



HAL
open science

Evolution des queues chez les Papilionidae (Lepidoptera) : approche macro-évolutive et expérimentale

Ariane Chotard

► To cite this version:

Ariane Chotard. Evolution des queues chez les Papilionidae (Lepidoptera) : approche macro-évolutive et expérimentale. *Ecologie, Environnement*. Museum national d'histoire naturelle - MNHN PARIS, 2022. Français. NNT : 2022MNHN0009 . tel-04959261

HAL Id: tel-04959261

<https://theses.hal.science/tel-04959261v1>

Submitted on 20 Feb 2025

HAL is a multi-disciplinary open access archive for the deposit and dissemination of scientific research documents, whether they are published or not. The documents may come from teaching and research institutions in France or abroad, or from public or private research centers.

L'archive ouverte pluridisciplinaire **HAL**, est destinée au dépôt et à la diffusion de documents scientifiques de niveau recherche, publiés ou non, émanant des établissements d'enseignement et de recherche français ou étrangers, des laboratoires publics ou privés.



Muséum National d'Histoire Naturelle

Ecole doctorale Science de la nature et de l'Homme : écologie et évolution – ED227

Institut de Systématique, Evolution, Biodiversité (UMR 7205)

Evolution of tails in Swallowtail butterflies (Papilionidae, Lepidoptera): macro-evolutionary and experimental approaches

Ariane Chotard

Thèse de doctorat d'Ecologie Evolutive

Dirigée par **Vincent Debat & Violaine Llaurens**

Présentée et soutenue publiquement le 16 décembre 2022 devant le jury :

Patricia Beldade, Professor, Universidade de Lisboa	Rapportrice
Gilles Escarguel, Assistant professor, Université de Lyon 1	Rapporteur
Marianne Elias, DR CNRS, Muséum National d'Histoire Naturelle	Examinatrice
Claire Mérot, CR CNRS, Université de Rennes 1	Examinatrice
Rodolphe Rougerie, Assistant professor, Muséum National d'Histoire Naturelle	Invité
Vincent Debat, Assistant professor, Muséum National d'Histoire Naturelle	Directeur
Violaine Llaurens, DR CNRS, Muséum National d'Histoire Naturelle	Directrice

**Evolution of tails in Swallowtail butterflies
(Papilionidae, Lepidoptera): macro-evolutionary
and experimental approaches**



Ariane Chotard

“Faithless is he that says farewell when the road darkens.”

“Not all those who wander are lost.”

— J.R.R. Tolkien

Acknowledgements

J'aimerais tout d'abord remercier Patrícia Beldade, Gilles Escarguel, Marianne Elias, Claire Mérot et Rodolphe Rougerie d'avoir accepté d'évaluer ma thèse de doctorat. J'espère sincèrement que vous prendrez autant de plaisir à la lire que j'en ai eu à travailler sur ce sujet pendant ces trois ans.

Vincent, Violaine, il n'y a pas mille façons de dire merci dans notre langue alors qu'il y a au moins mille choses pour lesquelles j'aimerais vous témoigner ma gratitude. Merci évidemment de m'avoir tant appris. Merci pour votre écoute et vos infatigables encouragements. Merci pour ces échanges passionnants, ces conseils innombrables qui, je le sais, me serviront toute ma vie. Merci de m'avoir accompagné, du premier jusqu'au dernier jour (celui où, d'ailleurs, j'écris ces lignes, à la fois si difficiles et si simples à mettre sur le papier). Merci pour votre rigoureuse bienveillance. Je verse dans l'oxymore parce qu'à mes yeux, elle illustre très bien votre complémentarité.

Vincent, merci de m'avoir réappris à m'émerveiller, à retrouver pourquoi j'aimais, j'aime, la Science.

Violaine, merci de comprendre, toujours. Merci de m'avoir réappris à croire en moi et à faire taire mes doutes.

Ce travail n'aurait pas été possible sans le concours scientifique d'un bon nombre de personnes. Un grand merci

à Fabien Condamine pour m'avoir immensément aidé sur les analyses de diversification (et pour m'avoir accueilli à l'ISEM, cette semaine intensive fût plus qu'enrichissante), ainsi que pour ton enthousiasme communicatif et ta réactivité qui frôle le surhumain.

à Michel Baguette pour nous avoir aiguillés dans les méandres de la montagne ariégeoise (sans ton aide, nous n'aurions certainement pas trouvé autant de Flambés),

à Alexis Chainé (et ses 72 adorables mésanges), Anthony Herrel et Thierry Descamps, pour votre enthousiasme, votre disponibilité et vos compétences respectives, qui ont

permis à notre super papier de voir le jour (et d'être publié en un temps record !). Je ne pouvais pas rêver mieux comme première expérience de publication.

à Ramiro Godoy-Diana et Roméo Antier, pour vos précieux conseils en biomécanique et pour nous avoir accueilli à l'ESPCI.

à Jérôme Barbut, pour avoir toujours été là quand j'essayais de me retrouver dans les collections et pour tes nombreux conseils et anecdotes de terrain incroyables. Merci aussi pour ce cours d'étalage de papillons, dont j'hésite à appliquer les enseignements, ayant mis presque un mois à retrouver la sensibilité de mes doigts.

à toute l'équipe étendue du labo : Sylvain, Marianne, Raph, Céline, Arnaud, pour cette formidable ambiance de travail, motivante et chaleureuse.

En parlant d'équipe, je tiens à faire une mention spéciale aux copains du labo, sans qui ces trois ans auraient été bien ternes. Joséphine et Camille, j'espère avoir été une aussi bonne encadrante que vous avez été de bons stagiaires. Un immense merci à Camille, Charline, Léa, Ludo, Vio, Pierre et Agathe, comme on avait l'habitude de dire, mes « frères et sœurs de thèse ». Merci pour ces pauses café, ces escapades en conférences (même en visio, on s'est débrouillés pour rendre ça un peu spécial), ces tours à la ménageries, ces sessions d'escalade, ces discussions dont la diversité est impossible à retranscrire, ces soirées, de celles confinées à arpenter les plaines de Tamriel à celles en vrai, qui duraient jusqu'au petit matin. Merci aussi évidemment pour votre aide scientifique, de la biomécanique en passant par la morphométrie, la classification taxonomique ou les mathématiques, merci d'avoir partagé tous ces bouts de codes R, ces workflows et bien sûr, tous ces conseils.

Et ma transition pour la suite est toute trouvée : durant ces trois ans, j'ai eu la chance d'être entourée d'une myriade de personnes formidables, à qui j'ai quelques lignes à adresser.

Aux copains de la première heure (on remonte minimum de quatorze ans en arrière jusqu'à vingt), Claire, Zoé, Henri, Florence, Fleur, Mewan. Vous avez toujours été là et je ne me fais aucun doute que cela sera toujours le cas. Merci pour ces si précieux souvenirs, il me tarde d'en écrire plein d'autres. Je sais la chance que j'ai de vous avoir dans ma vie depuis tout ce temps.

Aux copains de licence et de master, vous êtes trop nombreux pour que je vous nomme tous pardon (petite mention spéciale à Daphné, mon binôme de toujours). Merci à tous pour ces cinq années passionnantes, ces travaux de groupe, ces révisions, ces UE aux bords de l'eau, la vie de terrain à Foljuif ou à l'IEES... bref toute cette vie étudiante dont j'ai de merveilleux souvenirs.

Merci à mes copains d'aventure : Olivia, Niamh, Luc, Claire, Michaël, Alexis, Mélanie, Io, Fleur, Carla, Greg. Je n'ai pas eu beaucoup l'occasion de souffler pendant ma thèse (*i.e.*, je ne me suis pas donné beaucoup l'occasion de souffler), alors les quelques jours par an où je m'en échappais ont une saveur particulière. Merci pour ces plongées, ces sessions d'escalade, ces randonnées, ces soirées autour du feu, ces chamallows, ces levers et ces couchers de soleil. La vie est si simple à vos côtés. Merci pour cette bouffée d'air frais qui, à chaque fois, me redonnait l'envie de rêver.

Alain Couté, merci pour tes enseignements, tu m'as appris presque tout ce que je sais sur la plongée. Je penserai à toi à chaque fois que je croiserai une *Elysia timida*.

Merci à ma famille, de sang comme de cœur, pour votre affection et votre soutien indéfectibles sans lesquels je ne serai pas devenue la personne que je suis.

Papa, Maman, merci pour tout. Simplement tout. Je pourrai écrire un roman sur tout ce que vous avez fait pour moi ou à quel point je vous aime, mais vous le savez déjà.

Merci à Alexandra Elbakyan pour son dévouement et sa contribution à rendre le savoir scientifique accessible à tous.tes les chercheurs.euses, sans lesquels mon travail de thèse n'aurait clairement pas été aisé.

Enfin, merci à toutes celles qui, anonymes ou panthéonisées, ont œuvré, combattu pour chaque droit, pour chaque liberté. Celles dont les luttes et les sacrifices me donne le droit, aujourd'hui, d'écrire ces lignes.

Abstract (english version)

The evolution of butterfly wing shape is driven by multiple selective, phylogenetic and developmental influences. In my thesis, I focused on the evolution of wing shape in Papilionidae, a butterfly family presenting a high diversity of wing shapes. Papilionidae are collectively referred to as Swallowtail butterflies, owing to the tails that many species harbour on the hindwings. While this feature is particularly striking and diversified, its evolutionary drivers have never been investigated. *Did tails evolve neutrally? What are the selective pressures affecting it? Do forewings and hindwings evolve independently?* By combining micro- and macro-evolutionary approaches, my thesis aimed at answering these questions and identifying the main factors affecting the evolution of wing shape, with a particular focus on hindwing tails. Focusing on *Iphiclides podalirius*, I first tested whether tails deflect birds attacks away from the butterfly body (the *deflecting effect* hypothesis; Chapter I). I showed that natural wing damages mostly concern hindwings tails and colour-pattern, suggestive of predation attempts; I then conducted a behavioural assay with dummy butterflies, and showed that great tits (*Parus major*) focus their attacks on the tails; finally, quantifying the mechanical properties of fresh wings, I found that the tails are particularly fragile. Altogether, these results support a deflecting effect of hindwing tails, suggesting that predation is an important selective driver of the evolution of tails in butterflies. I then investigated the relative aerodynamic importance of tails in flapping flight (the *aerodynamic effect* hypothesis; Chapter II), conducting flight analyses of phenotypically altered *I. podalirius*. I showed that hindwing tails have a significant stabilising impact on flapping flight, suggesting that selection on aerodynamic performance likely affects the evolution of tails. Based on these experimental results, I then quantified the variation of fore- and hindwing wing shape at the macro-evolutionary scale (across the Papilionidae family; Chapter III). I compared the shape diversity and evolutionary rate among the two wings, and tested the link between diversification and phenotypic disparity. I specifically characterized the evolution of the tail at the family level. My results show that hindwings are strikingly more diversified than forewings, suggesting contrasted selective regimes on the two pairs of wings. Forewings might be under stabilizing selection in relation to flight anteromotorism, while hindwings might be submitted to a diversity of selective pressures.

Our results on *I. podalirius* suggest a possible trade-off between attack deflection and aerodynamic effects, promoting the diversity of hindwing shape, and particularly the evolutionary lability of tails and associated colour patterns. Contrary to previous work, my results also suggest a tight coevolution of the two wing pairs, the presence of tails possibly affecting the selection on the forewings. Overall, this study shows that the combination of behavioural ecology and macro-evolutionary studies might shed light on key factors affecting morphological evolution.

Altogether, my PhD work has brought some insights on the selection pressures involved in hindwing tail evolution and highlighted the complex links existing between forewings and hindwings evolution, between contrasted selection, developmental constraints and co-evolution.

Résumé (version française)

L'évolution de la forme des ailes des papillons est déterminée par de multiples influences sélectives, phylogénétiques et développementales. Durant ma thèse, je me suis concentrée sur l'évolution de la forme des ailes chez les Papilionidae, une famille de papillons présentant une grande diversité de formes d'ailes. Cette famille doit son nom aux queues que de nombreuses espèces arborent sur les ailes postérieures. Si cette caractéristique est particulièrement frappante et diversifiée, ses déterminants évolutifs n'ont jamais été étudiés. *Les queues ont-elles évolué de manière neutre ? Quelles sont les pressions de sélection en jeu ? Les ailes antérieures et les ailes postérieures évoluent-elles indépendamment ?* En combinant des approches micro- et macro-évolutives, ma thèse vise à répondre à ces questions et à identifier les principaux facteurs affectant l'évolution de la forme des ailes, avec un accent particulier mis sur l'évolution des queues des ailes postérieures. En prenant pour espèce modèle *Iphiclides podalirius*, j'ai d'abord testé si les queues déviaient les attaques des oiseaux du corps des papillons (hypothèse de l'effet de déflexion ; Chapitre I). J'ai montré que les dommages naturels aux ailes concernaient principalement les queues et les motifs de couleur des ailes postérieures, suggérant des tentatives de prédation ; j'ai ensuite réalisé un test comportemental et montré que les mésanges charbonnières (*Parus major*) concentraient leurs attaques sur les queues ; enfin, en quantifiant les propriétés mécaniques des ailes, j'ai constaté que les queues étaient particulièrement fragiles. Dans l'ensemble, ces résultats confirment l'effet défecteur des queues des ailes postérieures, suggérant que la prédation est un facteur sélectif important de l'évolution des queues chez les papillons. J'ai ensuite étudié l'importance aérodynamique relative des queues durant le vol battu (hypothèse de l'effet aérodynamique ; Chapitre II), en effectuant des analyses de vol sur des *I. podalirius* phénotypiquement modifiés. J'ai montré que les queues des ailes postérieures avaient un effet stabilisateur significatif sur le vol battu, suggérant que la sélection sur la performance aérodynamique affecte probablement l'évolution des queues. Sur la base de ces résultats expérimentaux, j'ai ensuite quantifié la variation de la forme des ailes antérieures et postérieures à l'échelle macro-évolutive (dans toute la famille des Papilionidae ; Chapitre III). J'ai comparé la diversité des formes et le taux d'évolution des deux paires d'ailes, et testé le lien entre diversification et disparité phénotypique. J'ai

spécifiquement caractérisé l'évolution de la queue au niveau de la famille. Mes résultats montrent que les ailes postérieures sont étonnamment plus diversifiées que les ailes antérieures, ce qui suggère des régimes sélectifs contrastés sur les deux paires d'ailes. Les ailes antérieures pourraient être soumises à une sélection stabilisante, en lien avec l'antéromotricité du vol, tandis que les ailes postérieures pourraient être soumises à une diversité de pressions sélectives. Nos résultats *sur I. podalirius* suggèrent un compromis évolutif possible entre la déviation des attaques et les effets aérodynamiques, favorisant la diversité de la forme des ailes postérieures, et particulièrement la labilité évolutive des queues et des motifs de couleur associés. Contrairement aux travaux précédents, mes résultats suggèrent également une coévolution étroite des deux paires d'ailes, la présence des queues pouvant affecter la sélection sur les ailes antérieures. Dans l'ensemble, cette étude montre que la combinaison de l'écologie comportementale et des études macro-évolutives peut faire la lumière sur les facteurs clés de l'évolution morphologique.

Dans l'ensemble, mon travail de thèse a permis de mieux comprendre les pressions de sélection impliquées dans l'évolution de la queue des ailes postérieures et a mis en évidence les liens complexes existant entre l'évolution des ailes antérieures et des ailes postérieures, entre sélection contrastée, contraintes de développement et coévolution.

Table of content

INTRODUCTION	1
I – Trait variation, a complex equation.....	2
II - Lepidopteran wing: a complex trait.....	3
1) The development of Lepidopteran wings, a highly conserved and constrained process.....	3
2) Does aerodynamics generate contrasted evolution between forewings and hindwings?	4
3) Natural and sexual selection on shape and colour-pattern of wings	5
4) Why and how do hindwing tails evolve in Papilionidae?.....	7
III - <i>Iphiclides podalirius</i> as a model species for investigating hindwing tail evolution.	13
IV - Main questions and objectives of the thesis	16
CHAPTER I: EVIDENCE OF ATTACK DEFLECTION SUGGESTS ADAPTIVE EVOLUTION OF WING TAILS IN BUTTERFLIES	21
Introduction.....	23
Materials & Methods.....	26
1) Field sampling	26
2) Assessing the distribution of wing damage in the wild.....	26
3) Behavioural experiment with birds.....	27
4) Mechanical resistance of the wings	29
Results.....	32
1) Natural wing damage mostly affects the tails	32
2) Behavioural experiments with birds reveal preferential attacks on hindwing tail and colour pattern	33
3) Hindwings and in particular hindwing tails are more easily damaged.....	34
Discussion	36

1) Adaptive evolution of hindwing tails promoted by predator behaviour.....	36
2) Adaptive syndrome of predation deflection	38
Conclusion	40
Supplementary	42

CHAPTER II: THE EFFECTS OF HINDWING TAILS ON FLAPPING FLIGHT PERFORMANCES IN THE SWALLOWTAIL BUTTERFLY IPHICLIDES PODALIRIUS SUGGEST AN ADAPTIVE EVOLUTION OF BUTTERFLY TAILS.....47

Introduction.....	49
Materials & Methods	51
1) Sampling	51
2) Experimental groups	51
3) Experimental setup.....	52
4) Flight trials	52
5) Quantification of flight trajectory	53
6) Statistical analyses	55
Results	57
Discussion.....	61
1) Butterfly wing tails contribute to flapping flight performance	61
2) A trade-off between deflection and flight abilities.....	61

CHAPTER III: SELECTION AND CONSTRAINTS SHAPE THE MACROEVOLUTION OF HINDWING TAILS IN PAPILIONIDAE65

Introduction.....	67
Materials & Methods	70

1) Taxon sampling	70
2) Phylogenetic data.....	70
3) Imaging.....	70
4) Geometric morphometrics	70
5) Aspect Ratio as a proxy for gliding performance	71
6) Hindwing tail.....	71
7) Phylogenetic signal.....	72
8) Estimating the effect of biomes on wing shape evolution	73
9) Comparing the evolution of the two types of wings: diversity, evolution rate and sexual dimorphism.....	73
10) Covariation between the wings and impact of the tail on forewing evolution	74
11) Testing the effect of wing shape variation on species diversification	74
12) Estimating the rate of wing shape evolution	75
13) Developmental integration of wings	75
14) Impact of the chosen macro-evolutionary scale: zoom on two genera.....	76
Results.....	77
Contrasted evolution of the two pairs of wings	77
Shared developmental constraints between forewing and hindwing	80
Evolution of sexual dimorphism in hindwing and forewing	80
Testing for the effect of wing shape variation on species diversification?	81
Multiple emergences and losses of hindwing tail.....	82
Testing the effect of hindwing tail on the forewing shape.....	83
Discussion	87
Supplementary	92
DISCUSSION.....	109
1) Ancestral wing shape and multiple evolution of tails	110
2) What bridges can be built between macro and micro-evolutionary results?.....	113
Perspectives.....	118

Conclusion 121

**ANNEX I: INVENTORY OF THE NATIONAL MUSEUM OF NATURAL
HISTORY COLLECTIONS: PAPILIONIDAE 123**

**ANNEX II: PATTERNS OF MORPHOLOGICAL VARIATION SHED LIGHT
ON THE ADAPTIVE EVOLUTION OF EYESPOTS MODULARITY IN THE
BUTTERFLY MORPHO TELEMACHUS..... 159**

Introduction..... 161

Materials & Methods 164

- 1) Butterfly Samples..... 164
- 2) Estimating eyespot conspicuousness..... 165
- 3) Measuring eyespot size and shape: Imaging and morphometric measurements 165
- 4) Assessing patterns of variations and covariations 167

Results 169

- 1) Contrasted levels of conspicuousness among eyespots in *M. telemachus* 169
- 2) The shape of always-visible eyespots is more variable and asymmetrical in *M. telemachus* 170
- 3) Conditionally-displayed eyespots form a developmental module in *M. telemachus* 172

Discussion..... 175

- 1) Differential eyespot variability in *M. telemachus* shaped by contrasted selection regimes 175
- 2) Phenotypic covariation: integration within eyespots, modularity among eyespots..... 177
- 3) Phenotypic covariation: functional and developmental modularities match in *M. telemachus*... 178

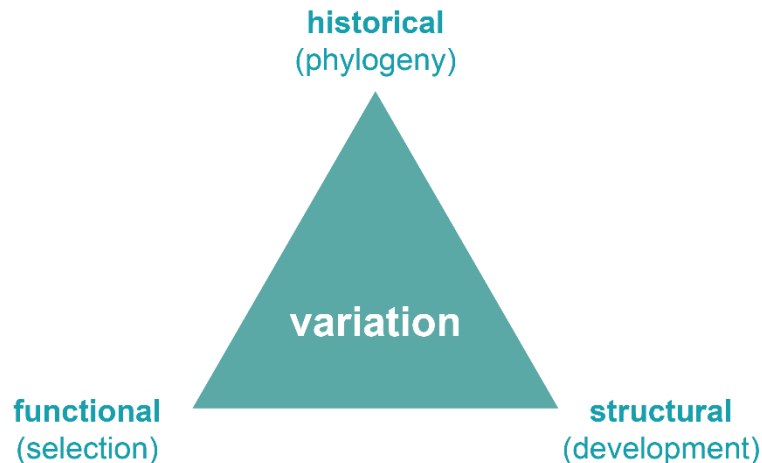
Supplementary 180

BIBLIOGRAPHY 185

Introduction

I – Trait variation, a complex equation

All phenotypic traits, either morphological or behavioural, are the evolutionary results of multiple functional, historical and structural influences.



Understanding the evolution of a trait could be compared to the resolution of a polynomial equation with infinite unknowns and dimensions. Of course, the immense majority of the terms of this equation is, and will always remain, unknown. And yet, identifying some terms can strongly modify our vision of the equation, and constitute a precious clue for understanding Evolution. Some of these terms imply an adaptive effect on the trait, while others are associated with a neutral divergence.

Firstly, the independent identification of the terms of the equation is a preliminary step to solving the global equation. But as some selective factors will promote a certain variation of our trait while other pressures will select other trait values, the relative importance of these different pressures will condition trait variation. In parallel, traits do not vary independently of each other. Some selective forces induce an increased fitness of a trait at the expense of a decreased fitness in another trait. This notion of « trade-off » is essential to understand trait evolution (the “functional” + “structural” forces). For example, a lot of secondary sexual characters associated with display increase

reproductive success but decrease survival, due to predation exposure or limited resource allocation (Garland *et al.*, 2022).

Secondly, at each time unit t , the equation is constrained by all previous states $t-n$ (the “historical” + “structural” forces). In line with the concept of adaptive landscape described by Wright (1932), the position of a trait in the landscape is the result of its previous positions. Therefore, its possibilities of variations are dependent of the past evolutionary road. Some high fitness peaks are accessible only after passing through many other peaks. Some roads are astonishing and tortuous. One of the best examples is the concept of exaptation. Exaptation is, as defined by Gould and Vrba in 1982, “*a character, previously shaped by natural selection for a particular function (an adaptation), coopted for a new use*” or “*a character whose origin cannot be ascribed to the direct action of natural selection (a nonadaptation), coopted for a current use*”. An emblematic example of exaptation is theropods feathers; the primary selection pressures that drove feathers evolution are still debated, from body insulation, manoeuvrability, brooding, camouflage to display, but feathers were only secondary recruited for aerodynamic functions (Ostrom, 1974; Prum and Brush, 2002; Foth *et al.*, 2014).

How do we balance the selective, historical and developmental components of our equation? The main challenge is the lack of prediction on the actual developmental constraints acting on the traits, as well as the reliance on models of neutral trait evolution at large evolutionary scales. Nevertheless, some traits are still relevant to disentangle the equation, using key developmental and historical properties such as serial homology. This homology between traits allows to decipher developmental and selective processes acting on trait variations. In this thesis, I focused on the evolution of emblematic serially homologous traits: Lepidopteran wings.

II - Lepidopteran wing: a complex trait

1) The development of Lepidopteran wings, a highly conserved and constrained process

Lepidoptera is an ancient order, that originated nearly 300 million years ago (Kawahara *et al.*, 2019). *Lepidoptera* display two pairs of wings, like all other pterygotes (main

lineage of insects: *e.g.*, *Orthoptera*, *Diptera*...). Nevertheless, contrary to other pterygotes, Lepidopteran wings are covered with scales (in Ancient Greek, λείψ, lepis means « scale » and πτερόν, pterón means « wing »). Pterygotes wings are formed by the transformation of ancestral segments with limbs, through the repression of some homeobox genes: forewings on the second thoracic segment and hindwings on the third thoracic segment (Carroll, 1995; Carroll *et al.*, 2005). The forewings and hindwings are then serially homologous. Serially homologous traits stem from the repetition of the same developmental pathway in different locations of the body (Hall, 1995), like vertebrate teeth (Van Valen, 1994). They are relevant traits to identify how selection regime can overcome the effect of developmental constraints acting on phenotypic evolution (*e.g.*, Allen 2008).

Firstly, the modularity pattern across serial homologues could reflect the prevailing effect of developmental *vs.* selective factors affecting trait evolution (Beldade and Brakefield, 2003; Breuker *et al.*, 2006; Allen, 2008). Indeed, they are expected to exhibit tight covariations due to their shared developmental basis (Young and Hallgrímsson, 2005), and these covariations could be broken down by heterogeneous selection across the elements of a series (Wagner and Altenberg, 1996; Melo and Marroig, 2015). During my master's thesis, I focused on the effect of selection on developmental modularity, using wing eyespots in the butterfly *Morpho telemachus* as a case-study (see Annex II).

Secondly, the phenotypic differentiation of serial homologues may inform on the selective regime acting on repeated modules. Usually, ancestral insect is assumed to display similar forewings and hindwings, like the Orthopteran wings observed nowadays (Carroll *et al.*, 2005). Differential selection acting on this ancestral phenotype results, for example, to the reduction of hindwings into halteres in Diptera. In Lepidoptera, morphological differences between forewings and hindwings are also observed, and this difference is likely caused by different selection pressures, notably aerodynamics.

2) Does aerodynamics generate contrasted evolution between forewings and hindwings?

Lepidoptera have an anteromotoric flight, *i.e.*, they predominantly use their forewings during flight (Dudley, 2002; Jantzen and Eisner, 2008). Wing shape variation may strongly influence flight performances. Flight abilities might be shaped by selective

pressures exerted by predators (enhancing endurance for instance), sexual selection (inter-sexual selection through mating display or inter-sexual selection through fight), or by competition for resources. These different behaviours might promote contrasted wing morphologies (Le Roy *et al.*, 2019b, 2021) and wing shape evolution likely results from the trade-off in performance in different aspect of flights. Selection on aerodynamic properties might be higher on forewings than hindwings, resulting in divergent evolution of forewings from the homologous hindwings. In contrast, hindwings shape may be shaped by multiple selective processes, such as predator avoidance or mating (see below), possibly leading to a higher shape diversity in Lepidoptera. Moreover, Lepidopteran wings evolution is largely more complex than forewings/hindwings differentiation.

Because wing shape and colour-pattern both contribute to the visual appearance of butterflies, they are usually assumed to evolve in concert. They form so-called complex phenotypes, whereby multiple selection pressures generated by predators and conspecifics promote specific associations between wing shapes and colours.

3) Natural and sexual selection on shape and colour-pattern of wings

Predation generates powerful selection promoting the evolution of defensive traits (Ruxton *et al.*, 2004). In butterfly wings, predation has selected many anti-predator morphologies, combining colour-pattern and wing shape, either (1) limiting detection, (2) preventing attack after detection and/or (3) enhancing survival after an attack. These anti-predators morphologies are diverse and are likely to depend on the nature and intensity of predation pressures (Aluthwattha *et al.*, 2017).

(1) Detection by predators may be limited by a cryptic aspect of the wings: butterflies can then be confounded with their environment by the predators. For example, in *Kallima* butterflies, disruptive coloration and wing shape make the butterfly look like a dead-leaf. Because birds rarely distinguish these butterflies from leaves, this specific association between colour pattern and wing shape likely improve survival (Stoddard, 2012).

(2) Avoiding attack after detection may involve the joint evolution of aposematic coloration and particular wing shape. For example, in some skipper butterflies (family *Hesperiidae*), colour pattern (white patches on dark background) and wing shape

(extended butterfly hindwings) form an “evasive signal” and drive learning and avoidance of butterflies by avian predators (Linke *et al.*, 2022).

(3) Traits enhancing survival after an attack can also be promoted. Wing shape and colour can generate deflection effects by directing predator attacks towards poorly vulnerable area of the prey body or towards the opposite direction of the escape trajectory (Ruxton *et al.*, 2004; Humphreys and Ruxton, 2018). For example, in Lycaenidae, hindwings frequently display particular wing shape (tiny tails and wide anal angle) and conspicuous colour patterns hypothesized to mimic a head with moving antennae (the ‘false head effect’). This ‘false-heads’ are likely to deflect attacks away from vital parts (Robbins, 1980, 1981).

The association of wing shape and colour pattern could also be under sexual selection. For example, in *Papilio dardanus*, females are polymorphic, with andromorph forms (displaying hindwing tails and black and yellow colour pattern) and mimic forms (for example, the *hippocoonides* form displaying no tail and black and with colour-pattern). It has been shown that males preferred mimic females (*hippocoonides*) than andromorph. Wing shape and colour-pattern associated with *hippocoonides* form are then co-selected (Cook *et al.*, 1994).

While the developmental determinism and selective effects driving the evolution of butterfly colour-pattern are well known, the factors underlying wing shape evolution are still poorly documented in Lepidoptera. Lepidopteran wing shape are widely diversified, what factors are involved in the diversification of this trait? Is this diversification neutral or adaptive? Can we identify ecological factors driving its evolution?

A remarkable feature of wing shape is tail. Tail is a very common trait in butterflies, but its developmental bases and the evolutionary forces acting on its emergence and loss are unknown. Tail is a very variable character, by its presence (we indeed find tails in many groups, but they are remarkably absent from others) but also by its shape and size. The tails of moths such as Saturniidae have been well studied: tails divert bats from attacking moth bodies (Barber *et al.*, 2015) by blurring the echolocation signal perceived by predators, thus diminishing strike efficiency (Rubin *et al.*, 2018). Surprisingly for such a

prominent trait, the evolution of tails in day-light butterflies is comparatively remarkably unknown. What selection pressures act on their evolution?

4) Why and how do hindwing tails evolve in Papilionidae?

Hindwing tail can be defined as a protrusion of the wing margin. Such tails are widespread among day-flying Lepidoptera and have evolved many times independently. For example, tails are observed in some species of day-flying moths, like Uranidae (Figure 1A), and in many species across butterfly families, with the countless tailed Papilionidae (Swallowtail butterflies) species, the double-tailed Charaxinae (Figure 1B), the tiny tailed Riodinidae (Figure 1C) and Lycaenidae (Figure 1D), and the few Hesperidae (Figure 1E) and even fewer Pieridae tailed species (Figure 1F).

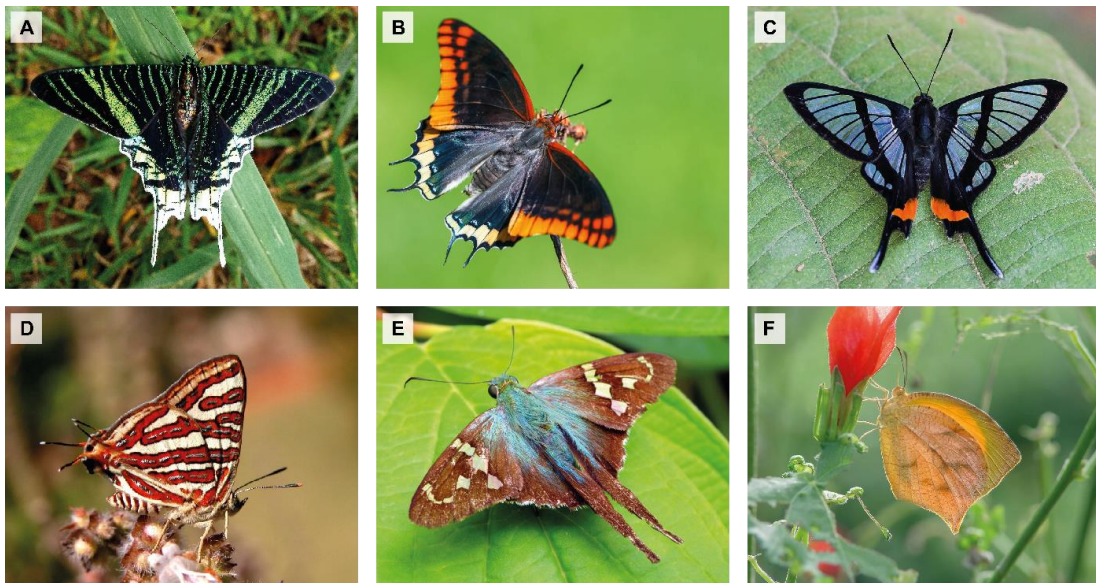


Figure 1: (A) *Urani leilus*. (B) *Charaxes jasius*. (C) *Chorinea licursis*. (D) *Cigaritis vulcanus*. (E) *Urbanus proteus*. (F) *Pyrisitia proterpia*. Credits photo: (B) Adam Gor, (C) Ailton Cândido de Almeida, (E) Andea Kay, (F) Bill Bouton.

Swallowtail butterflies are particularly well known for their conspicuous tails, they even take their name from this characteristic. They harbour highly diversified hindwing tails (Figure 2), but the evolutionary determinants driving the evolution of these tails have never been formally investigated.

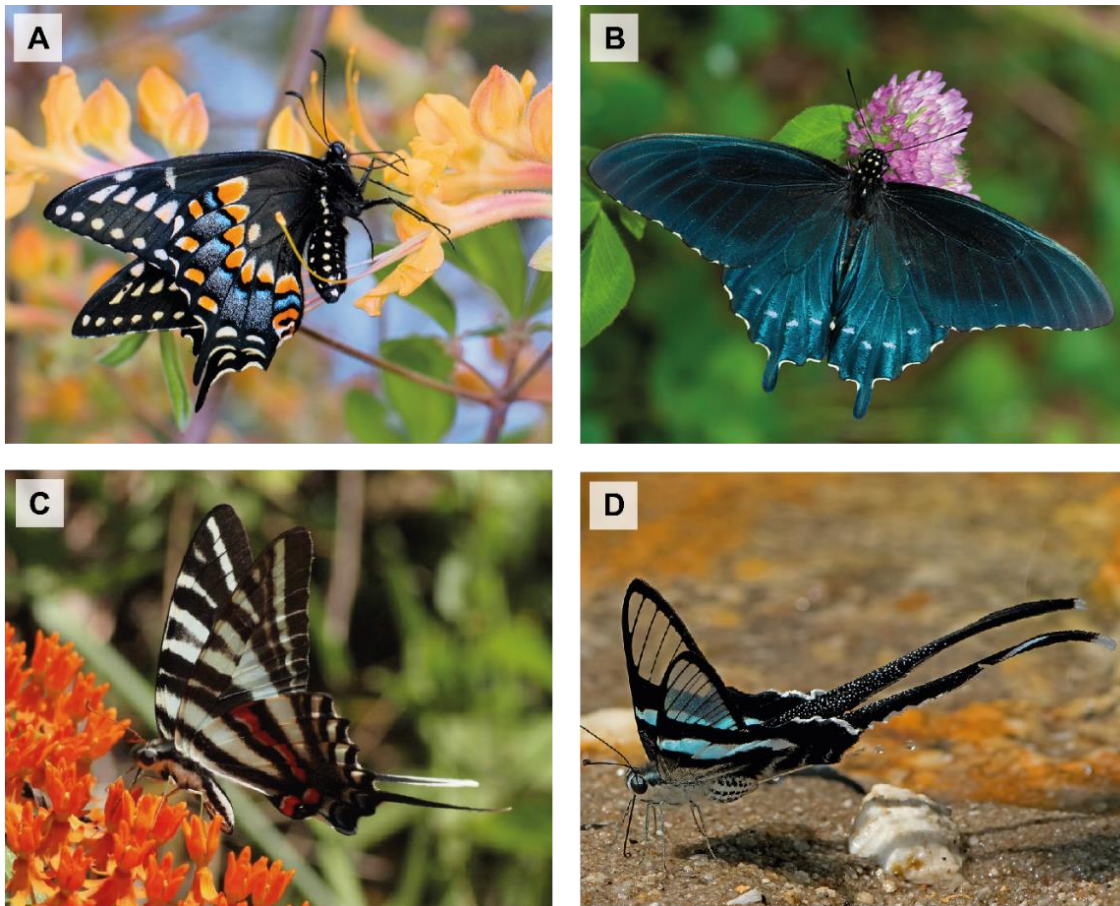


Figure 2: (A) *Papilio polyxenes*. (B) *Battus philenor*. (C) *Erutytides marcellus*. (D) *Lamproptera meges*. Photo credits: (A) Sara Bright, (B) Jerry Green, (C) Bibb County, (D) Tom Stratford.

Papilionidae is one of the seven families of butterflies (Papilionoidea, [Espeland *et al.*, 2018](#)), which counts between 570 and 620 described species depending on the studies ([Allio *et al.*, 2020](#); [Museum für Naturkunde Berlin, GloBIS](#)). The latest time-calibrated phylogeny of Papilionidae counts 408 species distributed over 31 genera (data from ([Allio *et al.*, 2020, 2021](#)), see Figure 9 for illustration) and was used as a reference for the macroevolutionary studies carried out in this thesis. Tails are found in many species of this group, but are notably absent in some. What are the factors involved in the diversification of this trait?

Based on the literature, two main selective hypotheses have been put forward:

The predation deflection hypothesis: tails could attract predators attention and deflect their attacks away from the vital body parts, thereby increasing escape probability

(Ruxton *et al.*, 2004). This hypothesis was long proposed for Lycaenidae (Cott, 1940). These butterflies display wings with contrasting stripes converging toward the anal angle (and so presumably leading the predator's eye), contiguous between forewing and hindwing, an anal angle with conspicuous colour pattern (eyespot, lunules) and one or several tails. Experimental studies on *Arawacus aetolus* and others Lycaenidae species demonstrated that the combined effect of wing pattern and shape deflected predator attacks from the actual head (Robbins, 1980, 1981). Tail may thus attract predator attacks on the edges of the hindwings, away from the thorax/head (vital parts) of the butterfly. More recently, behavioural experiments with spiders showed that *Calycopis cecrops* butterflies, displaying false-head hindwings, escaped more frequently than butterflies from other species lacking these false-heads (Sourakov, 2013). Papilionidae wing tails evolution could also be shaped by predator behaviour. Nevertheless, the predator community feeding on Papilionidae might be drastically different from Lycaenidae. Lycaenidae are small-size butterflies whose predators are mainly invertebrate. In contrast, predation on Papilionidae, on average larger butterflies, mostly involves vertebrate predators, and birds in particular (Pinheiro, 2011; Pinheiro and Cintra, 2017; Páez *et al.*, 2021). The deflection effect of tails has not been investigated in Papilionidae, and call for behavioural experiments involving birds.

The aerodynamic hypothesis: a wind tunnel study in the Papilionidae *Graphium polices* showed that tails could improve aerodynamic performance, particularly by stabilizing gliding flight (Park *et al.*, 2010). The evolution of tails could therefore be promoted in species where gliding flight performance are crucial, as for example in canopy species. The effect of tails on flapping flight has not been studied at all.

Some others selection pressures certainly influence the evolution of tails in some species:

- **Camouflage/masquerade:** In *Papilio nobilis* and *Meandrusa payeni* (Figure 3) tails are associated with specific coloration, making these butterflies hardly distinguishable from the surrounding vegetation / looks like fallen leaves. The evolution of tail may have been promoted by increased survival in individuals with irregular shapes.

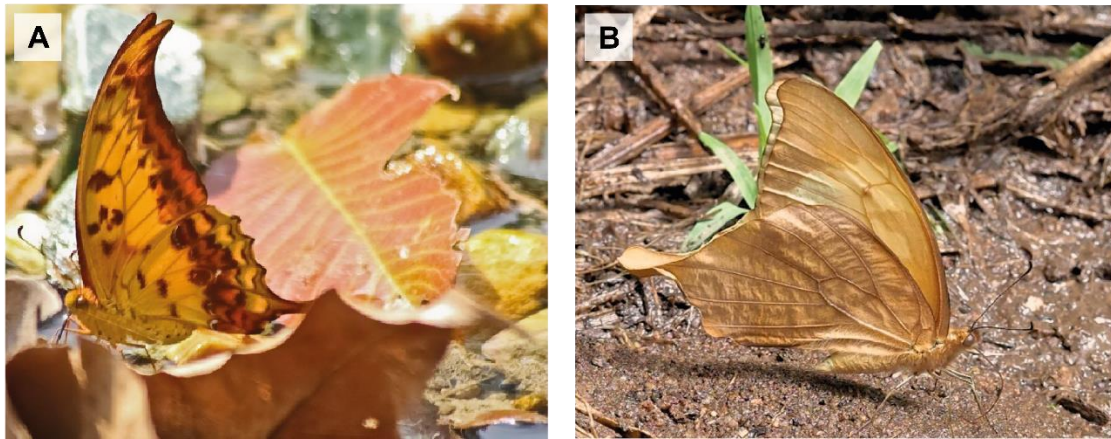


Figure 3: (A) *Meandrusa payeni*. (B) *Papilio nobilis*. Photo credits: (A) Tarun Karmakar, (B) N.P. Kibale.

- **Aposematism / Mullerian mimicry:** Some Papilionidae lineages feed on host plants of the Aristolochiaceae family, known for their high toxicity (Ehrlich and Raven, 1964 but see [Condamine et al., 2012](#) for a review). Caterpillars sequester toxins (e.g., aristolochic acids), and these sequestered compounds are still found in adults (e.g., *Pachliopta aristolochiae*, [Wu et al., 2000](#); *Battus philenor*, [Fordyce, 2000](#)). In the Troidini tribe, large number of species are described for their aposematic coloration, i.e., genus *Atrophaneura*, *Byasa*, *Losaria*, and *Pachliopta* (also known as pipevine butterflies – see Figure 4 for illustration). Those butterflies display conspicuous red coloration on body and hindwings, that make them particularly recognizable by predators. Moreover, this colour-pattern is often associated with particular wavy hindwing shape and very often tails. The particular shape of the wing is likely to participate to the aposematic signal ([Sekimura and Nijhout, 2017](#)).

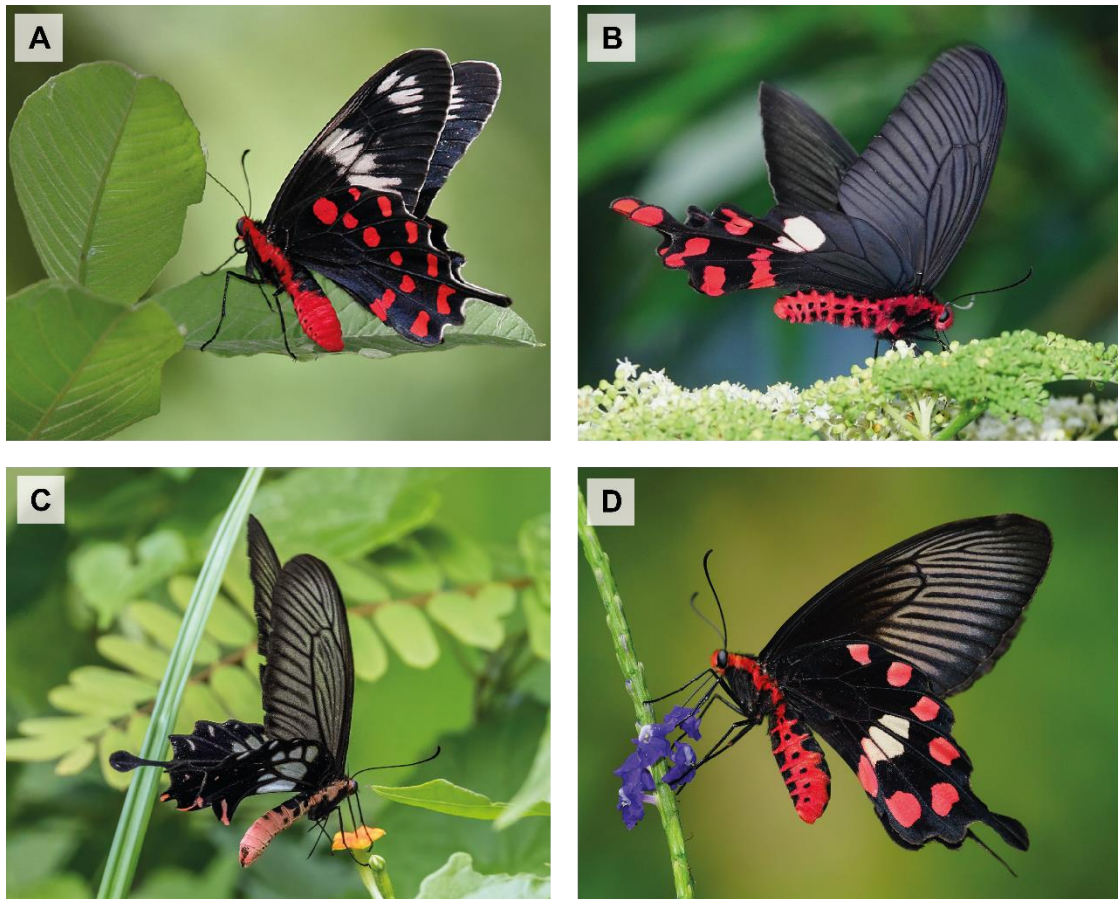


Figure 4: (A) *Atrophaneura hector*. (B) *Byasa polyeuctes*. (C) *Losaria coon*. (D) *Pachliopta aristolochiae*.

- Batesian mimicry:** some palatable species (especially from the *Papilio* genus) display mimetic wing colour pattern resembling some defended species. Both tails and colour-pattern are likely promoted by the protection gained from mimicry towards defended species living in sympatry. For example, *Papilio polyxenes asterius* is mimetic to *Battus philenor* – see Figure 5 (Codella and Lederhouse, 1989). Interestingly, in some *Papilio* species, mimicry is observed only in females. For example, *Papilio memnon* has monomorphic males without tail and polymorphic females. Some females have mimetic coloration and tails, enhancing resemblance with local defended species (16 females forms listed in Clarke *et al.*, 1968).

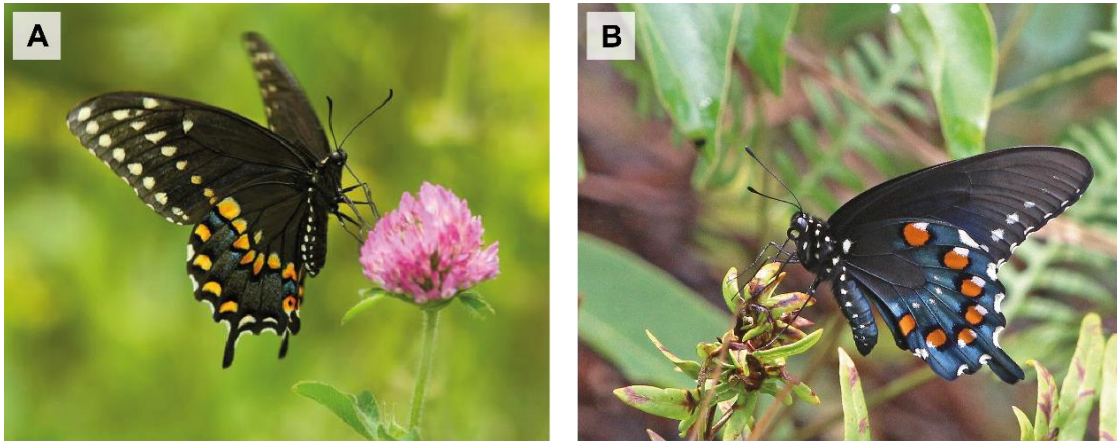


Figure 5: (A) *Papilio polyxenes asterius*. (B) *Battus philenor*. Photo credits: (A) Denis Dumoulin, (B) Mary Keim.

- **Sexual selection:** by participating in the mimetic signal, tails could indirectly be under sexual selection due to reproductive interference related to mimicry (*e.g.*, *Papilio glaucus*, [Pliske, 1972](#)) or to frequency-dependence preferential mating with Batesian females forms ([Kunte, 2009](#)). In others non-mimetic species, tails could, contrary to the hypothesis of flight stabilization, be an honest signal of quality for females, especially if they generate an aerodynamic cost (like bird tails, *e.g.*, in hummingbirds, [Clark and Dudley, 2009](#)).

In a nutshell, the wide diversity of hindwing tails in Papilionidae could result from multiple selection pressures, but the evolutionary dynamics of this trait has never been investigated and no experimental test for fitness advantages associated with hindwing tails has been conducted.

III - *Iphiclides podalirius* as a model species for investigating hindwing tail evolution.

Iphiclides podalirius (1758, Linnaeus) is a large palearctic butterfly and is one of the most emblematic species of butterfly in Europe. We even find traces of it in naturalist engravings prior to its taxonomic description (Figure 6A).

This species displays long tails associated with a salient colour pattern on hindwings: an orange eyespot and four blue lunules with strong UV reflectance (Gaunet *et al.*, 2019). The combination of hindwing tail and colour pattern is very conspicuous (Figure 6B), and especially for predators sensitive to UV reflection, such as songbirds (Cuthill *et al.*, 2000). Moreover, the four wings exhibit black stripes over a pale background, contiguous between forewings and hindwing in resting position, pointing towards the anal edge. These visual characteristics fit the characteristics listed in Robbins, 1981 as contributing to a deflecting effect. *Iphiclides podalirius* has a characteristic gliding flight: males are usually found flying on a hilltop (“hill-topping”), competing for the best spot and ultimately, for the females. Males are then sometimes seen fighting with others males. These environmental conditions (winds and predation exposure) and their courting behaviour require particular individual aerodynamic performances (such as flight stabilization, acceleration power...).

The use of this species as an experimental model allowed us to test concomitantly the two main selective hypotheses on tail evolution (predation deflection and aerodynamics) and understand if and how they can co-occur.

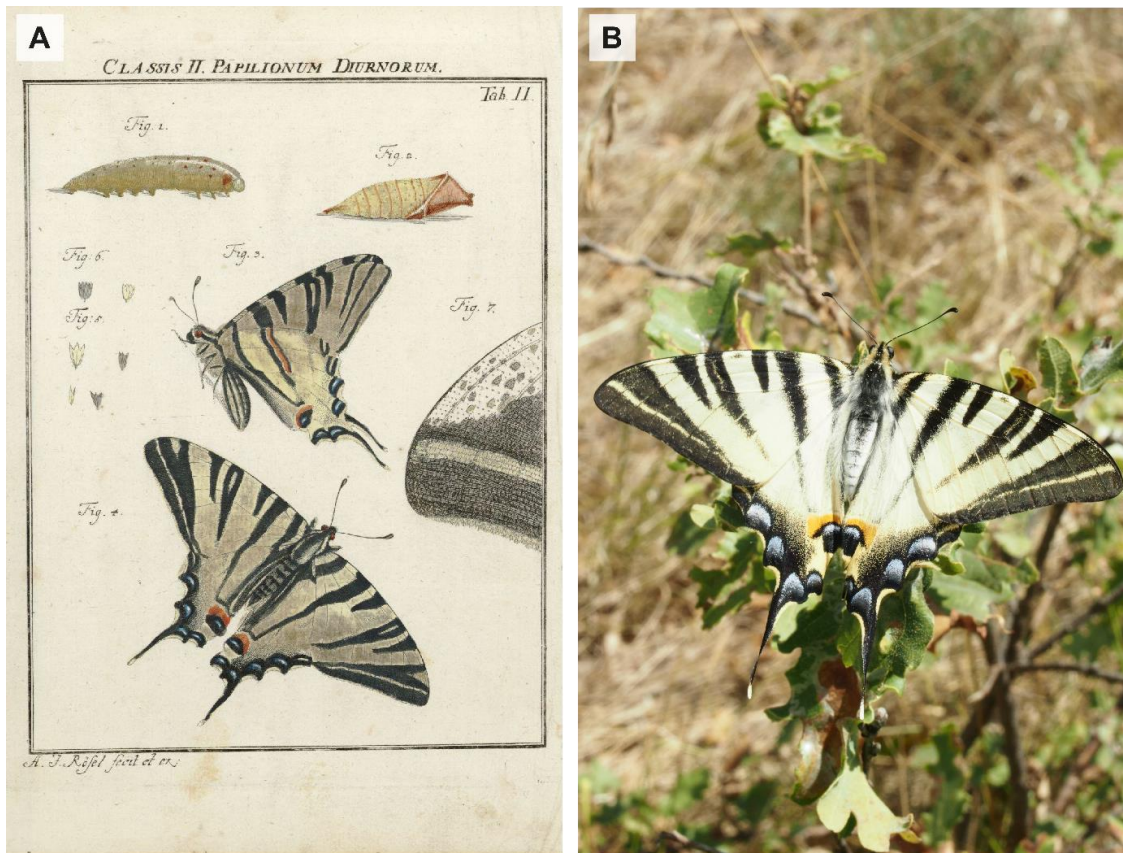


Figure 6: (A) Engraving dating from 1746, from *In welchem die in sechs Classen eingetheilte Papilionen mit ihrem Ursprung*, Verwa, 1746. (B) Photograph of an *Iphiclides podalirius*, perching on a young oak tree (Ariège, summer 2020). Credits photo: Ariane Chotard.

Box 1: *Iphiclides podalirius* ecology, distribution and life-cycle

The spatial distribution of *Iphiclides podalirius* spans from North-West Africa to the Central Asia through the Mediterranean area (Wiemers and Gottsberger, 2010). This species is usually observed between 0 and 2000m altitude (Gaunet *et al.*, 2019; Lafranchis and Delmas, 2015), at the top limestone slope. Two or three generations can occur within a year (Scheller and Wohlfahrt, 1981; Wohlfahrt, 1979). In France, *I. podalirius* is bivoltine, with a spring-generation in April-May and a summer-generation in July-August (data from the Suivi Temporel des Rhopalocères de France - STERF).

The life cycle of *I. podalirius* lasts about 2-3 month, with 3 caterpillar stages. The most common host plants are fruit trees of the genus *Prunus*, pear tree *Pyrus communis* and hawthorn *Crataegus monogyna* (Stefanescu *et al.*, 2006). Adults are nectarivore, feeding on blue/violet flowers (*e.g.*, thistle or lavender, pers.obs Ariane Chotard) and oligophagous (Stefanescu *et al.*, 2006). Its known predators are mainly avian (black redstart *Phoenicurus ochruros*, blue tit *Cyanistes caeruleus*, great tit *Parus major*, pers.obs. Michel Baguette and Luc Legal).

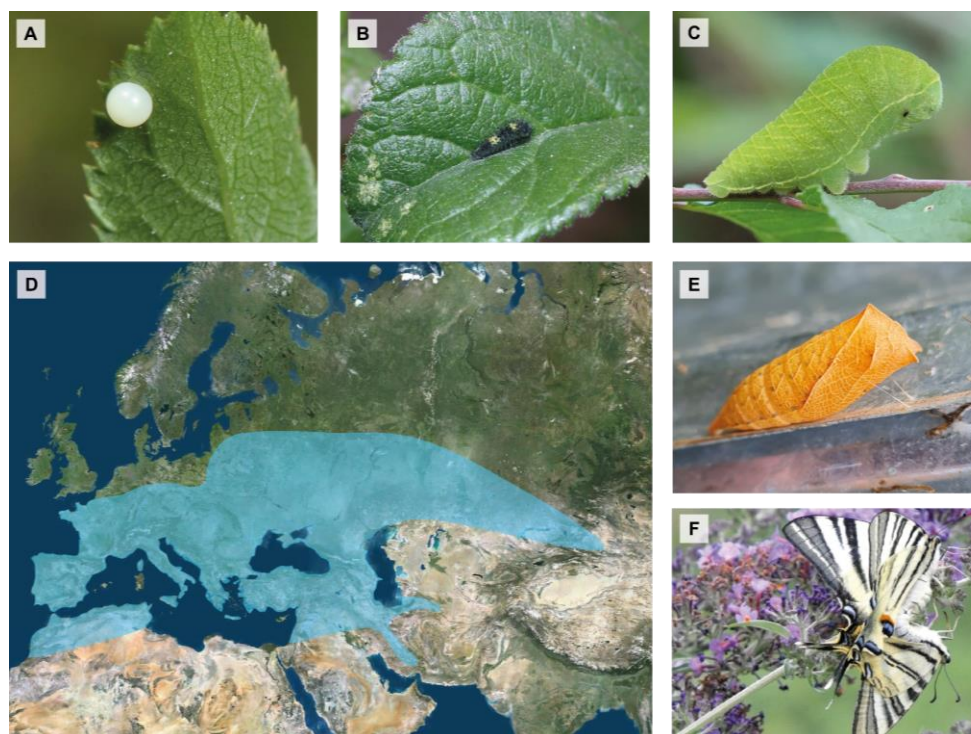


Figure 7: (A) Egg stage. (B) Caterpillar stage n°1. (C) Caterpillar stage n°. (D) Spatial distribution of *I. podalirius*, adapted from Wiemers and Gottsberger 2010. (E) Pupae stage. (F) Mating. Credits photos: (A, B) Philippe Mothiron, (C) Jessica Joachim, (E) Denis Ivanov, (F) Dege.

IV - Main questions and objectives of the thesis

The evolution of wing shape in Papilionidae is likely driven by multiple selective, phylogenetical and developmental influences (Figure 8):

- The serial homology between forewings and hindwings implies tight covariations due to their shared developmental basis. *To what extent does the hindwing shape evolve independently of the forewing shape?*
- Tail has also independently emerged in many Lepidoptera (e.g., Saturniidae and Charaxinae illustrated in Figure 8). *What is the importance of phylogenetic constraints on its evolution in Papilionidae? What was the ancestral state for wing shape in Papilionidae?*
- There are many selective pressures that may influence the evolution of the tail (predation deflection and aerodynamics display in Figure 8). *Are they concomitant? antagonistic?*

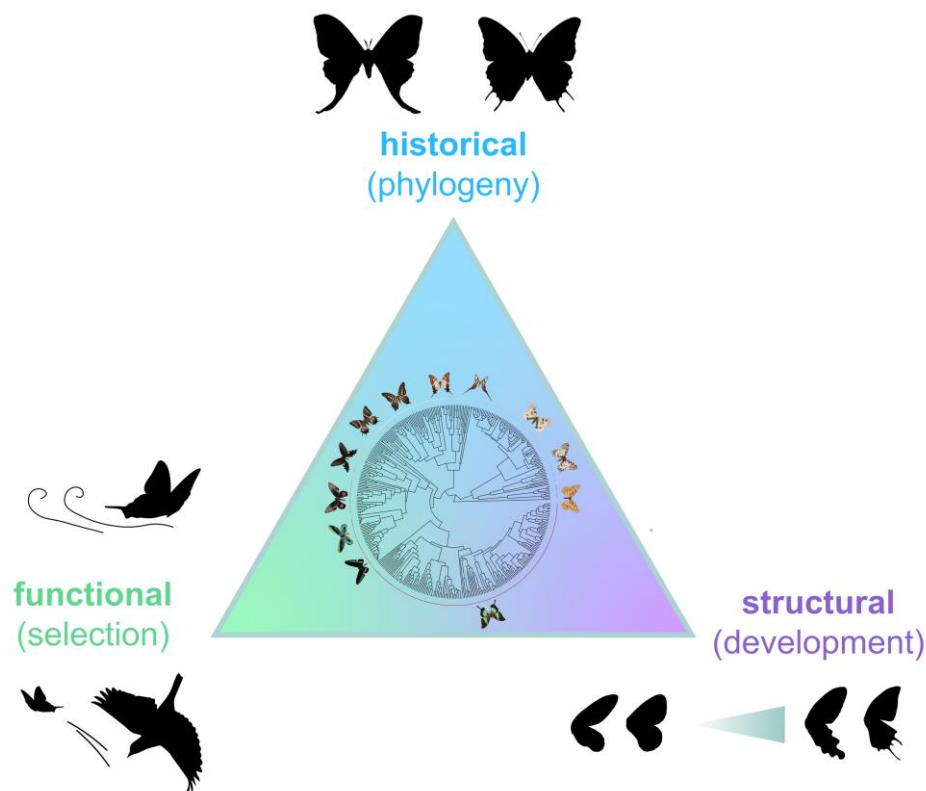


Figure 8: Theoretical scheme of **historical** (phylogenetic constraints), **structural** (developmental constraints due to forewing/hindwing serial homology) and **functional** (multiple selection pressures, here, predation deflection and aerodynamics) influences driving Papilionidae wing shape evolution.

The objective of my thesis was to identify the main evolutionary drivers, using an original combination of macro- and micro-evolutionary approaches.

I first tested two hypotheses of selective factors promoting the evolution of tails by focusing on the swallowtail *Iphiclides podalirius*.

In Chapter I, I conducted an integrative approach including three complementary experiments to test the deflection effect of hindwing tails: (1) The quantification of wing damages within a large wild population of *I. podalirius*. (2) A standardized behavioural assay employing dummy butterflies with real *I. podalirius* wings to study the location of attacks by great tits *Parus major*. (3) The characterization of the mechanical properties of fresh wings of *I. podalirius*.

In Chapter II, I investigated the relative aerodynamical importance of tails in flapping flight, conducting flight analyses of phenotypically altered *I. podalirius*.

Based on these experimental results, I then quantified the variation of Papilionidae wing shape at the macro-evolutionary scale (Chapter III).

I focused on the differential evolution of the shape of the forewings and hindwings, to test for contrasted selection on the fore- and hindwings at a large phylogenetic scale (Figure 9). I thus compared their shape diversity, their evolutionary rates, and the link between diversification and phenotypic disparity. I specifically characterized the evolution of the tail at the family level.

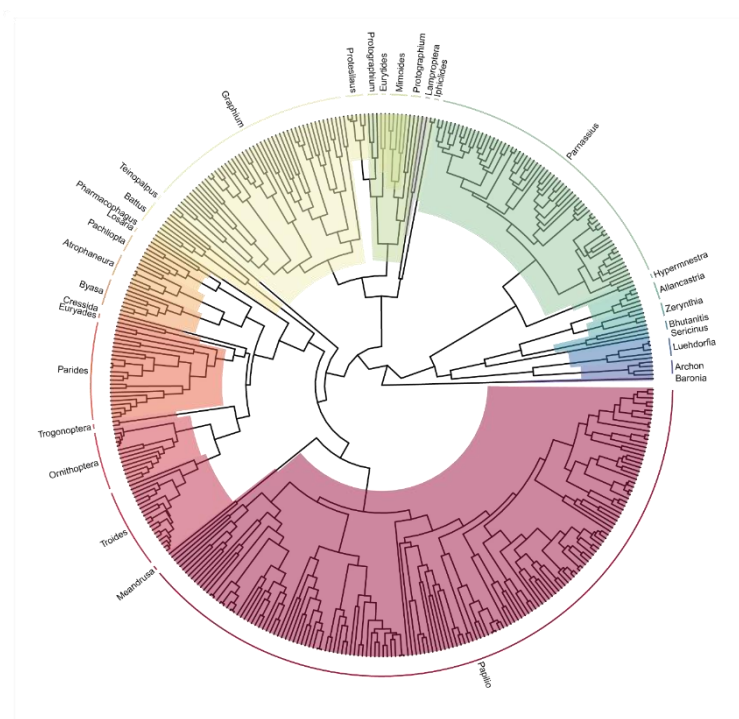


Figure 9: Papilionidae phylogeny from Allio *et al.* 2021, 408 species on 31 genera.

This work implied the complete inventory of the Papilionidae collections of the National Museum of Natural History of Paris, available in Annex I.

Chapter I

Evidence of attack deflection suggests adaptive evolution of wing tails in butterflies

Ariane Chotard¹, Joséphine Ledamoisel¹, Thierry Decamps², Anthony Herrel², Alexis S. Chainé³, Violaine Llaurens¹ and Vincent Debat¹

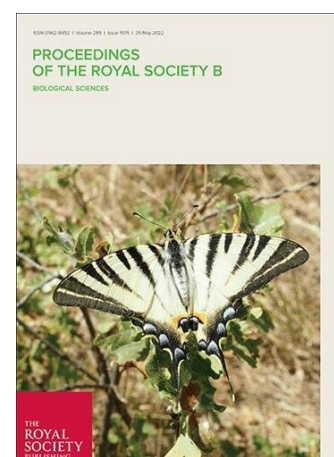
Institutions:

¹Institut de Systématique, Evolution, Biodiversité (ISYEB, UMR 7205), Muséum National d'Histoire Naturelle, CNRS, Sorbonne Université, EPHE, UA, Paris, France

²Unité Mixte de Recherche Mécanismes Adaptatifs et Evolution (MECADEV, UMR 7179), Muséum National d'Histoire Naturelle, CNRS, Paris, France

³Station d'Ecologie Théorique et Expérimentale du CNRS (SETE, UAR 2029), Moulis, France

Published: Chotard A, Ledamoisel J, Decamps T, Herrel A, Chainé AS, Llaurens V, Debat V. 2022. Evidence of attack deflection suggests adaptive evolution of wing tails in butterflies. *Proc R Soc B*. 289(1975):20220562. <https://doi.org/10.1098/rspb.2022.0562>



Abstract: Predation is a powerful selective force shaping many behavioural and morphological traits in prey species. The deflection of predator attacks from vital parts of the prey usually involves the coordinated evolution of prey body shape and colour. Here, we test the deflection effect of hindwing (HW) tails in the swallowtail butterfly *Iphiclides podalirius*. In this species, HWs display long tails associated with a conspicuous colour pattern. By surveying the wings within a wild population of *I. podalirius*, we observed that wing damage was much more frequent on the tails. We then used a standardized behavioural assay employing dummy butterflies with real *I. podalirius* wings to study the location of attacks by great tits *Parus major*. Wing tails and conspicuous coloration of the HWs were struck more often than the rest of the body by birds. Finally, we characterized the mechanical properties of fresh wings and found that the tail vein was more fragile than the others, suggesting facilitated escape ability of butterflies attacked at this location. Our results clearly support the deflective effect of HW tails and suggest that predation is an important selective driver of the evolution of wing tails and colour pattern in butterflies.

Keywords: *attack deflection, Papilionidae, butterfly tails, adaptive evolution, wing damage, mechanical resistance of wings*

Introduction

Predation often affects the evolution of multiple morphological and behavioural traits in prey species. While many traits limiting predator attacks evolve, traits increasing survival after an attack have also been repeatedly promoted by natural selection (Bateman *et al.*, 2014). Traits enhancing attack deflection, by attracting strikes towards a conspicuous body part, indeed limit damage to vital parts and increase escape probability (Ruxton *et al.*, 2004). The conspicuous coloration on the tails of some lizard species has been suggested to promote attacks on the tails, therefore limiting wounds on other parts of the body (Watson *et al.*, 2012; Guidi *et al.*, 2021). The attraction towards conspicuous tails can also be reinforced by striped body coloration, directing the attention of predators towards the tail (Murali and Kodandaramaiah, 2016). In salamanders, defensive posture increases tail conspicuousness (Myette *et al.*, 2019), suggesting that both body shape and colour, as well as behaviour, may contribute to the deflecting effect. The emergence of a deflecting effect may thus result from a joint evolution of several morphological and behavioural traits (reviewed in Arnold, 1984 for lizards). In butterflies, the joint evolution of hindwing (HW) tails and specific behaviour enhancing attack deflection has been shown in Lycaenidae. In these butterflies, the HWs frequently display tiny tails, conspicuous colour patterns and a specific behaviour involving tails movements, hypothesized to mimic a head with moving antennae (the ‘false head effect’, Robbins, 1981; Wourms and Wasserman, 1985). The ‘false-head’ tails of Lycaenidae are likely to deflect attacks away from vital parts (Robbins, 1981). Laboratory experiments with spiders indeed showed that *Calycopis cecrops* butterflies, displaying false-head HWs, escaped more frequently than butterflies from other species where HWs do not display such false-heads (Sourakov, 2013). In museum collections, the prevalence of individuals with symmetrically damaged HWs, interpreted as beak marks of failed predator attacks, has been shown to be higher in Lycaenidae species with wing tails, when compared with species without a tail or with a less conspicuous colour pattern (Novelo Galicia *et al.*, 2019). This suggests that the deflecting effect associated with HW tails might rely on the joint evolution of wing shape, colour pattern and behaviour, promoted by the attack behaviour of predators relying on visual cues. Such a deflecting effect may lead to the loss of the attacked body part, but with limited effect on survival. In lizards and salamanders, tails can be detached without severely impacting survival of the attacked

animal (*i.e.*, autotomy, [Beneski, 1989](#); [Cooper, 1998](#)). In butterflies, wing margins displaying eyespots are preferentially attacked (*e.g.*, in *Bicyclus anynana*, [Chan *et al.*, 2021](#); in *Lopinga achine*, [Olofsson *et al.*, 2010](#); see [Stevens, 2005](#) for a review). The loss of wing margins and especially HW margins has a low impact on butterflies flying abilities ([Le Roy *et al.*, 2019a](#)) and may therefore have a limited impact on survival. Butterflies are indeed commonly observed flying in the wild with such wing damage ([Molleman *et al.*, 2020](#)). The escape from predators after an attack might also be facilitated by enhanced fragility of the attacked parts of the wings. In *Pierella* butterflies, for instance, [Hill and Vaca \(2004\)](#) showed that the conspicuous areas of the HWs are associated with increased fragility, which may facilitate the escape after a predation attempt directed at this specific wing area. Similarly, in small passerine bird species, the feathers located in the zone most prone to the predator attacks are easier to remove [20]. The evolution of specific body parts with increased fragility might thus be promoted by predation pressure, because they enhance prey survival after an attack. The repeated evolution of HW tails in Lepidoptera could result from the selection exerted by predators on the evolution of traits that enhance deflection. The long, twisted wing tails of some Saturniidae moths have indeed been shown to divert bats from attacking moth bodies ([Barber *et al.*, 2015](#)). During flapping flight, the spinning tails indeed confuse the echolocation signal perceived by predators, thus diminishing strike efficiency ([Rubin *et al.*, 2018](#)). The evolution of wing tails in moths is thus likely to be promoted by the sensory system of their nocturnal predators. The deflecting effect of wing tails has also been suggested in day-flying butterflies facing diurnal predators relying on visual cues, but has been tested only in the very specific case of the false-head wing tail of Lycaenidae. In these small-size butterflies, predation is likely to be mostly exerted by invertebrate predators, such as jumping spiders. By contrast, a greater part of predation involves vertebrate predators, and birds in particular, for larger butterflies ([Pinheiro and Cintra, 2017](#)). Bird predation has indeed been suggested to exert significant selection on the evolution of butterfly wing morphology, especially on colour pattern ([Páez *et al.*, 2021](#); [Pinheiro, 2011](#)). Repeated evolution of tails has occurred many times in day-flying Lepidoptera, including some moths, like Uranidae, and all butterfly families, with the countless tailed Papilionidae (swallowtail) species, the double-tailed Charaxinae (Nymphalidae), the tiny tailed Riodinidae and Lycaenidae, and the few Hesperidae and even fewer Pieridae tailed species. Swallowtail butterflies are particularly well known for

their conspicuous, highly diversified HW tails (Owens *et al.*, 2020), but the selection exerted by predators on the repeated evolution of these tails has never been formally investigated. Here, we tested whether the evolution of tails might be promoted by attack deflection, using the swallowtail species *Iphiclides podalirius* (Linné, 1758 Lepidoptera, Papilionidae) as a case study. *Iphiclides podalirius* is a large Palaearctic butterfly with HWs displaying long tails associated with a salient colour pattern: an orange eyespot and four blue lunules with strong UV reflectance (Gaunet *et al.*, 2019). The combination of HW tail and colour pattern is, therefore, very conspicuous (Figure 3), and especially for predators sensitive to UV reflection, such as songbirds (Cuthill *et al.*, 2000). Moreover, the four wings exhibit convergent black stripes over a pale background, contiguous between forewings (FWs) and HWs in resting position, pointing towards the anal edge. This may enhance the attraction of a predator to the posterior part of the HW (Robbins, 1981). To test whether the evolution of wing tails in this species may stem from selection promoting traits enhancing attack deflection, we performed a series of three complementary experiments. First, we characterized the amount and location of damage on the wings of wild butterflies to test whether tails are more frequently lacking in surviving butterflies, possibly indicative of failed predation attempts. Second, we conducted experimental behavioural assays in captivity using an avian generalist predator, the great tit *Parus major*, and dummy butterflies made with real *I. podalirius* wings, in order to investigate the location of attacks. We specifically tested whether attacks are more frequently directed towards the HW tails and associated colour pattern as compared to the rest of the butterfly body. Finally, we used a specific experimental set up to estimate the force needed to tear wings at different locations. Preferentially attacked body parts are predicted to be more easily detached, as it would enhance the probability of escape of the butterfly after an attack (Hill and Vaca, 2004). This combination of experiments under controlled and natural conditions provides a test for the role of predator deflection in the adaptive evolution of wing shape, wing colour pattern and wing resistance in swallowtail butterflies.

Materials & Methods

1) Field sampling

Field sampling of *I. podalirius* was performed in Ariège (France) during the summer of 2020 (collection sites: 43°04'17.86"N, 01° 21'58.88"E; ca. 400m a.s.l., and 43°03'50.94"N, 01° 20'40.95"E; ca. 400m a.s.l.). We sampled a total of 138 wild individuals, with a large majority of males (132 males/six females), likely reflecting the patrolling behaviour displayed by males (hill topping). After their capture, butterflies were euthanized by hypothermia and their wings stretched out and dried.

2) Assessing the distribution of wing damage in the wild

The dorsal side of the FWs and HWs of the field-sampled individuals was photographed in controlled LED light conditions (Nikon D90, Camera lens: AF-S Micro Nikkor 60 mm 1 : 2.8G ED). Out of the 138 wild butterflies collected, 65 exhibited wing damage. We studied the location of missing wing areas, distinguishing damage occurring on HW and FW, and reported

the asymmetry of different types of damage (left and right damage with visually similar areas and positions were considered symmetric). A Pearson's χ^2 -test with Yates' continuity correction was used to test whether (1) damage was more often observed on HWs than on FWs, and (2) damage on HWs was more often asymmetric than damage on FWs. To finely quantify the distribution of missing wing areas, we then digitized the wing outlines of the 65 damaged butterflies and 10 intact individuals as references. We defined 300 semi-landmarks equally spaced along the outline of both the left- and right-reflected FWs and HWs, using *TpsDig2* (Rohlf, 2015). The average shape of intact butterflies was obtained with *TpsRelw*, (Rohlf, 2015), using a geometric morphometric approach (Adams *et al.*, 2004; Bookstein, 1997). The wing outline of each damaged individual was then manually superimposed on the average shape of intact butterflies, in order to characterize the missing area of each damaged wing. A heat map was then obtained by summing up the occurrences of missing areas at each pixel throughout the sample of damaged individuals, using *EImage* R package (Pau *et al.*, 2010), following (Le Roy *et al.*, 2019a). The heat map was then plotted with *autoimage* R package (French, 2017).

3) Behavioural experiment with birds

We conducted an experiment to determine the location of attacks by birds on *I. podalirius* wings between October 2020 and January 2021 at the Station d'Ecologie Théorique et Expérimentale du CNRS, France (near the collection sites). Great tits were caught in mist-nets in the vicinity of the research station, ringed, and housed in individual indoor/outdoor cages ($5 \times 1 \times 3$ m) and fed ad libitum with mealworms and sunflower seeds. After 2 days of habituation to captivity, we conducted behavioural experiments on 2 consecutive days during the 3 h after sunrise while birds did not have access to sources of food other than dummy butterflies. The whole experiment was repeated three times using new birds for a total of 72 different birds tested. Capture of wild birds was performed under permits from the French ringing office (CRBPO, permit no. 13619 to A.S.C.). Capture and holding of birds from the wild was approved by the Région Midi-Pyrénées (DIREN, no. 2019-s-09) in the Moulis experimental aviaries (Préfecture de l'Ariège, institutional permit no. SA-12-MC-054; Préfecture de l'Ariège, Certificat de Capacité, no. 09-321 to A.S.C.). We built 95 dummy butterflies, using actual wings of *I. podalirius* butterflies collected in the wild, glued on an artificial black cardboard body. The position of the glued wings corresponded to the natural position of butterflies at rest (Figure 1). A dummy was placed in each bird cage, about 1.5 m off the ground, using a wire fixed to the cage wall. This setting thus allowed the dummy to gently 'flutter' in the middle of the cage,

far enough from any perching site, to prevent close inspection by resting birds. The birds thus had to approach and potentially strike dummy butterflies while flying. Each cage was equipped with a camera filming continuously (Figure 1; electronic supplementary material, Figure S2). Two observers also monitored the 24 experimental cages: damaged dummies were replaced as soon as noted by the observers, to maximize the number of attacks on intact butterflies. After each experimental session, the birds were fed ad libitum until nightfall to minimize the stress generated by the experiment. The whole experiment was repeated for 2 consecutive days.

Analyses of videos recorded during the experiments were used to count the exact number of strikes performed by each bird on each dummy butterfly. Each strike was defined as a single touch of the beak on the dummy butterfly. The films were also used to assess the precise location of each strike on the butterfly body. Five categories of strike location

were defined: body, coastal part of the FW, distal part of the FW, HW colour pattern and HW tail (Figure 1). In some cases, the strike affected several locations at once. These ‘combined’ locations were considered as separate categories, leading to a total of eight possible targeted locations (Figure 3). Because a dummy could be attacked several times before it was replaced, we also recorded the order of each strike performed by the tested bird on the given dummy.

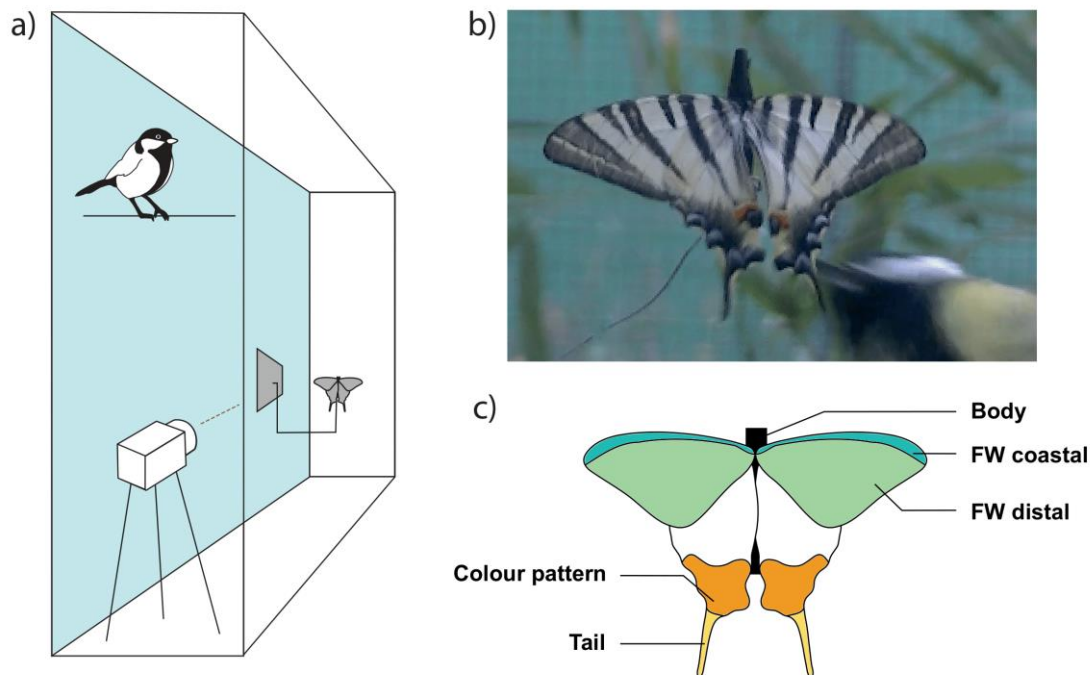


Figure 1: Experimental set-up for behavioural assay with wild-caught great tits. (a) Each experimental cage ($5 \times 1 \times 3$ m) was equipped with a video camera filming continuously. A butterfly dummy was fixed to the wall at about 1.5 m off the ground using a wire far enough from any perching site to prevent close inspection by the birds not in flight. (b) Picture of a butterfly dummy struck by a bird. (c) Schematic of a dummy butterfly composed of four real wings glued on an artificial black cardboard body. Five locations could be targeted by birds: body, FW coastal, FW distal, colour pattern and tail. Photograph of the set-up is given in electronic supplementary material, S2.

We first tested whether strikes occurred more often on the HWs than on the FWs, using a Pearson χ^2 -test with Yates' continuity correction. To test whether the different parts of the wings were equally prone to attack, we applied a generalized binomial regression model for the probability of attack, using strike location and strike rank order as effects and considering all specimens and sessions (including birds that did not attack). An analysis of variance was then applied (ANOVA type II, *Anova* function in the R package *car*, Fox *et al.*, 2021). To allow pairwise comparisons on the location categories, we

conducted a series of post hoc tests (*tukey_hsd* function in the R package *rstatix*, Kassambara, 2021).

4) Mechanical resistance of the wings

Experimental sample

We tested mechanical resistance of the different wing parts on 28 fresh *I. podalirius* butterflies (21 females and seven males) obtained as pupae from a commercial supplier (Worldwide Butterflies Ltd). After emergence, individuals were placed in individual cages to allow proper unfolding and drying of the wings, then placed in entomological envelopes to avoid wing damage. The butterflies were fed once a day with a mixture of water and honey, and maintained for 11 to 20 days depending on the time between emergence and the start of the experiments. Experiments were performed on freshly killed individuals to limit the effect of wing drying on mechanical properties post-mortem (Landowski *et al.*, 2020). In order to test whether the tails are more fragile, we compared the mechanical resistance of different regions of the wings (Figure 2). Specifically, we contrasted the vein located within the HW tail (M3H vein), with another HW vein located outside the colour pattern area (R5H vein). We also included the two developmentally homologous veins on the forewing (M3F and R5F, Racheli and Pariset, 1992). For each butterfly, the experiment was conducted on one HW and one FW. The four veins were measured in a randomized order to avoid any bias caused by the deformation of the wings due to previous tearing.

Experimental set-up

As wing parts involved in predator deflection are expected to be particularly fragile, we designed a custom experimental set-up adapted from Hill and Vaca (2004) and Devries (2002) to specifically estimate the mechanical resistance of different parts of the wings. When a bird catches the wing of a butterfly, the force exerted by the beak and the opposed escape movement of the butterfly likely induce tensile stresses on the wing. We thus compared the mechanical response of the different wing veins to a tensile force exerted in the direction of the vein, away from the body (Figure 2). Our set up was composed of a fixed part holding the wing and of a mobile part exerting traction on the wing (Figure 2; electronic supplementary material, figure S3). This mobile part was connected to the wing using a flattened and filed alligator clip with a squared 9 mm² piece of rubber

ensuring a soft and standardized contact with the wing. For each measurement, the clip was fixed at 3 mm from the edge of the wing. This clip was then connected to a piezo-electric force transducer (Kistler 9217A type 9207 serial no. 1275844), connected to a charge amplifier (Kistler type 5011). The force transducer was fixed on a linear table controlled by a motor (RS PRO, 12 V dc, 2400 g/cm), allowing constant traction. The charge from the force transducer was measured by the amplifier and sent to a Biopac AD unit. Forces were captured and analysed using Acq-Knowledge software (v. 4.1, BIOPAC Systems, Inc.). The variation of the force through time, from the onset of the motor to the total rupture of the wing was recorded for each trial. These response curves were first smoothed using a low-pass filter set at 20 Hz. Five summary variables were extracted from the response curve (Figure 2): (1) the maximum force exerted on the vein (estimating the maximum strength of the vein, noted F_{max}), (2) the time to the first break (T_1 ; shown by the first abrupt decrease in force), (3) the time to the complete rupture of the vein (T_{max} ; when the force returns to zero), (4) the slope (S) of the curve between the beginning of the pull and the point of maximum force (estimating the stiffness of the wing, see electronic supplementary material, S1) and (5) the impulse required for the complete rupture of the vein (J_{max}), assessed by the area under the curve. The forces were measured in Newtons (N) - note the force takes negative values since we measured a tensile force.

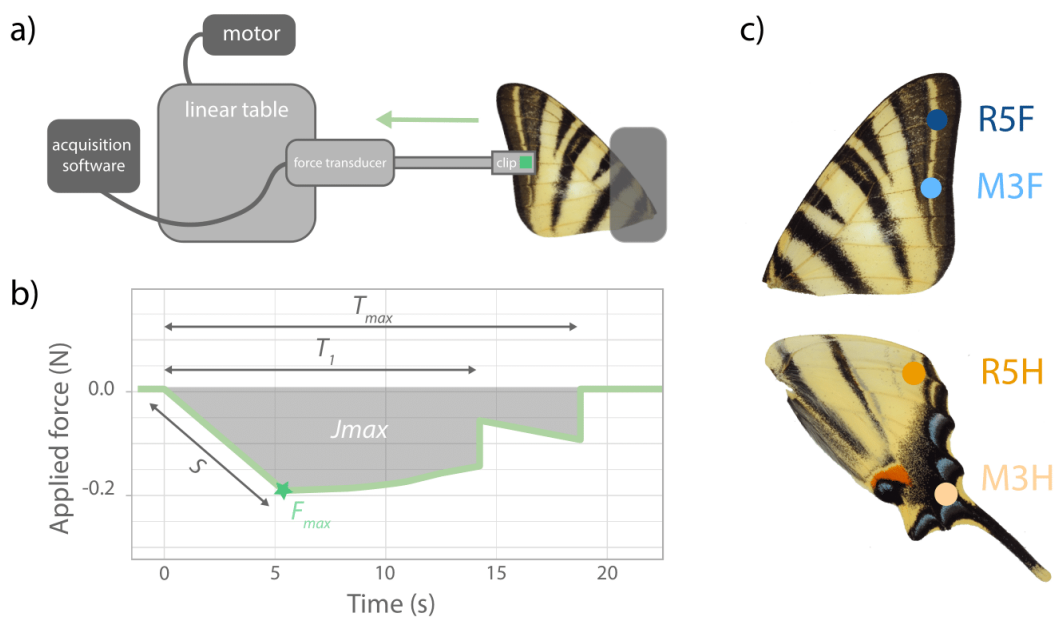


Figure 2: Experimental set-up designed to estimate the strength needed to break wings at different locations. (a) A custom set-up was built, composed of a mobile part (clip + force transducer + linear table) exerting traction on the

wing and a fixed part, holding the wing. (b) Summary variables derived from force profile: F_{\max} (the maximum force exerted on the vein), T_1 (the time to the first break), T_{\max} (the time to the complete rupture of the vein), S the slope of the curve (estimating the stiffness of the wing) and the area under the curve J_{\max} (indicating the impulse). (c) Locations of the four measured points with attachment on a vein at 3 mm from the edge of the wings. Hindwing tail resistance is measured at the point M3H. Photograph of the set-up is given in electronic supplementary material, S3.

The five mechanical parameters measured on the different veins were then compared using linear mixed models using wing (FW versus HW) and vein (M3 versus R5) as fixed effects, while butterfly ID, sex and the date of measurement session were set as random variables (*lmer* function in the R package *lmerTest*, [Kuznetsova et al., 2017](#)). The date of measurement session was added to account for potential differences in temperature and humidity across sessions possibly affecting the mechanical properties of the wing. For J_{\max} , there was some evidence that the wing and vein effects interacted. We thus modified the model to directly account for the four modalities of the vein effect (R5F, M3F, R5H and M3H). We analysed all models with a type III analysis of variance. All statistical analyses were carried out in R v. 4.0.3 ([R Core Team, 2018](#)).

Results

1) Natural wing damage mostly affects the tails

We hypothesized that a deflection effect should result in a higher proportion of wing damage on the deflecting wing areas in the wild. To test this hypothesis, we studied the location of wing damage in a natural population of *I. podalirius*. Among all wild individuals collected, 47.1% had wing damage. FWs were less often damaged than HWs (22.31% and 85.38%, respectively; $\chi^2 = 101.54$, $d.f. = 1$, $P < 0.001$). The frequency of individuals with missing HW tails in the wild was especially high: all 65 damaged individuals had at least one tail damaged (out of 130 wings tested, 82.3% had tail damaged). This result is illustrated by the heat map (Figure 5). Furthermore, damage on the HWs were more often asymmetrical (78.46%) than damage on the FWs (24.62%, $\chi^2 = 35.603$, $d.f. = 1$, $P < 0.001$).

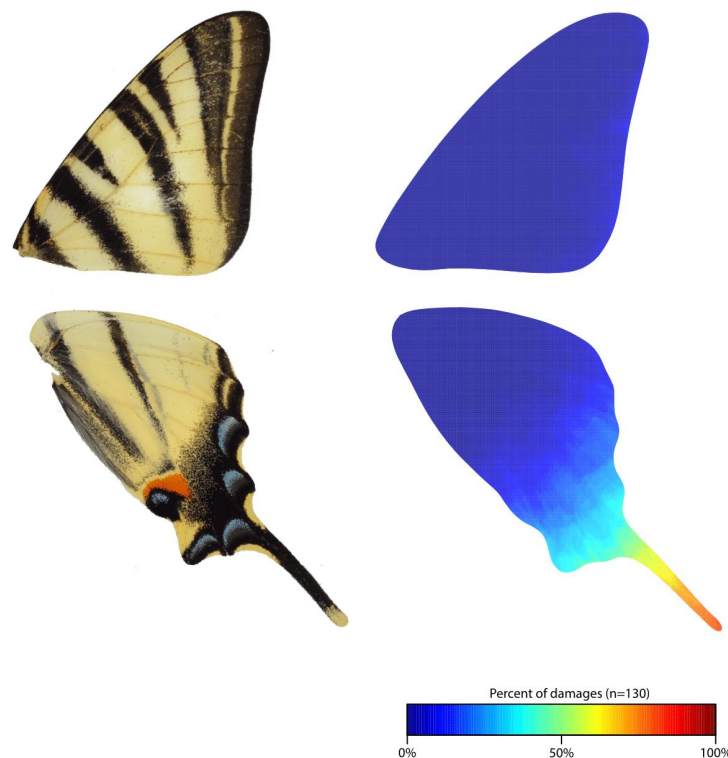


Figure 5: Heat map describing the spatial distribution of wing damage on a sample of wild *I. podalirius*. Left: photograph of *I. podalirius* wings. Right: proportion of naturally damaged wing locations. Data for left and right wings were pooled for each pair of wings (65 individuals, so 130 forewings and 130 hindwings). The most frequently damaged areas are shown in red, while intact areas are shown in blue (see colour scale).

2) Behavioural experiments with birds reveal preferential attacks on hindwing tail and colour pattern

Using the behavioural assays carried out with great tits, we investigated whether the attacks on dummy butterflies were directed towards the posterior part of the HWs (Figure 3), as expected under the hypothesis of a deflecting effect induced by the butterfly morphology. Among the 72 birds tested, only 17 attacked the dummy butterflies, resulting in 65 recorded strikes. Because some strikes occurred outside of the field of view of the camera, the targeted part of the dummy could be determined in only 59 of these strikes. The HWs were more often targeted by the birds (43 strikes; 72.9%) than the FWs (16 strikes; 27.1%) ($\chi^2 = 12.36$, $d.f. = 1$, $P < 0.001$). The probability of attack strongly depended on the wing location (LR $\chi^2 = 141.21$, $d.f. = 8$, $P < 0.001$): there was strong evidence that strikes jointly targeting the tail and the colour pattern of the HWs (23 attacks; 39%) were more frequent than strikes on any other body part (see detailed statistical tests in Table 1). By contrast, no evidence for an effect of the attack ranking on attack probability was found (see detailed statistical tests in electronic supplementary material, table S1).

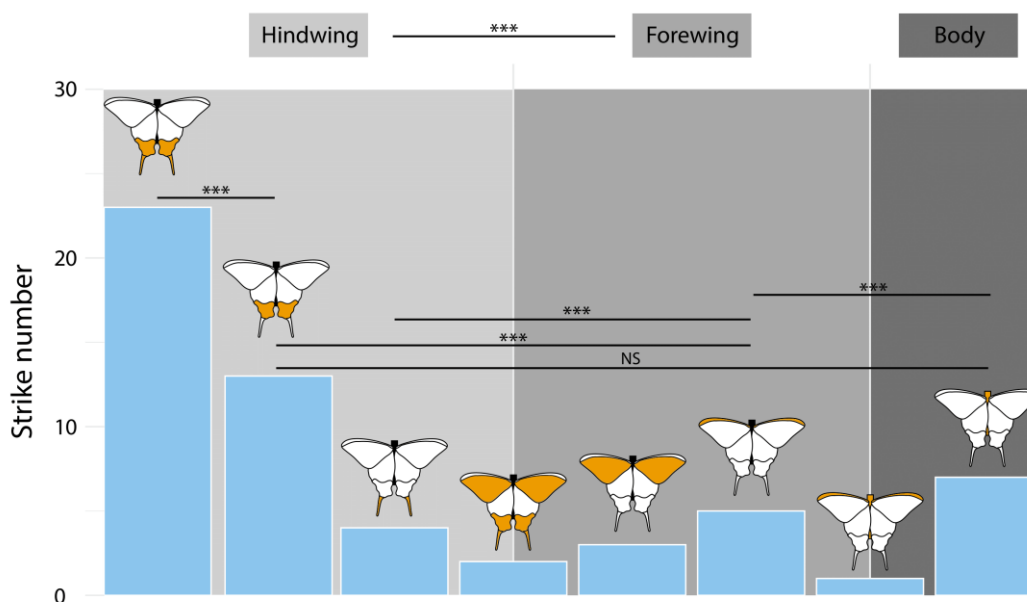


Figure 3: Locations of bird strikes on the dummy butterflies, recorded during six experimental sessions on 72 captured *Parus major* using butterfly dummies built with real wings of *I. podalirius*. A total of 59 strikes were recorded. Each category is defined by the location targeted by a bird in a single strike and represented in orange on each associated butterfly scheme. Only essential statistical comparisons are represented; see details in table 1. Video in electronic supplementary material, movies S1–S2.

Table 1 Post hoc comparisons of bird strike numbers on the dummy butterflies between attack locations. Eight categories of location were defined: body, FW coastal, FW distal, colour pattern, tail, FW coastal + body, tail + colour pattern and tail + colour pattern + FW distal.

Locations	Parameters	Body	Colour pattern	FW distal	FW coastal	FW coastal + Body	Tail	Tail + Colour pattern	Tail + Colour pattern + FW distal
Body	estimate								
	<i>P</i>								
Colour pattern	estimate	-1.110							
	<i>P</i>	0.684							
FW distal	estimate	5.218	6.328						
	<i>P</i>	< 0.001	< 0.001						
FW coastal	estimate	6.328	7.438	1.110					
	<i>P</i>	< 0.001	< 0.001	0.965					
FW coastal + Body	estimate	-1.665	-0.555	-6.883	-7.994				
	<i>P</i>	0.960	1.000	< 0.001	< 0.001				
Tail	estimate	2.109	3.220	-3.109	-4.219	3.775			
	<i>P</i>	0.213	< 0.001	0.057	< 0.001	0.210			
Tail + Colour pattern	estimate	3.109	4.219	-2.109	-3.220	4.774	0.999		
	<i>P</i>	< 0.001	< 0.001	0.190	< 0.001	0.014	0.897		
Tail + Colour pattern + FW distal	estimate	2.109	3.220	-3.109	-4.219	3.775	0	-0.999	
	<i>P</i>	0.548	0.040	0.200	< 0.001	0.324	1	0.983	
Intact	estimate	-1.000	-1.000	-1.000	-1.000	-1.000	1	1	1
	<i>P</i>	< 0.001	< 0.001	< 0.001	< 0.001	< 0.001	< 0.001	< 0.001	< 0.001

3) Hindwings and in particular hindwing tails are more easily damaged

We then tested whether the HW region with the tail and conspicuous colour pattern is more fragile than the rest of both wings, as expected if they are involved in a deflecting effect. There was a strong evidence that time to first rupture (T_1) and the time to total rupture (T_{max}) were lower in HWs veins than FW veins (Figure 4, see statistical tests in Table 2). J_{max} , the impulse required to fully rupture the vein (as assessed by the area under the response curve; Figure 2) was smaller for the HW tail vein (M3H) than for any other veins (M5H: $t = -2.42$; $p = 0.019$; M3F; $t = -2.48$; $p = 0.016$; M5F: $t = -1.88$, $p = 0.06$). The slope of the force profile, S , reflects the stiffness of the wing: the greater the slope, the stiffer the veins (equations in electronic supplementary material, S1). There was strong evidence that HW veins had higher force profile slopes than FW veins (Figure 4, details in Table 2), indicating that they are stiffer. Finally, a weak evidence for a lower F_{max} (maximum force applied to the vein) in the HWs than in the FWs was found ($F = 3.11$; $p = 0.082$, Table 2).

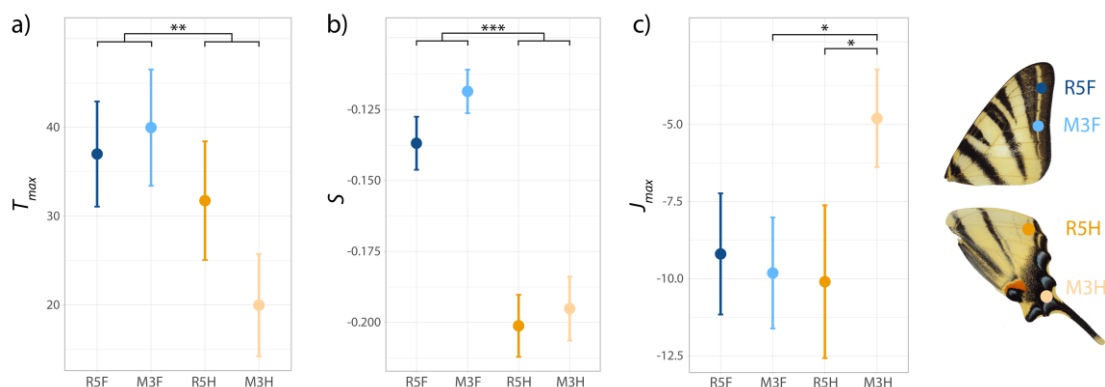


Figure 4: Variation in mechanical resistance in different areas of the forewings and hindwings of fresh *I. podalirius* samples ($n = 28$). On each of the 28 butterflies, four locations were studied, corresponding to four different veins (R5F, M3F, R5H and M3H). Means and standard errors are indicated as well as significant differences between locations. Three mechanical variables per wing location are reported (a) T_{max} (the time to the complete rupture of the vein). (b) S , the slope of the curve (estimating the stiffness of the wing) and (c) J_{max} , the area under the curve (a measure of impulse).

Table 2: Summary of the linear mixed-effects models describing the effect of wing (forewing/hindwing) and vein (M3/R5) on the five mechanical parameters measured during the mechanical resistance experiment in different areas of the forewings and hindwings of fresh *I. podalirius* samples ($n = 28$): F_{max} (the maximum force exerted on the vein), T_1 (the time to the first break), T_{max} (the time to the complete rupture of the vein), S (estimating the stiffness of the wing) and J_{max} (the impulse required for the complete rupture of the vein). These five models were analysed with a type III analysis of variance.

	Wing			Vein			Wing:Vein		
	<i>df</i>	<i>F-value</i>	<i>p-value</i>	<i>df</i>	<i>F-value</i>	<i>p-value</i>	<i>df</i>	<i>F-value</i>	<i>p-value</i>
F_{max}	75.8500	3.1006	0.0823	75.6680	0.0180	0.8937	75.791	1.3071	0.2565
T_1	44.4160	17.7794	< 0.001 ***	44.1520	0.8624	0.3581	44.793	2.7123	0.1066
T_{max}	67.7270	7.9865	0.0062 **	64.3680	1.1973	0.2779	63.458	2.1050	0.1517
S	69.0870	60.4044	< 0.001 ***	68.9320	1.3691	0.2460	70.49	0.3050	0.5825
E_{max}	64.036	1.8635	0.1770	58.537	2.0436	0.1582	57.844	4.1549	0.04609 *

Discussion

Our multi-pronged approach combining behavioural experiments, biomechanical measurements and survey in natural population provides strong evidence of a deflecting effect of HW tails in *I. podalirius*, opening new research avenues on the predation pressures involved in the evolution of tails in butterflies.

1) Adaptive evolution of hindwing tails promoted by predator behaviour

Our behavioural trials showed that attacks by great tits on *I. podalirius* are highly biased towards the HW tails and colour pattern. This provides strong support for a deflective effect generated by both colour pattern and tail on predators. Only a small fraction of the tested birds actually attacked the dummies. This could suggest that *I. podalirius* butterflies are not the usual prey consumed by great tits (Naef-Daenzer *et al.*, 2000), especially during the season when the tests were carried out (late autumn and winter), where they mostly rely on seeds rather than on insects. Our behavioural experiments are thus relevant for the behaviour of generalist predators that are probably naive to the phenotypes of the tested butterflies, a likely situation in nature, as no specialist predator is known for *I. podalirius*. Some of the birds nevertheless repeatedly attacked the posterior area of the HWs, consecutively targeting the two tails, showing a particularly strong interest for this location (see electronic supplementary material, movie S1). Birds typically flew above the butterflies, patrolling the cage at 3 m high and dummies had their tails oriented towards the ground, at about 1.5 m high. The high frequency of attacks on the tails therefore did not result from an easier access to the tails due to a positional bias. To the contrary, birds adjusted their trajectory to attack from below (see electronic supplementary material, S4; movie S2), suggesting they were specifically targeting the tails. The combination of tails and associated conspicuous colour pattern is thus probably very attractive to predators, inducing the observed pattern of attack locations. Given the tested birds preferentially attacked the distal area of the HW, we would expect that this wing area should be easier to tear off. Such enhanced fragility would facilitate butterfly escape and may thus be promoted by natural selection generated by the behaviour of birds. Our analysis of the mechanical resistance of wing veins indeed shows that HW veins, and especially the vein located within the tail, are less resistant to the application of a tensile force and break sooner than FW veins. Whether the measured difference in strength

would have a significant impact during a predator attack is unknown but the forces tested are relevant to the type of strikes observed in our behavioural experiment. The enhanced fragility of the HW vein located within the tail is thus consistent with the deflection hypothesis. It should increase escape probability, while preserving the integrity of the wing and reducing aerodynamic costs. Interestingly, in *Pierella* butterflies, the conspicuous white patch of the HW, found by Hill and Vaca (2004) to have increased fragility, contains the M3H vein, *i.e.*, the vein located within the tail in *I. podalirius*, that was found to be the stiffest and the earliest to break in our study. The M3H vein could have enhanced fragility in many butterfly species, therefore promoting the evolution of conspicuousness in these wing areas, enhancing survival after an attack. The evolution of such an association should especially be favoured if butterflies missing this wing area still survive in the wild. The large abundance of tailless *I. podalirius* flying in the wild indeed testifies to the limited aerodynamic consequences of such damage. Tail loss does not prevent these damaged butterflies from performing their typical hill-topping behaviour and is thus likely to have a limited impact on their fitness. The distribution of damage across the wings in the natural population of *I. podalirius* also confirms that HW tails are more prone to attack than any other part of the wing (Figure 5). Inferring predation from butterfly wing damage alone can be misleading because damage can stem from a diversity of sources, including interactions with conspecifics (Alcock, 1996; Carvalho *et al.*, 2016) or collision with obstacles (Foster and Cartar, 2011; Le Roy *et al.*, 2019a). However, the pattern we found is still consistent with an increased attack rate on HW tails. While damage due to collisions should be symmetrical as seen on FWs, the prevalence of asymmetric damage on the tails of *I. podalirius* matches the hypothesis of predator attacks during flight or when butterflies are at rest, typically perching on high branches with their wings wide open (Figure 1). This also suggests that symmetry in the tail is not critical for aerodynamics. Our survey in a natural population thus reinforces the evidence for the adaptive evolution of tail and colour pattern in *I. podalirius*, where the benefits in terms of escape ability may exceed the costs of wing damage. Considered together, (1) the strong prevalence of the attacks on the HW tails and associated colour pattern, (2) the reduced strength or the corresponding parts of the wings and (3) the very high incidence of natural wing damage on the tails, provide evidence for the adaptive evolution of HWs tails in *I. podalirius* via a deflecting effect of predator attacks. The effect of attack deflection on the evolution of wing tails in day-flying butterflies has only been

demonstrated in the peculiar case of false head morphology in Lycaenidae (Robbins, 1981; Wourms and Wasserman, 1985). Our study suggests that predation can be a major selective pressure involved in the evolution of HW tails in butterflies. HW tails have evolved multiple independent times throughout the diversification of butterflies and are associated with an important diversity of colour patterns (McKenna *et al.*, 2020). Their size and shape are highly variable across species, ranging from slightly scalloped margins to long tails. Poorly developed tails might be sufficient to induce attack deflection: for example, a high rate of attack (as assessed by the frequency of wing damage) was reported on the barely prominent, but colourful, hindtips of the Burmese jungle queen butterfly (Tonner *et al.*, 1993). This underlines the importance of the joint effect of wing shape and colour and suggests that the predator's behaviour can promote the gradual evolution of HW tails. Altogether, our results point to the combined evolution of different traits involved in predator deflection, namely HWshape, fragility and colour patterns, as well as behaviour, jointly forming an adaptive syndrome.

2) Adaptive syndrome of predation deflection

In our experiments with birds, tails alone were targeted in a large proportion of the trials, but most attacks involved a combination of the tails and associated colour pattern. This strongly suggests that the visual effect triggering attack deflection in *I. podalirius* is jointly induced by the tails and the colour pattern, including the blue marks and the orange eyespots on the HW, and possibly the black stripes pointing at the tails. The deflection effect therefore probably relies on the evolution of a series of traits, including wing shape, wing colour pattern and wing mechanical resistance. The joint versus sequential nature of the evolution of these different traits is largely unknown and might depend on the developmental and genetic bases of the traits involved in deflective syndromes, as well as the different selection pressures acting on each of those traits. Associations between HW tails and peculiar colour patterns promoted by predation pressure have been described for butterfly species involved in Batesian mimicry. In *Papilio memnon*, for instance, some females display HW tails and red coloration resembling the toxic species *Pachliopta coon* on the Malay peninsula while other females have no tail and an alternative yellow colour pattern mimicking *Troides helena* in Northern Borneo (Clarke *et al.*, 1968). These two traits are controlled by different loci and the linkage disequilibrium between these loci might have been promoted by the selective advantages

brought by mimicry (Llaurens *et al.*, 2017). Nevertheless, the association between well-developed tails and conspicuous colour elements is not universal in Papilionidae: for example, *Papilio ulysses* tails and surrounding wing parts are completely black, while in *Papilio demodocus*, conspicuous distal eyespots are observed in tailless HWs. Shared developmental pathways in wing shape and colour pattern might promote their joint evolution, so that the emergence of deflective syndromes can be facilitated in some lineages. Alternatively, species ecology might trigger strong selection promoting linkage disequilibrium between loci controlling traits enhancing deflection. The combined evolution of traits limiting predation also frequently extends to behaviour. Whether the behaviour emerges before or after the evolution of morphological traits involved in deflection is an open question. In *I. podalirius*, the perching position with wings wide open possibly enhances the deflecting effect provided by HW tails but might have been promoted for its effect on thermoregulation (Rawlins, 1980) before the evolution of tails. Adaptive syndromes involving the evolution of both morphological and behavioural traits promoted by predator behaviour have been observed in other Lepidoptera. In some species, hidden conspicuous coloration can be suddenly uncovered when threatened by a predator, inducing a startling effect (*e.g.*, in *Catocala nupta*, Kim *et al.*, 2020) or attracting predator attention to specific eyespot locations (*e.g.*, in *Archeoprepona chromus*, Sourakov, 2015). The evolutionary sequence of these behavioural and morphological traits has been investigated experimentally by testing the deterring effect of both traits independently. These experiments suggest that behavioural changes might have preceded the evolution of conspicuous coloration, because sudden movements can be sufficient to induce strong deterrence (Holmes *et al.*, 2018). Whether a similar ‘behaviour first’ evolutionary sequence is involved in the evolution of deflective syndromes should be investigated. Important selective trade-offs between predator deflection and flight abilities might also influence the evolution of deflective syndromes in Lepidoptera, therefore constraining wing areas involved in such syndromes. Anteromotorism being a shared characteristic of butterflies (Dudley, 2002), HW fragility might be ancestral, and conspicuous marks might have secondarily been favoured on these weaker wings. In Papilionidae, HW shape is indeed strikingly more diversified than FW shape (Owens *et al.*, 2020) in agreement with lower aerodynamic constraints on the HWs. The study of aerodynamic forces applied to an artificial model of a butterfly with tails suggests that HW tails increase the lift of the butterfly during gliding (Park *et al.*, 2010). Preservation

of flight capacity through the maintenance of tail integrity, and in particular a sufficient strength to withstand the pressure forces applied during flapping, could act as an evolutionary tradeoff with the selection of mechanical weakness. The selective pressures acting on each of the traits involved in these deflective syndromes should now be studied independently and compared in species with contrasted ecologies and levels of phylogenetic proximity to determine the evolutionary forces involved in the emergence of deflective syndromes.

Conclusion

The diversity of wing tails observed in Lepidoptera suggests they have evolved multiple times, therefore raising the question of the selective pressures involved. Based on our combined analysis of natural wing damage, biomechanical resistance of the wings and behavioural interactions with bird in the species *I. podalirius*, we provide direct evidence for an effect of natural selection exerted by predators on HW tail evolution, promoting traits enhancing attack deflection away from the vital body parts. Our study therefore opens up new research avenues on the relative effect of predation pressure versus other selective forces involved in the evolution of HW tails in butterflies. We also highlight that such a deflective effect may have emerged from a sequential evolution of a suite of traits, including wing shape, wing colour patterns and wing mechanical properties. These questions should stimulate new research on the developmental and selective origin of the traits involved in deflective syndromes in various butterfly species.

Ethics. Capture of wild birds was performed under permits from the French ringing office (CRBPO, permit no. 13619 to A.S.C.). Capture and holding of birds from the wild was approved by the Région Midi-Pyrénées (DIREN, no. 2019-s-09) in the Moulis experimental aviaries (Préfecture de l'Ariège, institutional permit no. SA-12-MC- 054; Préfecture de l'Ariège, Certificat de Capacité, no. 09-321 to A.S.C.).

Data accessibility. The dataset is available at the Dryad Digital Repository: <https://doi.org/10.5061/dryad.jm63xsjd6>. The data are provided in the electronic supplementary material: <https://doi.org/10.6084/m9.figshare.c.5965921>.

Authors' contributions. A.C.: conceptualization, data curation, formal analysis, funding acquisition, investigation, methodology, project administration, resources, visualization, writing—original draft, writing—review and editing; J.L.: data curation, formal analysis, investigation; T.D.: methodology, resources, software; A.H.: methodology, resources, writing—review and editing; A.S.C.: funding acquisition, methodology, project administration, resources, writing—review and editing; V.L.: methodology, supervision, writing—review and editing; V.D.: conceptualization, funding acquisition, investigation, methodology, project administration, supervision, writing—review and editing. All authors gave final approval for publication and agreed to be held accountable for the work performed therein.

Conflict of interest declaration. We declare we have no competing interests.

Funding. Aviary work was supported by ANR-SoCo to A.S.C. and the Laboratoire d'Excellence (LABEX) entitled TULIP (ANR-10- LABX-41).

Acknowledgements. We would like to thank Michel Baguette for his advice on sampling sites for *Iphiclides podalirius*, Camille Le Roy for his protocol on the analysis of wing damage, Thomas Crouchet for his assistance during the behavioural assay, Fabienne Tékéoglou for her last-minute help saving the November experiment, Ramiro Godoy-Diana and Roméo Antier for their advice on biomechanics and material deformation.

Supplementary

Supplementary 1: Physical characterisation of the tensile strength of the wing (Basset *et al.*, 2007)

The behaviour of a material in a tensile test is given by Hooke's law:

$$\sigma = E \cdot \varepsilon \quad [1]$$

With: E the Young's modulus of the material (an intrinsic modulus of elasticity of the material)

σ the stress applied to the sample (N/mm²)

ε the resulting strain of the specimen

The stress and strain of the sample are given by the following equations

$$\sigma = \frac{F}{S} \quad [2] \qquad \varepsilon = \frac{L - L_0}{L_0} \quad [3]$$

With: F the force applied to the sample (N)

S the area of the sample normal to the force (mm²)

L_0 the initial length of the sample before traction (mm)

L the length of the sample after traction (mm)

Thus, according to the equation [1] the behaviour of a material in a tensile test can be characterised by the following equation:

$$F = E \cdot S \cdot \frac{L - L_0}{L_0} \quad [4]$$

Knowing that our results represent the force exerted on a vein as a function of time, and that the elapsed time is proportional to the deformation of the material (because the tensile force is applied to the wing in a constant manner), then the slope measured for each curve profile is equivalent to:

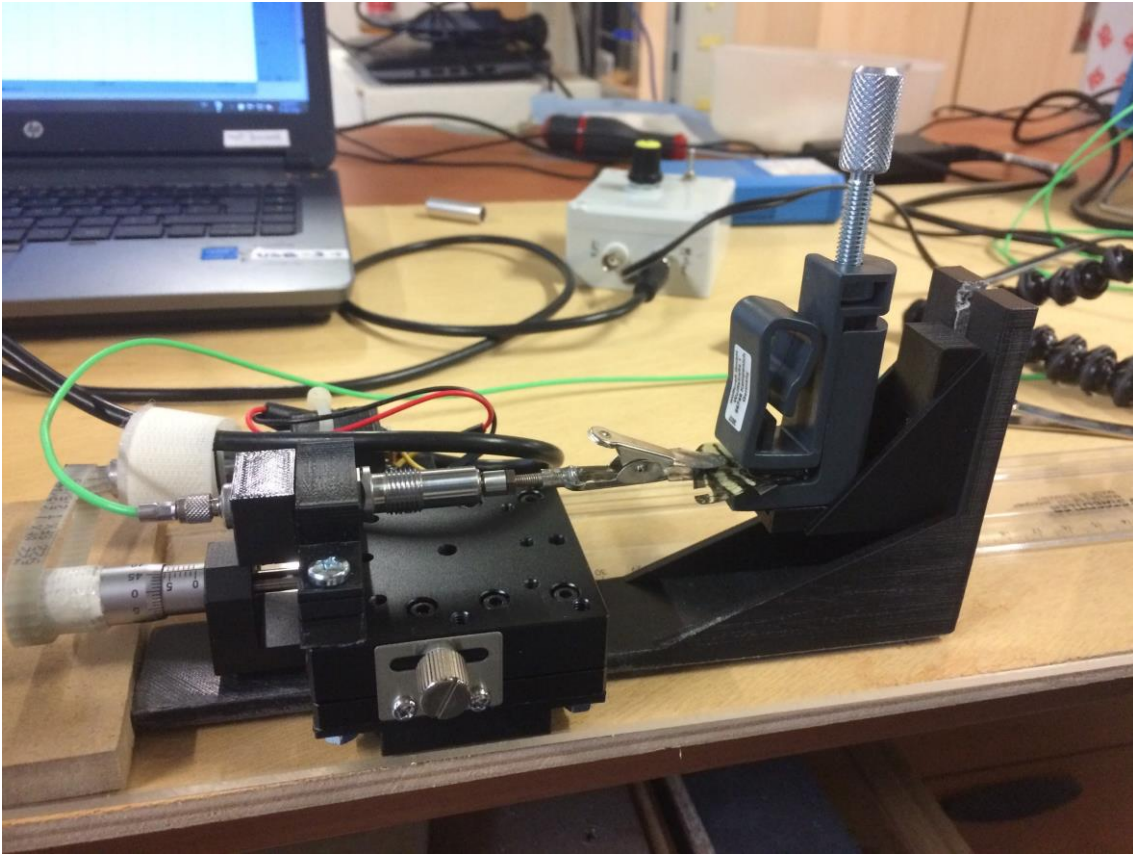
$$\beta = E.S \quad [5]$$

The slope measured on our curve gives us an idea of the order of magnitude of the Young's modulus. The greater the slope, the stiffer the vein.

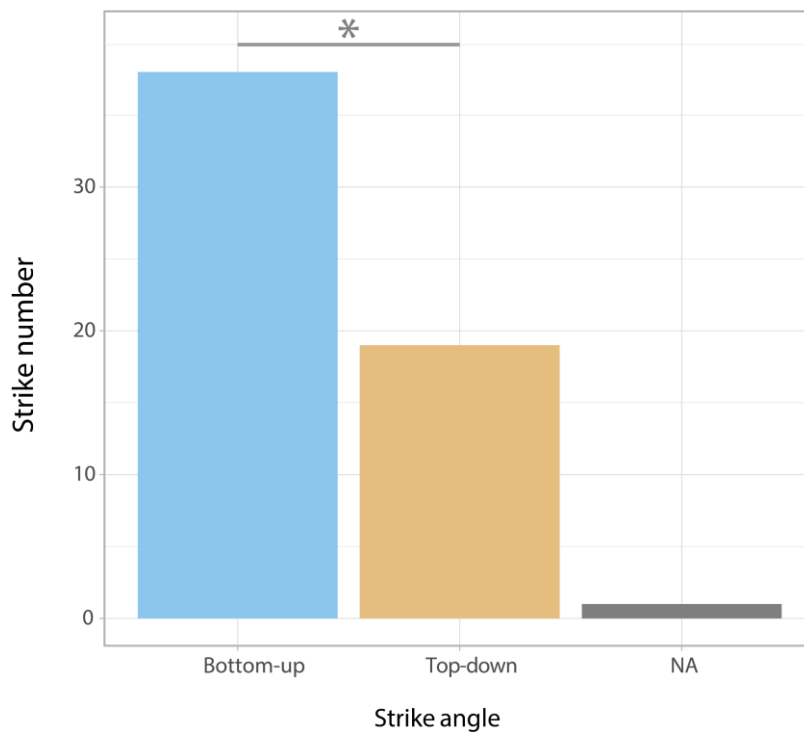
Supplementary materials S2: Photograph of the experimental setup for behavioural assay with wild-caught great tits.



Supplementary materials S3: Photograph of the experimental setup to estimate the force needed to tear the wings at different locations



Supplementary materials S4: Strike trajectories of birds (n=59). We tested whether strikes occurred more often with a bottom-up trajectory than a top-down trajectory using a Pearson Chi-squared test. Bottom-up trajectories (n=33) are more frequent than top-down (n=19) ($\chi^2 = 6.3333$, $df = 1$, $P = 0.012$).



Supplementary table 1: Post Hoc comparisons of bird strike numbers on the dummy butterflies between rank order of attacks. Each strike was characterised by its rank order, from 1 to 7.

Rank order	Parameters	1	2	3	4	5	6
1	estimate						
	<i>P</i>						
2	estimate	0.999					
	<i>P</i>	0.0491					
3	estimate	0.721	-0.276				
	<i>P</i>	0.325	0.982				
4	estimate	0.666	-0.333	-0.055			
	<i>P</i>	0.424	0.955	1			
5	estimate	0.888	-0.111	0.167	0.222		
	<i>P</i>	0.116	1	0.999	0.994		
6	estimate	0.722	-0.276	0	0.055	-0.167	
	<i>P</i>	0.325	0.982	1	0	0.999	
7	estimate	0.666	-0.333	-0.055	0	-0.222	-0.055
	<i>P</i>	0.424	0.955	1	1	0.994	1

Supplementary movie 1: Video of three sequential strikes performed by a great tit on a dummy butterfly. Strikes are shown at normal speed then slowed down 10 times.

Supplementary movie 2: Video of one strike performed by a great tit on a dummy butterfly. Strike is shown at normal speed then slowed down 10 times.

Chapter II

The effects of hindwing tails on flapping flight performances in the swallowtail butterfly *Iphiclides podalirius* suggest an adaptive evolution of butterfly tails

Ariane Chotard¹, Camille Laurain, Camille Le Roy², Violaine Llaurens¹ and Vincent Debat¹

Affiliations:

¹Institut de Systématique, Evolution, Biodiversité (ISYEB, UMR 7205), Muséum National d'Histoire Naturelle, CNRS, Sorbonne Université, EPHE, UA, Paris, France.

² Experimental Zoology Group, Wageningen University, 6709 PG Wageningen, Netherlands.

In prep

Abstract: The evolution of wing shape in flying animals is greatly influenced by the associated aerodynamic properties, because flying abilities are crucial for numerous fitness-related behaviours, such as foraging, migration, escape from predators, male-male contests or courtship. Nevertheless, the impact of selection on flight behavior on the evolution of hindwing shape has been scarcely studied. In Lepidoptera, hindwing tails have independently emerged in various clades, but its effect on flight has only been investigated using model wings placed in a wind tunnel. These researches suggested a significant effect of the tails on gliding performance, with an aerodynamic impact on lift and gliding stability. However, our recent study on *I. podalirius* showed that (1) wing damage was much more frequent on the tails, (2) wing tails and conspicuous coloration of the hindwings were struck more often than the rest of the body by birds and (3) the tail vein was more fragile than the others. These results clearly support the deflective effect of hindwing tails and suggest that predation is an important selective driver of the evolution of wing tails and colour pattern in butterflies (Chotard *et al.*, 2022). Such preferential attack rate on the hindwing might imply aerodynamic costs, because tails are likely to be lost during the life of butterflies. The effect of the tails on flight behavior and performance thus needs to be tested to understand the potential selective conflicts between deflective and aerodynamic properties associated with tails. In this word, we investigated the relative aerodynamical importance of tails in flapping flight, conducting flight analyses of phenotypically altered *I. podalirius*. We showed that hindwing tails have a significant effect on flight stabilization, suggesting that aerodynamics is also a selective driver of tails evolution.

Keywords: *Papilionidae*, *aerodynamics*, *wing morphology*, *flight behaviour*, *evolutionary trade-off*.

Acknowledgements: We would like to thank Michel Baguette for his advice on sampling sites for *Iphiclides podalirius* and all the professionals of the Station d'Ecologie Théorique et Expérimentale SETE (Moulis, France) for their technical assistance.

Introduction

The evolution of wing shape in flying animals is greatly influenced by the associated aerodynamic properties, because flying abilities are crucial for numerous fitness-related behaviour, such as foraging, migration, escape from predators, male-male contests or courtship. In Lepidoptera, hindwing tails have independently emerged in various clades, from moth to butterflies. In the Papilionidae family for instance, 48 percent of species display tails on the hindwings in at least one sex (Chapter III - [Chotard *et al. in prep.*](#)). Yet, the evolutionary forces promoting the multiple evolution of hindwing tails are still largely unknown.

In particular, the impact of selection on flight behavior on the evolution of hindwing shape has been scarcely studied. The effect of hindwing tail on flight has only been investigated using model wings placed in a wind tunnel and suggested a significant effect of the tails on gliding performance, with an aerodynamic impact on lift and gliding stability ([Park *et al.*, 2010](#)). Nevertheless, experimental analyses using actual butterflies with clipped or naturally damaged wings suggested that hindwings play a less important role in flight than forewings ([Jantzen and Eisner, 2008](#)): while forewings are necessary to produce the lift required to fly, hindwings mostly impact flight maneuverability. A higher frequency of wing damage is indeed observed on the hindwings as compared to the forewings in wild-caught butterflies ([Molleman *et al.*, 2020](#); [Chotard *et al.*, 2022](#)), suggesting that hindwing damage has a limited impact on flight and survival. Selection acting on flight performance might thus be more relaxed on hindwings as compared to forewings. The higher interspecific variation in hindwing shape ([Owens *et al.*, 2020](#); [Strauss, 1990](#); Chapter III - [Chotard *et al. in prep.*](#)) also suggest that heterogeneous selective processes might promote a higher diversification of hindwing morphology.

In both butterflies and moths, behavioral experiments with predators have suggested a positive effect of hindwing tail on the escape abilities. The long, twisted tails observed in some moth species have been shown to interfere with bats echolocation, thus efficiently deflecting their attacks away from the insect body ([Barber *et al.*, 2015](#); [Rubin *et al.*, 2018](#)). A similar effect has been documented in day-flying butterflies where the tails may deflect

attacks of visual predators away from vital parts of the body. The false-head morphology generated by the hindwing tails of Lycaenidae has indeed been suggested to favor the escape from predators (Robbins, 1981; Sourakov, 2013; Novelo Galicia *et al.*, 2019). More recently, behavioral experiments carried with captive birds revealed that tails of the swallowtail *Iphiclides podalirius* are more often attacked than any other wing part (Chotard *et al.*, 2022). The wing tail was also shown to be more easily teared apart than other wing part, therefore further enhancing escape probability. Such increased survival after an attacked might be a powerful selective process promoting the evolution of hindwings in many species of butterflies.

Nevertheless, such preferential attack rate on the hindwing might imply aerodynamic costs, because tails are likely to be lost during the life of butterflies. Indeed, in natural population of *I. podalirius* for instance about 47.1 percent of collected individuals lack at least one tail (Chotard *et al.*, 2022). The effect of the tails on flight behavior and performance thus needs to be tested to understand the potential selective conflicts between deflective and aerodynamic properties associated with tails.

Here, we thus experimentally manipulated the hindwings of *I. podalirius* butterflies and investigated the impact of such manipulations on flight behavior in controlled conditions. Using a highspeed videographic system, we indeed recorded the flight trajectories and compared the flight behaviour of individuals with intact and experimentally modified wings.

Materials & Methods

1) Sampling

Field sampling of *I. podalirius* was performed in Ariège (France) during the summer of 2020 (collection sites: 43°04'17.86"N, 01° 21'58.88"E; ca. 400m a.s.l., and 43°03'50.94"N, 01° 20'40.95"E; ca. 400m a.s.l.). We captured butterflies with hand-nets, and placed them in entomological envelopes to avoid any wing damage, next to a bottle of frozen water preventing overheating, for a few hours at most (until the experiments were conducted). For this experiment, we only selected intact specimens, sampling a total of 27 wild male. Experiments were then conducted in the Station d'Ecologie Théorique et Expérimentale SETE (Moulis, France).

2) Experimental groups

To estimate the effect of hindwing tails on flight behaviour, five treatments were applied to modify the morphology of the wings (see Figure 2B): (1) Individuals with intact wings; (2) Individuals with both tails clipped; (3) Individuals with tails clipped and then reglued again to their natural location. (4) Individuals with lateral parts of the hindwings clipped. In this treatment we removed a wing area with a size similar to the tail area; (5) Individuals with lateral parts clipped and then reglued again at their natural location. To glue the previously clipped part back to the hindwings (treatments 3 and 5), we used clear nail polish, allowing a fast and efficient adhesion using an extremely small amount of product, a classic technique in entomotaxy (Gibb *et al.*, 2006).

Intact individuals (treatment 1) were used as a control group (in particular to quantify the variability of flight behaviour carried out by the same individuals). Individuals with clipped tails (treatment 2) and with glued tails (treatment 3) were used to test whether tails have an effect on flight behaviour. Individuals with clipped lateral wing parts (treatment 4) and glued lateral parts (treatment 5) were used to test whether the effect of hindwing clipping on flight was specific to tails, or rather a generic effect of a loss of wing surface. Finally, the glued treatments (3 and 5) allow to test whether the effect of the wing clipping on flight is due to an aerodynamic impact, or to a behavioural effect

stemming from the manipulation of the butterflies (*e.g.*, individual stress). Assuming that the clipping generates mainly an aerodynamic effect, we expect that gluing the missing part may partially restore the control flight behaviour.

3) Experimental setup

To study the flight behaviour of the tested butterflies, we used a large indoor insectary (6m × 3m × 3.5m) equipped with a stereoscopic videography system, consisting of two cameras (GoPro Hero5 Black and GoPro Hero4 Black; temporal resolution: 240 frames/second; spatial resolution: 848 × 480 pixels) positioned orthogonally (see Figure 1): one camera was mounted horizontally on a tripod, and provided a side view of the flight path. The second camera was located on the ceiling, facing downwards, and thus provided a top view. The insectary temperature conditions were permanently controlled and regulated.

The butterflies were released 60 cm from the ground, from the darkest area of the cage, so that they usually flew directly to the much-brighter opposite wall (Figure 1). We discard flight sequences where the butterflies did not cross the whole cages, to keep comparable of flight sequences.

4) Flight trials

Twenty-seven individuals were used in the experiment. Each individual was used in different treatments. Their phenotype was sequentially modified: first the flight behaviour of the intact butterfly was recorded (treatment 1), then its behaviour when clipped (either treatment 2 or 4) and glued (either treatment 3 or 5) were captured. To account for potential biases related to the handling of butterflies, their fatigue and variation due to individual behavioural effects, we defined 7 combinations of trials, to which individual were randomly assigned. (a) 1-1-1; (b) 1-2-2; (c) 1-2-3; (d) 1-3-3; (e) 1-4-4; (f) 1-4-5; (g) 1-5-5. For example, the combination 1-2-3 corresponded to the sequence “Intact” - “Clipped tails” - “Reglued tails”. A sequence is so defined by 3 takes (in our example, take 1 = “Intact”, take 2 = “Clipped tails”, take 3 = “Reglued tails”) and for each take, we aimed at recording 3 flights to account for intra-individual variability. To continue our example, the sequence “1-2-3” include 3 flights in treatment 1, follow by 3 flights in

treatment 2 and then 3 flights in treatment 3, for a total of 9 flights aimed by sequence. In total, 185 flights were included in the analyses (treatment 1: n -flights = 95, n -individuals = 24; treatment 2: n -flights = 17, n -individuals = 6; treatment 3: n -flights = 40, n -individuals = 10; treatment 4: n -flights = 17, n -individuals = 5; treatment 5: n -flights = 16, n -individuals = 5).

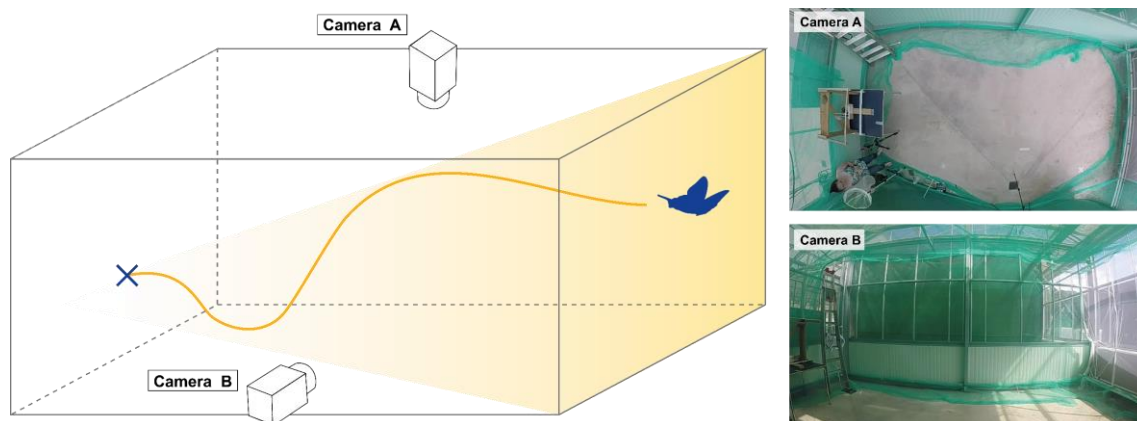


Figure 1: Schematic and photograph of the experimental setup used to reconstruct the three-dimensional trajectories of butterflies, constituted of a large indoor insectary (6m × 3m × 3.5m) equipped with two orthogonally positioned video cameras.

5) Quantification of flight trajectory

The analyses of the videography data were carried out using MATLAB (Mathworks Inc). The background of the stereoscopic video sequences was first subtracted. The views obtained from the two cameras were then synchronized using a reference frame.

Calibrations – To calibrate the distances within the experimental cage, we used the direct linear transformation (DLT) technique by digitizing the positions of a wand moved throughout the insectary before each film session (Theriault *et al.*, 2014; Le Roy *et al.*, 2021). Wand tracking was performed using *DeepLabCut DLC* (Mathis *et al.* 2018), running on *Tensorflow* (Abadi *et al.*, 2016), for 15 calibrations and *easyWand* for 7 (Theriault *et al.*, 2014). *DLC* is a deep learning software, designed for position interpolation in animal movement analyses. We trained *DLC* using 500 frames per view (sampled using *DLC* clustering algorithm, maximizing the variance between selected frames). Computation of the DLT coefficients and frame distortion (fisheye effect) due to wide-angle settings were performed using *DLTdv8a* (Theriault *et al.*, 2014)

Flight trajectories - we digitized the flight trajectory by tracking the butterfly body (*i.e.*, a single point) and extracting the corresponding 3D coordinates at each frame, using *DLC* (previously trained with 500 frames selected along a uniform distribution). DLT coefficients corresponding to the flight session were computed on the obtained coordinates. Finally, flight trajectories were smoothed using a linear Kalman filter ([Welch and Bishop, 1995](#)) – see Figure 2A.

Flight parameters - We used the 3D trajectories to estimate seven relevant parameters summarizing the flight behaviour carried by butterflies under the different treatment (see Table 1). We selected flight parameters based on the percentage of explained variability and correlation: we kept the most explanatory and least redundant parameters (Figure 1). The highest correlation between the pairs of our parameters was 0.7 and the average correlation was 0.08.

Table 1: Description of the flight parameters.

Parameters	Description
Velocity V (m.s ⁻¹)	Speed V is the magnitude of the change of a position over time. For a frame i , the instantaneous speed is: $v(i) = \frac{\sqrt{(x_{i+1}-x_{i-1})^2+(y_{i+1}-y_{i-1})^2+(z_{i+1}-z_{i-1})^2}}{t_{i+1}-t_{i-1}}$, with x , y and z coordinates were digitized and t the instantaneous time at frame i .
Acceleration A (m.s ⁻²)	Acceleration A was computed as the derivative of velocity. For a frame i , the instantaneous acceleration is: $a(i) = \frac{d}{dt} v(i)$ where v correspond to the instantaneous velocity at frame i .
Sinuosity S (vertical and horizontal)	Sinuosity (<i>i.e.</i> , the erraticism of a trajectory) was computed as the ratio of the actual distance covered along the flight path, over the distance between start and end positions: $S = \frac{\sum \sqrt{(x_{i+1}-x_{i-1})^2+(y_{i+1}-y_{i-1})^2+(z_{i+1}-z_{i-1})^2}}{\sqrt{(x_{start}-x_{end})^2+(y_{start}-y_{end})^2+(z_{start}-z_{end})^2}}$, where i corresponds to the frame in which the x , y and z coordinates were digitized, and xyz_{start} / xyz_{end} corresponds to the first and last coordinates digitized. We separately considered the horizontal and vertical component of Sinuosity S , to decompose the aerodynamic characteristics of the studied flights.
Wingbeat frequency f (Hz)	Wingbeat frequency f was computed as the number of wingbeats executed per unit of time: $f = \frac{wing\ beats}{time}$, where time is the duration of flight.
Ascent angle γ (°)	The ascent angle γ is equivalent to the angle between the velocity vector and the horizontal plane: $\gamma = \tan^{-1}\left(\frac{U_{vertical}}{U_{horizontal}}\right)$, where $U_{vertical}$ and $U_{horizontal}$ are the vertical and horizontal components of the velocity.
Number of change heading	Number of change heading was computed as the number of times turning acceleration vector (<i>i.e.</i> , the orthogonal projection of the acceleration vector in the plan orthogonal to the velocity vector) is passing from one to another side from the velocity vector: $t[x_i]^2 + t[y_i]^2 > or < 0.5$, with t the turning acceleration on a point of x and y coordinates, at frame i .

6) Statistical analyses

All statistical analyses were carried out in R version 4.1.3 (R Core Team 2022).

We first performed a PCA (function *prcomp* in the R package *stats*, Bolar, 2019) on all measured parameters from the flight trajectories (Figure 2B). We then tested the effect of the treatment on flight using a MANOVA applied to the set of parameters with

“treatment” as a factor, followed by pairwise permutation MANOVAs (function *pairwise.perm.manova* in the R package *RVAideMemoire*, [Hervé, 2022](#)). Finally, we tested the effect of the treatment on each of the seven flight parameters using Linear Mixed-Effects Models (function *lme* in the R package *nlme*, [Pinheiro et al., 2022](#)), with treatment as fixed effect. We defined the take, the flight number and the individual identity as random effects. For the case of wingbeat frequency parameter, results were ambiguous (treatments 2, 3, 4 and 5 displayed higher wingbeat frequency than treatment 1), so we completed the analysis with pairwise comparisons (function *glht* in the R package *multcomp*, [Hothorn et al., 2022](#)).

Results

The PCA performed on all flight parameters shows a difference in flight behaviour/performances between the treatments. The flights performed by individuals with clipped/glued tails (treatments 2 and 3) indeed differed from the flight behavior performed by intact and clipped/glued lateral parts butterflies (treatments 1, 4, 5; Figure 2C). The first dimension of the PCA is driven by the horizontal and vertical sinuosity and the number of changes of heading, which reflected the erraticism of flights. The second dimension of PCA is driven by variation in acceleration and velocity. The clipped tails butterflies diverge from all the other treatment, exhibiting a higher sinuosity and changes of heading, reflecting an erratic flight. Butterflies with clipped tails also had a reduced velocity and acceleration, suggesting a negative effect of tails clipping on aerodynamic performance during flapping flight. Interestingly, butterflies with the glued tails display a flight more similar to intact individuals, suggesting that regluing the tails partly restores natural flight capacities.

The PCA also did not revealed any difference in flight behavior between intact butterflies (treatment 1) and individuals with a clipped lateral part (treatment 4 and 5), suggesting that the loss of a lateral part has a limited effect on flight.

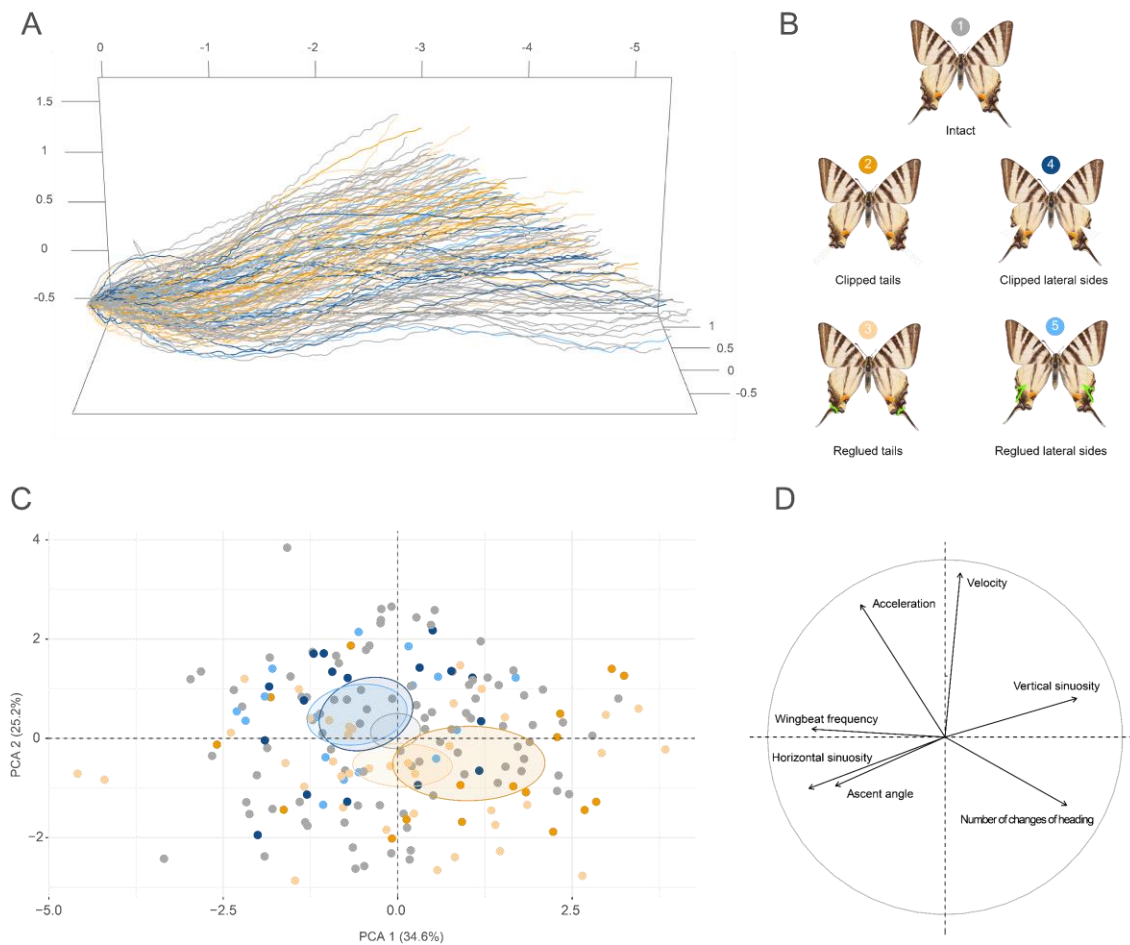


Figure 2: A) The 185 smoothed trajectories analysed showed together (n -flights: treatment 1 = 95, treatment 2 = 17, treatment 3 = 40, treatment 4 = 17, treatment 5 = 16). (B) Phenotypical treatments. (C) Principal components analysis showing the difference of flight between treatments. Ellipses are plot around each group mean points. (D) Flight parameters associated with PCA dimensions 1 and 2.

These results are supported by the MANOVA performed on all flight parameters where the treatment had a significant effect on flight behavior ($df = 4$, Pillai = 0.3812, approximation of F -value = 2.6636, $num\ df = 28$, $den\ df = 708$, P -value < 0.001 ***). The pairwise permutation MANOVAs (Table 2) revealed a significant difference between the flights performed by intact butterflies (treatment 1) compared to butterflies with clipped tails (treatment 2) and individuals with glued tails (treatment 3). On the contrary, no difference was detected between the flights of intact individuals and those of individuals with clipped lateral parts, suggesting a lack of aerodynamic and behavioral effect of this wing part. This comparison between manipulation of the tails vs. other hindwing area

suggest that the tails have a more significant effect on flight behavior, probably through its impact on aerodynamic property.

Table 2: Pairwise permutation MANOVA on all flight parameters (Horizontal sinuosity, Vertical sinuosity, Velocity, Acceleration, Horizontal radius of curvature, Ascent angle, Number of changes of heading) between treatments (1, 2, 3, 4, 5). Significant comparisons are indicated in bold.

	Intact (1)	Clipped tails (2)	Glued tails (3)	Clipped lateral (4)
Clipped tails (2)	0.0047	-	-	-
Glued tails (3)	0.0010	0.0425	-	-
Clipped lateral (4)	0.3685	0.1819	0.0010	-
Glued lateral (5)	0.5805	0.0272	0.0037	0.4484

Clipped tails individuals indeed accelerate less than intact individuals, and their trajectories are more sinuous (-16.3% for acceleration and +55.6% for vertical sinuosity, Figure 3 – see Supplementary for detailed results). In contrast, no effect of the clipping of the lateral wing parts was detected on these flight parameters. This further confirms that the effect of tails clipping on flight trajectory is not due to a generic wing surface reduction, but rather to a specific aerodynamic effect of the tails. Velocity and change of heading are only significantly different from intact state for treatments 3 and 5 respectively. As these are our control treatments, we cannot draw any conclusion on the impact of tail/lateral parts clip. Finally, clipped and reglued tails individuals displayed slight increase in wingbeat frequency and the same trend is observed for clipped and reglued lateral parts individuals. Pairwise comparisons are only significant for the treatment 4 – treatment 1 and treatment 5 – treatment 1 (details in Supplementary), suggesting that clipping of tails seems have less effect on wingbeat frequency than clipping of lateral side.

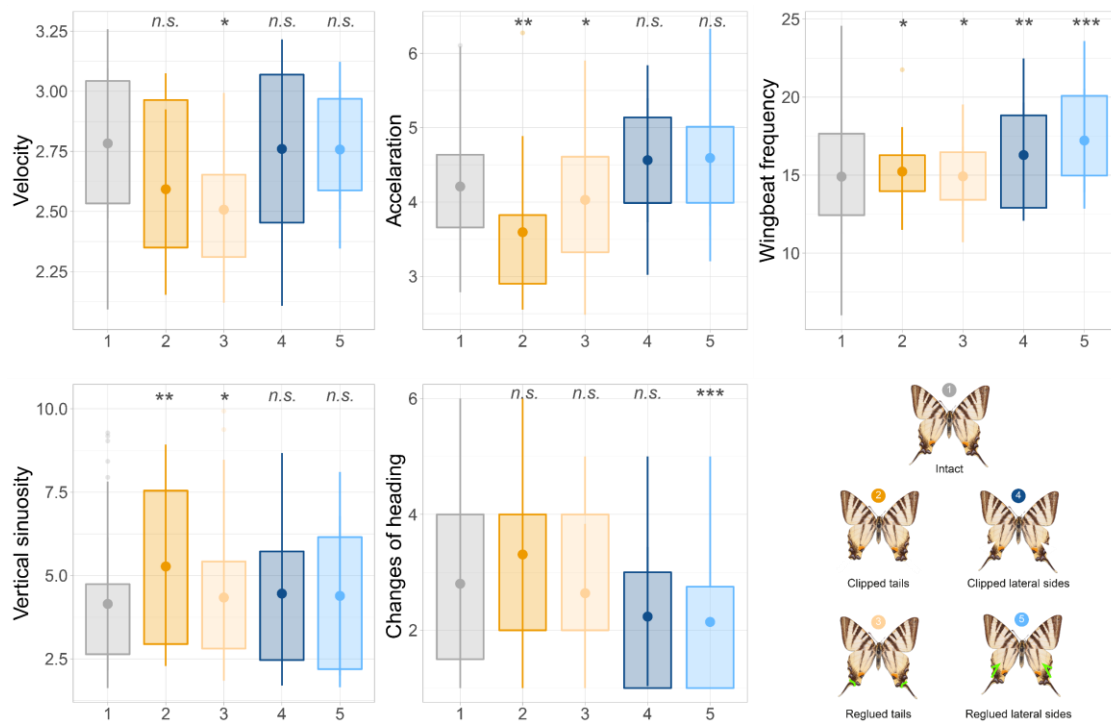


Figure 3: Difference of flight parameters between treatments – mean and quantile displayed in boxplot, the distribution is graphically reduced to first and last 5% of observations to facilitate reading. The p-values from *lmer* models are displayed as: *n.s.* = *P-value* > 0.05; * = *P-value* < 0.05; ** = *P-value* < 0.01; *** = *P-value* < 0.001.

Discussion

1) Butterfly wing tails contribute to flapping flight performance

By manipulating the hindwing shape, our behavioural experiment reveals that the ablation of the tails has a marked effect on the flight of *I. podalirius* butterflies, by decreasing acceleration and vertical stability. This suggests that the tails significantly contribute to flight abilities in this Papilionidae species. This result is consistent with the wind-tunnel experiments carried out on Papilionidae model wings showing that hindwings tails enhance lift and longitudinal static stability in gliding flight (Park *et al.*, 2010). Since the flight sequences recorded in our experiments were most exclusively flapping flight – the somewhat stressful captivity conditions likely induced escape flight – butterfly tails therefore appear to impact both flapping and gliding flight capacities.

In contrast, we detected limited effect of an ablation of a lateral part of the hindwing. In a previous study of natural wing damage in *Morpho* butterflies (Le Roy *et al.*, 2019a), we reported a similarly limited effect of hindwing damage on flight. These results are compatible with the generally expected limited contribution of hindwings to flight performance. The marked effect of tails loss on flight thus suggest that specific aerodynamic properties are associated to hindwing tails.

2) A trade-off between deflection and flight abilities

The evidence of a dual effect of tails on both flight capacities and attack deflection in *I. podalirius* suggests that the evolution of hindwing tails in these butterflies could have been promoted by at least two selective pressures: the selection exerted by predators promoting attack deflection, and the selection on aerodynamic performances. Nevertheless, the deflecting effect of tails frequently leads to their loss during the life of the butterflies: many *I. podalirius* fly without tails in the wild and this loss seems to impact their flight abilities. There is therefore a cost to predator deflection, and the evolution of tails might result from an evolutionary trade-off between attack deflection and flight performances.

Hindwing tails were frequently gained and lost during the diversification of Lepidoptera. In Papilionidae, a phylogenetic analysis of tail evolution recently suggested that the ancestor probably had tailed hindwings, and that tails were lost – and also regained – many times independently in this family (Chapter III, [Chotard *et al. in prep*](#)). The trade-off generated by the conflicting selective pressures stemming from deflection and aerodynamics might contribute to these repeated tail gains and losses at macro-evolutionary scale. Such antagonistic selective pressures acting on morphological variation (referred to as ‘*functional conflict*’ in [Garland *et al., 2022*](#)) have been suggested to be a key factor shaping morphological evolution. For example, in the damselflies *Lestes sponsa*, sexual and natural selection in relation to aerodynamic performance tend to favor different wing shapes ([Outomuro *et al., 2016*](#)), resulting in the evolution of intermediate wing shape phenotypes in nature. In lizards, tail autotomy is an advantageous trait in terms of predator escape, but is very costly energetically and for locomotion. Advantages and costs depend on the intensity of predation and on the selection generated by adaptation to different microhabitats, and may why autotomy is restricted to some taxa ([Bateman and Fleming, 2009](#)).

As for lizard tails, the benefits butterfly wing tails provide in terms of attack deflection must overcome the aerodynamic costs of their loss, for deflection to evolve. And this balance is likely variable within and across species, depending on the ecological conditions, and in particular, on the relative strength of predation pressure. These antagonistic selective forces may contribute to the diversity of tail size and shape observed across Papilionidae species, but also to the diversity of color patterns associated with tails. In some species, thin tails are associated with conspicuous colors, and in particular stripes and eyespots, contributing to the deflection effects. In other species, large, “spatula” shaped tails, possibly contributing to lift ([Norberg, 1995](#)), are associated with dull or even black colorations (Figure 4). This suggests that in these taxa, the selection pressures related to aerodynamics might be preponderant.

The impact of trade-offs on the diversification of traits is controversial: some authors have suggested they limit traits evolution, by constraining the set of possible phenotypes (*e.g.*, [Walker, 2007](#)). Recent studies, however, rather suggest that trade-offs promote the evolutionary diversification of the associated structures along the line of equilibrium

(Holzman *et al.*, 2012; Corn *et al.*, 2021; Burrell and Muñoz, 2022). In fishes for instance, the trade-off between suction-feeding and bite force has been suggested to play a strong role in the diversification of the skull morphology (Corn *et al.*, 2021). Similarly, the trade-off between attack deflection and aerodynamic performance might have fueled the diversification of butterfly hindwing tails and color patterns in Papilionidae.



Figure 4: (left to right) *Iphiclides podalirius*, *Graphium pazala*, *Byasa alcinous*, *Papilio buddha*

Chapter III

Selection and constraints shape the macroevolution of hindwing tails in *Papilionidae*

Ariane Chotard¹, Agathe Puissant¹, Fabien Condamine², Violaine Llaurens¹
and Vincent Debat¹

Affiliations:

¹Institut de Systématique, Evolution, Biodiversité (ISYEB, UMR 7205), Muséum National d'Histoire Naturelle, CNRS, Sorbonne Université, EPHE, UA, Paris, France

² Institut des Sciences de l'Evolution de Montpellier (ISEM, UMR 5554), IRD, UM, CNRS, EPH, Montpellier, France

In prep

Abstract:

The shape of butterfly wings is extremely diversified across species, but the complex phylogenetic and developmental constraints influencing its evolution makes it difficult to identify the selection pressures involved. Here we investigate the evolution of the shape of both pairs of wings across the whole Papilionidae family (ca. 600 species), using a large sample of butterflies from Museum collection. Using a geometric morphometric approach, we finely describe the evolution of hind and forewing shape throughout the Papilionidae family. We tested for contrasted selection on the fore- and hindwings at a large phylogenetic scale. We compared their shape diversity, their evolutionary rates, and the link between diversification and phenotypic disparity. A remarkable feature of wing shape is tail. Tail is a very common trait in butterflies, but its developmental bases and the evolutionary forces acting on its emergence and loss are unknown. What selection pressures act on their evolution? We then assess the evolutionary lability of hindwing tails, testing for their multiple independent evolution. Finally, by comparing wing shapes of males and females, we contrast the evolution of sexual dimorphism between the two pairs of wings, to estimate the significance of sexual selection or differential natural selection across sexes on their evolution. Our results shed light that forewings and hindwings evolution could be a signature for different selection regimes while highlighting a possible co-evolution of forewing and hindwing shape driven by aerodynamics.

Acknowledgements: We would like to thank Julien Clavel for his advice on multivariate phylogenetic analysis and Jérôme Barbut and Joel Minet for their assistance into the entomological collections.

Keywords: *Lepidoptera, comparative analyses, geometric morphometrics, wing shape evolution, tails.*

Introduction

The shape of butterfly wings is extremely diversified across species. Quantifying the effect of phylogenetic constraints *vs.* of the contrasted selective pressures encountered in different ecological niches on the diversification of wing shape is highly challenging (see [Le Roy *et al.*, 2019b](#) for a review). Since flying capacities are a key component for both survival and reproductive success in butterflies, aerodynamic constraints are likely to impose strong selection on wing shape evolution. The selection regime generated by these aerodynamic constraints is likely to depend on the specialization into different habitat and on life-history traits that might differ among species, therefore playing a role in the diversification of wing shape at the macro-evolutionary scale. For example, adaptation to contrasted environments in *Morpho* butterflies has resulted in the divergence of wing shape between species observed in the canopy *vs.* understory micro-habitats: the elongated wings are observed in canopy species, associated with a slow gliding flight, while the rounded wings are displayed in understory species, associated with a powerful flap-gliding flight putatively adaptive to their cluttered micro-habitat ([Le Roy *et al.*, 2021](#)). Similarly, at the micro-evolutionary scale, the long-range migrations observed in the butterfly *Danaus plexipus* favour the evolution of wing morphologies associated with reduced aerodynamic costs: in migrating populations, elongated wings are associated with an extensive use of gliding flight ([Altizer and Davis, 2009](#)). While the effect of aerodynamic constraints is likely to play a substantial role in the evolution of the forewings, their effect could be milder on the evolution of the hindwings. Wing damages caused on the hindwings have indeed been reported to have a smaller effect on flight capacities than damages on the forewings in several butterfly species ([Jantzen and Eisner, 2008](#); [Le Roy *et al.*, 2019a](#)). Selection generated by aerodynamic constraints might thus be less important on the hindwings as compared to forewings, producing contrasted evolution between the two wing pairs ([Owens *et al.*, 2020](#)).

Flight behaviours are involved in a wide range of life history traits, such as search for larval host plants, nectar sources, mates, and new territory ([Scoble, 1992](#)), and that wing shape are intrinsically linked to flight performances, we could expected that some wings morphologies would opening novel ecological niches previously unavailable and so, be

motor of adaptive radiation. This is for example the case of the hypocone in mammals (Hunter and Jernvall, 1995), that allowed colonization of new environments (in particular exploitation of new resources) and so, generated an adaptive radiation. In Papilionidae, host plant shifts have been considered a major factor driving evolutionary radiations (Fordyce, 2010; Condamine *et al.*, 2012), but wing shape role in this diversification remains unknown.

Many Lepidopteran species display tails with various shapes and sizes on the hindwing, and the evolutionary forces involved in the independent emergence of this striking morphological variation is still largely unknown. In Saturniidae moths, the long-twisted tails observed on the hindwings were shown to deflect bat attacks, by interfering with the echolocation signal and reducing strike efficiency (Barber *et al.*, 2015; Rubin *et al.*, 2018). Many butterfly species also display long and conspicuous hindwing tails, such as the Swallowtails (Papilionidae), but the adaptive effect of these tails is currently not documented. Yet in Lycaenidae, hindwing tails are often associated with particular colour patterns, jointly resembling the butterfly's head. This false-head has been hypothesized to deflect predators attacks away from the vital parts (Robbins, 1981). For example, *Calycopis cecrops* butterflies, that display false-heads, escape predators attacks more frequently than butterflies from other species lacking false-head (Sourakov, 2013). In the Papilionidae species *Iphioides podalirius* behavioural experiments have shown that captive birds tend to strike butterfly wings predominantly on the tails, consistent with the deflective effect hypothesis (Chotard *et al.*, 2022). These data suggest that predation may promote the evolution of hindwing tails in Lepidoptera. Nevertheless, the evolution of hindwing could also be influenced by their associated aerodynamic properties. Park *et al.*, (2010) indeed suggested that hindwing tails might contribute to the stability of gliding flight. Studying the multiple emergences of hindwing tails throughout the history of the diversification of Papilionidae might shed light on the relative effects of neutral divergence vs. adaptation to contrasted habitats on the evolution of this conspicuous trait.

Here we investigate the evolution of the shape of both pairs of wings across the whole Papilionidae family (ca. 600 species), using a large sample of males and females from Museum collection. The phylogenetic relationships between Papilionidae species have been precisely established for this family (Allio *et al.*, 2021) allowing us to account for

phylogenetic effects acting on the diversification of wings, enabling to disentangle historical constraints from selective effects affecting the wing shape evolution.

Using a geometric morphometric approach, we finely describe the evolution of hind and forewing shape throughout the Papilionidae family. We first test whether the two wing types evolve at different paces, and whether hindwings are more diversified than forewings, as reported in some sub-clades of *Papilio* (Owens *et al.*, 2020) and in Ithomiini and Heliconiini butterflies (Strauss, 1990). We then assess the evolutionary lability of hindwing tails, testing for their multiple independent evolution. To test whether tails affect the aerodynamics of flight and particularly the selection imposed on forewings, we then assess the effect of the presence of tails on the evolution of forewing shape. Finally, by comparing wing shapes of males and females, we contrast the evolution of sexual dimorphism between the two pairs of wings, to estimate the significance of sexual selection or differential natural selection across sexes on their evolution.

Materials & Methods

1) Taxon sampling

Butterfly specimens were sampled in the collections of the National Museum of Natural History in Paris (MNHN), aiming at covering all species included in the latest phylogeny of Allio *et al.* (2021). We thus gathered 1318 specimens (746 males and 572 females) from 337 species.

2) Phylogenetic data

We used the recently published phylogeny of Allio *et al.*, (2021) to account for the effect of phylogenetic distances on phenotypic divergence. The congruence with our morphological data is 82.6%.

3) Imaging

The dorsal and ventral sides of each specimen were photographed in a photo studio using a Nikon D90 camera (Camera lens: AF-S Micro Nikkor 60 mm 1:2.8G ED). We used controlled LED lights and standardized positions for both the specimens and the camera to minimize shape distortion due to parallax.

4) Geometric morphometrics

We then used a geometric morphometric approach based on landmarks and semi-landmarks to quantify butterfly wings shape and size (Bookstein, 1997; Adams *et al.*, 2004; see Chazot *et al.*, 2016 for a similar approach). We defined 18 and 19 landmarks (LM) on the fore- and hindwing respectively, at veins intersection and vein termini (as shown in Figure 1). To describe the wing outline, we then used 110 and 145 semi-landmarks (SL) on fore- and hindwings respectively. We did not add LM on the coastal outline of the forewing because veins are very often fused. Similarly, we excluded the anal outline of the hindwing, because this part of the wing was folded or missing in a large number of specimens, and also harbours inner marginal androconial brushes in some species (*e.g.*, genus *Ornithoptera*, Parsons, 1996), making it difficult to define SL. We

digitized LM/SL on scaled photos using the software *TpsDig2* (Rohlf, 2015). For both wings, all landmarks were then superimposed using a generalized Procrustes analysis (Rohlf and Slice, 1990) implemented in the *gpagen* function of the R package *geomorph* (Adams and Otárola-Castillo, 2013). The sliding of the SL was performed by minimizing the bending energy (Mitteroecker and Gunz, 2009). Sexes were separated because of the apparent diversity of sexual dimorphism across species within the family. The centroid size was computed and used as an estimator of wing size in subsequent analyses.

$$\text{Centroid size} = \sqrt{\sum_{i=1}^n ((y_i - \bar{y})^2 + (x_i - \bar{x})^2)}$$

We checked and validated for the repeatability of our measurements, as well as the presence of allometry (Supplementary 2). As analysis suggested allometric effects, we added the size as fixed effect in our analyses of wing shape.

5) Aspect Ratio as a proxy for gliding performance

To estimate the effect of wing shape variation on aerodynamic performances, we also computed the forewing aspect ratio (*AR*), as the ratio of wing length to width. *AR* is a classical descriptor of wing shape, shown to correlate with flight performance (see Le Roy *et al.*, 2019b for a review). A high *AR*, corresponding to long and narrow wings, is generally associated with a stable flight and high gliding performances. In contrast, a low *AR*, corresponding to short and large wings, is generally associated with a high manoeuvrability.

6) Hindwing tail

The presence/absence of a tail was noted: for the 80 species not found in the collections, we used the entomological monography of Nakae (2021). We thus assessed the presence/absence of tails in the 408 species described in the phylogeny of Allio *et al.*, (2021).

The length of the tail (TL) was measured on all specimens, as the distance between the LM located at the tip of the tail ($M3$ – see Figure 1) and the middle of the vector $M2$ - $Cu1$. Note that for the species *Ornithoptera meridionalis* and *O. paradisea*, whose males display tails on $Cu2$ vein instead of $M3$, we estimated TL using the $Cu1$ - $Cu2$ distance – see Supplementary 1). To compare the different species, TL was standardized using the hindwing centroid size. We compared TL between males and females using a Paired Samples T-test.

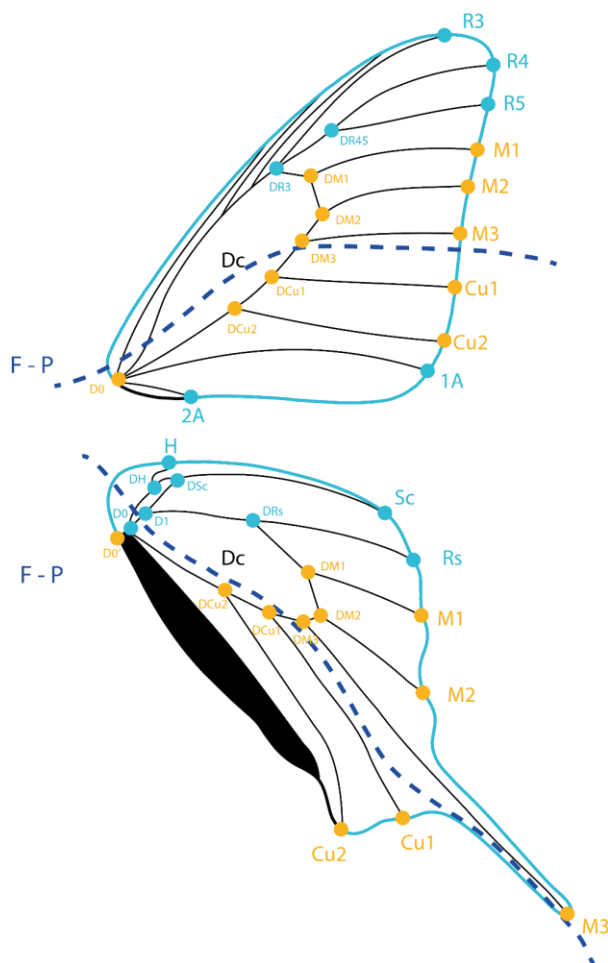


Figure 1: Typical structure of veins in the forewing and hindwing of Papilionidae, showing the position of the landmarks (LM) and semi-landmarks (SL) used. The wing veins are labelled with conventional vein names (Subcosta = Sc; Radius = R; Media = M; Cubitus = Cu; and Anal vein = A, Stark *et al.*, 1999). LM are indicated by dots (orange for developmental homologous LM between forewing and hindwing, blue for the others), resulting in 18 LM on the forewing and 19 LM on the hindwing. SL are positioned on the wings outline (blue line between the LM). The numbers of SL *per* outline section are distributed as follows. Forewing: D0-R3 = 50; R3-R4 = 5; R4-R5 = 5; R5-M1 = 5; M1- M2= 5; M2- M3= 5; M3- Cu1= 5; Cu1-Cu2 = 5; Cu2-1A = 5, 1A-2A = 20. Hindwing: D0'-H = 10; H-Sc = 15; Sc-Rs = 15; Rs-M1 = 20; M1- M2= 20; M2- M3= 30; M3- Cu1= 20; Cu1-Cu2 = 15. Theoretical developmental module (adapted from Abbasi and Marcus, 2017) are defined by the F-P compartment boundaries (indicated by dotted lines). The module n°1 includes LM: M1, M2, M3, DM3, D32, DM1. The module n°2 includes LM: Cu1, Cu2, D0, DCu2, DCu1.

7) Phylogenetic signal

The phylogenetic signal associated with shape variation was computed using Adam's *Kmult* (function *physignal* in the R package *geomorph*, Adams and Otárola-Castillo, 2013). The phylogenetic signal of univariate quantitative traits (*i.e.*, wing size, forewing aspect ratio (AR), standardized tail length (TL) and shape sexual dimorphism) was

estimated using Blomberg's K (function *phylosig* in the R package *phytools*, Revell, 2012). The phylogenetic signal of the presence/absence of the tail was assessed using Fritz and Purvis D (Fritz and Purvis, 2010), using the *phylo.d* function (R package *caper*, Orme *et al.*, 2013).

8) Estimating the effect of biomes on wing shape evolution

To assess the effect of environmental and ecological conditions on the evolution of wing shape, we used the 10 biomes defined by Gamboa *et al.*, (2022). The effect of biome on wing shape was tested, using a phylogenetic Procrustes ANOVAs (function *procD.pgls* in the R package *geomorph*, Adams and Otárola-Castillo, 2013). We focused on species whose distribution was restricted to a single biome, therefore performing our analysis on a subsample of 141 species for males and of 109 species for females. We also tested the effect of biome on presence/absence of tails on this subsample, using the same method.

9) Comparing the evolution of the two types of wings: diversity, evolution rate and sexual dimorphism

To test whether wing shape diversity was significantly different between fore- and hindwings, we compared their relative levels of variation, focusing on a subset of landmarks considered homologous between fore- and hindwings (see Figure 1). We superimposed this subset of landmarks in a new generalized Procrustes analysis pooling hindwings and forewings. We quantified the levels of variation in the shape of forewings and hindwings respectively, by computing the centroid size of the corresponding clouds of dots in the PCA space. We estimated and compared evolutionary rates of fore- and hindwings using the *compare.evol.rates* function (R package *geomorph*, Adams and Otárola-Castillo, 2013). For both wings, sexual dimorphism of wing shape was computed in each species (for which the two sexes were available, that is 268) as the Euclidian distance between the average male and female phenotypes in the common morphospace. The correlation between forewing and hindwing dimorphism was assessed (Phylogenetic *Pearson's* coefficient, using the *phyl.vcv* function of the R package *phytools*, Revell, 2012). The phylogenetic signal associated with shape variation was computed using

Adam's *Kmult* (using the *physignal* function in the R package *geomorph*, Adams and Otárola-Castillo, 2013).

10) Covariation between the wings and impact of the tail on forewing evolution

To assess the correlation between forewing and hindwing shapes, we performed a phylogenetic Partial Least Squares regression (PLS) between the FW and HW average shape (all LM and SL), using the *phylo.integration* function (R package *geomorph*, Adams and Otárola-Castillo, 2013). We assessed the effect of the presence/absence of the tail and of tail length on forewing shape and *AR* using phylogenetic Procrustes ANOVAs.

11) Testing the effect of wing shape variation on species diversification

Wing shape: To test whether species diversification rates vary among clades depending on wing shape, we relied on a Bayesian Analysis of Macroevolutionary Mixture (BAMM, Rabosky, 2014). We used the PC1 coordinates of average shape per species as a proxy for wing shape variation. BAMM analyses were run with four MCMC for 20 million generations, sampling every 20,000th and a conservative value for the compound Poisson prior (CPP=1). To account for non-random incomplete taxon sampling using the implemented analytical correction, we set a sampling fraction per genus based on the known species diversity of each genus. Mixing and convergence among runs (ESS > 200 after 15% burn-in) were assessed with the R package *BAMMtools* 2.1. We then tested whether the evolution of wing shape was correlated with the diversification rate estimated using Structured Rate Permutations on Phylogenies (*i.e.*, STRAPP, using the *traitDependentBAMM* function of the R package *BAMMtools*, Rabosky *et al.*, 2014).

Presence/absence of tail: To quantify the diversification associated with the presence / absence of tail along the phylogeny, we applied a series of birth–death models. First, we fitted Binary State Speciation and Extinction (BiSSE) models as implemented in the R package *diversitree* (FitzJohn, 2012) and Hidden State Speciation and Extinction (HiSSE) models as implemented in the R package *hisse* (Beaulieu and O'Meara, 2016). The complete procedure is detailed in Supplementary 3. The HiSSE model accounts for unmeasured factors (“hidden” states) that could impact diversification rates in addition to the trait of interest, so we used it as a complement to the BiSSE model.

12) Estimating the rate of wing shape evolution

Wing shape: to analyse the dynamics of shape evolution through time and compare it between fore- and hindwings in the two sexes, we used *RRphylo* function of the *RRphylo* R package (Raia *et al.*, 2022). This function allowed us to estimate the evolutionary rate variation of shape (a high-dimensional object) through time. Using BAMM, we estimated the numbers of shifts of shape evolution and compared it to the number of shifts expected under neutral evolution (Brownian motion). Finally, we modelled wing shape Disparity Through Time (DTT) using the *dtl* function of the R package *geiger* (Pennell *et al.*, 2014). We used the average squared Euclidean distance among all pairs of species average shape as a metric for disparity (the most common metric in macroevolution, Ciampaglio *et al.*, 2001). The DTT method calculates mean trait relative disparity and compares the observed trait disparity throughout the phylogeny to a null model of Brownian-motion evolution of the trait estimated using 1,000 simulations assuming the same phylogenetic tree. If the computed DTT falls outside the simulated neutral 95% interval, the disparity is significantly higher or lower than expected under Brownian motion, indicating a non-neutral evolution of the trait of interest (Blackburn *et al.*, 2013; Colombo *et al.*, 2015). We computed DTT on the first two PCA dimensions. Presence/absence of tail: The BiSSE models allowed us to (1) estimate the numbers of shifts between tailed/untailed states and compare it to the number expected under neutral evolution, (2) estimate the transition rates between tailed/untailed states, (3) infer the ancestral states of presence/absence of the tail at each node (function *asr.marginal* R package *divesitree*, FitzJohn, 2012). We also modelled disparity through time (DTT) of tail presence, tail length, and forewing aspect ratio using the *dtl* function of the R package *geiger* (Pennell *et al.*, 2014).

13) Developmental integration of wings

We computed the modularity of FW and HW and compared them using the *phylo.modularity* function (R package *geomorph*, Adams and Otárola-Castillo, 2013). This function uses the covariance matrix to quantify the CR coefficient between all pairs of LM (Adams, 2016), which is then compared to a distribution of values obtained by randomly assigning LM to hypothetical modules. We tested two such modularity hypotheses: the first was based on Abbasi and Marcus (2017), which described the Far-

Posterior (F-P) compartment boundary, and associated positional organizer along the M3 vein (see Figure 1), which opposed the compartments close to the coastal edge, and the more distal compartments of the wing (called the F-P repartition below). The second characterized the opposition between LM defined on the Termini and LM defined by vein Intersections (called the T-I repartition below).

We then computed the correlation matrix between homologous LM using the *dotcorr* function of the *paleomorph* package (Lucas and Goswami, 2017) in order visualize covariations between LM of each wing.

14) Impact of the chosen macro-evolutionary scale: zoom on two genera

To investigate if the trends that we observed at the family level were general or clade-specific, all the above analyses were also conducted independently on the clades *Papilio* (n = 30) and *Graphium* (n = 39), which both contain a large number of species with a large diversity of wing shape and tail size.

Results

Contrasted evolution of the two pairs of wings

We first analyzed the variation of each wing separately, considering the full sets of LM and SL.

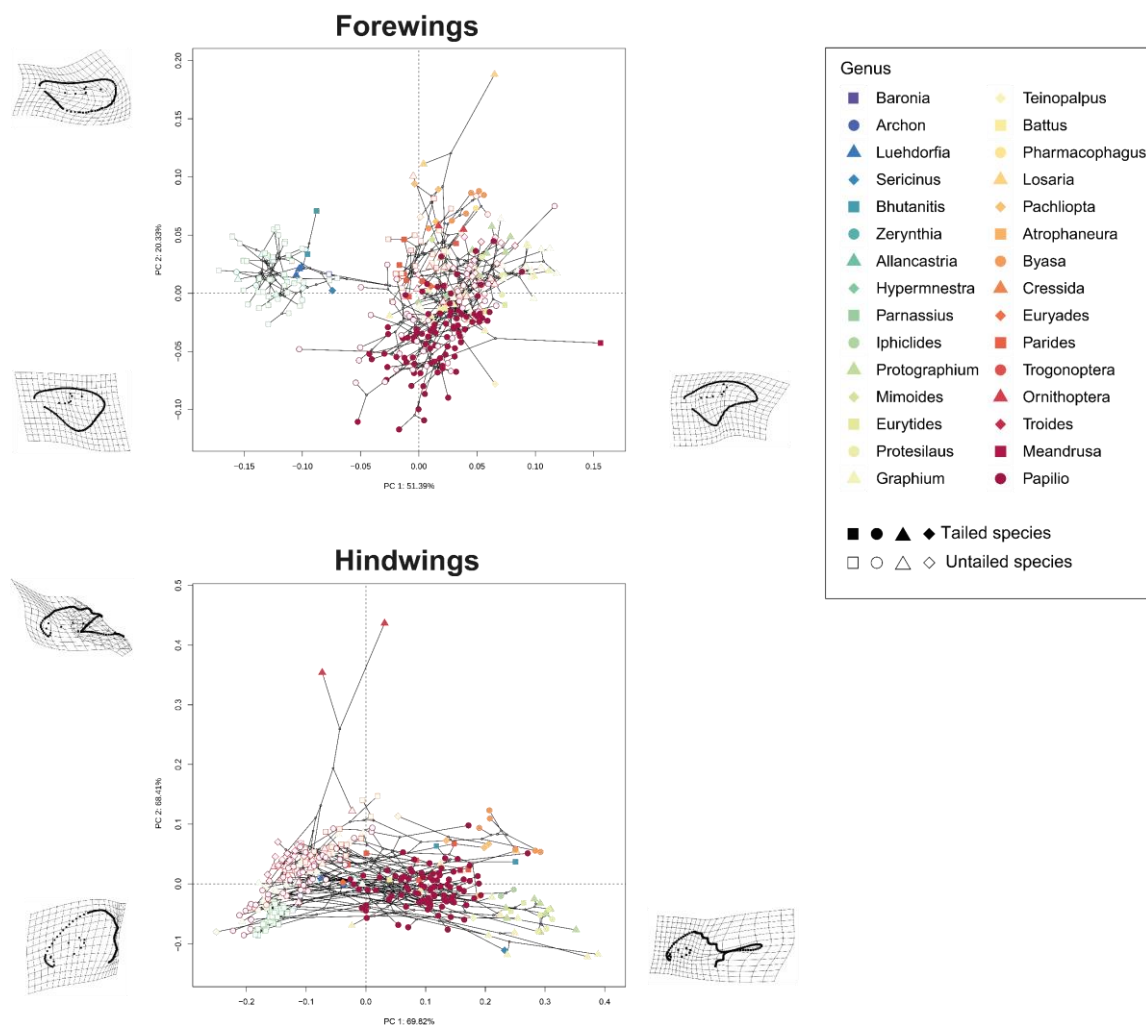


Figure 2: Phylomorphospaces describing variations across species mean shapes for the forewing (top) and hindwing (bottom) (n=328 species; males only). For both wings, we first conducted a PCA on Procrustes coordinates and visualized the shape changes associated with the PCs using the *picknplot.shape* function of the R package *geomorph* (Adams and Otárola-Castillo 2013). Phylogenetic relationships among species are visualized by black lines. The genera are ordered according to their position in the phylogeny (from the first to branch off *Baronia* to the most derived *Papilio*). Filled symbols: presence of tails; open symbols: absence of tails.

For forewing shape (Figure 2), the first axis opposes rounded wings (mostly found in *Parnassius* species) to elongated and pointy wings of most other species of the Papilionidae family. The second axis opposes wings differing in their aspect ratio, with elongated wings on the positive values and wide wings on the negative ones. Species average shapes appear to largely cluster according to the phylogenetic structure, a visual signal confirmed by the strong phylogenetic signal (Male: $K = 0.73$, $P < 0.001$; Female: $K = 0.64$, $P < 0.001$). The evolution of forewing AR also presents a significant phylogenetic signal (Male: $K = 0.37$, $P < 0.001$; Female: $K = 0.36$, $P < 0.001$).

For hindwing shape (Figure 2) the first axis clearly opposes species with and without tails; the second axis is driven by a variation on the coastal edge. Remarkably, many genera include species of both morphologies (tailed and untailed), as shown by the many shifts between the two morphological groups and the corresponding long phylogenetic lines parallel to PC1. The phylogenetic signal of hindwing shape evolution is significant, but with lower values than those found for forewing (Male: $K = 0.53$, $P < 0.001$. Female: $K = 0.46$, $P < 0.001$), likely due to these repeated shifts in wing shape.

We also detected a significant phylogenetic signal in the evolution of wing size, for both sexes, again presenting lower values for hindwings (FWM: $K = 0.76$, $P < 0.001$; FWF: $K = 0.84$, $P < 0.001$; HWM: $K = 0.53$, $P < 0.001$; HWF: $K = 0.57$, $P < 0.001$), suggesting a more labile size in hindwings than in forewings.

The DTT analysis detected a discernible departure ($P < 0.05$) from the null model of Brownian evolution of the disparity of forewing shape (PC1), especially at the beginning of the evolutionary history of Papilionidae (Supplementary 4). This disparity of forewing shape is smaller than expected under neutral model, which suggests a selection around an optimum. At the opposite side, the disparity of hindwing shape seemed slightly higher than expected under neutral model at the end of evolutionary history (Supplementary 4), which suggests a heterogeneous selection.

Nevertheless, we did not find any significant effect of biomes on wing shape (Table 1), indicating that adaptation to different biome was necessarily fueling changes in wing shapes.

Table 1: Results of the Procrustes ANOVA between forewing/hindwing shape and biome effect.

	Males average shape					Females average shape						
		<i>df</i>	<i>SS</i>	<i>MS</i>	<i>F</i>	<i>P</i>		<i>df</i>	<i>SS</i>	<i>MS</i>	<i>F</i>	<i>P</i>
Forewing	Centroid size FW	1	0.0001	0.0001	0.6938	0.65423	Centroid size FW	1	0.0004	0.0004	2.0136	0.08209
	Biomes	7	0.0021	0.0003	1.4542	0.0676	Biomes	7	0.0016	0.0002	1.1360	0.2486
	Residuals	132	0.0267	0.0002			Residuals	109	0.0224	0.0002		
Hindwing	Centroid size HW	1	0.0151	0.0151	16.1268	< 0.001***	Centroid size HW	1	0.0119	0.0119	14.8504	< 0.001***
	Biomes	7	0.0089	0.0013	1.3622	0.1526	Biomes	7	0.0068	0.0010	1.2216	0.2025
	Residuals	132	0.1235	0.0009			Residuals	109	0.0873	0.0008		

We then focused on the set of common landmarks across the two wings, allowing a direct comparison of their relative variation (Figure 1). The variation of shape was almost 2.66 times higher in hindwing than in forewing, as shown by the different centroid size of the clouds of hindwing and forewing dots on this morphospace (Hindwing: 5.09; Forewing: 1.91, Supplementary 5). Accordingly, the evolutionary rate of hindwing shape was 3.8 higher than that of the forewing shape (Males: forewing rate = 1.35×10^{-5} , hindwing rate = 5.20×10^{-5} , *P-value* = 0.001; Females: forewing rate = 1.12×10^{-5} , hindwing rate = 4.32×10^{-5} , *P-value* = 0.001 – Supplementary 6).

As shown on Figure 3, the number of evolutionary rate shifts for hindwing shape was largely higher in the hindwing in both sex (males *n*-shifts = 13.16 ± 3.69 ; females *n*-shifts = 12.35 ± 3.54) than in the forewing shape (males *n*-shifts = 3.77 ± 2.25 ; females *n*-shifts = 3.46 ± 2.16).

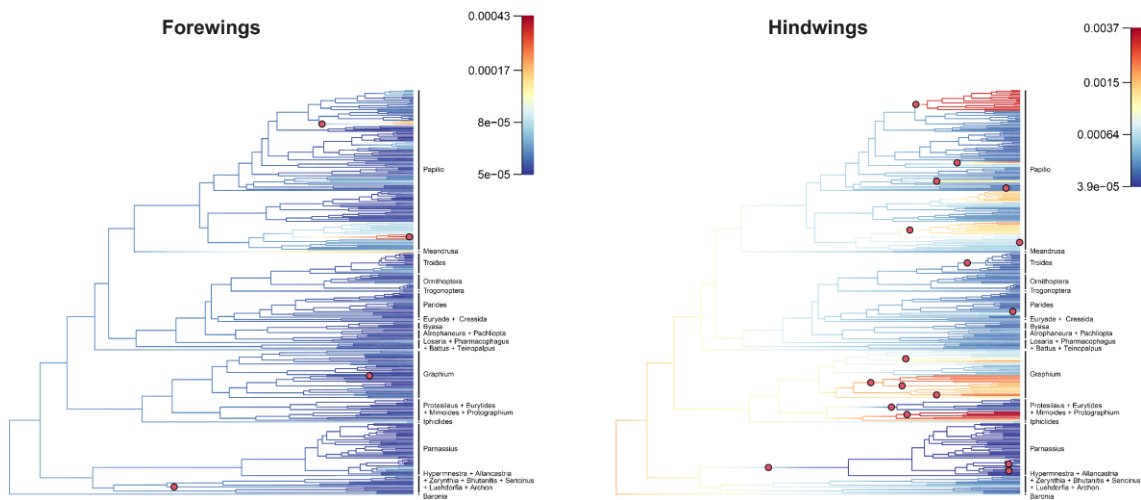


Figure 3: Wing shape evolution rate through time in males from the Papilionidae family ($n\text{-species} = 328$), obtained with the R package BAMMtools (Rabosky *et al.*, 2014). Wing shape is defined as the PC1 coordinate of species on Phylomorphospace.

Shared developmental constraints between forewing and hindwing

Forewings are more tightly integrated than hindwings (**Supplementary 7**): while no modularity is detected within the forewing (FWM: CR = 1.0685, $P\text{-value} = 0.1455$; FWF: CR = 1.0686, $P\text{-value} = 0.1273$), we found some support for a modular structure of the hindwing, in agreement with the F-P partition (HWM: CR = 1.0460, $P\text{-value} = 0.0294$; HWF: CR = 1.0491, $P\text{-value} = 0.0269$). In others words, LM more tightly covary within the hypothetical developmental modules than with LM of the other module.

We also tested if the T-I partition was supported by data and we found a significant modular signal in all wing venations (FM: CR = 1.0231, $P\text{-value} = 0.003$; FF: CR = 1.0274, $P\text{-value} = 0.003$; HM: CR = 1.0360, $P\text{-value} = 0.003$; HF: CR = 1.0355, $P\text{-value} = 0.003$). So, FW and HW venations shows a similar modularity pattern, opposing the edge of the wing of the central disc.

Evolution of sexual dimorphism in hindwing and forewing

The shape sexual dimorphism was 1.46 smaller for forewing (0.042 ± 0.003) than on hindwing shape (0.062 ± 0.061), considering the configurations of homologous LM across wings (Figure 4). The forewing and hindwing dimorphism were weakly but

significantly correlated (Phylogenetic Pearson's coefficient = 0.30, $df = 266$, P -value < 0.001). We didn't detect significant phylogenetic signal for dimorphism in forewings ($K = 0.199$, $P = 0.051$) but we did for hindwings ($K = 0.314$, $P < 0.05$). Sexual selection and /or sexually different selective forces acting on the different sexes might contribute to the more heterogeneous evolution of hindwing shape as compared to forewings.

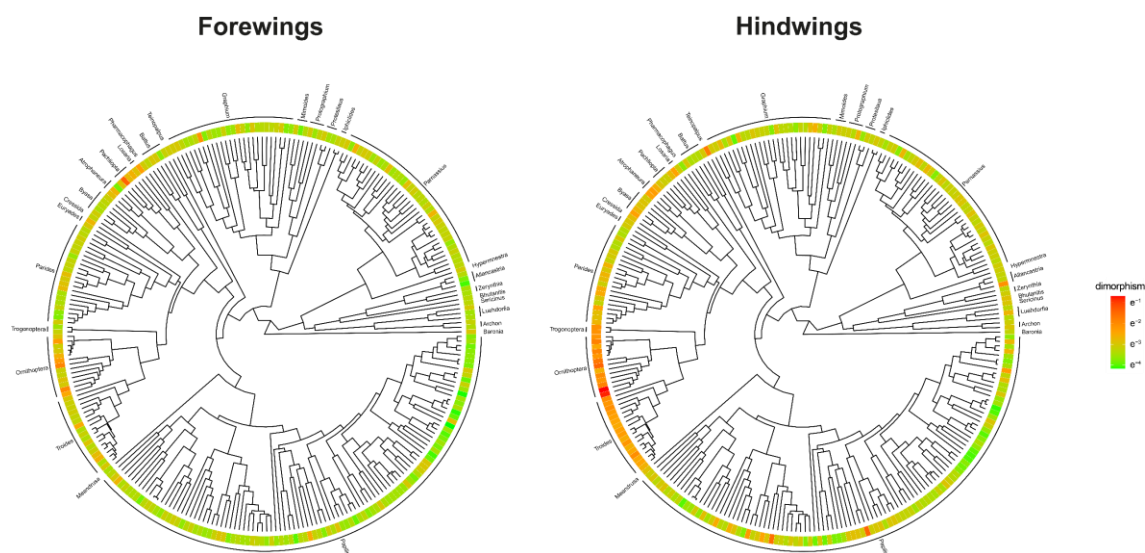


Figure 4: Sexual dimorphism for forewing and hindwing shape ($n = 268$ species). Dimorphism is expressed as the Euclidian distance between male and female average phenotype in the morphospace (defined by homologous LM).

Testing for the effect of wing shape variation on species diversification?

No correlation was detected between diversification rates and wing shape evolutionary rates (FM: $r = 0.0251$, $P = 0.64$; FF: $r = -0.13$, $P = 0.58$; HM: $r = 0.20$, $P = 0.68$; HF: $r = 0.42$, $P = 0.24$). Nevertheless, the MCMC analysis of the BiSSE model applied to the presence/absence of the tail on the hindwing inferred significantly higher speciation rates for species with hindwing lacking tails, resulting in higher net diversification in lineages without tails (results for males in Supplementary 8, in Supplementary 9 for females, tables in Supplementary 10 & Supplementary 11). The same results are found using HiSSE (Supplementary 12, tables in Supplementary 13 & Supplementary 14).

Multiple emergences and losses of hindwing tail

The number of inferred shifts for tail evolution ($n\text{-shift} = 56.45 \pm 5.73$) was largely higher than expected under a Brownian motion (Figure 5 for males, see females in Supplementary 15). We also counted many speciation events associated with each of the states, respectively 226 for tailed state and 181 for untailed state (Supplementary 16).

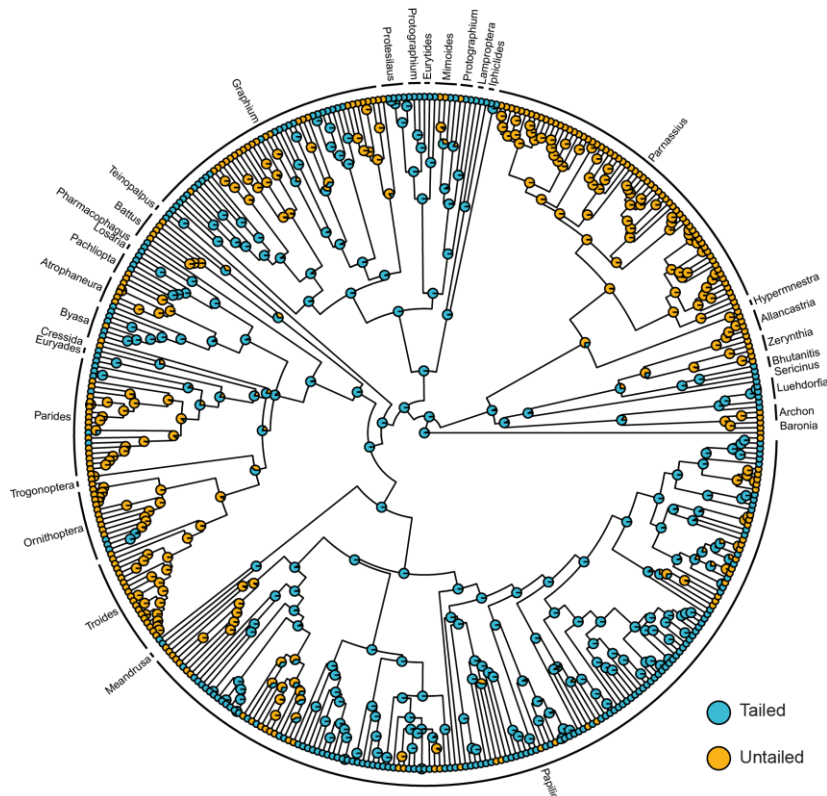


Figure 5: Evolution of tails on the hindwings in Papilionidae. The presence and absence of tails on the hindwings in the different species is shown in blue and orange respectively. Ancestral state estimation from BiSSE based on the best-fitting diversification model ($n\text{-species} = 408$ species, estimate from male forms, see **Supplementary 15** for female forms). The ancestor of Papilionidae is inferred as tailed. Untailed lineages appeared recently and multiple times across the phylogeny.

Focusing on the evolution of tails, we detected a significant phylogenetic signal for tail presence ($D: -0.031$; Probability of E(D) resulting from no (random) phylogenetic structure: 0; Probability of E(D) resulting from Brownian phylogenetic structure: 0.613), but also for tail length TL (Males: $K = 0.51$, $P < 0.001$; Females: $K = 0.41$, $P < 0.001$). We didn't find any significant difference between males and females TL ($t\text{-value} = 1.75$, $df = 267$, $P\text{-value} = 0.08$)

The disparity-through-time plots for the Tail presence, *TL* and *AR* revealed a significant increase in disparity during the recent evolutionary history of family (Figure 6). This excess of disparity indicates that related species are more different from each other than expected under neutral evolution.

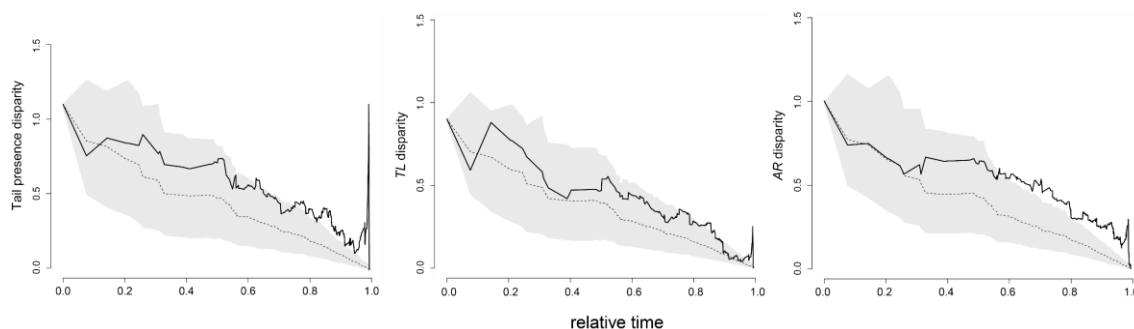


Figure 6: Disparity-through-time for Tail presence, *TL* and *AR* in relative time (from -70Ma to present). Solid black lines represent the observed disparity, while the dotted lines and shaded grey interval represent the median and 95% confidence intervals from BM simulations, respectively.

The emergence and losses of hindwing tail might play a role in specialisation into different micro habitat, and could in turn impact the evolution of the forewing by imposing different aerodynamic effects during flight.

Testing the effect of hindwing tail on the forewing shape

We found a significant correlation between forewing and hindwing average shape of males ($r\text{-PLS} = 0.286$, $P < 0.001$) and females ($r\text{-PLS} = 0.356$, $P < 0.001$) – see Supplementary 17 & 18 for details. Procrustes regression showed a significant effect of *TL* on FW shape (Table 2).

Table 2: Results of the Procrustes regression between forewing shape and *TL* in Papilionidae species.

	Variable	Forewing Male					Forewing Female				
		<i>Df</i>	<i>SS</i>	<i>MS</i>	<i>F</i>	<i>P</i>	<i>Df</i>	<i>SS</i>	<i>MS</i>	<i>F</i>	<i>P</i>
Phylogenetic Procrustes regression	<i>TL</i>	1	0.001	0.001	2.541	0.021 *	1	0.001	0.001	4.422	0.007 **
	Residuals	326	0.074	0.000			269	0.058	0.000		
Non-phylogenetic Procrustes regression	Variable	<i>Df</i>	<i>SS</i>	<i>MS</i>	<i>F</i>	<i>P</i>	<i>Df</i>	<i>SS</i>	<i>MS</i>	<i>F</i>	<i>P</i>
	<i>TL</i>	1	0.185	0.185	23.946	0.001 **	1	0.174	0.174	26.072	0.001 **
	Residuals	326	2.517	0.008			269	1.797	0.007		

The presence of hindwing tails has a strong effect on forewing shape, but this effect becomes non-significant when controlling for phylogenetic distances (Table 3).

Table 3: Results of the Procrustes ANOVA between forewing shape and tail presence in Papilionidae species.

	Variable	Forewing Male					Forewing Female				
		<i>Df</i>	<i>SS</i>	<i>MS</i>	<i>F</i>	<i>P</i>	<i>Df</i>	<i>SS</i>	<i>MS</i>	<i>F</i>	<i>P</i>
Phylogenetic Procrustes ANOVA	Tail presence	1	0.000	0.000	1.312	0.227	1	0.001	0.001	2.525	0.050
	Residuals	326	0.074	0.000			269	0.059	0.000		
Non-phylogenetic Procrustes ANOVA	Variable	<i>Df</i>	<i>SS</i>	<i>MS</i>	<i>F</i>	<i>P</i>	<i>Df</i>	<i>SS</i>	<i>MS</i>	<i>F</i>	<i>P</i>
	Tail presence	1	0.163	0.163	20.924	0.001 **	1	0.164	0.164	24.394	0.001 **
	Residuals	326	2.539	0.008			269	1.808	0.007		

For tail presence, non-phylogenetic ANOVA showed a significant effect on *AR* (results for females in Figure 7, see Supplementary 19 for males, details in

Table 4), and this effect remained significant when corrected by phylogeny, but only in females. Note that this males/females difference is not related to the different sample size for each sex: the same analysis conducted for males considering only the species common with females gives the same results.

Table 4: Results of the ANOVA between *AR* and tail presence in Papilionidae species.

	AR Males				AR Females					
		<i>Estimate</i>	<i>StdErr</i>	<i>t value</i>	<i>P</i>		<i>Estimate</i>	<i>StdErr</i>	<i>t value</i>	<i>P</i>
Phylogenetic ANOVA	Intercept	1.6493	0.2564	6.4321	< 0.001 ***	Intercept	1.5183	0.2388	6.3569	< 0.001 ***
	<i>Tail presence</i>	-0.0333	0.0367	-0.9050	0.3662	<i>Tail presence</i>	-0.0961	0.0404	-2.3811	< 0.05 *
	<i>Centroid size FW</i>	0.0053	0.0023	2.2824	< 0.05 *	<i>Centroid size FW</i>	0.0071	0.0021	3.4132	< 0.001 ***
Non-phylogenetic ANOVA	Intercept	1.6269	0.0709	22.9340	< 0.001 ***	Intercept	1.6321	0.0629	25.9390	< 0.001 ***
	<i>Tail presence</i>	-0.1396	0.0367	-3.8080	< 0.001 ***	<i>Tail presence</i>	-0.2024	0.0369	-5.4840	< 0.001 ***
	<i>Centroid size FW</i>	0.0055	0.0017	3.1560	< 0.01 **	<i>Centroid size FW</i>	0.0048	0.0014	3.4140	< 0.001 ***

For *TL*, non-phylogenetic regression showed a significant effect on *AR*, but this effect becomes non-significant when controlling for phylogenetic distances (results for females in Figure 7, see Supplementary 19 for males, details in

Table 4 & Table 5).

Table 5: Results of the regression between *AR* and *TL* in Papilionidae species.

	AR Males				AR Females					
		<i>Estimate</i>	<i>StdErr</i>	<i>t value</i>	<i>P</i>		<i>Estimate</i>	<i>StdErr</i>	<i>t value</i>	<i>P</i>
Phylogenetic regression	Intercept	1.6435	0.2581	6.3683	< 0.001 ***	Intercept	1.4991	0.2410	6.2195	< 0.001 ***
	<i>TL</i>	-0.2238	0.6477	-0.3456	0.7299	<i>TL</i>	-0.5698	0.6456	-0.8826	0.3783
	<i>Centroid size FW</i>	0.0052	0.0023	2.2545	< 0.05 *	<i>Centroid size FW</i>	0.0070	0.0021	3.3646	< 0.001 ***
Non-phylogenetic regression	Intercept	1.6556	0.0720	22.9970	< 0.001 ***	Intercept	1.6510	0.0649	25.4270	< 0.001 ***
	<i>TL</i>	-2.2320	0.5298	-4.2130	< 0.001 ***	<i>TL</i>	-2.9893	0.5922	-5.0470	< 0.001 ***
	<i>Centroid size FW</i>	0.0052	0.0017	3.0100	< 0.01 **	<i>Centroid size FW</i>	0.0047	0.0014	3.3150	< 0.01 **

While the effect of hindwing tail on forewing shape tends to be weak at this large macroevolutionary scale, on the contrary in the *Graphium* clade where we observed several transitions between tailed and untailed hindwings (see Figure 5), the forewing *AR*, in turn, was strongly impacted by the presence of a tail, and depended on its length: species with long tails tended to present low *AR* forewings (see results for females Figure 7, for males see Supplementary 19 - tables in Supplementary 20 & 21). Nevertheless, this trend was not observed in the *Papilio* clade, where a lot of transitions between tailed and untailed hindwings also happened. In the *Papilio* clade the tail presence and *TL* had weak effects on the forewing shape and *AR*. The contrasted results in these two clades

confirms that the evolution of wing shape is clearly heterogeneous across clades, as is the covariation between the two pairs of wings.

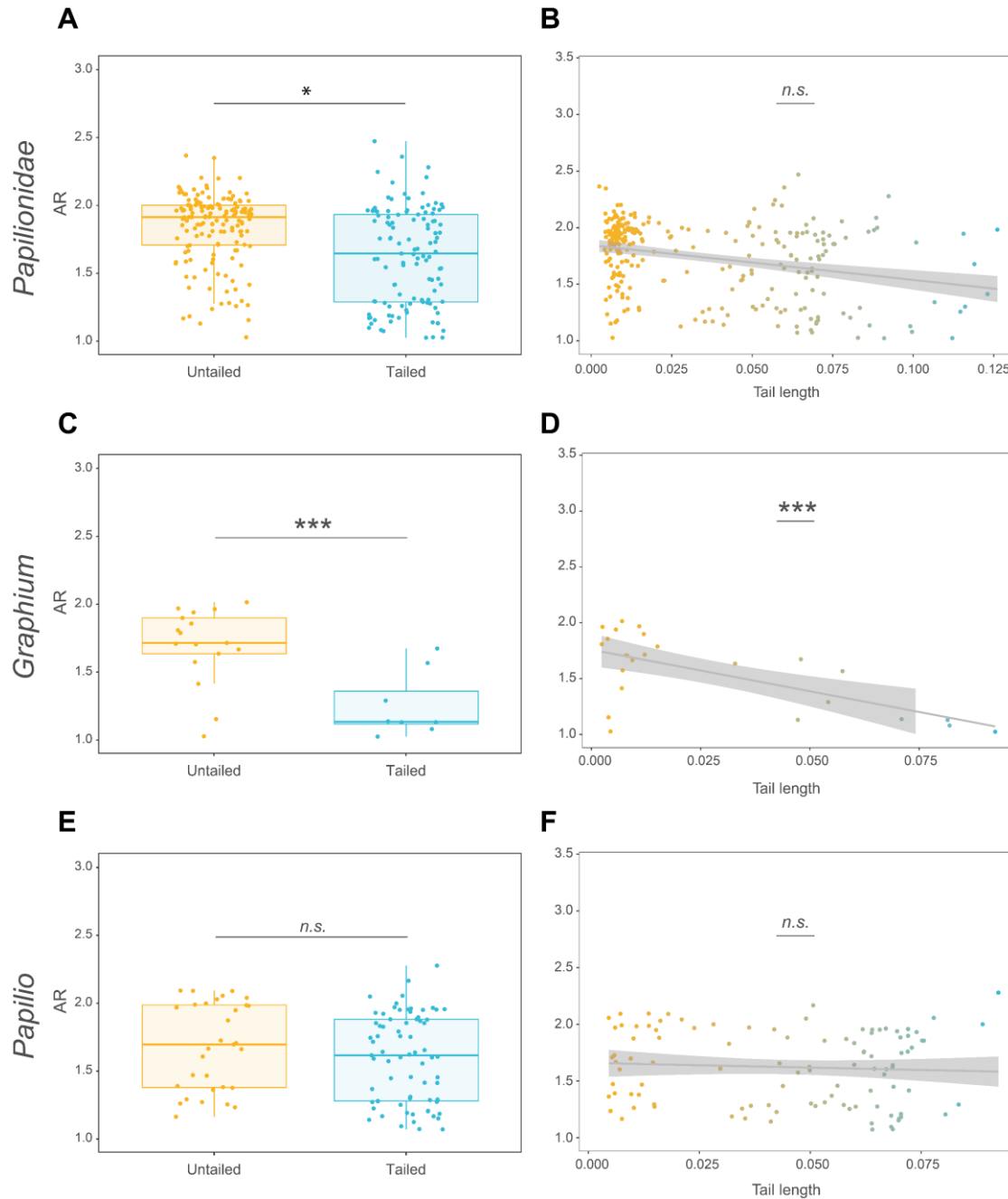


Figure 7: Difference of AR females between Untailed and Tailed species in (A) Papilionidae (n -species = 270 species), (C) *Graphium* (n -species = 24 species), (E) *Papilio* (n -species = 103 species). Difference of AR according to TL in (B) Papilionidae, (D) *Graphium*, (F) *Papilio*. Significance of the results from phylogenetic regression/ANOVA are displayed.

Discussion

Contrasted evolution of forewings and hindwings: a signature for different selection regimes?

Our study on macro-evolutionary patterns of shape variation in Papilionidae revealed that forewing shape was much less diversified than hindwing shape. Forewing variations among species was indeed associated with a stronger phylogenetic signal and a slower evolutionary rate. The forewing shape DTT was also lower than expected under a neutral model, suggesting convergent evolution of shape, potentially driven by stabilizing selection (with one fitness optimum), especially at the beginning of the evolutionary history. In contrast, hindwing shape DTT was higher than expected under a Brownian model of evolution, suggesting a heterogeneous selection, with many optima. This difference was reflected in 3.5 higher number of phenotypic shifts observed in hindwing shape evolution as compared to forewings. This difference of evolution between the two wing pairs suggested different selection regimes, in agreement with the results previously obtained in other butterflies, *e.g.*, *Papilio* (Owens *et al.*, 2020) and in Ithomiini and Heliconiini butterflies (Strauss, 1990).

In butterflies, flight abilities have been involved in crucial behaviours, including feeding, finding mates and host plants, likely imposing a strong selection on wing shape. The strength of this selection likely varied with the aerodynamic effects generated by the different wing parts. The lower diversity of the forewing shape thus suggested a higher importance of forewings for flight, in agreement with the hypothesis of a predominantly anteromotoric flight in butterflies (Dudley, 2002; Jantzen and Eisner, 2008).

Although less diversified than hindwings, forewings nevertheless displayed some sharp differences among genera: for example, *Parnassius* species forewing shape was strikingly divergent from all other Papilionidae species, with a rounder outline. Because most *Parnassius* species have a mountainous distribution, such divergence may reflect a particular adaptation to flight in high altitude. In the genus *Heliconius* for instance, species with a geographic range with higher altitude displayed rounder wings as compared to closely-related species observed in lowland habitats (Montejo-Kovacevich *et al.*, 2019).

The high diversity of hindwing shape, mostly driven by the evolution of tails, suggested a higher diversity of selective pressures involved. Although little is known about the aerodynamic importance of hindwings, a stabilizing effect of tails on gliding flight was reported by [Park *et al.*, \(2010\)](#). Selection promoting gliding flight may have then favoured the evolution of tails. Gliding flight is an energy-saving flight mode. This gliding flight behaviour could be specifically promoted in species where long-distance flights are commonly observed, like in migrating ([Altizer and Davis, 2009](#); [Dockx, 2007](#)) or extensively-patrolling butterflies ([Berwaerts *et al.*, 2002](#); [Cespedes *et al.*, 2015](#); [Le Roy *et al.*, 2019a](#)). Here, the frequent gains and losses of tails observed throughout the diversification of Papilionidae may reflect the contrasted importance of gliding flight across species, shaped by their different ecologies.

Contrasted predation pressures may have promoted the diversity of hindwing shapes. A recent experiment on the Papilionidae butterfly *Iphiclides podalirius* suggested a deflecting effect of tails, suggesting that predator behaviour may have promoted the evolution of tails enhancing butterfly survival after an attack ([Chotard *et al.*, 2022](#)). Beak marks observed in wild Papilionidae have suggested that these butterflies were submitted to a particularly strong predation pressure ([Kiritani *et al.*, 2013](#); [Ota *et al.*, 2014](#)). The strength of predation pressure was likely different across species, and a heterogeneity in predation pressure may have also explained the frequent gain and loss of tails and the diversity of their size and shape.

Selection imposed by predators may have also affected different parts of the wings differently. The low integration of hindwings is consistent with a heterogeneous selection affecting hindwings. The deflective effect of tails indeed implied a particular selection on the posterior, distal part of the wing, as opposed to the anterior part. Such heterogeneous selection across the hindwing may have decreased its integration. Theory indeed predicts a reduced integration in structures whose parts are submitted to different selective pressures (*e.g.*, [Breuker *et al.*, 2006](#); [Wagner and Altenberg, 1996](#)).

Our study also highlighted a higher level of sexual dimorphism in hindwing than forewing shape. Sexual selection and /or different selective forces acting on the two sexes may have contributed to the more heterogeneous evolution of hindwing shape. Tail length was

generally not sexually dimorphic in our study, suggesting that tails were not sexually selected and do not trigger the higher dimorphism of hindwing shape. This result matched recent findings on *Papilio machaon*, showing that dimorphism of tails was fully explained by allometry (Koutrouditsou and Nudds, 2021). The female-limited mimicry founded in many species of Papilionidae (e.g., Kunte, 2009) could also contribute to dimorphism. The prevalence of aposematic signals on the hindwings of chemically-defended species (e.g., genus *Pachliopta*), including both wing colour patterns and shape, may have explained the higher sexual shape dimorphism of the hindwings.

Wing shape and species diversification, a relative independence

One of our hypotheses was that wing shape could be causally linked to an increased diversification rate. This hypothesis was based on the “key innovation” concept (Heard and Hauser, 1995). Nevertheless, our analyses have not been able to demonstrate such an effect in Papilionidae wing shape. This result could be explained by the complex nature of our trait of interest. First, wing shape are defined by high-dimensional object, that are not supported by current methods for diversification analysis. We were forced to degrade our dataset, and to use only the first dimension of our PCA as proxy of our shape. This methodological choice greatly reduces the amount of shape variance accounted for in the models. Second, wing shape are subject to multiple selection pressures, whose variations implications in terms of fitness are not unidirectional. A homogeneous signal at family level is therefore not necessarily a likely scenario.

Co-evolution of forewing and hindwing shape: an aerodynamic effect?

In a previous study carried out on Papilionidae butterflies, it has been suggested that the two pairs of wings likely diversified independently (Owens *et al.*, 2020). While our analyses detected different patterns of diversification consistent with contrasted selective regimes, they nevertheless showed a significant correlation between forewing and hindwing shapes. This correlation remained significant when accounting for phylogenetic structure, suggesting that the co-diversification of both wings could stem from a joint selection acting on both wings. The length of the tail significantly affected forewing shape, and the presence of the tail was associated with a lower forewing aspect ratio, especially in females. These results clearly showed that the two wing types coevolve in Papilionidae.

The negative association between forewing AR and hindwing tails suggest an aerodynamic effect of tails that might modify the selective pressures affecting forewing shape.

In birds, sexually-selected elongated tails have been suggested to decrease flight performance by increasing drag, thereby incurring metabolic costs (e.g., Evans and Thomas, 1992; Thomas, 1993; Clark and Dudley, 2009). This aerodynamic cost was suggested to be compensated by an increased wingspan (Evans and Thomas, 1992; Swallow and Husak, 2011). In butterflies, considering that low AR wings were associated with fast manoeuvrable flapping flight, the reduced AR of tailed Papilionidae species may have indicated a compensation of an increased drag induced by the tails during flapping flight. This hypothesis should be tested by quantifying the effect of tails upon flapping flight, and comparing tailed and untailed species, or phenotypically manipulated individuals.

The association between tails and reduced forewing AR might also be interpreted through its effect on gliding flight performances. According to Park *et al.*, (2010), tails improved gliding flight by enhancing lift and stability, both characteristics also favoured by high forewing AR . The absence of tails would have thus induced a decrease in gliding flight performance, that could be compensated by long and narrow forewings. However, this effect of tails on butterflies gliding performances has only been investigated in a single species of Papilionidae, using a rigid model placed in a wind tunnel.

The co-evolution of the two pairs of wings, and in particular of hindwing tails and forewing AR could be further complicated by the deflection effect of tails. Attack deflection paradoxically implies that tails will often be lost through failed predation attempts. The evolution of the forewing shape would thus depend on the aerodynamic effects of the presence of tails but also of their sudden absence, possibly favouring intermediate forewing shapes.

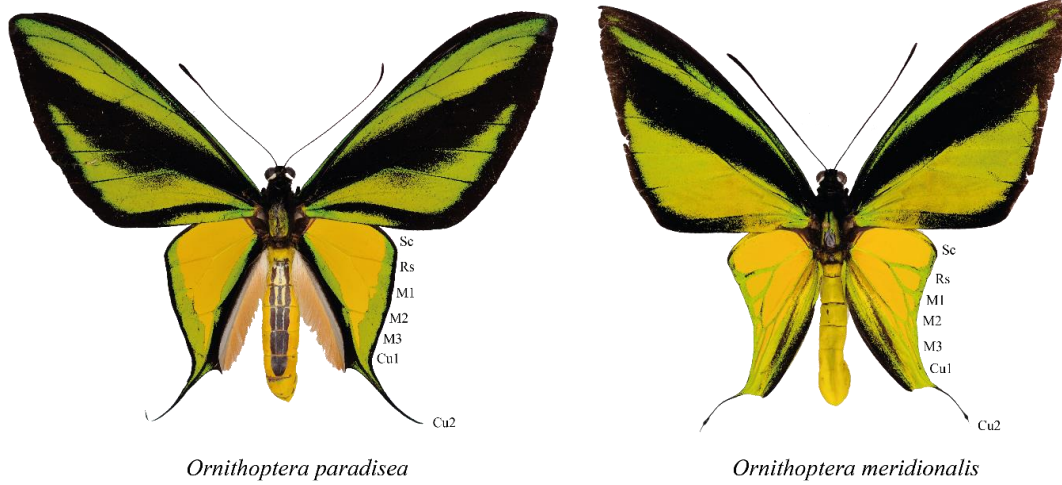
Interestingly, the covariation between tails and forewing shape was lost when considering the genus *Papilio* only, but was stronger in the genus *Graphium*. While tails seem to have evolved and regressed several times in both *Papilio* and *Graphium* (Figure 5), the factors

affecting their evolution might be different in these two genera. For example, mimicry is extremely common in *Papilio* (Kunte, 2009; Zakharov *et al.*, 2004), but rare in *Graphium*. While tail evolution might mostly stem from mimetic interactions with defended species in *Papilio*, tail evolution is more likely to be linked to predator deflection in *Graphium*. These contrasted selection regimes are likely to affect the coevolution of hindwing tails and forewing shape.

Generally, selection on flight is likely to be very different across species, depending on their ecology, with strong consequences on patterns of evolution of hindwing and forewing shape. Such a heterogeneity of signal across phylogenetic scales makes the identification of precise adaptive causes to large scale patterns of morphological diversity highly challenging. Nevertheless, our study on Papilionidae showed that the combination of behavioural ecology data and macro-evolutionary studies might shed light on key factors affecting morphological evolution.

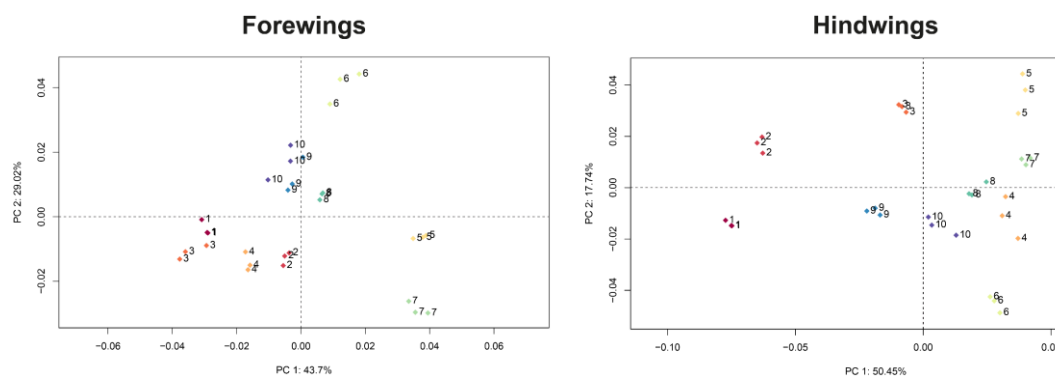
Supplementary

Supplementary 1: *Ornithoptera paradisea* and *Ornithoptera meridionalis* photograph. These two species display tail on Cu2 vein.



Supplementary 2: Preliminary analyses: repeatability and allometry

To check the repeatability of our measurements, a sub-sample of 10 individuals of the same species was measured 3 times. Individuals from the same species were used to ensure that ME was negligible relative to the interspecific signal used in our study. We then conducted a principal component analysis (PCA) to check the morphological distances between measures of a same individual were smaller than inter-individual differences. The validation of this condition (**Error! Reference source not found.**) allowed us to validate our protocol.



PCA repeatability check. Each number correspond to an individual (n=10 individuals).

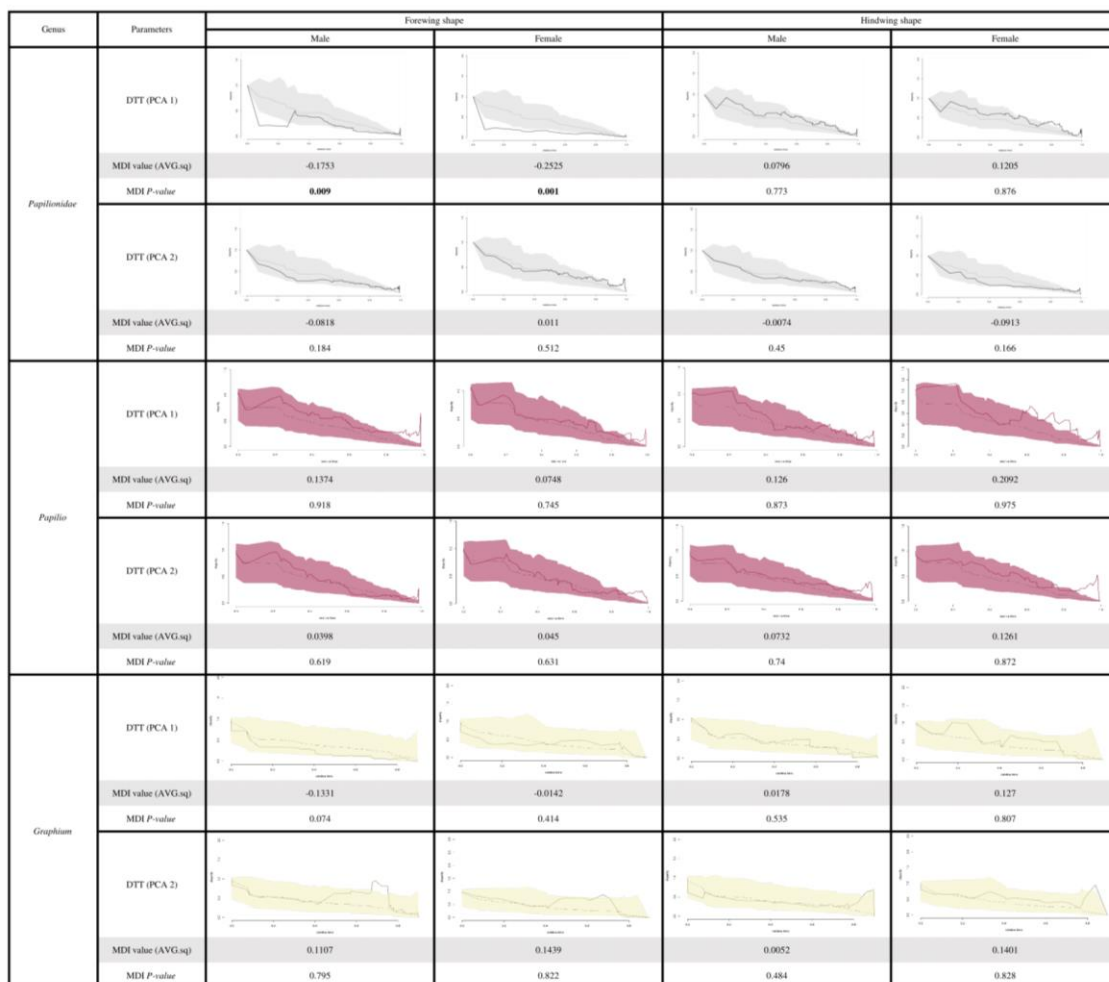
To assess whether larger butterflies tended to display a different shape (allometric shape variation), we used a phylogenetic regressions of average shape on average centroid size per species and sex (function *procD.pgls* R package *geomorph* - Adams and Otárola-Castillo 2013). A significant correlation was detected for both wings in both sexes (Forewings, Males $Df = 1$, $F = 5.584$, $P < 0.001$; Females: $Df = 1$, $F = 5.1721$, $P < 0.001$; Hindwings, Males: $Df = 1$, $F = 33.273$, $P < 0.001$; Females: $Df = 1$, $F = 30.945$, $P < 0.001$), suggesting allometric effects. So, we added the size as fixed effect in all of our analyses of wing shape.

Supplementary 3: BiSSE models

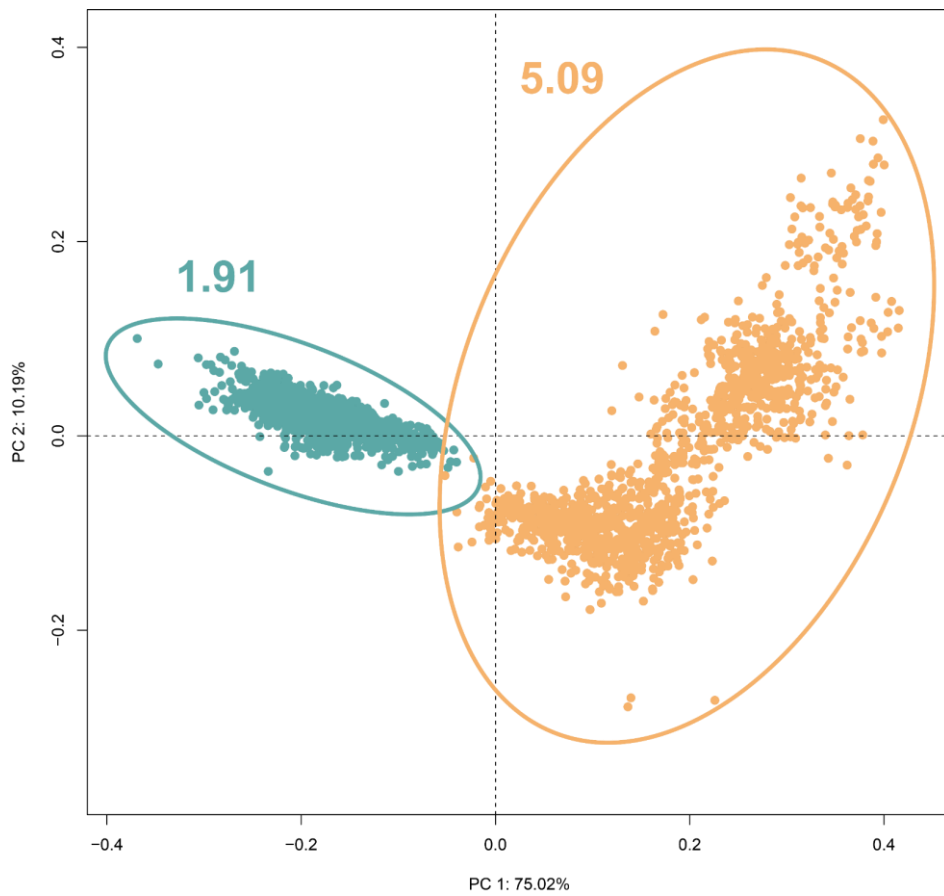
To quantify the evolution of the presence (“Tailed” state, noted “T”) / absence (“Untailed” state, noted “U”) of tail along the phylogeny and the diversification rates associated to each trait state, we applied a series of birth–death models. First, we fitted Binary State Speciation and Extinction (BiSSE) models as implemented in the R package *diversitree*, (FitzJohn 2012) and Hidden State Speciation and Extinction (HiSSE) models as implemented in the R package *hisse* (Beaulieu and O’Meara 2016).

The BiSSE model has six distinct parameters: two speciation rates without character change (*i.e.*, without morphological shift) associated with untailed hindwings (hereafter “U”, λ_U), or with tailed hindwings (hereafter “T”, λ_T), two extinction rates associated with untailed (μ_U) and tailed (μ_T) species, and two transition rates (*i.e.*, morphological shift) with one from untailed to tailed ($q_{U \rightarrow T}$), and from tailed to untailed ($q_{T \rightarrow U}$). Net diversification rates, denoted as $D = \text{speciation } (\lambda) - \text{extinction } (\mu)$, were then computed (D_U and D_T for diversification rates associated with untailed and tailed species respectively). We used the functions *make.bisse* to construct the likelihood function of the model based on the data, and the functions *constrain* and *find.mle* to apply different diversification scenarios going from the most simple (all rates are equal, no effect of the trait) to the most complex model (each rate is free to vary). To limit the biases related to the reconstruction of the molecular phylogeny, we conducted our analyses across 100 randomly sampled trees from the BEAST posterior distribution. We optimized the fit of all models using maximum likelihood and evaluated model performance using the corrected Akaike information criterion (AICc). For the best fitting model, we used the maximum clade credibility tree of Papilionidae and a Markov Chain Monte Carlo (MCMC) approach to examine the confidence interval of the parameter estimates. Following the recommendations from FitzJohn (2012), we used an exponential prior $1/(2r)$ and started the chain with the parameters obtained by maximum likelihood. We ran 20,000 steps of MCMC and applied a burn-in of 2,000 steps.

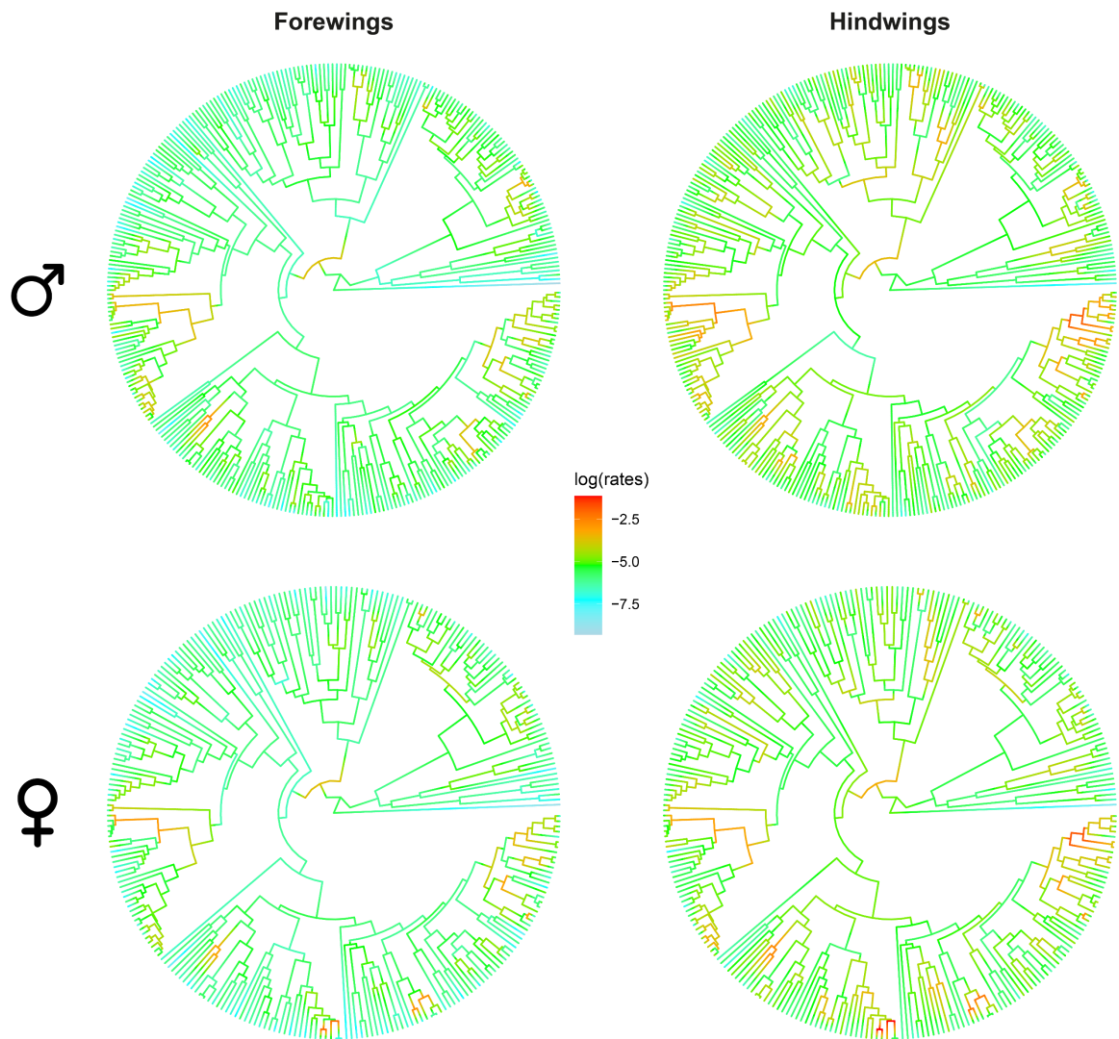
Supplementary 4: Disparity Through Time of FW and HW average shape (the top two PCA dimensions) for all Papilionidae (male forms, $n = 328$ species; female forms, $n = 270$ species), *Papilio* genera (male forms, $n = 129$ species; female forms, $n = 103$ species) and *Graphium* genera (male forms, $n = 37$ species; female forms, $n = 24$ species).



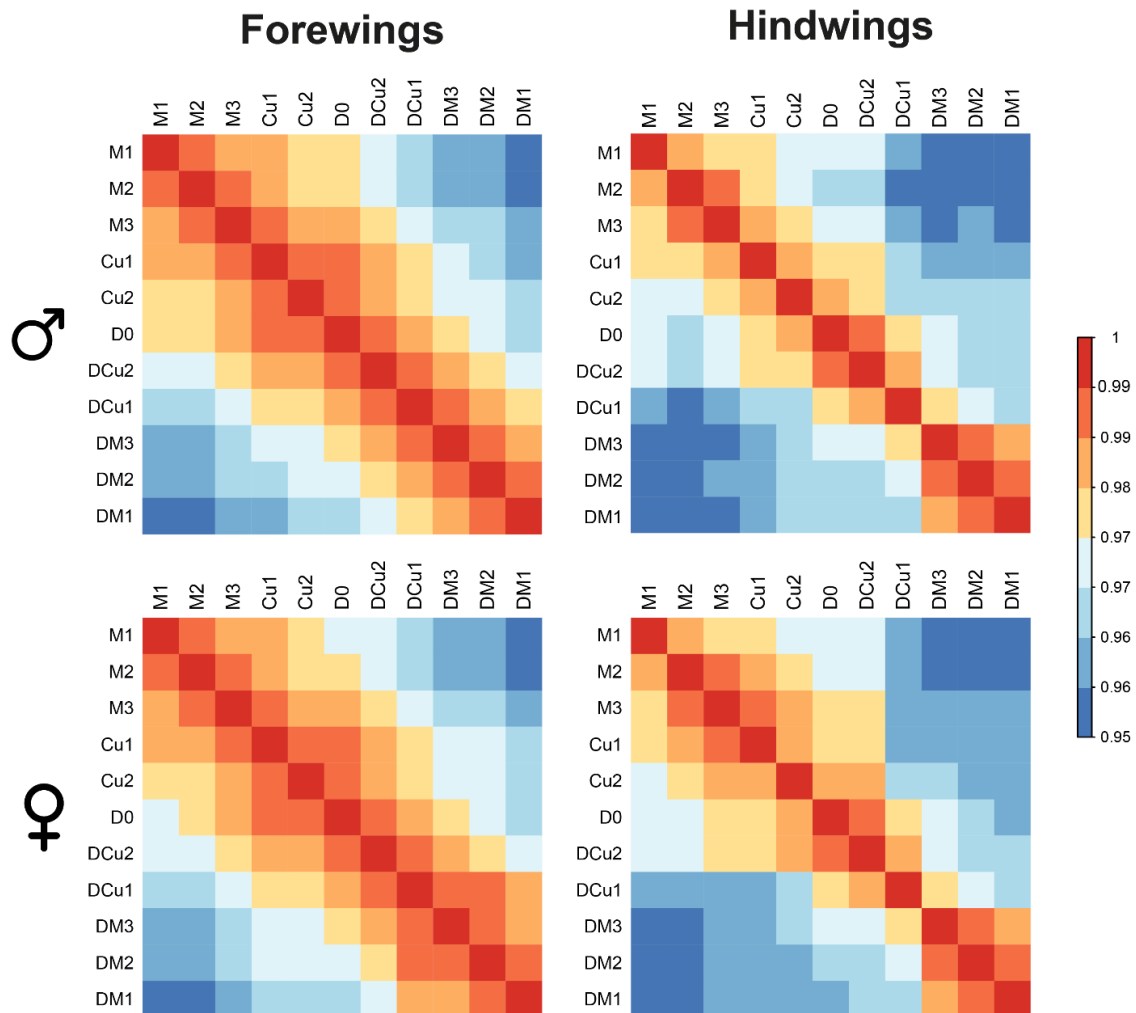
Supplementary 5: PCA performed on the 11 landmarks considered as developmentally homologous between forewing and hindwing (all individuals sex combined, $n = 1318$). The variation in shape of forewings and hindwing respectively was estimated by the centroid size of the corresponding cloud of dots in the PCA space.



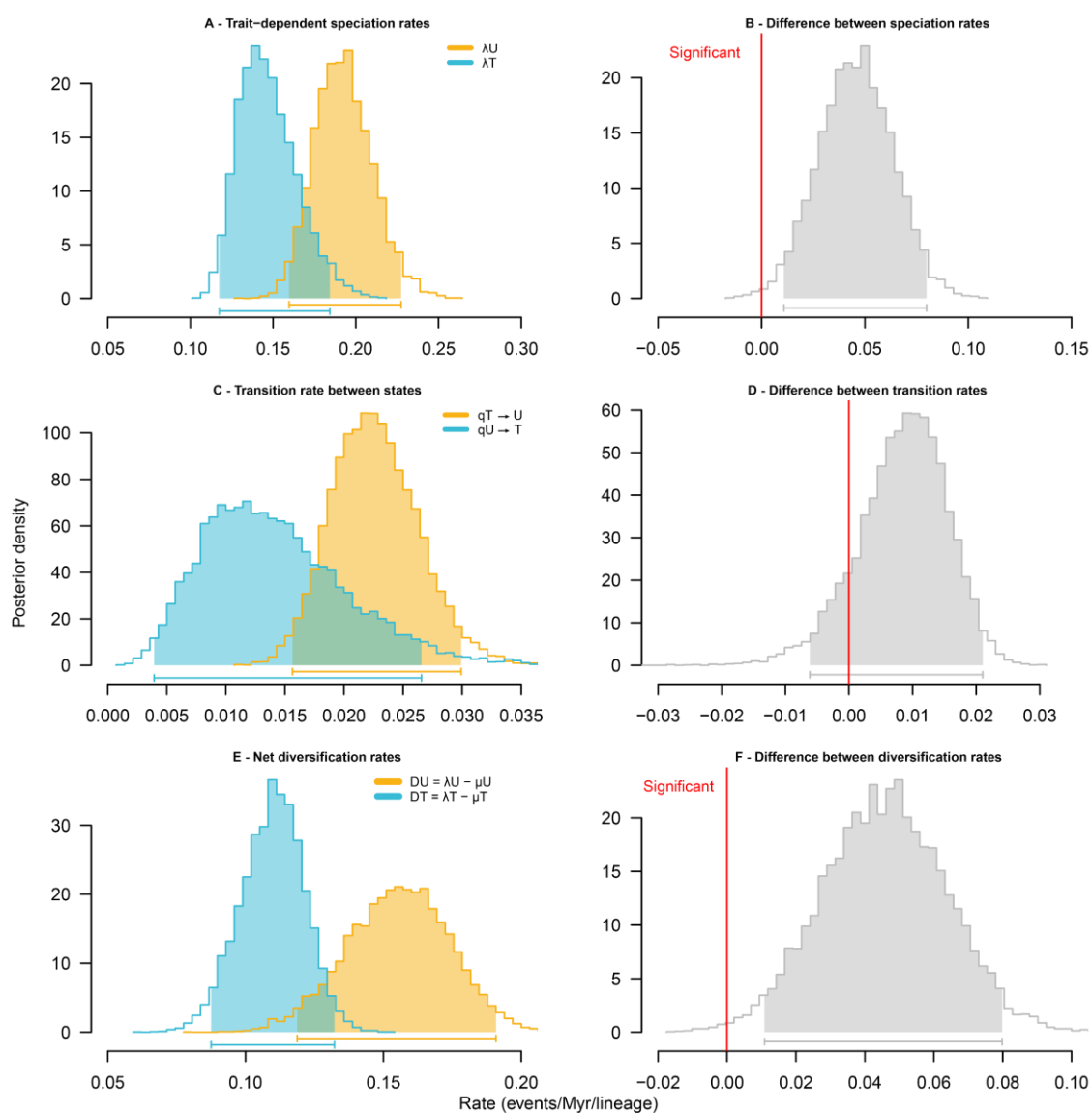
Supplementary 6: Evolution rate of forewing and hindwing shape



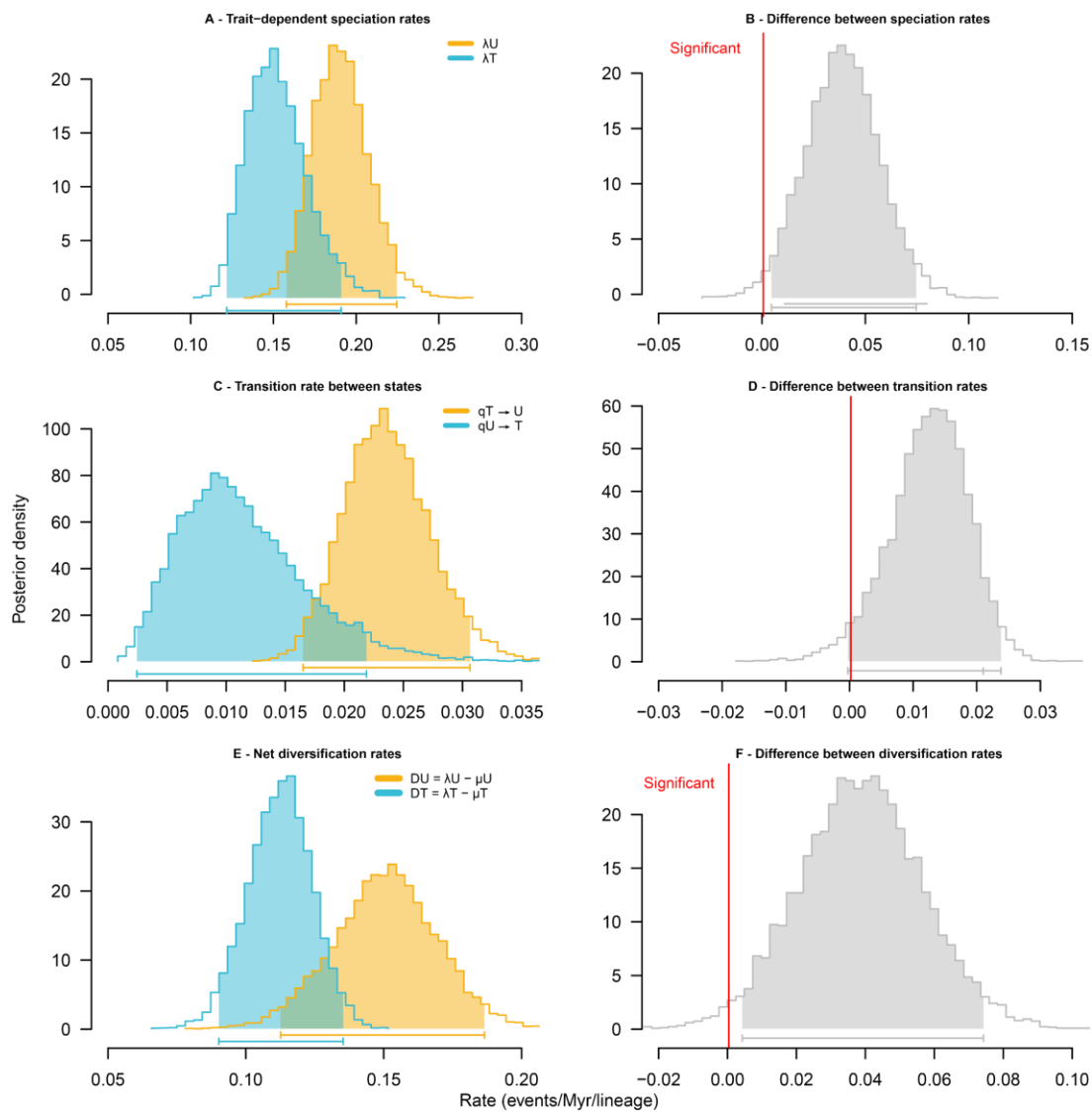
Supplementary 7: Contrasted patterns of modularity observed in FW and HW venation, assessed by correlation matrices of homologous LM.



Supplementary 8: Posterior distributions of trait-dependent (A) speciation, (C) transition between states « Tailed » (T) and « Untailed » (U), (E) diversification as estimated by the best fitted model from BiSSE (lambda q free = with equal extinction rates between the « Tailed » and « Untailed » states). Colours correspond to the states « Tailed » (blue) and « Untailed » (orange). Each posterior distribution is compared to a neutral distribution (Brownian motion), the significance of the comparison is mentioned if verified. Results for 408 species, male forms.



Supplementary 9: Posterior distributions of trait-dependent (A) speciation, (C) transition between states « Tailed » (T) and « Untailed » (U), (E) diversification as estimated by the best fitted model from BiSSE (lambda q free = with equal extinction rates between the « Tailed » and « Untailed » states). Colours correspond to the states « Tailed » (blue) and « Untailed » (orange). Each posterior distribution is compared to a neutral distribution (Brownian motion), the significance of the comparison is mentioned if verified. Results for 408 species, females forms.



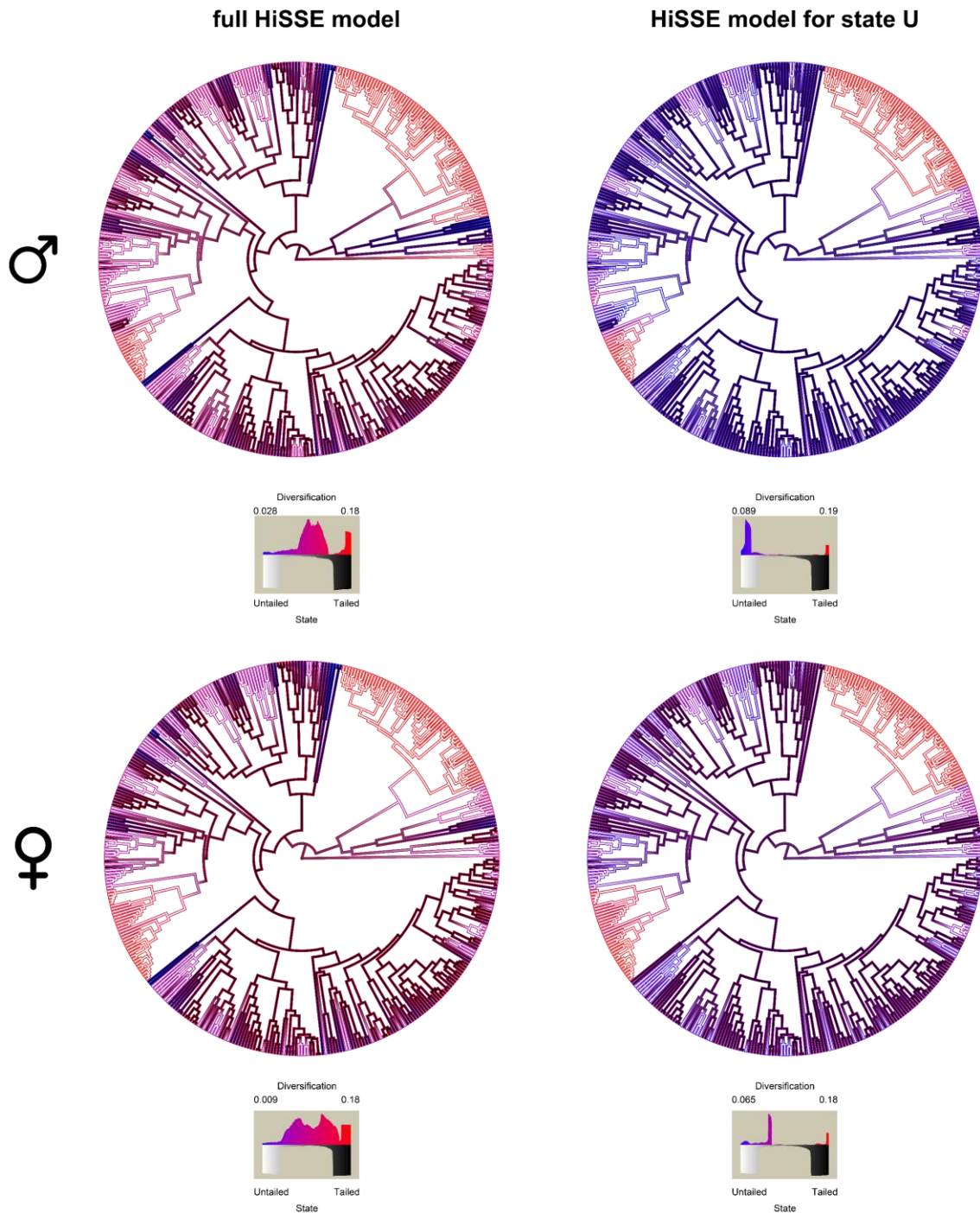
Supplementary 10: Model comparison for the BISSE analyses (male forms, $n = 408$ species). In BISSE the parameters are λ speciation and μ extinction in the « Tailed » (T) and « Untailed » (U) species, as well as q transitions from the Tailed to Untailed state (qTU), and from Untailed to Tailed state (qUT). We denote NP= number of parameters; log L, the log-likelihood; AICc, the corrected Akaike Information Criterion; SE, the standard error. The best model is indicated in bold.

Model	NP	logL	AICc	λU	λT	μU	μT	$qU \rightarrow T$	$qT \rightarrow U$	SE _{logL}	SE _{AICc}	SE λU	SE λT	SE μU	SE μT	SE $qU \rightarrow T$	SE $qT \rightarrow U$
full.free	6	-1541.1641	3094.5376	0.1551	0.1071	0.046	0.0018	0.004	0.0231	9.7557	19.5114	0.0036	0.0024	0.0019	0.0003	0.0001	0.0006
λ .free	4	-1545.0515	3098.2023	0.1435	0.1104		0.0159	0.0162		9.7522	19.5044	0.0033	0.0026	0.001		0.0004	
μ .free	5	-1544.3499	3098.8491	0.1363	0.1193	0.0007	0.0315	0.0315	0.0189	9.7515	19.5029	0.0031	0.0027	0.0003	0.001	0.001	
λ , μ .free	5	-1541.6863	3093.5219	0.1403	0.1116	0.0137		0.0052	0.0189	9.7516	19.5032	0.0032	0.0026	0.001		0.0001	0.0004
μ , q .free	4	-1544.7718	3097.6429		0.1316	0.0002	0.047	0.0141		9.7543	19.5086	0.0029	0.0026	0.0001	0.0011	0.0003	
λ , q .free	5	-1543.1793	3096.5078		0.1289	0.0064	0.0364	0.0061	0.0167	9.7541	19.5081	0.0029	0.0029	0.0009	0.0011	0.0002	0.0004
Null model	3	-1548.1976	3102.4546		0.1319		0.0315	0.017	0.017	9.7596	19.5193	0.003	0.003	0.0011	0.0011	0.0004	
q .free	4	-1543.9645	3096.0282		0.1319		0.0315	0.005	0.0198	9.7596	19.5192	0.003	0.003	0.0011	0.0011	0.0001	0.0004

Supplementary 11: Model comparison for the BISSE analyses (female forms, $n = 408$ species).

Model	NP	logL	AICc	λU	λT	μU	μT	$qU \rightarrow T$	$qT \rightarrow U$	SE _{logL}	SE _{AICc}	SE λU	SE λT	SE μU	SE μT	SE $qU \rightarrow T$	SE $qT \rightarrow U$
full.free	6	-1539.9542	3092.1179	0.1546	0.1052	0.0393	0.0026	0.0061	0.0217	9.755	19.5101	0.0036	0.0024	0.0019	0.0004	0.0002	0.0005
λ .free	4	-1541.9121	3091.9236	0.1454	0.1063		0.0131	0.0161		9.7493	19.4986	0.0033	0.0025	0.0009		0.0004	
μ .free	5	-1541.5518	3093.2528	0.1398	0.1121	0.0013	0.0234	0.0234	0.0183	9.7488	19.4977	0.0031	0.0026	0.0005	0.0009	0.0009	
λ , μ .free	5	-1540.3025	3090.7542	0.1422	0.1085	0.012		0.0076	0.0183	9.7517	19.5034	0.0032	0.0025	0.0009		0.0002	0.0004
μ , q .free	4	-1542.5898	3093.2788		0.1316	0.0001	0.048	0.014		9.7544	19.5089	0.0029	0.0029	0.0001	0.0011	0.0003	
λ , q .free	5	-1542.0814	3094.312		0.1293	0.0021	0.0406	0.0092	0.0155	9.7552	19.5105	0.0029	0.0029	0.0005	0.0011	0.0003	0.0004
Null model	3	-1546.214	3098.4874		0.1316		0.0314	0.0169	0.0169	9.7603	19.5206	0.003	0.003	0.0011	0.0011	0.0004	
q .free	4	-1543.4347	3094.9686		0.1316		0.0315	0.0069	0.0195	9.7614	19.5228	0.003	0.003	0.0011	0.0011	0.0002	0.0004

Supplementary 12: Results of HiSSE analysis (male or females forms, $n = 408$ species), showing significantly higher speciation rates for species with hindwing lacking tails, resulting in higher net diversification in lineages without tails. The two best HiSSE models are displayed: the “full HiSSE model” and the “HiSSE model for state U”.



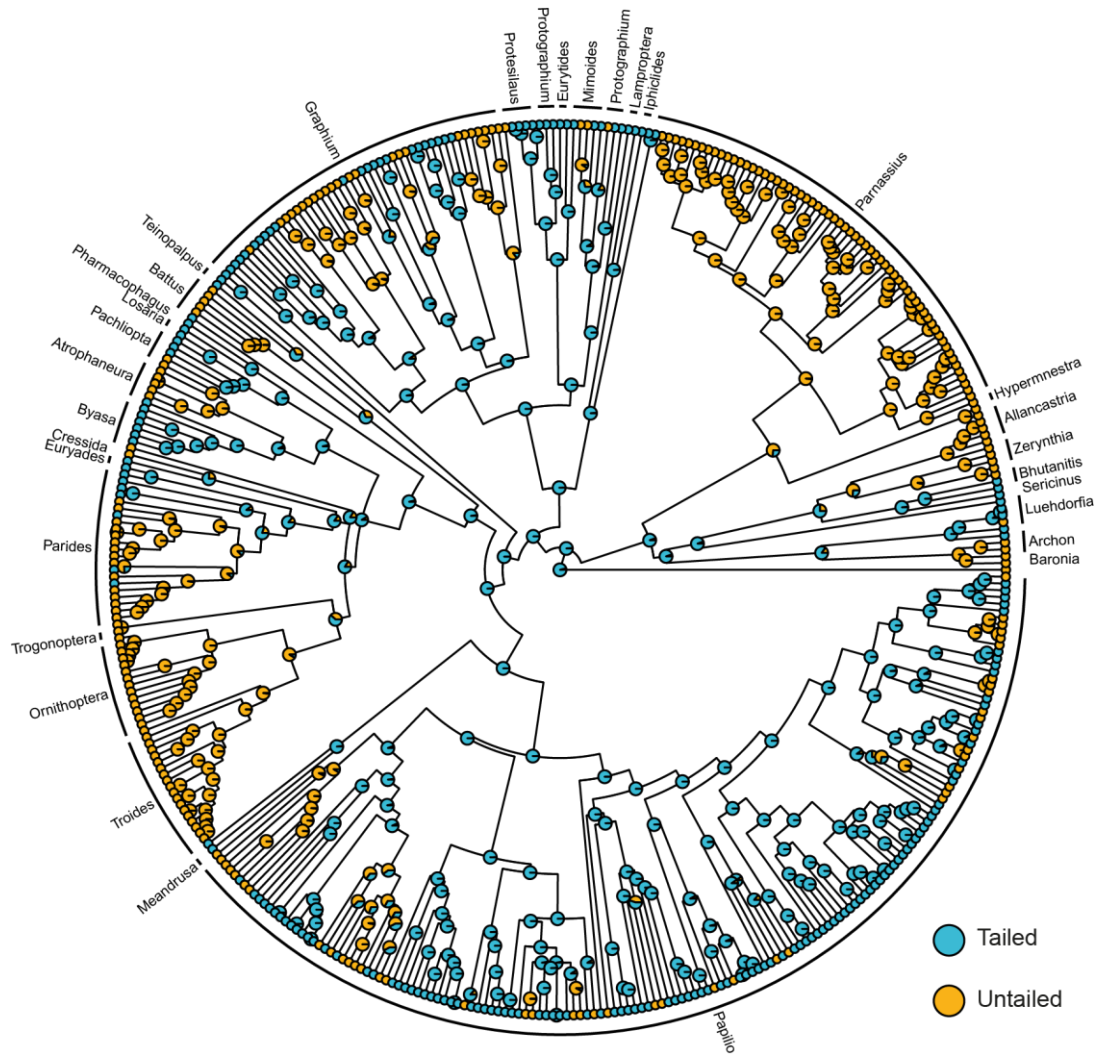
Supplementary 13: Model comparison for the HISSE analyses (male forms, $n = 408$ species). In HISSE the parameters are λ speciation and μ extinction in the « Tailed » (T) and « Untailed » (U) species, as well as q transitions from the Tailed to Untailed state (qTU), and from Untailed to the Tailed state (qUT). ‘‘A’’ and ‘‘B’’ correspond to the unmeasured factors (‘‘hidden’’ states) of the model. We denote NP= number of parameters; log L, the log-likelihood; AICc, the corrected Akaike Information Criterion; SE, the standard error. The best model is indicated in bold.

Model	NP	logL	AICc	λ_{UA}	λ_{TA}	λ_{UB}	λ_{TB}	μ_{UA}	μ_{TA}	μ_{UB}	μ_{TB}	q_{UATA}	q_{UAUB}	q_{TAUA}	q_{TATB}	q_{UBTA}	q_{UBTB}	q_{UBUA}	q_{TBTA}	q_{TBUB}
CID model	5	-1551.048	3112.246	0.027		0.134		0		0.0177		0.0056	-	0.0188	-	-	-	-	-	-
full HISSE model	6	-1554.091	3120.392	0.1365	0.0963	-	-	0.0196	0	-	-	0.0165	0.0061	0.0196	-	-	-	0	-	-
HISSE model for state U	10	-1543.183	3106.92	0.0945	0.0973	0.1922	-	0.0053	0	0	-	0.0054	-	0.0257	0.0285	-	-	-	0.0091	-
HISSE model for state T	10	-1546.457	3113.467	0.1355	0.1226	-	0.0319	0.0228	0	-	0.0127	0	0	0.0049	0	0	0.0206	-	0.0367	0.0247
full HISSE model	16	-1534.363	3102.117	0.1768	0.0412	0.0949	0.1295	0	0.0146	0	0	0	0	0.0049	0	0	0.0206	-	0.0367	0.0247

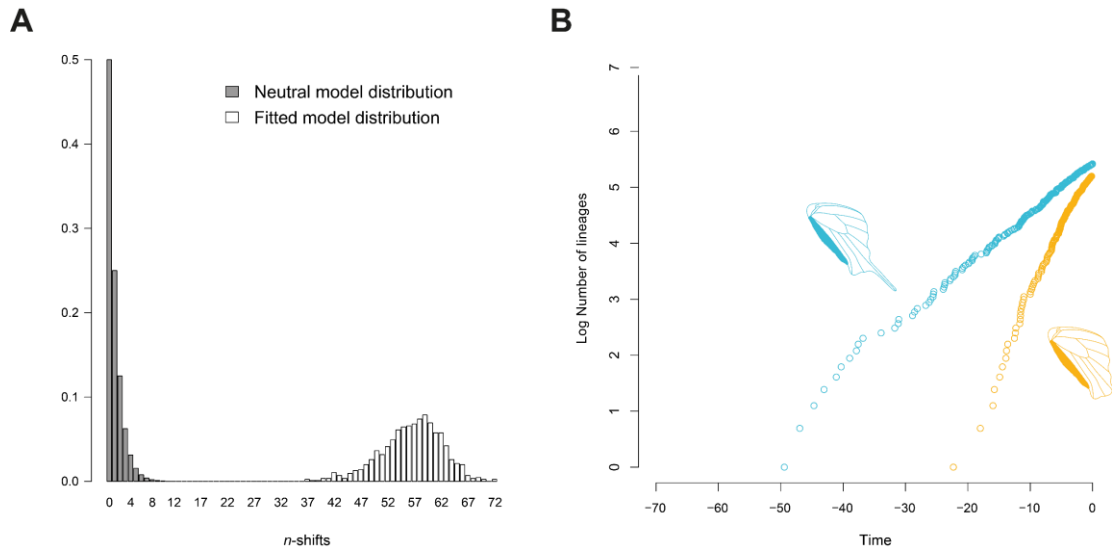
Supplementary 14: Model comparison for the HISSE analyses (female forms, $n = 408$ species).

Model	NP	logL	AICc	λ_{UA}	λ_{TA}	λ_{UB}	λ_{TB}	μ_{UA}	μ_{TA}	μ_{UB}	μ_{TB}	q_{UATA}	q_{UAUB}	q_{TAUA}	q_{TATB}	q_{UBTA}	q_{UBTB}	q_{UBUA}	q_{TBTA}	q_{TBUB}	
CID model	5	-1552.843	3115.836	0.0275		0.1332		0		0.0164		0.0037	-	0.0198	-	-	-	-	-	-	
full HISSE model	6	-1555.047	3122.304	0.1359	0.0983	-	-	0.0245	0	-	-	0.0037	-	0.0198	-	-	-	-	-	-	
HISSE model for state U	10	-1543.678	3107.91	0.0962	0.1018	0.1751	-	0.0314	0	0	-	0.0143	0.0063	0.0238	-	-	-	0	-	-	
HISSE model for state T	10	-1547.237	3115.028	0.1347	0.1225	-	0.0289	0.0262	0	-	0.0039	0.0036	-	0.0267	0.0285	-	-	-	0.0107	-	
full HISSE model	16	-1534.594	3102.578	0.1754	0.0422	0.0942	0.137	0	0.0363	0.0344	0	0	0	0	0	0	0.0124	0.0054	-	0.0405	0.0327

Supplementary 15: Evolution of tails on the hindwings in Papilionidae. The presence and absence of tails on the hindwings in the different species is shown in blue and orange respectively. Ancestral state estimation from BiSSE based on the best-fitting diversification model (n -species = 408 species, estimate from female forms). The ancestor of Papilionidae is inferred as tailed. Untailed lineages appeared recently and multiple times across the phylogeny.



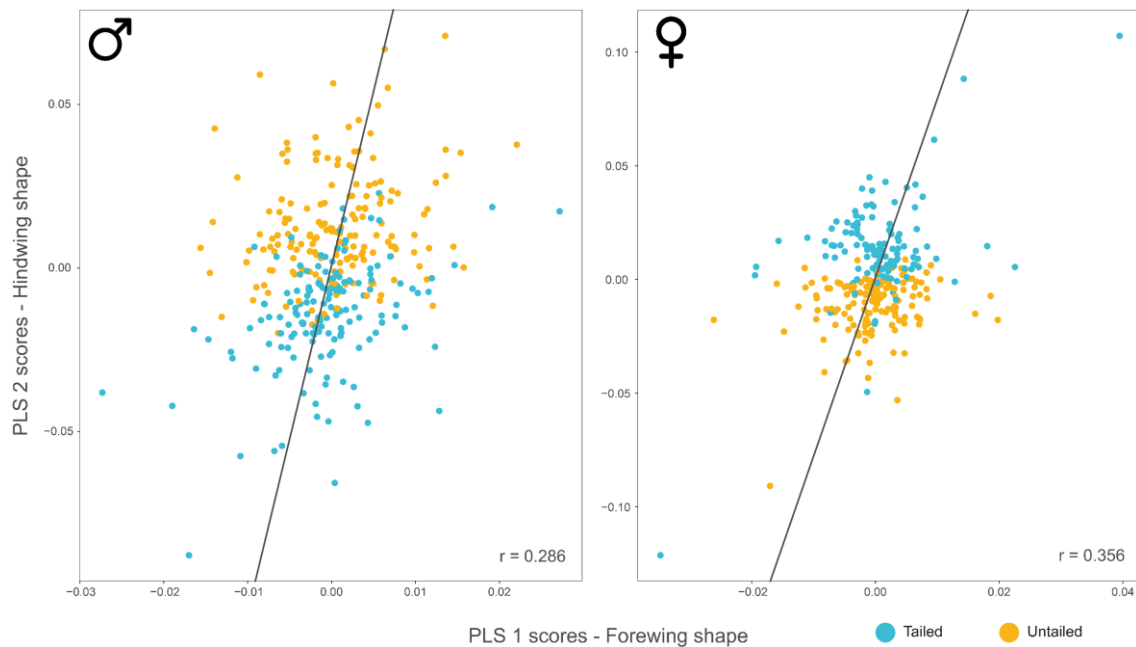
Supplementary 16: (A) Numbers of morphological shifts between tailed/untailed state, inferred with BAMM under a neutral model and a fitted model. (B) Cladogenetic events associated with each state (tailed/untailed).



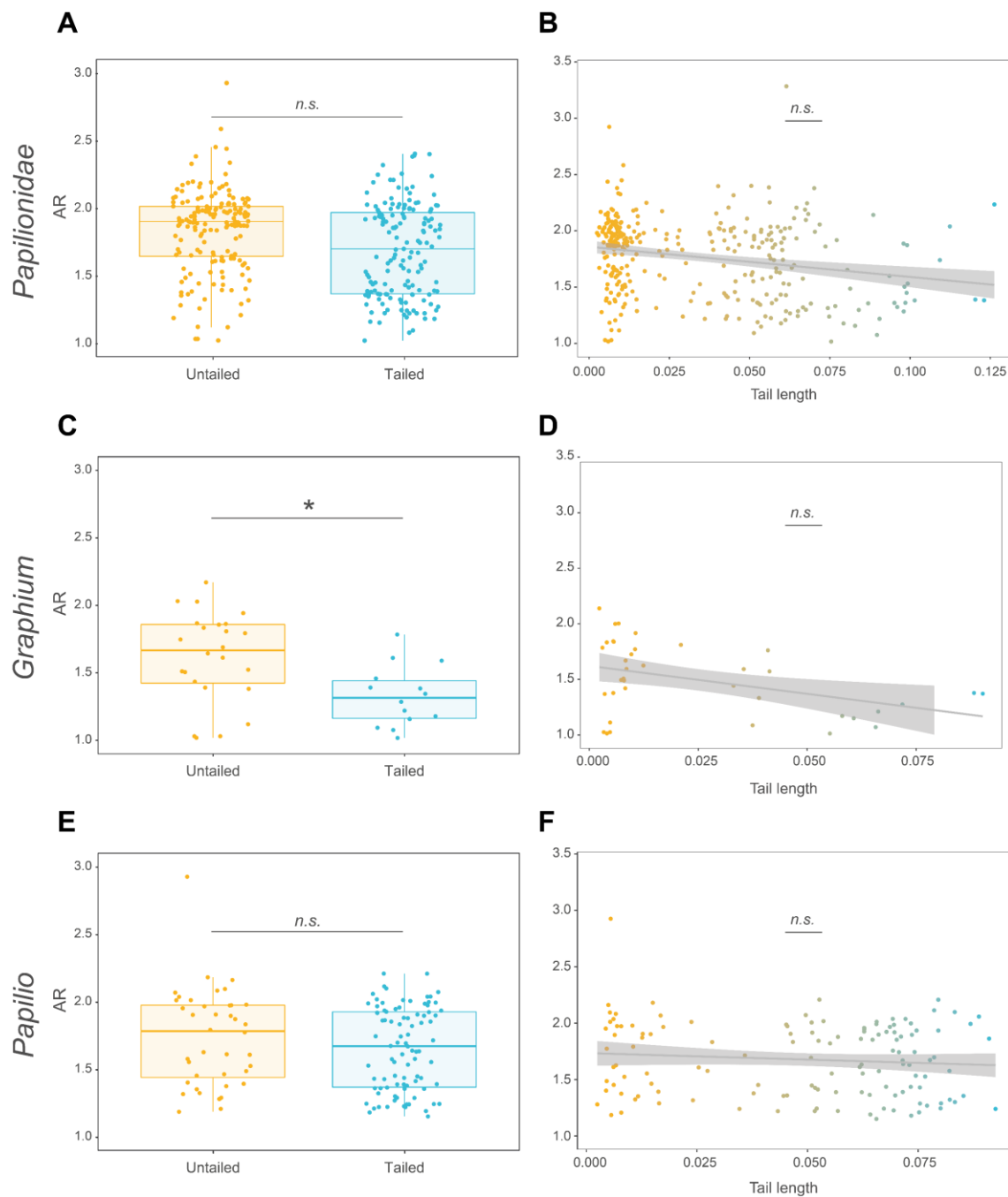
Supplementary 17: Results of the 2B-PLS performed on forewing and hindwing shape, in all Papilionidae (male forms, $n = 328$ species: female forms, $n = 270$ species), *Papilio* genera (male forms, $n = 129$ species: female forms, $n = 103$ species) and *Graphium* genera (male forms, $n = 37$ species: female forms, $n = 24$ species).

		<i>Papilionidae</i>	<i>Papilio</i>	<i>Graphium</i>
Male	r-PLS	0.286	0.27	0.599
	Effect Size (Z)	3.0967	1.4648	2.3321
	P-value	0.001 ***	0.073	0.008 **
Female	r-PLS	0.356	0.414	0.591
	Effect Size (Z)	4.197	2.8559	1.8442
	P-value	0.001 ***	0.003 **	0.031 *

Supplementary 18: 2B-PLS performed on forewing and hindwing shape, in Papilionidae (male forms, $n = 328$ species: female forms, $n = 270$ species).



Supplementary 19: Difference of AR males between Untailed and Tailed species in (A) Papilionidae (n -species = 328 species), (C) *Graphium* (n -species = 37 species), (E) *Papilio* (n -species = 129 species). Difference of AR according to TL in (B) Papilionidae, (D) *Graphium*, (F) *Papilio*. Significance of the results from phylogenetic regression/ANOVA are displayed.



Discussion

1) Ancestral wing shape and multiple evolution of tails



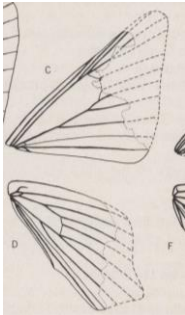

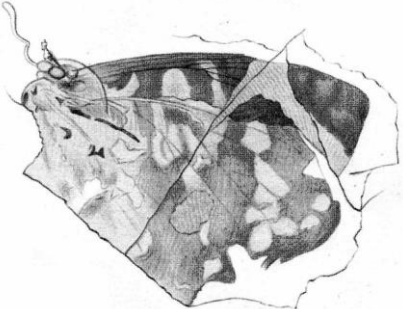
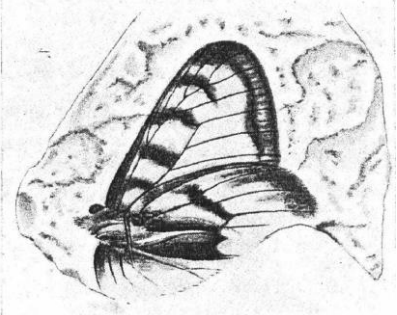

As described in Chapter III, multiple gains and losses of hindwing tails have occurred throughout the diversification of Papilionidae butterflies. Hindwing tails have also evolved multiple times in other butterfly families (see McKenna *et al.*, 2020) and moths (*e.g.*, Saturniidae). Tails emerged most frequently at M3 veins, but can also be founded in others locations (such as Cu1 or Cu2 veins), concomitantly or not. Furthermore, polymorphism in the presence/absence of tails is also observed in Papilionidae, such as in *P. memnon* or *P. dardanus*. Hindwing tail thus appears as an evolutionary labile trait in Lepidoptera, whose multiple gains and losses might be facilitated by limited developmental constraints. In Papilionidae, the reconstruction of family ancestral phenotype (- 67.28 Ma) suggests the presence of hindwing tail. Surprisingly, the basal taxon *Baronia brevicornis* does not display hindwing tail. Similarly, only some species of Papilionidae sister-family Hesperidae, display tails (Li *et al.*, 2019). As in many insect taxa, Lepidoptera fossils are quite scarce. To our knowledge, only four fossils of swallowtails are registered (see Table 1):

- *Doritites bosniackii* (Rebel, 1898)
- *Praepapillio colorado* (Durden and Rose, 1978)
- *Praepapillio gracilis* (Durden and Rose, 1978)
- *Thaites rumaniana* (Scudder, 1875)

The first switch between tailed/untailed states inferred by ancestral state reconstruction suggests a date of -28.60 Ma (at the node separating the clades *Parnassius* and *Hypermnestra*), earlier than the *Thaites rumaniana* and *Doritites bosniackii* dating. The wing phenotype of these fossils is thus not relevant to confirm our ancestral state inference. Moreover, these fossils are incomplete, precisely in the hindwings anal area, preventing any conclusion on the presence/absence of tails. However, the species *Praepapillio colorado* and *Praepapillio gracilis* are older, and display reduced tails on the M3 vein.

The fossil record of Papilionidae does not allow validating our inference, but the existence of two species exhibiting a hindwing boundary protrusion on the M3 vein is consistent with our results, and confirms the evolutionary lability of hindwing tails in Papilionidae.

Table 1: Register of Papilionidae fossils species: species name, estimated age, sketch or scheme of the reconstructed wing venation, holotype photograph when available. Illustrations are from their respective publications.

Species	Age	Scheme/drawing	Photograph
<i>Praepapillio colorado</i>	- 48Ma		
<i>Paepapillio gracilis</i>	- 48 Ma		
<i>Thaites rumaniana</i>	- 23Ma		
<i>Doritites bosniackii</i>	Miocene [-23.03; - 5.33] Ma		

Our macro-evolutionary study of hindwing tail evolution was consistent with a flexible development facilitating the multiple gains and losses of this trait. The developmental decoupling of wing margin determination and dorso-ventral (DV) boundary formation likely facilitated the diversification of specialized wing shapes in moths and butterflies (Macdonald *et al.*, 2010). Contrary to other insects, the imaginal disk DV boundary does not determine the final shape of the wing. The adult wing shape is determined by a molecular “cookie cutter”, involving the expression of *wingless* (*wg*) and a transcription factor (*Cut*), inducing apoptosis of border cells. This specific molecular mechanism allows the shape of adult wing to drastically differ from the imaginal disk boundary (Figure 1).



Figure 1: Hindwing shape developmental determination. (A) *Battus philenor* hindwing, (B) *Cut* expression, and (C) *wg* expression in fifth-instar wing discs presage formation of the wing tail (t) and the anal fold (a). (Figure 4 in Macdonald *et al.* 2010).

Moreover, the tail vein (M3) is located exactly at the boundary between two wing compartments, defined by long-range decapentaplegic-like signal (*dpp-like*, (Abbasi and Marcus, 2017; McKenna *et al.*, 2020)). The *dpp* concentration establishes a set of nested domains of gene expression along the wing, defining the location of wing veins (Klein, 2001). Small variations in the concentration of this morphogen could induce important wing outline variations at the M3 veins. While the selection pressures possibly involved are unknown, adaptive radiations have been suggested to occur primarily along the genetic lines of least resistance, because of the constraining effects of genetic correlations (Schluter, 1996). This suggests the removal of a developmental constraint on Lepidoptera wing shape has facilitated a morphological radiation and the multiple gain and losses of tails observed throughout the diversification of Lepidoptera. Such a release in a developmental constraint associated with a burst of morphological evolution has been documented in *Heteropsis* butterflies (family Mycalesina), that gained an independent developmental control of their eyespot colour

composition. This developmental innovation allowed a morphological radiation in this genus (Brattström *et al.*, 2020).

Our disparity analyses suggested that the tail does not simply behave as a neutral trait but exhibited a diversification pattern with higher level of lability than expected under a simple Brownian motion model (Chapter III). To pinpoint the potential selective mechanisms underlying the evolution of this trait, we then relied on micro-evolutionary studies focusing on a single model species (Chapters I and II).

2) What bridges can be built between macro and micro-evolutionary results?

Aerodynamics vs. deflection: an evolutionary trade-off?

Our experimental approaches on the species *Iphiclides podalirius* revealed the effect of hindwing tails on attack deflection (Chapter I) and stabilization of flight (Chapter II). These effects can have important consequences on the survival of the butterflies and are thus likely to be influenced by natural selection. Nevertheless, they could generate antagonistic selective pressures on the evolution of hindwing tails. The deflecting effect of tails indeed frequently leads to their loss during the life of the butterflies. There is therefore a cost to predation deflection, and the evolution of tails might result from an evolutionary trade-off between attack deflection and flight performances. Should this trade-off exist in other Papilionidae species, the specific ecological constraints encountered in different taxa could then balance the cost and benefits of attack deflection and flight abilities respectively, and might explain the frequent gain and loss of the tail throughout Papilionidae. Moreover, it has been shown that traits more closely tied to trade-offs evolve more rapidly: in Neotropical cichlid fishes, jaws evolution are subject to a trade-off between velocity and force. Generalist species (with unspecialized jaws, positioned in the middle of the trade-off between velocity and force) displayed a higher phenotypical evolution rate than specialized species (Burress and Muñoz, 2022). A similar result was found at larger evolutionary scale in Actinopterygii, between suction specialized species and generalist species (Corn *et al.*, 2021). Our results are consistent with those finding: we measured a strikingly higher phenotypical evolution rate for hindwings shape than for forewings shape (Chapter III), consistent with an hindwings shape evolution influenced by multiple selection pressures (trade-off) vs. forewing shape evolution under homogeneous selection.

Deflective phenotype, an adaptive syndrome driven by predators in Papilionidae?

Papilionidae are widespread around the world, occupying all continents (except Antarctic), and it is highly challenging to characterize the selective pressures acting on tail evolution within each and every species. Nevertheless, associations between hindwing tails and specific colour pattern can be observed in different Papilionidae genera, suggesting that predation might have independently promoted similar deflecting syndromes in different clades. For example, many *Graphium*, *Protesilaus Eurytides* or *Protographium* species display black and white stripes on the two pairs of wings, conspicuous colour-pattern at the tips hindwings (eyespot and blue markings) and long and thin tails, similarly to *I. podalirius* (see Figure 2). The evolution of the tails in these different clades could thus have been favoured by intense predation promoting traits enhancing deflection.



Figure 2: (left to right) *Iphiclides podalirius*, *Graphium pazala*, *Eurytides servile*, *Protesilaus molops*. These four species from different Papilionidae genera harbour a “deflector phenotype”: black and white stripes on the two pairs of wings, conspicuous colour-pattern at the tips hindwings (eyespot and blue markings) and long and thin tails.

Whether the evolution of hindwing tails might have been first promoted because of the associated aerodynamic performances (possibly enhancing predator avoidance or mating probability), and then selection generated by predators promoted specific colour pattern associated with the tail is currently unknown. We can imagine different evolutionary sequences including three components (see on Figure 3): (A) selection of tails aerodynamic effects, (B) selection of tails attack deflection effects (C) selection of a deflective colour-patterns.

The order of appearance of the different traits involved in the deflecting effects or the aerodynamic effect (which also involved a coordinated evolution of forewing shape, see Chapter III) is a key evolutionary question that remains to be investigated. It is also quite

possible that this evolutionary sequence was different between taxa harbouring such “deflector phenotypes” (Figure 2), thereby resulting from convergent evolution.

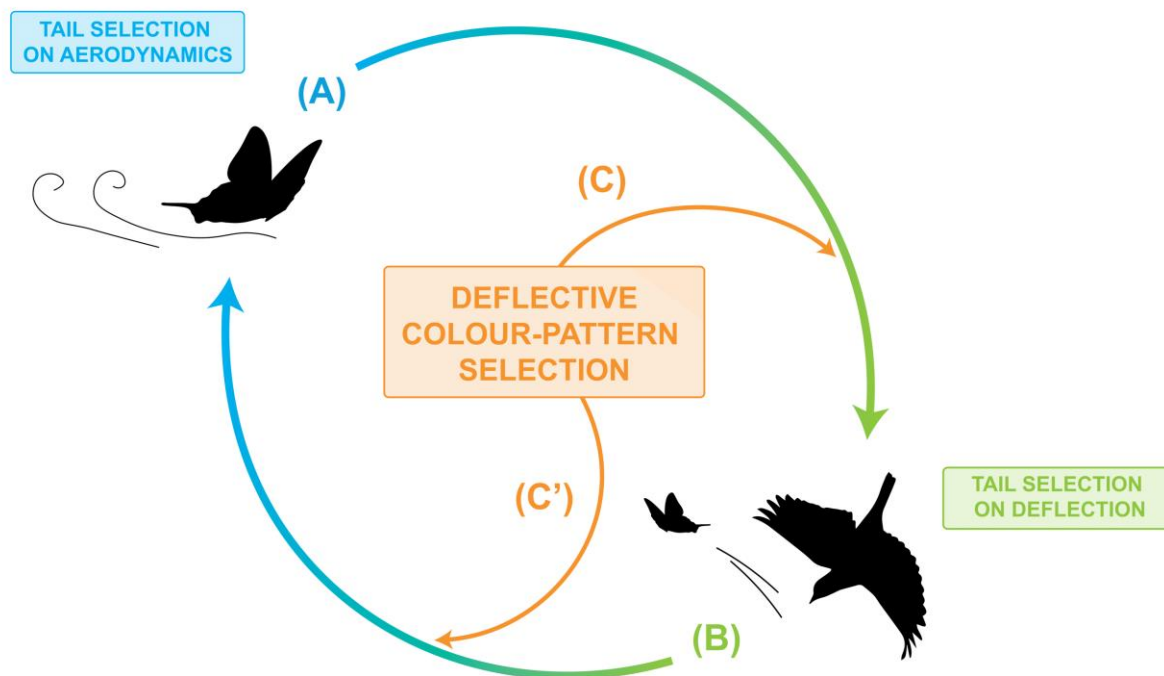


Figure 3: Possible evolutionary sequences between (A) selection of tails aerodynamic effects, (B) selection of tails attack deflection effects (C) selection of a deflective colour-pattern. The sequence could start by a selection of tails before colour-pattern (start at A or B) and vice versa. Likewise, selection of a deflective colour-pattern could occur before (C) or after (C') selection of tails attack deflection effects

Color-pattern and tails co-evolution

The evolution of wing shape and that of wing colour patterns appear to be tightly connected. This is particularly striking in species that combine hindwing tails and deflective colour-pattern, but other combinations of traits can be observed at the family level. Here, I propose a raw classification of such phenotypical traits associations in Papilionidae, considering four trait categories:

- Aposematic / non-aposomatic colour-pattern
- Deflector / non-deflector colour-pattern
- Toxic / non-toxic species
- Spatulated tail / thin tail / non tail

While these categories rely on traits that vary quantitatively and thus likely oversimplify the reality, they nevertheless provide a global picture of the various combinations of traits observed throughout the family. Only the male phenotype and the dorsal side of the wings are considered (for example, this analyse don't take into consideration many cases of Batesian mimicry in females of the genus *Papilio*). While many combinations are possible, we can observe preferred trait associations (Figure 4). The most frequent combinations are:

- (1) No tail / non-deflector / aposematic / toxic = 29.9%
- (2) Thin tail / deflector / non-aposematic / non-toxic = 15.9%
- (3) Spatulated tail / non-deflector / non-aposematic / non-toxic = 13.5%
- (4) No tail / non-deflector / non-aposematic / non-toxic = 13.0%

The second category corresponds to the “deflection syndrome” cited above. Selection pressures occurring on tails evolution in species belonging to different categories might be very different from the selection characterized in *I. podalirius*. This categorisation suggests non-random association between wing shape and colour pattern, and raises the question of the evolutionary path leading the evolution of shape/colour pattern syndromes.

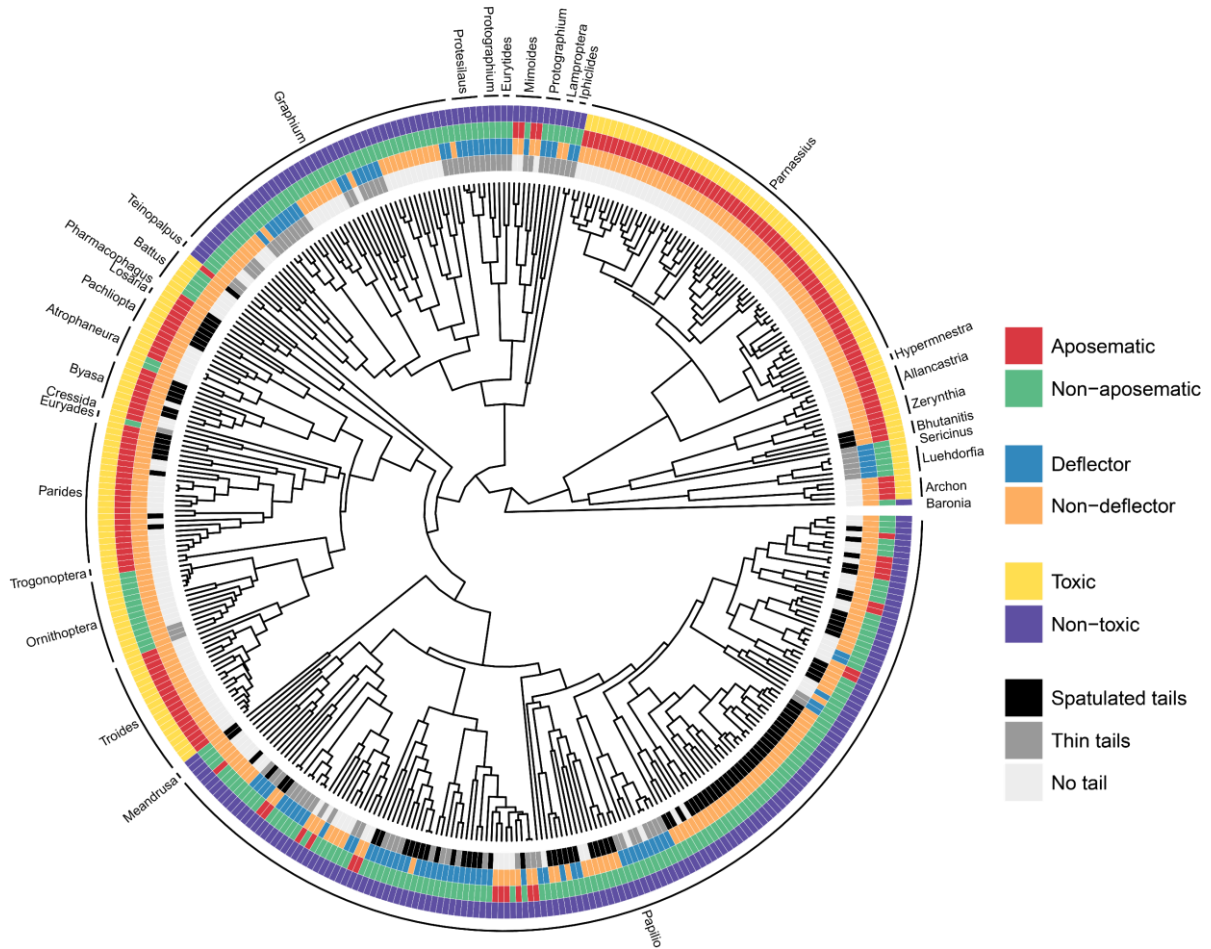


Figure 4: Phylogenetic tree of 408 Papilionidae species with associated phenotypic traits: presence of absence of aposematic colour pattern on dorsal wings sides, presence of absence of deflecting colour pattern on dorsal wings sides, presence of absence of toxicity in imago phase, shape of tails (spatulated/thin/absent).

Perspectives

Investigating the effect of tails on gliding flight performances at the macro-evolutionary scale.

The role of tails in gliding flight at the macro-evolutionary scale could be investigated using Computational Fluid Dynamics simulations. This method allows detailed analysis of the airflow characteristics, and has provided promising results when applied to insects flight (Sane, 2003; Le Roy *et al.*, 2021). Especially, tails have been suggested to increase the lift and longitudinal static stability during gliding flight (Park *et al.*, 2010). This lift increase is due to a modification of air-flow profile, through the creation of a low-pressure region close to the upper wing surface. Nevertheless, others studies (Martin and Carpenter, 1977; Brodsky, 1994) suggested that tail induced a drag reduction, which is not observed in Park *et al.*, (2010) or in Ortega Ancel *et al.*, (2017). In the latter case, however, the lift-to-drag values of *Protographium leosthenes* were not measured in natural position of the wings. At rest as well as in flight, Papilionidae hindwing tails are in the body axis and not outwards, as was done in the study of Ortega Ancel *et al.*, (2017). It is possible that this aberrant position of the wings has influenced the result. A “grey zone” still exists in the involvement of tail in the aerodynamics of gliding flight. Computational Fluid Dynamics simulations applied to the shapes of different Papilionidae species could allow estimating the effect of wing shape and tails on the lift-to-drag ratio, and thus quantify the gliding performances associated with the presence and absence of tails.

Investigating the shape / colour-pattern evolution

The joint evolution between wing shape (and more specifically hindwing tail) and colour pattern could be investigated using a combination of micro-evolutionary (1) and macro-evolutionary (2) approaches:

- (1) Behavioural essays using phenotypically modified dummies to investigate the relative importance of tail and colour-pattern in predator learning avoidance. In skippers, tails and colour-pattern are both involved in predators learning avoidance when associated with escaping ability of butterflies (Linke *et al.*, 2022). We could imagine the same type of experiments, to test:
 - if tails and/or deflective colour-pattern are used by predators to avoidance learning when associated with a deflective effect (if the predator attacks on the hindwing, it breaks and the butterfly escapes)

- if tails and/or aposematic colour-pattern are used by predators to avoidance learning when associated with prey unpalatability

(2) At the family level, we could characterize colour-patterns and study to what extent its evolution is correlated with that of wing shape.

Methodological considerations: Colour pattern could be defined as factor modalities (for example “deflector” or “aposematic” as see above), allowing a simple but intuitive approach on evolutionary sequence and then determine to what extent some wing shapes are preferentially associated with some colour patterns and in what order did these features appear. Nevertheless, as wing shape, colour-pattern is a complex trait, constituted of many sub-traits (*e.g.*, “deflection phenotype” = eyespots + blue lunules + convergent stripes) that are not necessarily present in all species. As well as, an aposematic colour-pattern can be defined in many ways. By definition, aposematic signals manipulate the predator by sending a signal of unpalatability (see [Mappes *et al.*, 2005](#) for a review) so it is actually quite difficult to determine the aposematism of a trait independently of the involved predator. Consider colour pattern as contiguous and multidimensional trait (define by a “colour-space”, exactly as shape could be defined by a morphospace of n dimensions) could provide solutions to these problems and then constitute a complementary approach. One could thus consider:

- automatically define phenotypical groups in colour-space and morphospace and studied their preferentially association. This would be a more reproducible and less biased approach to the one presented in Figure 4. As see above, a possible perspective of our work on the deflecting effect of the tails would be to characterize to what extent tails are associated with a deflector colour-pattern at family level and inferred their respective ancestral states and then determined the associated evolutionary sequence. The same type of analysis could be conducted on aposematic colour-pattern.
- studying the evolution of colour pattern and as continuous traits, and compared their evolutionary patterns (switch of evolution rate positions, correlation between some of colour-space and morpho-space dimensions...). As well as, this approach will allow us to quantify convergence and divergence events of shape at family level. Here, we presented a preliminary result, conducted on males and females mean wing shape

(Figure 5). This analysis could be coupled we colour-pattern convergences/divergences pattern to estimate in what extend these events are correlated.

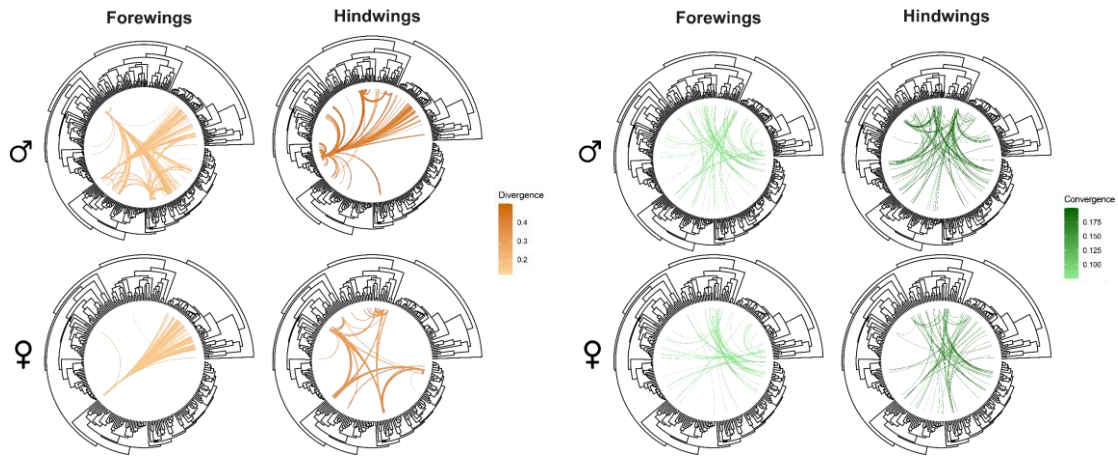


Figure 5: Convergences and divergence events in forewings and hindwings average shape for males ($n\text{-species} = 328$) and females forms ($n\text{-species} = 271$). Among all significant shape convergence/divergence recorded, only values above the first quartile Q1 are plotted.

Conclusion

Overall, the study of Papilionidae wing shape evolution, initiated with my PhD, has brought some insights on the selection pressures involved in tail evolution and highlighted the complex links existing between forewings and hindwings evolution, between a contrasted selection, developmental constraints and co-evolution.

Annex I

Inventory of the National Museum of Natural History collections: Papilionidae

Taxonomy				Collections						
Family	Subfamily	Tribes	Genus	Subgenus	Species	Sub-Species	Ancient name	Comspecific	Specimens	Total number
Papilionidae	Bacotinae	Bacotini	<i>Bacotia</i>		<i>brevicornis</i>				4 (Mexico)	4
Papilionidae	Papilioninae	Papilionini	<i>Papilio</i>	<i>Priniceps</i>	<i>rex</i>	<i>regulus</i> <i>schalzei</i> <i>absyrticus</i> <i>commata</i>			6 (Kenya) + 3 (form armoldi - Congo) 4 (Cameroun) 7 (Ehiopis) 3 (Kenya)	9 4 7 3
Papilionidae	Papilioninae	Papilionini	<i>Papilio</i>	<i>Priniceps</i>	<i>phorcus</i>	<i>congoanus</i> <i>amazegei</i> <i>nykanus</i>			33+29+19 (Guinea/Ivory Coast/Sierra Leone) 10+30+28+30+14(Congo/Ouganda) 30+14+34+15 (Kenya) 2 (East Africa)	81 112 93 2
Papilionidae	Papilioninae	Papilionini	<i>Papilio</i>	<i>Priniceps</i>	<i>constantinus</i>	<i>dardanus</i>			24 (East Africa)	24
Papilionidae	Papilioninae	Papilionini	<i>Papilio</i>	<i>Priniceps</i>	<i>meriones</i>	<i>dardanus</i>			27 + 20 + 14 + 16 (Madagascar) + 1 (female andromorphic - Madagascar)	78
Papilionidae	Papilioninae	Papilionini	<i>Papilio</i>	<i>Priniceps</i>	<i>dardanus</i>	<i>antimorii</i> <i>polytraphus</i> <i>fibulus</i> <i>cenea</i>			30 + 30 + 35+34+29 + 30+47 (males/females andromorphic - Guinea/Ivory Coast/Congo/Gabon/Ouganda) + 16+37+41 (females nimis - Guinea/Congo/Cameroun) 32+37+40+41+27 (males/females andromorphic - Ehiopie/Eritrea) + 1 (form albicola - Ehiopis) + 35 (form antimorii female - Ehiopis) + 4 (female form niavolice) 47+31 (males - East Africa) + 19 (female form nimis alluaudi - Kenya/Zimbabwe/Central African Republic/Ivory Coast)	289 217 78
Papilionidae	Papilioninae	Papilionini	<i>Papilio</i>	<i>Priniceps</i>	<i>dardanus</i>	<i>benetti</i>			38 (males/females andromorphic - East Africa/Zanzibar) + 1 (form male discopunctatus - Mozambique) 1 (male/female andromorphic) + 24 (female form nimis cenea - Afrique du Sud/Orientale)	39 1
Papilionidae	Papilioninae	Papilionini	<i>Papilio</i>	<i>Priniceps</i>	<i>humberti</i>				18 (Grande Comore)	18
Papilionidae	Papilioninae	Papilionini	<i>Papilio</i>	<i>Priniceps</i>	<i>delalandei</i>	<i>delalandei</i>			29 + 18 (Madagascar)	47
Papilionidae	Papilioninae	Papilionini	<i>Papilio</i>	<i>Priniceps</i>	<i>lormieri</i>	<i>lormieri</i> <i>crocea</i> <i>semikana</i>			20+20+17+14+12 (Congo/Gabon/Republique Centrafricque) 4 (Ouganda)	83 4 3
Papilionidae	Papilioninae	Papilionini	<i>Papilio</i>	<i>Priniceps</i>	<i>demodocus</i>	<i>demodocus</i>			29 + 32 (Madagascar) + 17 (La Reunion) + 35 (Mauricio) + 35+36+32+37+35+36+34+34+37+33+36+24+26+25+33+18 (Ouganda/Congo/Tanzanie/Ivory Coast/Ehiopie/Colore/Gabon) + 21 (form nubilis - Congo) + 2 (form terat - Angola) + 12 (form confluus - Congo/Guinee/Ivory Coast) + 5 (form albicans - Sierra Leone/Ouganda/Angola)	760
Papilionidae	Papilioninae	Papilionini	<i>Papilio</i>	<i>Priniceps</i>	<i>erithonioides</i>	<i>benetti</i>			2 (Yemen)	2
Papilionidae	Papilioninae	Papilionini	<i>Papilio</i>	<i>Priniceps</i>	<i>demoleus</i>	<i>movans</i> <i>demoleus</i> <i>siboninus</i> <i>novoguineensis</i>			35 (Ile de NW Madagascar) 15 (Vietnam) 5 (Laos) + 27 (India) + 1 + 2 (Arabie) + 13 (Sri Lanka) + 1 (Taiwan) + 5 (Thaïlande) + 4 (Cambodia) + 4+37+12+46+15 (Vietnam/China) 4 (Indonésie) + 12 (Australie)	15 163 16 4
Papilionidae	Papilioninae	Papilionini	<i>Papilio</i>	<i>Priniceps</i>	<i>groscomathi</i>	<i>groscomathi</i>			21 (NW Madagascar)	21
Papilionidae	Papilioninae	Papilionini	<i>Papilio</i>	<i>Priniceps</i>	<i>maoridana</i>	<i>maoridana</i>			27 (riviere Morondava Mahabo - Madagascar)	27
Papilionidae	Papilioninae	Papilionini	<i>Papilio</i>	<i>Priniceps</i>	<i>epiphorbus</i>	<i>nobilis</i> <i>lerysi</i>			33 + 30 + 31 + 29 + 5 (Madagascar) 25+23 (East Africa) 1 (Congo)	128 48 1
Papilionidae	Papilioninae	Papilionini	<i>Papilio</i>	<i>Priniceps</i>	<i>orbiculus</i>	<i>orbiculus</i>			28 + 30 (Madagascar)	58
Papilionidae	Papilioninae	Papilionini	<i>Papilio</i>	<i>Priniceps</i>	<i>menestheus</i>	<i>menestheus</i>			20 + 20 + 14 + 7 (Sierra Leone/Ivory Coast/Guinea/Beneegal)	61
Papilionidae	Papilioninae	Papilionini	<i>Papilio</i>	<i>Priniceps</i>	<i>mangara</i>	<i>mangara</i>			39 + 6 (Madagascar) + 20 (phenotype différent - Madagascar)	65
Papilionidae	Papilioninae	Papilionini	<i>Papilio</i>	<i>Priniceps</i>	<i>hesperus</i>	<i>hesperus</i> <i>pellax</i>			20+20+18+8 (Cameroun/Congo/Guinea) + 6 (form masculatissima - Ivory Coast/Guinea/Sierra Leone/Libéria) 9 + 11 (Libéria/Guinea)	66 20
Papilionidae	Papilioninae	Papilionini	<i>Papilio</i>	<i>Priniceps</i>	<i>leucotaenia</i>	<i>leucotaenia</i>			10 (East Africa)	0
Papilionidae	Papilioninae	Papilionini	<i>Papilio</i>	<i>Priniceps</i>	<i>horribilis</i>	<i>horribilis</i>			2	0
Papilionidae	Papilioninae	Papilionini	<i>Papilio</i>	<i>Priniceps</i>	<i>espharator</i>	<i>espharator</i>				0
Papilionidae	Papilioninae	Papilionini	<i>Papilio</i>	<i>Priniceps</i>	<i>pebidanus</i>	<i>pebidanus</i>				0
Papilionidae	Papilioninae	Papilionini	<i>Papilio</i>	<i>Priniceps</i>	<i>ophidiocephalus</i>	<i>ophidiocephalus</i>			17 (Tanzanie)	17
Papilionidae	Papilioninae	Papilionini	<i>Papilio</i>	<i>Priniceps</i>	<i>phalacro</i>	<i>phalacro</i>			3 (Afrique du Sud)	3
Papilionidae	Papilioninae	Papilionini	<i>Papilio</i>	<i>Priniceps</i>	<i>zuluensis</i>	<i>zuluensis</i>			3 (Congo)	3
Papilionidae	Papilioninae	Papilionini	<i>Papilio</i>	<i>Priniceps</i>	<i>demolitor</i>	<i>demolitor</i>			3 (Vietnam/Laos) + 30+30+8 (Indonésie)	71

Papilionidae	Papilioninae	Papilio	<i>energetes</i>					1 (Indonesia)	1
Papilionidae	Papilioninae	Papilio	<i>egon</i>	<i>nobeli</i>				5 (Vietnam)	5
Papilionidae	Papilioninae	Papilio	<i>nerites</i>	<i>egon</i>				16+5 (Indonesia)	21
Papilionidae	Papilioninae		<i>romulus</i>				<i>nubilus (hybrid) ovce</i> <i>M. nepheles</i> + <i>sakomala</i> + <i>walkeri</i>	2 (Indonesia)	2
Papilionidae	Papilioninae		<i>protes</i>					6 (Vietnam) + 7 (females forms polytes Vietnam) + 2 (females forms cynus Vietnam + Cambodia) + 3 (females forms stichus) + 10+30+30+30+30+25+25 (Sri Lanka/India/China)	199
Papilionidae	Papilioninae		<i>radhausula</i>					28 +25+25+29+30+12 (China/Vietnam)	146
Papilionidae	Papilioninae		<i>jovinus</i>					3 (China)	3
Papilionidae	Papilioninae		<i>nikobarus</i>					24+30+30+21 (Indonesia)	105
Papilionidae	Papilioninae		<i>flexus</i>					12 (Indonesia)	12
Papilionidae	Papilioninae		<i>mesius</i>					6 (Indonesia)	6
Papilionidae	Papilioninae		<i>setra</i>					1 (Indonesia)	1
Papilionidae	Papilioninae		<i>timorensis</i>					1 (Indonesia)	1
Papilionidae	Papilioninae		<i>alphates</i>					4 (Indonesia)	4
Papilionidae	Papilioninae		<i>protes</i>					5+7 (Japan)	12
Papilionidae	Papilioninae		<i>protenor</i>	<i>alcindor</i>				6 (Indonesia)	6
Papilionidae	Papilioninae		<i>euprotenor</i>	<i>protenor</i>				20 +20+16+6+11 (China/Thibet)	62
Papilionidae	Papilioninae		<i>amara</i>					10+20 +11 (India)	41
Papilionidae	Papilioninae		<i>memnon</i>					6 (Taiwan)	6
Papilionidae	Papilioninae		<i>egonor</i>					20+20+10 +8 (Indonesia) + 10+6 (female form homedon - India) + 2 (female form gyrus - Indonesia) + 12 +2 (female form hiera - Indonesia) + 1 (female form dobera - Indonesia) + 1 (female form isarcha - Indonesia) + 1 (female form imperiosa - Indonesia) + 15 (female form achates - India/Indonesia)	107
Papilionidae	Papilioninae		<i>ancus</i>	<i>memnon</i>				20+20+20+20+20+2+16 (India/China/Taiwan) + 13 +18 (female form agenor - Thailand/Vietnam) + 7+9 (female form bulterianus - India) + 16+16 +11 (female form alcanor - India/Cambodia/Vietnam) + 3 +2 (female form thetonius - India) + 1 (female form vinius - China) + 1 (female form phoenix - China) + 8 (female form esperi - Malaysia)	227
Papilionidae	Papilioninae		<i>pyveri</i>					8 (Indonesia) + 3 (female form trochila - Indonesia) + 4 (female form aneus - Indonesia) + 2 (female form ityla - Indonesia) + 1 (female form butis)	18
Papilionidae	Papilioninae		<i>perichas</i>					3 (Japan)	3
Papilionidae	Papilioninae		<i>thunbergi</i>					1 (Indonesia)	1
Papilionidae	Papilioninae		<i>christianae</i>					1 (Indonesia)	1
Papilionidae	Papilioninae		<i>singkepensis</i>					7 (Japan)	7
Papilionidae	Papilioninae		<i>oemonaus</i>					2 (Indonesia)	2
Papilionidae	Papilioninae							3 (Indonesia)	3
Papilionidae	Papilioninae							15 (Philippines) + 4 (female form semperius - Philippines) + 1 (female form obscura - Philippines) + 1 (female form etibala - Philippines)	21
Papilionidae	Papilioninae		<i>deiphobus</i>					7 (Indonesia) + 3 (form hypoxanthus - Indonesia) + 10 (form flavo - Indonesia)	22
Papilionidae	Papilioninae		<i>deiphobus</i>					16 (Indonesia)	16
Papilionidae	Papilioninae							10 (Indonesia)	10
Papilionidae	Papilioninae							5 (Taiwan)	5
Papilionidae	Papilioninae							7 (Japan) + 4 (China) + 2 (Corea) + 9 (form mucus - Thibet/China)	22
Papilionidae	Papilioninae		<i>chaon</i>				<i>chaon</i> + <i>nubilus (hybrid) ovce</i> <i>M. pebeser</i>	6+18 (Vietnam) + 1 (Laos) + 19+18 (India/China)	62
Papilionidae	Papilioninae		<i>stromus</i>					2 (Indonesia)	2
Papilionidae	Papilioninae		<i>nepheles</i>					12 (Indonesia)	12
Papilionidae	Papilioninae		<i>albithemus</i>					9 (Indonesia)	9
Papilionidae	Papilioninae		<i>sinatus</i>					15 + 3 (Indonesia)	18
Papilionidae	Papilioninae		<i>mahadeva</i>					13+16 (Malaysia)	29
Papilionidae	Papilioninae		<i>argens</i>					3 (Vietnam) + 4 (Thailand)	7
Papilionidae	Papilioninae		<i>adranus</i>					20+16 (Australia)	36
Papilionidae	Papilioninae		<i>gortanus</i>					4 (Indonesia)	4
Papilionidae	Papilioninae		<i>ketanus</i>					Indonesia	2
Papilionidae	Papilioninae		<i>kisvanus</i>					5 (Indonesia)	5
Papilionidae	Papilioninae							1 (Indonesia)	1

Papilionidae	Papilioninae	Papilionini	Papilio	Meneclides	argus	<i>adallo</i> <i>acastus</i>			7 (Papua New Guinea) + 2 (female form thuria - Papua New Guinea)	9
						<i>omneus</i>			10 (Papua New Guinea)	10
						<i>ortus</i>			15+8 (Papua New Guinea) + 4 (female form leporina - Indonesia) + 1 (female form timoxeta - Papua New Guinea) + 6 (female form oncsinus - Papua New Guinea/Indonesia)	34
						<i>websteri</i>			2 (Papua New Guinea) + 1 (female form ximene - Papua New Guinea) + 2 (female form nymphasa - Papua New Guinea)	5
Papilionidae	Papilioninae	Papilionini	Papilio	Meneclides	gambirius	<i>gambirius</i>			1 (Papua New Guinea) + 1 (female form bistarcklamus - Salomon island) + 1 (female form sapaea - Salomon island)	3
						<i>bridgeri</i>			5 (Indonesia)	5
						<i>oreque</i>			4 (Salomon island) + 2 (form goret - Salomon island)	6
Papilionidae	Papilioninae	Papilionini	Papilio	Meneclides	bridgeri	<i>oreque</i>			2 (Salomon island)	2
						<i>prospero</i>			2 (Salomon island)	2
						<i>tryoni</i>			2 (Salomon island)	2
						<i>hecatæus</i>			2 (Papua New Guinea)	2
Papilionidae	Papilioninae	Papilionini	Papilio	Meneclides	solens	<i>solens</i>			11 (Indonesia)	11
						<i>limber</i>			3 (Indonesia)	3
						<i>albanus</i>			4 (Vietnam/Thailand)	4
						<i>heringi</i>			3 (Papua New Guinea)	3
						<i>helonus</i>			19+17+16+18+20 (India/China/Malaysia/Vietnam/Laos) + 3	0
						<i>fortunius</i>			3 (Taiwan)	93
						<i>dikcha</i>			9 (India)	9
						<i>mooracens</i>			4 (Japan)	4
						<i>palawanicus</i>			4 (Sri Lanka)	4
						<i>iserialus</i>			10 (Philippines)	10
						<i>engonus</i>			20+13 (Indonesia)	0
						<i>amysithor</i>			17 (New Caledonia)	33
						<i>acharua</i>			3 (Indonesia)	17
						<i>alkmentor</i>			10+14+4 (India) + 5+11 (form leucocellis - India)	3
						<i>platanius</i>			1 (China)	44
						<i>nizaror</i>			1 (Indonesia)	1
						<i>ledeburia</i>			12+13 (Indonesia)	25
						<i>perverus</i>			12+25+20 (Philippines)	57
						<i>ambax</i>			4 (Philippines)	4
						<i>artanus</i>			24 + 11 (Papua New Guinea) + 5 (female form ambracii - Papua New Guinea) + 3 (female form nova - Papua New Guinea)	43
						<i>esippus</i>			1 (Papua New Guinea)	1
						<i>antimo</i>			9 (Australia)	9
						<i>ascalaphus</i>			1	1
						<i>ascalaphus</i>			12+10 (Indonesia) + 1 (female form rubiger - Indonesia)	23
						<i>bootes</i>			2 (Indonesia)	2
						<i>canopus</i>			3 (Indonesia)	3
						<i>castor</i>			10 (Thbet)	10
						<i>demetrius</i>			7 (India)	7
						<i>formosanus</i>			10 (Australia) + 2 (Papua New Guinea) + 2 (Thbet)	14
						<i>pharazangus</i>			30+23 (India/China)	53
						<i>demetrius</i>			1 (Vietnam)	1
						<i>dravidarum</i>			4 (Taiwan)	4
						<i>eriskirei</i>			2 (China)	2
						<i>encheator</i>			5+15 (Japan)	20
									4 (Indonesia)	4
									5 (India)	5
									16+3 (Papua New Guinea)	0
										19

Papilionidae	Papilioninae	Papilio	<i>Menclaides</i>	<i>enchenor</i>	<i>novobornensis</i>				2 (Papua New Guinea)	2
Papilionidae	Papilioninae	Papilio			<i>depilis</i>				2 (Papua New Guinea)	2
Papilionidae	Papilioninae	Papilio			<i>neohomoveranus</i>				1 (Papua New Guinea)	1
Papilionidae	Papilioninae	Papilionini			<i>minimatus</i>				1	1
Papilionidae	Papilioninae				<i>andersonis</i>				1	1
Papilionidae	Papilioninae				<i>miniferus</i>				1	1
Papilionidae	Papilioninae				<i>maules</i>				2 (Indonesia)	2
Papilionidae	Papilioninae				<i>obsolens</i>				1	1
Papilionidae	Papilioninae				<i>fuscus</i>				20+1 (Indonesia)	21
Papilionidae	Papilioninae				<i>beccani</i>				15 + 6 (Papua New Guinea)	21
Papilionidae	Papilioninae				<i>thomsoni</i>				6 (Indonesia)	6
Papilionidae	Papilioninae				<i>rotata</i>				1 (Indonesia)	1
Papilionidae	Papilioninae				<i>ellix</i>				2 (Papua New Guinea)	2
Papilionidae	Papilioninae				<i>laniponius</i>				2 (Papua New Guinea)	2
Papilionidae	Papilioninae				<i>hasterti</i>				4 (Solomon Island)	4
Papilionidae	Papilioninae				<i>lapathus</i>				8 (Indonesia)	8
Papilionidae	Papilioninae	Papilionini	<i>Menclaides</i>	<i>Jucus</i>	<i>porothemus</i>				4 (Indonesia)	4
Papilionidae	Papilioninae				<i>tababona</i>				1 (Indonesia)	1
Papilionidae	Papilioninae				<i>perthax</i>				6 (Indonesia)	6
Papilionidae	Papilioninae				<i>capareus</i>				10 (Australia)	10
Papilionidae	Papilioninae				<i>xenophilus</i>				1 (Solomon Island)	1
Papilionidae	Papilioninae				<i>ombrianus</i>				1 (Indonesia)	1
Papilionidae	Papilioninae				<i>andamanicus</i>				1 (India)	1
Papilionidae	Papilioninae				<i>dayaxus</i>				Indonesia	2
Papilionidae	Papilioninae				<i>capareus</i>				6 (Australia)	6
Papilionidae	Papilioninae				?				12	12
Papilionidae	Papilioninae	Papilio	<i>Menclaides</i>	<i>prexaspes</i>					3 (Vietnam) + 3 (Malaysia)	6
Papilionidae	Papilioninae	Papilio	<i>Menclaides</i>	<i>gedefroi</i>					3 (Solomon Island)	3
Papilionidae	Papilioninae	Papilio	<i>Menclaides</i>	<i>hysaxtes</i>						0
Papilionidae	Papilioninae	Papilio	<i>Menclaides</i>	<i>hysaxtes</i>					1	1
Papilionidae	Papilioninae	Papilio	<i>Menclaides</i>	<i>inopinatius</i>					6 (Indonesia)	6
Papilionidae	Papilioninae	Papilio	<i>Menclaides</i>	<i>iswara</i>					5 (India)	5
Papilionidae	Papilioninae	Papilio	<i>Menclaides</i>	<i>iswara</i>					3 (Indonesia)	3
Papilionidae	Papilioninae	Papilio	<i>Menclaides</i>	<i>iswaranides</i>						0
Papilionidae	Papilioninae	Papilio	<i>Menclaides</i>	<i>janata</i>					8 (India)	8
Papilionidae	Papilioninae	Papilio	<i>Menclaides</i>	<i>janata</i>					1 (Indonesia)	1
Papilionidae	Papilioninae	Papilio	<i>Menclaides</i>	<i>lampisus</i>					2 (Indonesia)	2
Papilionidae	Papilioninae	Papilio	<i>Menclaides</i>	<i>larnedon</i>					1 (India)	1
Papilionidae	Papilioninae	Papilio	<i>Menclaides</i>	<i>lowii</i>					5 (Philippines)	5
Papilionidae	Papilioninae	Papilio	<i>Menclaides</i>	<i>mayo</i>					2 (Indonesia)	2
Papilionidae	Papilioninae	Papilio	<i>Menclaides</i>	<i>phetas</i>					4 (Solomon Island)	4
Papilionidae	Papilioninae	Papilionini			<i>pinisongi</i>				5 (Papua New Guinea)	5
Papilionidae	Papilioninae	Papilionini			<i>pinisongi</i>				3 (Papua New Guinea)	3
Papilionidae	Papilioninae	Papilionini			<i>pinisongi</i>				12 + 12 (India)	24
Papilionidae	Papilioninae	Papilio	<i>Menclaides</i>	<i>polymnestor</i>					4 + 16 + 5 (Sri Lanka)	25
Papilionidae	Papilioninae	Papilio	<i>Menclaides</i>	<i>sataptes</i>					6 (Indonesia)	6
Papilionidae	Papilioninae	Papilio	<i>Menclaides</i>	<i>sataptes</i>					2 (Indonesia)	2
Papilionidae	Papilioninae	Papilio	<i>Menclaides</i>	<i>schmelzi</i>					1 (Philippines)	1
Papilionidae	Papilioninae	Papilio	<i>Menclaides</i>	<i>schmelzi</i>					6 (Fiji Island)	6
Papilionidae	Papilioninae	Papilio	<i>Menclaides</i>	<i>weyneri</i>					2 (Papua New Guinea)	2
Papilionidae	Papilioninae	Papilio	<i>Menclaides</i>	<i>woolfordipolychus</i>					2 (Solomon Island)	2
Papilionidae	Papilioninae	Papilio	<i>Menclaides</i>	<i>woolfordipolychus</i>					15 (Solomon Island) + 1 (form echnica - Solomon Island)	16
Papilionidae	Papilioninae	Papilio	<i>Menclaides</i>	<i>laucus</i>					2	2
Papilionidae	Papilioninae	Papilio	<i>Menclaides</i>	<i>antel</i>					1	1

Papilionidae	Papilioninae	Papilionini	<i>Papilio</i>	<i>Eleppone</i>	<i>anaeus</i>				14 (Australia)	14
Papilionidae	Papilioninae	Papilionini	<i>Papilio</i>	<i>Achillides</i>	<i>monckii</i>					0
Papilionidae	Papilioninae	Papilionini				<i>okunowensis</i>		<i>okunowensis + polycator</i>		2 (Japan)
Papilionidae	Papilioninae	Papilionini				<i>formosanus</i>				3 (Taiwan)
Papilionidae	Papilioninae	Papilionini				<i>hianoi</i>				10+24 (China/Tibet) + 8 (form gladiator - China/Vietnam)
Papilionidae	Papilioninae	Papilionini	<i>Papilio</i>	<i>Achillides</i>	<i>hianoi</i>					12 (Japan)
Papilionidae	Papilioninae	Papilionini				<i>maiae</i>				13 (Tibet)
Papilionidae	Papilioninae	Papilionini				<i>trimpfator</i>				14 (China/Russia) + 12 (Japan) + 12+4 (form radde - Japan/Russia/China)
Papilionidae	Papilioninae	Papilionini				<i>significans</i>				3 (India/Cambodia)
Papilionidae	Papilioninae	Papilionini				<i>ganesa</i>				5 (China/India)
Papilionidae	Papilioninae	Papilionini	<i>Papilio</i>	<i>Achillides</i>	<i>dehmanni</i>					18 + 22 (India) + 3 (form poophytia - India)
Papilionidae	Papilioninae	Papilionini	<i>Papilio</i>	<i>Achillides</i>	<i>ryukyuensis</i>					5 (China/Japan)
Papilionidae	Papilioninae	Papilionini	<i>Papilio</i>	<i>Achillides</i>	<i>polycator</i>					6+12 (China/India)
Papilionidae	Papilioninae	Papilionini				<i>chinensis</i>		<i>hermosanus</i>		8+18 (China/Tibet)
Papilionidae	Papilioninae	Papilionini				<i>pisiphernes</i>				1 (Taiwan) + 5 (Vietnam)
Papilionidae	Papilioninae	Papilionini				<i>paris</i>				28+21 (India/Vietnam/Laos) + 8 (form splendifer - India)
Papilionidae	Papilioninae	Papilionini				<i>batacorum</i>				3 (Sumatra)
Papilionidae	Papilioninae	Papilionini				<i>sealeris</i>				16 (Java) + 4 (form - Java)
Papilionidae	Papilioninae	Papilionini				<i>tengerensis</i>				3 (Java) + 3 (form privata - Java)
Papilionidae	Papilioninae	Papilionini				<i>tomilana</i>				4 (India)
Papilionidae	Papilioninae	Papilionini				<i>hermosanus</i>				3 (Taiwan)
Papilionidae	Papilioninae	Papilionini	<i>Papilio</i>	<i>Achillides</i>	<i>hermosanus</i>					3 (Java)
Papilionidae	Papilioninae	Papilionini	<i>Papilio</i>	<i>Achillides</i>	<i>arjuna</i>					4 (Indonesia)
Papilionidae	Papilioninae	Papilionini	<i>Papilio</i>	<i>Achillides</i>	<i>lorquinianus</i>					1 (Indonesia)
Papilionidae	Papilioninae	Papilionini				<i>manauatus</i>				1 (Indonesia)
Papilionidae	Papilioninae	Papilionini				<i>ulysses</i>				8 (Indonesia) + 3
Papilionidae	Papilioninae	Papilionini				<i>oxyares</i>				1 (Indonesia)
Papilionidae	Papilioninae	Papilionini	<i>Papilio</i>	<i>Achillides</i>	<i>ulysses</i>					12+1 (Papua New Guinea) + 1 (female form conjuncta - Papua New Guinea) + 1 (female form transiens - Papua New Guinea)
Papilionidae	Papilioninae	Papilionini				<i>anaeus</i>				5+6 (Australia)
Papilionidae	Papilioninae	Papilionini				<i>peesa</i>				3 (Papua New Guinea)
Papilionidae	Papilioninae	Papilionini				<i>amblyus</i>				1 (Papua New Guinea)
Papilionidae	Papilioninae	Papilionini				<i>gabrielis</i>				1 (female form cymippe)
Papilionidae	Papilioninae	Papilionini				<i>nigerrimus</i>				8 (Indonesia)
Papilionidae	Papilioninae	Papilionini	<i>Papilio</i>	<i>Achillides</i>	<i>orsippus</i>					20 (New Caledonia)
Papilionidae	Papilioninae	Papilionini	<i>Papilio</i>	<i>Achillides</i>	<i>telegonus</i>					6 (New Caledonia)
Papilionidae	Papilioninae	Papilionini	<i>Papilio</i>	<i>Achillides</i>	<i>montrozieri</i>					14 (New Caledonia)
Papilionidae	Papilioninae	Papilionini				<i>arcularius</i>				2 (China) + 13 (India)
Papilionidae	Papilioninae	Papilionini	<i>Papilio</i>	<i>Achillides</i>	<i>arcularius</i>					1+3 (India)
Papilionidae	Papilioninae	Papilionini	<i>Papilio</i>	<i>Achillides</i>	<i>arcularius</i>					14+3 (Indonesia)
Papilionidae	Papilioninae	Papilionini	<i>Papilio</i>	<i>Achillides</i>	<i>blaneti</i>					7 (India)
Papilionidae	Papilioninae	Papilionini	<i>Papilio</i>	<i>Achillides</i>	<i>budha</i>					13 (India) + 8 (form montianus - India)
Papilionidae	Papilioninae	Papilionini	<i>Papilio</i>	<i>Achillides</i>	<i>ebharae</i>					8 (Philippines)
Papilionidae	Papilioninae	Papilionini	<i>Papilio</i>	<i>Achillides</i>	<i>crino</i>					3 (Vietnam)
Papilionidae	Papilioninae	Papilionini	<i>Papilio</i>	<i>Achillides</i>	<i>decidua</i>			<i>decidua</i>		2 (Vietnam)
Papilionidae	Papilioninae	Papilionini	<i>Papilio</i>	<i>Achillides</i>	<i>disalis</i>					2 (Taiwan)
Papilionidae	Papilioninae	Papilionini	<i>Papilio</i>	<i>Achillides</i>	<i>elephanor</i>					2 (India)
Papilionidae	Papilioninae	Papilionini	<i>Papilio</i>	<i>Achillides</i>	<i>hermeli</i>					2 (Taiwan)
Papilionidae	Papilioninae	Papilionini	<i>Papilio</i>	<i>Achillides</i>	<i>hopponis</i>			<i>hopponis</i>		2 (Taiwan)
Papilionidae	Papilioninae	Papilionini				<i>karua</i>				8 (Java)

Papilionidae	Papilioninae	Papilionini	Papilio	Achillides	karna	carneatus				2 (Borneo)	2
Papilionidae	Papilioninae	Papilionini	Papilio	Achillides	krishna	alexandra				1 (Sumatra)	1
Papilionidae	Papilioninae	Papilionini	Papilio	Achillides		charici				6 (India)	6
Papilionidae	Papilioninae	Papilionini	Papilio	Achillides	neumogeni					2 (China/Thibet)	2
Papilionidae	Papilioninae	Papilionini	Papilio	Achillides	pollinatus					3 (Indonésie)	3
Papilionidae	Papilioninae	Papilionini	Papilio	Achillides	perantus					2 (Java)	2
Papilionidae	Papilioninae	Papilionini	Papilio	Achillides						4 (Philippines)	4
Papilionidae	Papilioninae	Papilionini	Papilio	Achillides						10 (Malaysia/Indonésie)	10
Papilionidae	Papilioninae	Papilionini	Papilio	Achillides						19 (Java)	19
Papilionidae	Papilioninae	Papilionini	Papilio	Achillides						3 (Philippines)	3
Papilionidae	Papilioninae	Papilionini	Papilio	Achillides						1 (Java)	1
Papilionidae	Papilioninae	Papilionini	Papilio	Achillides						1	1
Papilionidae	Papilioninae	Papilionini	Papilio	Achillides						4 (Indonésie)	4
Papilionidae	Papilioninae	Papilionini	Papilio	Achillides	pericles					1	1
Papilionidae	Papilioninae	Papilionini	Papilio	Achillides	syfianus					7 (Thibet)	7
Papilionidae	Papilioninae	Papilionini	Papilio	Stenoprius	suthus					36 + 29 + 27 (China)	92
Papilionidae	Papilioninae	Papilionini	Papilio	Stenoprius						6 + 34 (Japan)	40
Papilionidae	Papilioninae	Papilionini	Papilio	Stenoprius						1 (Taiwan)	1
Papilionidae	Papilioninae	Papilionini	Papilio	Stenoprius						25 (Thibet)	25
Papilionidae	Papilioninae	Papilionini	Papilio	Stenoprius	banguetanus						0
Papilionidae	Papilioninae	Papilionini	Papilio	Stenoprius	india					5 (USA)	5
Papilionidae	Papilioninae	Papilionini	Papilio	Stenoprius	hippocrates					14 (male Corsea) + 4 (female Corsea) + 3 (male Sardaigne) + 3 (female Sardaigne)	24
Papilionidae	Papilioninae	Papilionini	Papilio	Stenoprius						35 (Japan)	35
Papilionidae	Papilioninae	Papilionini	Papilio	Stenoprius						43 (France/Grece) + 9 (Vancluse) + 12 (Basses Alpes) + 2 (Var) + 26 (Alpes Maritimes) + 47 (Spagne/Portugal) + 17 (Liban/Cypré) + 54 (Haute Vienne/Laire/Auge) + 7 (Isère) + 17 (Savoie) + 20 (Alpes Maritimes) + 7 (Aberdeen) + 52+22+11 (Ile de France) + 4 (Ardennes) + 5 (Bretagne) + 9 (sous localités) + 45 (France/Angleterre) + 26 (Pyrenées Orientales) + 4 (Bouches du Rhône) + 8 (Var) + 32 (Central Europe) + 19 (Corse) + 48 (Siberia/Uruguay) + 55 (Nord Est France) + 45 (Suisse/Italie) + 17 (Central Europe) + 49 (Caucasus/Paléarctique) + 20 (France) + 4 (Pyrenées Orientales) + 8 (Libanon) + 4 (Grece) + 4 (Méditerranée) + 5 (Italie) + 2 (France)	869
Papilionidae	Papilioninae	Papilionini	Papilio	Stenoprius	nachuon	nachuon					
Papilionidae	Papilioninae	Papilionini	Papilio	Stenoprius	alpheraki					2	2
Papilionidae	Papilioninae	Papilionini	Papilio	Stenoprius	everetti					2	2
Papilionidae	Papilioninae	Papilionini	Papilio	Stenoprius	annae					16 (Bhoutan/Thibet/China)	16
Papilionidae	Papilioninae	Papilionini	Papilio	Stenoprius	neoChimantus					13 (Thibet)	13
Papilionidae	Papilioninae	Papilionini	Papilio	Stenoprius	archus					3 (China/Thibet)	3
Papilionidae	Papilioninae	Papilionini	Papilio	Stenoprius	septentrionalis					42 (China)	42
Papilionidae	Papilioninae	Papilionini	Papilio	Stenoprius	mauritanicus					36 (Maroc)	36
Papilionidae	Papilioninae	Papilionini	Papilio	Stenoprius	irous					44+22 (Persia)	66
Papilionidae	Papilioninae	Papilionini	Papilio	Stenoprius	urulanus					6	6
Papilionidae	Papilioninae	Papilionini	Papilio	Stenoprius	alaska					4 (Alaska)	4
Papilionidae	Papilioninae	Papilionini	Papilio	Stenoprius	orientis					9 (Sibéria)	9
Papilionidae	Papilioninae	Papilionini	Papilio	Stenoprius	sachalinensis					1 (Ile Sakhaline)	1
Papilionidae	Papilioninae	Papilionini	Papilio	Stenoprius	pradipharis					29 (Indie)	29
Papilionidae	Papilioninae	Papilionini	Papilio	Stenoprius	asuticus					2	2
Papilionidae	Papilioninae	Papilionini	Papilio	Stenoprius	ladakensis					3 (Indie)	3
Papilionidae	Papilioninae	Papilionini	Papilio	Stenoprius	ruprethe					1	1
Papilionidae	Papilioninae	Papilionini	Papilio	Stenoprius	mauritanicus					19 (Algérie)	19
Papilionidae	Papilioninae	Papilionini	Papilio	Stenoprius	subarctic					17 (Sibéria)	17
Papilionidae	Papilioninae	Papilionini	Papilio	Stenoprius	stikimensis					1 (USA)	1
Papilionidae	Papilioninae	Papilionini	Papilio	Stenoprius	oregonus					0	0
Papilionidae	Papilioninae	Papilionini	Papilio	Stenoprius	seficson					17 (USA)	17
Papilionidae	Papilioninae	Papilionini	Papilio	Stenoprius						gathica + nitra	
Papilionidae	Papilioninae	Papilionini	Papilio	Stenoprius						coloro + kalli (hybride avec Pimacana) + midata	
Papilionidae	Papilioninae	Papilionini	Papilio	Stenoprius						31 (USA/Equator)	31
Papilionidae	Papilioninae	Papilionini	Papilio	Stenoprius						18 (Canada/USA/Mexico)	18
Papilionidae	Papilioninae	Papilionini	Papilio	Stenoprius						8 (Panama) + 6 (Amérique Centrale)	14

Papilionidae	Papilioninae	Papilio	Pterourus	zegeus	<i>areolatus</i>		3+16 (Colombia)	19
					<i>rosenbergi</i>		1 (Equator)	1
					<i>barclasi</i>		2 (Colombia)	2
					<i>chrysochilus</i>		3 (Peru) + 1 (form silenus - Peru)	4
					<i>heliasar</i>		1	1
Papilionidae	Papilioninae	Papilio	Pterourus	neyi			1 (Equator)	1
					<i>elycia</i>		6 (form elycia Vietnam) + 3 (form oupape Vietnam) + 5 (form janus Vietnam) + 4 (form papone Vietnam) + 8 (form dissimila Vietnam) + 32+30+29 +40+41+30+30+6 (China/India)	264
Papilionidae	Papilioninae	Papilio	Chilasa	elycia			1 (Philippines)	1
					<i>panoptus</i>		4 (India)	4
					<i>flavolimbatus</i>		12 (Sri Lanka/Philippines)	12
					<i>lankavara</i>		5 (Philippines)	5
					<i>polephates</i>		21 (India/China)	21
					<i>epysides</i>		1 (Taiwan)	1
					<i>hypochra</i>		1 (Laos)	1
					<i>curvatus</i>		7 (China)	7
					<i>horatus</i>		3 (Thibet)	3
					<i>ageator</i>		24 (India/China)	24
					<i>govindra</i>		8 (Taiwan/Thibet)	8
					<i>agator</i>		3 (Papua New Guinea)	3
					<i>govindra</i>		0	0
					<i>telarchus</i>		4 (form telarchus Vietnam) + 1 (form danisepu Vietnam) + 1 (Vietnam) + 13 (Laos/China)	19
					<i>telarchus</i>		6 + 6 (Indonesia)	12
					<i>paradasa</i>		3 (Java)	3
					<i>muscus</i>		2 (Sumatra)	2
					<i>arigma</i>		17 (Sumatra)	17
					<i>slateri</i>		21 (India/China)	21
					<i>marginata</i>		4 (Laos)	4
					<i>avayanus</i>		3 (India/Indonesia)	3
					<i>hevisani</i>		1 (Indonesia) + 3 (form persides - Indonesia)	4
							7 (Salomon island)	7
							0	0
							5+20 +20USA/Mexico)	45
							0	0
					<i>ihous</i>		13 (French Guiana/Suriname)	13
					<i>autocles</i>		15+18 (Mexico/Guatemala/Peru/Honduras/Nicaragua)	33
					<i>maeter</i>		19 +20+20 (Colombia/Costa Rica/Venezuela)	59
					<i>cinrus</i>		12+16+6 (Peru/Equator)	34
					<i>brasilensis</i>		9+16+16+17+3 (Brazil/Argentina)	61
					<i>thoumides</i>		12 (Paraguay/Argentina)	12
							3 (Cuba)	3
					<i>lyciphron</i>		10 +26 (Paraguay/Brazil) + 4 (female form pirithous - Paraguay/Brazil)	36
					<i>hippomedon</i>		8 (Colombia/Venezuela)	8
					<i>phantus</i>		5 (Colombia/Bolivia/Peru)	5
					<i>anchisades</i>		6 (Honduras/Costa Rica)	6
					<i>idarus</i>		9+18+31+20 (French Guiana/Guatemala/Colombia/Peru/Venezuela)	78
					<i>capys</i>		15+10 (Mexico/Venezuela)	25
							32+20 (Brazil)	52
							14 (Guatemala)	14
							15+22 (Brazil) + 10 +3(female form hectorides - Brazil) + 1 (female form melania - Paraguay) + 2 (female form catamelis)	55
					<i>robules</i>		1 (Colombia)	1

Papilionidae	Papilioninae	Papilionini	Papilio	<i>Heracles</i>	<i>torquatus</i>	<i>torquatus</i>					16 (Bolivia/Colombia/Peru)	16
Papilionidae	Papilioninae	Papilionini			<i>orchlanius</i>	<i>orchlanius</i>					1+4 (French Guyana) + 1 (female form caudius - Amazonie) + 5 (female form thersa - French Guyana)	11
Papilionidae	Papilioninae	Papilionini	Papilio	<i>Heracles</i>	<i>polybus</i>	<i>polybus</i>					30 (Brazil)	30
Papilionidae	Papilioninae	Papilionini	Papilio		<i>andracemon</i>	<i>andracemon</i>					5+15 (Cuba)	20
Papilionidae	Papilioninae	Papilionini	Papilio		<i>tailori</i>	<i>tailori</i>					2 (Cuba)	2
Papilionidae	Papilioninae	Papilionini	Papilio	<i>Heracles</i>	<i>andragens</i>	<i>andragens</i>					20 +9 (Colombia/Venezuela/Equator) +4 (female form pirambus - French Guyana)	33
Papilionidae	Papilioninae	Papilionini	Papilio	<i>Heracles</i>	<i>landicus</i>	<i>landicus</i>					3+11 (Peru) + 1 (spandromorphic - Brazil)	15
Papilionidae	Papilioninae	Papilionini	Papilio	<i>Heracles</i>	<i>epidaurus</i>	<i>epidaurus</i>					14 (Haiti/Guatemala/Honduras/Mexico)	14
Papilionidae	Papilioninae	Papilionini	Papilio	<i>Heracles</i>	<i>aristodemus</i>	<i>aristodemus</i>			<i>hyrnalidae</i>		3 (Haiti)	0
Papilionidae	Papilioninae	Papilionini	Papilio	<i>Heracles</i>	<i>teneres</i>	<i>teneres</i>					5 (Cuba)	5
Papilionidae	Papilioninae	Papilionini	Papilio		<i>poecanus</i>	<i>poecanus</i>						0
Papilionidae	Papilioninae	Papilionini	Papilio	<i>Heracles</i>	<i>aristor</i>	<i>aristor</i>					4 (Cuba)	0
Papilionidae	Papilioninae	Papilionini	Papilio	<i>Heracles</i>	<i>caiguandubus</i>	<i>caiguandubus</i>					3 (Colombia)	4
Papilionidae	Papilioninae	Papilionini	Papilio	<i>Heracles</i>	<i>ebanoides</i>	<i>ebanoides</i>			<i>despassosi + muroni</i>			3
Papilionidae	Papilioninae	Papilionini	Papilio	<i>Heracles</i>	<i>epeneus</i>	<i>epeneus</i>					3 (Equator)	3
Papilionidae	Papilioninae	Papilionini	Papilio	<i>Heracles</i>	<i>garleppi</i>	<i>garleppi</i>					8 (French Guyana/Equator)	8
Papilionidae	Papilioninae	Papilionini	Papilio	<i>Heracles</i>	<i>limeros</i>	<i>limeros</i>			<i>tasos (hybride avec P. torquatus)</i>		3 (Brazil)	3
Papilionidae	Papilioninae	Papilionini	Papilio	<i>Heracles</i>	<i>bolai</i>	<i>bolai</i>					3 (Brazil)	3
Papilionidae	Papilioninae	Papilionini	Papilio	<i>Heracles</i>	<i>humabaus</i>	<i>humabaus</i>					11 (Venezuela)	11
Papilionidae	Papilioninae	Papilionini	Papilio	<i>Heracles</i>	<i>hypsson</i>	<i>hypsson</i>					9 (French Guyana/Bolivia) + 1 (female form amosis - French Guyana) + 3 (female form paransis - French Guyana)	13
Papilionidae	Papilioninae	Papilionini	Papilio		<i>phylon</i>	<i>phylon</i>					2 (Equator)	2
Papilionidae	Papilioninae	Papilionini	Papilio	<i>Heracles</i>	<i>isidonus</i>	<i>isidonus</i>			<i>rhodotenus</i>		5 (Colombia/Equator)	5
Papilionidae	Papilioninae	Papilionini	Papilio		<i>lamarchei</i>	<i>lamarchei</i>					6+2 (Equator/Peru/Guatemala)	8
Papilionidae	Papilioninae	Papilionini	Papilio	<i>Heracles</i>	<i>machonides</i>	<i>machonides</i>					15 (Colombia/Equator)	15
Papilionidae	Papilioninae	Papilionini	Papilio	<i>Heracles</i>	<i>melanias</i>	<i>melanias</i>					2 (Bolivia)	2
Papilionidae	Papilioninae	Papilionini	Papilio	<i>Heracles</i>	<i>orythion</i>	<i>orythion</i>					3 (Haiti)	3
Papilionidae	Papilioninae	Papilionini	Papilio	<i>Heracles</i>	<i>oxyzus</i>	<i>oxyzus</i>					3 (Cuba)	0
Papilionidae	Papilioninae	Papilionini	Papilio	<i>Heracles</i>	<i>pocon</i>	<i>pocon</i>					11 (Peru)	3
Papilionidae	Papilioninae	Papilionini	Papilio	<i>Heracles</i>	<i>pelias</i>	<i>pelias</i>					5+12 (Colombia)	17
Papilionidae	Papilioninae	Papilionini	Papilio	<i>Heracles</i>	<i>peloides</i>	<i>peloides</i>					5 (Jamaica)	5
Papilionidae	Papilioninae	Papilionini	Papilio	<i>Heracles</i>	<i>phamaeus</i>	<i>phamaeus</i>					3 (Cuba)	3
Papilionidae	Papilioninae	Papilionini	Papilio	<i>Heracles</i>	<i>rogeri</i>	<i>rogeri</i>					33+30+30+2 (Mexico)	0
Papilionidae	Papilioninae	Papilionini	Papilio	<i>Heracles</i>	<i>therzites</i>	<i>therzites</i>					1 (Mexico)	95
Papilionidae	Papilioninae	Papilionini	Papilio	<i>Druryia</i>	<i>andracenus</i>	<i>andracenus</i>					4 (Jamaica)	1
Papilionidae	Papilioninae	Papilionini	Papilio	<i>Druryia</i>	<i>antimachus</i>	<i>antimachus</i>					4 (Gibson/Cameroon)	4
Papilionidae	Papilioninae	Papilionini	Papilio	<i>Druryia</i>	<i>arnoldiana</i>	<i>arnoldiana</i>			<i>arnoldi</i>		9+11+10+10+4+3 (Congo/Guinea/Sierra Leone/Central African Republic/Kenya)	4
Papilionidae	Papilioninae	Papilionini	Papilio	<i>Druryia</i>	<i>charopus</i>	<i>charopus</i>					9 (Ethiopia)	52
Papilionidae	Papilioninae	Papilionini	Papilio	<i>Druryia</i>	<i>ehimolentis</i>	<i>ehimolentis</i>					22 (Guinea/Congo)	22
Papilionidae	Papilioninae	Papilionini	Papilio	<i>Druryia</i>	<i>ehimolentis</i>	<i>ehimolentis</i>					25 +30+25+5+24+29+4+3+2+3+13 (Congo/Sierra Leone/Kenya) + 3 (form fusilis - Congo)	0
Papilionidae	Papilioninae	Papilionini	Papilio	<i>Druryia</i>	<i>ehimolentis</i>	<i>ehimolentis</i>			<i>bromius</i>		6 (Tanzanie)	210
Papilionidae	Papilioninae	Papilionini	Papilio	<i>Druryia</i>	<i>ehimolentis</i>	<i>ehimolentis</i>					24 (Ouganda)	6
Papilionidae	Papilioninae	Papilionini	Papilio	<i>Druryia</i>	<i>ehimolentis</i>	<i>ehimolentis</i>			<i>furvus</i>			24
Papilionidae	Papilioninae	Papilionini	Papilio	<i>Druryia</i>	<i>ehimolentis</i>	<i>ehimolentis</i>					39 (East Africa)	0
Papilionidae	Papilioninae	Papilionini	Papilio	<i>Druryia</i>	<i>ehimolentis</i>	<i>ehimolentis</i>			<i>precalaris</i>		3 (Congo)	95
Papilionidae	Papilioninae	Papilionini	Papilio	<i>Druryia</i>	<i>ehimolentis</i>	<i>ehimolentis</i>			<i>plagiatus</i>		6 (East Africa)	3
Papilionidae	Papilioninae	Papilionini	Papilio	<i>Druryia</i>	<i>ehimolentis</i>	<i>ehimolentis</i>						6

Papilionidae	Papilioninae	Papilionini	Papilio	Druryia	<i>cyproseoides</i>					24+24 +3(Sierra Leone/Libertia) + 7 (form lucifascia)	60
Papilionidae	Papilioninae	Papilionini	Papilio	Druryia	<i>demondi</i>					48 + 5 (East Africa) + 7 (form nicksi - Ethiopia)	0
Papilionidae	Papilioninae	Papilionini	Papilio	Druryia	<i>echeroides</i>					13 (Ethiopia)	60
Papilionidae	Papilioninae	Papilionini	Papilio	Druryia	<i>oscar</i>					19 (form zoroastres - East Africa) + 3 (form hamayeri - Congo) + 1 (form preussino - Ouganda)	23
Papilionidae	Papilioninae	Papilionini	Papilio	Druryia	<i>zoroastres</i>						0
Papilionidae	Papilioninae	Papilionini	Papilio	Druryia	<i>fermalus</i>						0
Papilionidae	Papilioninae	Papilionini	Papilio	Druryia	<i>fligrae</i>						0
Papilionidae	Papilioninae	Papilionini	Papilio	Druryia	<i>fuelliborni</i>					7 (form spocedi - Tanzania) + 1 (form kulleborni - Kenya)	8
Papilionidae	Papilioninae	Papilionini	Papilio	Druryia	<i>gullenus</i>					24+7 (Congo/Central African Republic)	31
Papilionidae	Papilioninae	Papilionini	Papilio	Druryia	<i>hornmani</i>					2 (East Africa)	2
Papilionidae	Papilioninae	Papilionini	Papilio	Druryia	<i>interjectana</i>						0
Papilionidae	Papilioninae	Papilionini	Papilio	Druryia	<i>jacksoni</i>					36+43 (East Africa)	79
Papilionidae	Papilioninae	Papilionini	Papilio	Druryia	<i>mackinnoni</i>					25+25+25+25+24(Kenya/Congo)	124
Papilionidae	Papilioninae	Papilionini	Papilio	Druryia	<i>maeseni</i>						0
Papilionidae	Papilioninae	Papilionini	Papilio	Druryia	<i>manili</i>					31 (Ile-de-France)	31
Papilionidae	Papilioninae	Papilionini	Papilio	Druryia	<i>mechowi</i>					11 (Guinea/Congo)	11
Papilionidae	Papilioninae	Papilionini	Papilio	Druryia	<i>whitalli</i>					6 (Ouganda)	6
Papilionidae	Papilioninae	Papilionini	Papilio	Druryia	<i>mechovianus</i>					9 (Congo)	9
Papilionidae	Papilioninae	Papilionini	Papilio	Druryia	<i>microps</i>						0
Papilionidae	Papilioninae	Papilionini	Papilio	Druryia	<i>niveus</i>					28 (Grande Comore)	28
Papilionidae	Papilioninae	Papilionini	Papilio	Druryia	<i>niveus</i>					16+21+24+25+19+27+22+21+27+25+18+24+35+38+44+34+22+13+20 +3(Afrique du Sud/Central African Republic/Zimbabwe/Guinea/Ivory Coast/Gabon/Kenya/Ethiopia)	516
Papilionidae	Papilioninae	Papilionini	Papilio	Druryia	<i>ovatus</i>					25 (Tanzania/Ouganda)	25
Papilionidae	Papilioninae	Papilionini	Papilio	Druryia	<i>phorbanta</i>					8 (Ethiopia)	8
Papilionidae	Papilioninae	Papilionini	Papilio	Druryia	<i>plagiatus</i>					2 (Sierra Leone)	2
Papilionidae	Papilioninae	Papilionini	Papilio	Druryia	<i>sosia</i>					19 (males - Cayenne) + 9 (females - Bourbon)	28
Papilionidae	Papilioninae	Papilionini	Papilio	Druryia	<i>blarui</i>					Sp. manquant (Secheles)	0
Papilionidae	Papilioninae	Papilionini	Papilio	Druryia	<i>affua</i>					6 (East Africa)	6
Papilionidae	Papilioninae	Papilionini	Papilio	Druryia	<i>zalmoxis</i>					23+16 (Congo/Sierra Leone/Central African Republic)	39
Papilionidae	Papilioninae	Papilionini	Papilio	Druryia	<i>zenobia</i>					2 (Congo)	2
Papilionidae	Papilioninae	Papilionini	Papilio	Druryia	<i>auratus</i>					11 + 12 + 11 + 12 (Congo/Cameroun)	46
Papilionidae	Papilioninae	Tenopulpini	Tenopulpus	-	<i>imperialis</i>					35 (Cote d'Ivoire/Ghana/Liberia)	35
Papilionidae	Papilioninae	Tenopulpini	Tenopulpus	-	<i>imperialis</i>					19 (India)	0
Papilionidae	Papilioninae	Tenopulpini	Tenopulpus	-	<i>himalicus</i>					15 (India)	19
Papilionidae	Papilioninae	Tenopulpini	Tenopulpus	-	<i>hercules</i>					4 (Tibet)	15
Papilionidae	Papilioninae	Tenopulpini	Tenopulpus	-	<i>poeyni</i>					2 (Indonesie) + 1	0
Papilionidae	Papilioninae	Tenopulpini	Tenopulpus	-	<i>cumbitatus</i>					8 (Vietnam/Malaysia)	8
Papilionidae	Papilioninae	Tenopulpini	Tenopulpus	-	<i>evan</i>					10 (India)	10
Papilionidae	Papilioninae	Tenopulpini	Tenopulpus	-	<i>brunei</i>					1 (Indonesie)	1
Papilionidae	Papilioninae	Tenopulpini	Tenopulpus	-	<i>gigas</i>					12 (India)	12
Papilionidae	Papilioninae	Tenopulpini	Tenopulpus	-	<i>sauteri</i>					3 (Sumatra Indonesie)	0
Papilionidae	Papilioninae	Tenopulpini	Tenopulpus	-	<i>luchinus</i>					3 (Celebes Indonesie)	3
Papilionidae	Papilioninae	Tenopulpini	Tenopulpus	-	<i>lugeni</i>					14 (India)	14
Papilionidae	Papilioninae	Tenopulpini	Tenopulpus	-	<i>aidanus</i>						0
Papilionidae	Papilioninae	Tenopulpini	Tenopulpus	-	<i>flachui</i>						0
Papilionidae	Papilioninae	Tenopulpini	Tenopulpus	-	<i>luchii</i>						0
Papilionidae	Papilioninae	Tenopulpini	Tenopulpus	-	<i>nox</i>					14 (Java Indonesie)	14
Papilionidae	Papilioninae	Tenopulpini	Tenopulpus	-	<i>noctis</i>					3 (Borneo/Java)	3
Papilionidae	Papilioninae	Tenopulpini	Tenopulpus	-	<i>nox</i>					2 (Java)	2
Papilionidae	Papilioninae	Tenopulpini	Tenopulpus	-	<i>noctula</i>					7 (Borneo)	7
Papilionidae	Papilioninae	Tenopulpini	Tenopulpus	-	<i>strix</i>					1	1

Papilionidae	Troidini	<i>Pachliopta</i>	-	<i>aristolochiae</i>	<i>gompipetis</i> <i>aristolochiae</i> <i>camaria</i> <i>cydonicus</i> <i>adaxus</i> <i>interpositus</i> <i>rhodopis</i> <i>brevicauda</i> <i>kozzeba</i> <i>anaphus</i> <i>amphidius</i> <i>philippus</i> <i>hulianus</i> <i>limbockenis</i> <i>austrorandanus</i>	12 (Cambodia/Vietnam) + 3 (Ile Adaman - India) + 9 (Vietnam) + 3 (Cambodia) 7+16 (India/Sikkim) + 26 (form diphtis - Sikkim/Java/India) + 25 (Jorlane/Malaysia/Sumatra/Thailand/Cambodia)	27
Papilionidae	Troidini	<i>Pachliopta</i>	-	<i>atropis</i>	2 (Ile Adaman/Nicebur - India)	2	
Papilionidae	Troidini	<i>Pachliopta</i>	-	<i>beccar</i>	12+17 (India)	29	
Papilionidae	Troidini	<i>Pachliopta</i>	-	<i>japon</i>	5 (Vietnam)	5	
Papilionidae	Troidini	<i>Pachliopta</i>	-	<i>kozzeba</i>	4 (Taiwan)	4	
Papilionidae	Troidini	<i>Pachliopta</i>	-	<i>leversis</i>	8 (China)	8	
Papilionidae	Troidini	<i>Pachliopta</i>	-	<i>liris</i>	1 (Philippines)	1	
Papilionidae	Troidini	<i>Pachliopta</i>	-	<i>maur</i>	9+18 (Philippines)	27	
Papilionidae	Troidini	<i>Pachliopta</i>	-	<i>oreon</i>	14 (Sumatra)	14	
Papilionidae	Troidini	<i>Pachliopta</i>	-	<i>paralysa</i>	8 (Sumatra)	8	
Papilionidae	Troidini	<i>Pachliopta</i>	-	<i>phlegon</i>	6 (Philippines)	6	
Papilionidae	Troidini	<i>Pachliopta</i>	-	<i>polydorus</i>	1 (Sumatra)	1	
Papilionidae	Troidini	<i>Pachliopta</i>	-	<i>prunus</i>	5 (Indonesia)	5	
Papilionidae	Troidini	<i>Pachliopta</i>	-	<i>sepius</i>	1 (Indonesia)	1	
Papilionidae	Troidini	<i>Pachliopta</i>	-	<i>schadenbergi</i>	2 (Indonesia)	2	
Papilionidae	Troidini	<i>Pachliopta</i>	-	<i>crecida</i>	1 (Indonesia)	1	
Papilionidae	Troidini	<i>Pachliopta</i>	-	<i>attenor</i>	30+15 (India/Sri Lanka)	45	
Papilionidae	Troidini	<i>Pachliopta</i>	-	<i>areucus</i>	3 (Sri Lanka)	3	
Papilionidae	Troidini	<i>Pachliopta</i>	-	<i>prunus</i>	2 (Philippine)	2	
Papilionidae	Troidini	<i>Pachliopta</i>	-	<i>prunus</i>	2 (Timor)	2	
Papilionidae	Troidini	<i>Pachliopta</i>	-	<i>prunus</i>	1	1	
Papilionidae	Troidini	<i>Pachliopta</i>	-	<i>prunus</i>	6 (Indonesia)	6	
Papilionidae	Troidini	<i>Pachliopta</i>	-	<i>prunus</i>	1 (Indonesia)	1	
Papilionidae	Troidini	<i>Pachliopta</i>	-	<i>prunus</i>	2 (Philippine)	2	
Papilionidae	Troidini	<i>Pachliopta</i>	-	<i>prunus</i>	1 (Indonesia)	1	
Papilionidae	Troidini	<i>Pachliopta</i>	-	<i>prunus</i>	1	1	
Papilionidae	Troidini	<i>Pachliopta</i>	-	<i>prunus</i>	5 (India)	5	
Papilionidae	Troidini	<i>Pachliopta</i>	-	<i>prunus</i>	7 (Sumatra)	7	
Papilionidae	Troidini	<i>Pachliopta</i>	-	<i>prunus</i>	2 (Indonesia)	2	
Papilionidae	Troidini	<i>Pachliopta</i>	-	<i>prunus</i>	3 (Indonesia)	3	
Papilionidae	Troidini	<i>Pachliopta</i>	-	<i>prunus</i>	5 (Papua New Guinea)	5	
Papilionidae	Troidini	<i>Pachliopta</i>	-	<i>prunus</i>	2 (Papua New Guinea)	2	
Papilionidae	Troidini	<i>Pachliopta</i>	-	<i>prunus</i>	2 (Papua New Guinea)	2	
Papilionidae	Troidini	<i>Pachliopta</i>	-	<i>prunus</i>	4 (Papua New Guinea)	4	
Papilionidae	Troidini	<i>Pachliopta</i>	-	<i>prunus</i>	14 (Indonesia)	14	
Papilionidae	Troidini	<i>Pachliopta</i>	-	<i>prunus</i>	2 (Indonesia)	2	
Papilionidae	Troidini	<i>Pachliopta</i>	-	<i>prunus</i>	3 (Indonesia)	3	
Papilionidae	Troidini	<i>Pachliopta</i>	-	<i>prunus</i>	1 (Timor)	1	
Papilionidae	Troidini	<i>Pachliopta</i>	-	<i>prunus</i>	2 (Australia)	2	
Papilionidae	Troidini	<i>Pachliopta</i>	-	<i>prunus</i>	2 (India)	2	
Papilionidae	Troidini	<i>Pachliopta</i>	-	<i>prunus</i>	3 (Indonesia/Papua New Guinea/India)	3	
Papilionidae	Troidini	<i>Pachliopta</i>	-	<i>prunus</i>	4 (Papua New Guinea)	4	
Papilionidae	Troidini	<i>Pachliopta</i>	-	<i>prunus</i>	2 (Papua New Guinea)	2	
Papilionidae	Troidini	<i>Pachliopta</i>	-	<i>prunus</i>	25 (Indonesia)	25	
Papilionidae	Troidini	<i>Pachliopta</i>	-	<i>prunus</i>	3 (Indonesia)	3	
Papilionidae	Troidini	<i>Pachliopta</i>	-	<i>prunus</i>	4 (Indonesia)	4	
Papilionidae	Troidini	<i>Pachliopta</i>	-	<i>prunus</i>	38+4 (Australia)	39	
Papilionidae	Troidini	<i>Pachliopta</i>	-	<i>prunus</i>	14 + 15	29	
Papilionidae	Troidini	<i>Pachliopta</i>	-	<i>prunus</i>	2 (Indonesia)	2	
Papilionidae	Troidini	<i>Pachliopta</i>	-	<i>prunus</i>	8 (Indonesia) + 5+6+6+3	28	

Papilionidae	Papilioninae	Troidini	<i>Ornithoptera</i>	-	<i>prunus</i>	<i>kerabu</i> <i>arriana</i> <i>poseidon</i> <i>boromani</i> <i>modensis</i> <i>coelestis</i> <i>arvilianus</i>	13+7 (Indonesia) 5+11+1 (Indonesia) 10+14+14+12+13+11+12+13+7 (Indonesia/Papua New Guinea/Australia) 3 (Papua New Guinea) 4 (Papua New Guinea) 2 4+12+7+8+8+7+8+2 (Solomon island/Papua New Guinea)	20 17 118 3 4
Papilionidae	Papilioninae	Troidini	<i>Ornithoptera</i>	-	<i>euphorion</i>		10+1+12 (Australia)	56
Papilionidae	Papilioninae	Troidini	<i>Ornithoptera</i>	-	<i>croesus</i>	<i>croesus</i> <i>balus</i>	10+1+8 (Indonesia) 12+8 (Indonesia)	33 29 20
Papilionidae	Papilioninae	Troidini	<i>Ornithoptera</i>	-	<i>goliath</i>	<i>proxa</i> <i>goliath</i> <i>sumon</i>	2 4 (Papua New Guinea) 5 (Papua New Guinea)	2 4 5
Papilionidae	Papilioninae	Troidini	<i>Ornithoptera</i>	-	<i>rethschildi</i>	<i>supremus</i>	2 (Papua New Guinea) 9 (Papua New Guinea)	2 9
Papilionidae	Papilioninae	Troidini	<i>Ornithoptera</i>	-	<i>paradisaea</i>	<i>paradisaea</i>	4 (Papua New Guinea) + 3 (female form <i>paradisaea</i> - Papua New Guinea)	7
Papilionidae	Papilioninae	Troidini	<i>Ornithoptera</i>	-	<i>arfakensis</i>	<i>flavescens</i> <i>flavescens</i>	3 (Papua New Guinea) 3 (Papua New Guinea)	3 5
Papilionidae	Papilioninae	Troidini	<i>Ornithoptera</i>	-	<i>tilhonis</i>	<i>maegerianus</i> <i>microstigma</i> <i>tilhonis</i>	5 (Papua New Guinea) 2 (Papua New Guinea)	5 2
Papilionidae	Papilioninae	Troidini	<i>Ornithoptera</i>	-	<i>albivandae</i>		6+4 (Papua New Guinea)	10
Papilionidae	Papilioninae	Troidini	<i>Ornithoptera</i>	-	<i>chamaca</i>		8 (Papua New Guinea)	8
Papilionidae	Papilioninae	Troidini	<i>Ornithoptera</i>	-	<i>meridionalis</i>		2 (Papua New Guinea)	2
Papilionidae	Papilioninae	Troidini	<i>Ornithoptera</i>	-	<i>richmondia</i>	<i>abakoe</i> (hybride <i>O. priamus</i>) <i>O. rethschildi</i> + <i>albivandae</i> (hybride <i>O. victrix</i>) + <i>chamaca</i>	21+5 (Australia)	26
Papilionidae	Papilioninae	Troidini	<i>Ornithoptera</i>	-	<i>victoriae</i>	<i>regis</i> <i>reginae</i> <i>victoriae</i> <i>rubianus</i> <i>epiphanes</i> <i>isabelle</i> <i>thomsonii</i> <i>aeacus</i> <i>scribanius</i> <i>malianus</i> <i>insularis</i> <i>formosanus</i> <i>ceberus</i> <i>ethycaetes</i> <i>spilota</i> <i>heliconides</i> <i>typhaon</i> <i>isara</i>	8 (Solomon island) + 13 (form <i>lancei</i> - Papua New Guinea + 2 (form <i>bunensis</i> - Solomon island) + 2 (form <i>alexis</i> - Papua New Guinea) + 2 (form <i>lancei</i> - Papua New Guinea) + 6 (form <i>gabriel</i> - Papua New Guinea) + 6 (form <i>bunensis</i> - Papua New Guinea) + 10 (hybride <i>allotri</i>) + 6 (Papua New Guinea) 3 (Solomon island) 3 (Solomon island) 3 (Solomon island) 1 (Solomon island) 5 (Solomon island) 5 (Vietnam) + 1 (Cambodia) 8 (Cambodia) + 18+9+20 (Thibet/India) 4 (Vietnam) 3 (Malaysia) 2 (Indonesia) 9 (Taiwan) 3 (form <i>ceberus</i> Vietnam) + 18+10 (India/Sri Lanka) + 2 (female form <i>gymnotella</i>) 4 (Vietnam) + 1 (female form <i>axello</i>) + 1 (female form <i>chongluahuang</i>) 1 (Indonesia) 2 (Indonesia) + 1 (female form <i>thypata</i>) 7 (Indonesia) + 4 (female form <i>spilota</i> - Indonesia) + 1 (female form <i>plycia</i> - Indonesia) 1 (Indonesia)	55 3 3 3 1 5 6 55 4 3 2 9 33 6 1 3 12 1 29 29 6 39 6
Papilionidae	Papilioninae	Troidini	<i>Troides</i>	-	<i>aeacus</i>	<i>aeacus</i>		2
Papilionidae	Papilioninae	Troidini	<i>Troides</i>	-	<i>helena</i>	<i>helena</i>		1
Papilionidae	Papilioninae	Troidini	<i>Troides</i>	-	<i>prattorum</i>	<i>prattorum</i>		6

Papilionidae	Papilioninae	Troidini	<i>Parides</i>		<i>erimedes</i>		<i>arcus</i>	<i>timius</i>	38+15 (Venezuela) 37+4 (Brazil/Mexico/Honduras/Guatemala)	53
					<i>mylotes</i>					41
					<i>myale</i>					25
					<i>atrophus</i>					23
					<i>ambros</i>					12
					<i>limius</i>					9
Papilionidae	Papilioninae	Troidini	<i>Parides</i>		<i>zocynthus</i>				8+6 (Brazil)	14
					<i>polyenus</i>				4 (Brazil)	4
					<i>neophilus</i>			<i>schuppi</i>	17 (French Guyana)	17
					<i>conus</i>				8 (Paraguay/Bolivia)	8
Papilionidae	Papilioninae	Troidini	<i>Parides</i>		<i>neophilus</i>				31+3 (Peru)	34
					<i>ecobius</i>				30 (Brazil)	30
					<i>parianus</i>				5 (Venezuela)	5
					<i>enrhaetes</i>				1 (Paraguay)	1
					<i>dracel</i>			<i>dracel + nephelion</i>	20 (Peru/Ecuador/Colombia)	20
					<i>seropis</i>				7 (Colombia) + 2 (variant - Panama)	7
					<i>oxyris</i>				5 (Venezuela)	5
					<i>albatus</i>				15 (Colombia)	15
					<i>cyonoides</i>				9 (Venezuela)	9
Papilionidae	Papilioninae	Troidini	<i>Parides</i>		<i>anchises</i>				14 (French Guyana) + 3 (female form ab - French Guyana)	14
					<i>orbignyus</i>				1 (Paraguay)	1
					<i>fortalei</i>				4 (Brazil)	4
					<i>bellos</i>				27 (Brazil/Ecuador)	27
					<i>nephelion</i>				17 + 12 (Paraguay/Brazil)	29
					<i>etias</i>				5 (Bolivia)	5
					<i>atimianus</i>				3 (Peru)	3
					<i>alceros</i>				6 (French Guyana)	6
					<i>bogotanus</i>				6 (Ecuador/Peru)	6
Papilionidae	Papilioninae	Troidini	<i>Parides</i>		<i>vermannus</i>				27 (French Guyana)	27
					<i>ynaraetes</i>				5 (Bolivia)	5
					<i>sesos</i>				7 (Mexico/Venezuela)	7
Papilionidae	Papilioninae	Troidini	<i>Parides</i>		<i>sexosaris</i>				17+32+7 (Bolivia/Ecuador/Mexico/Brazil/French Guyana/Peru)	56
					<i>taquinus</i>				10 (Colombia/Panama/Venezuela)	10
					<i>parulcescens</i>				3 (Bolivia)	3
Papilionidae	Papilioninae	Troidini	<i>Parides</i>		<i>phoebus</i>				7+10 (Mexico/Honduras)	17
					<i>ocdippus</i>				8 (Colombia)	8
Papilionidae	Papilioninae	Troidini	<i>Parides</i>		<i>childerense</i>				1 (Colombia)	1
					<i>amarcula</i>				6 (Ecuador)	6
					<i>ypilavilla</i>			<i>mithras</i>	19 (French Guyana)	19
Papilionidae	Papilioninae	Troidini	<i>Parides</i>		<i>chabrias</i>				11 (Amazon)	11
Papilionidae	Papilioninae	Troidini	<i>Parides</i>		<i>agenus</i>				18+8 (Brazil/Paraguay)	26
Papilionidae	Papilioninae	Troidini	<i>Parides</i>		<i>promeus</i>				23 (Brazil)	23
Papilionidae	Papilioninae	Troidini	<i>Parides</i>		<i>ascantus</i>				12 (Brazil)	12
Papilionidae	Papilioninae	Troidini	<i>Parides</i>		<i>huniclus</i>			<i>chamissentia</i>	15 (Brazil)	15
					<i>abodoris</i>				4 (Brazil)	4
					<i>perthebus</i>				4 (Argentina)	4
					<i>damocranes</i>				11 (Brazil/Argentina)	11
Papilionidae	Papilioninae	Troidini	<i>Parides</i>		<i>alopis</i>				3 (Mexico)	3
Papilionidae	Papilioninae	Troidini	<i>Parides</i>		<i>cuturna</i>				3 (Peru)	3
Papilionidae	Papilioninae	Troidini	<i>Parides</i>		<i>echmon</i>				18 (French Guyana/Brazil)	18
					<i>ergetes</i>				4 (French Guyana) + 4 (female form psander - French Guyana)	8
					<i>zaris</i>			<i>erdaes + polytelus</i>	11 (Venezuela/Honduras)	11
					<i>nov</i>				5 (Colombia)	5

Papilionidae	Troidini	<i>Parides</i>		<i>erithalton</i>			21 (Colombia/French Guiana) + 7 (variant - Colombia)	21
Papilionidae	Troidini	<i>Parides</i>		<i>subvates</i>			4 (Ecuador)	4
Papilionidae	Troidini	<i>Parides</i>		<i>polyschis</i>			17+10 (Honduras/Mexico/Costa Rica)	27
Papilionidae	Troidini	<i>Parides</i>		<i>xanthias</i>			4 (Peru)	4
Papilionidae	Troidini	<i>Parides</i>		<i>lucydes</i>			12 (Ecuador/Peru)	12
Papilionidae	Troidini	<i>Parides</i>		<i>alarces</i>			16 (Peru)	16
Papilionidae	Troidini	<i>Parides</i>					4 (Cuba)	4
Papilionidae	Troidini	<i>Parides</i>		<i>gumilochimus</i>				0
Papilionidae	Troidini	<i>Parides</i>		<i>hahneli</i>				26
Papilionidae	Troidini	<i>Parides</i>		<i>iphidamas</i>			26 (Honduras/Mexico/Guatemala)	26
Papilionidae	Troidini	<i>Parides</i>		<i>phalax</i>			12 (Colombia)	12
Papilionidae	Troidini	<i>Parides</i>		<i>colosyna</i>			2 (Ecuador)	2
Papilionidae	Troidini	<i>Parides</i>		<i>elatos</i>			1 (Colombia)	1
Papilionidae	Troidini	<i>Parides</i>		<i>truncata</i>			2 (Venezuela)	2
Papilionidae	Troidini	<i>Parides</i>		<i>klagesi</i>			7+3 (Mexico) + 7 (variant - Mexico)	0
Papilionidae	Troidini	<i>Parides</i>		<i>montezuma</i>			5 (Ecuador)	5
Papilionidae	Troidini	<i>Parides</i>		<i>orellana</i>			12 (Mexico/Guatemala) + 2 (variant - Mexico)	14
Papilionidae	Troidini	<i>Parides</i>		<i>panures</i>			2 (Ecuador)	2
Papilionidae	Troidini	<i>Parides</i>		<i>phidareus</i>			7+22 (Colombia/Venezuela)	29
Papilionidae	Troidini	<i>Parides</i>		<i>phosphorus</i>			1 (Ecuador)	1
Papilionidae	Troidini	<i>Parides</i>		<i>stimbuchi</i>			1 (Amazon)	1
Papilionidae	Troidini	<i>Parides</i>		<i>pizarro</i>			1 (French Guiana)	1
Papilionidae	Troidini	<i>Parides</i>		<i>quadatus</i>			5 (Bolivia/Peru)	5
Papilionidae	Troidini	<i>Parides</i>		<i>vercingerotzi</i>			3 (Peru)	3
Papilionidae	Troidini	<i>Parides</i>		<i>coelus</i>			4 (Peru)	4
Papilionidae	Troidini	<i>Parides</i>		<i>cocahuamba</i>			5 (Peru/Bolivia/Brazil)	5
Papilionidae	Troidini	<i>Parides</i>		<i>vatus</i>			(Ecuador/Guatemala/Colombia)	31
Papilionidae	Troidini	<i>Parides</i>		<i>belemus</i>			2 (French Guiana)	2
Papilionidae	Troidini	<i>Parides</i>		<i>belus</i>			12 (Peru/Ecuador) + 2 (female form belus - French Guiana)	14
Papilionidae	Troidini	<i>Parides</i>		<i>ingemus</i>			0	0
Papilionidae	Troidini	<i>Parides</i>		<i>crassus</i>			25+2 (Ecuador/Bolivia/French Guiana/Brazil) + 1 (form male lepidus - Colombia)	28
Papilionidae	Troidini	<i>Parides</i>		<i>polysiticus</i>			12 (Peru/Brazil/Paraguay)	12
Papilionidae	Troidini	<i>Parides</i>		<i>jinira</i>			14 (Brazil/Peru)	14
Papilionidae	Troidini	<i>Parides</i>		<i>hirata</i>			6 (USA)	6
Papilionidae	Troidini	<i>Parides</i>		<i>acada</i>			15 (Mexico)	15
Papilionidae	Troidini	<i>Parides</i>		<i>philenor</i>			4 (Mexico) + 26 (USA)	30
Papilionidae	Troidini	<i>Parides</i>		<i>archidamas + streckerianus</i>			10	10
Papilionidae	Troidini	<i>Parides</i>		<i>polyvates</i>			5 (Amazon/Habi)	5
Papilionidae	Troidini	<i>Parides</i>		<i>jamaicus</i>			5 (Jamaica)	5
Papilionidae	Troidini	<i>Parides</i>		<i>senodamas</i>			7 (Martinique)	7
Papilionidae	Troidini	<i>Parides</i>		<i>neodamas</i>			4 (Guadeloupe)	4
Papilionidae	Troidini	<i>Parides</i>		<i>streckerianus</i>			9+2 (Colombia/Peru/Venezuela)	11
Papilionidae	Troidini	<i>Parides</i>		<i>poludamas</i>			36+34+33+12 (French Guiana/Brazil/Mexico/Cuba/Colombia/Venezuela/Argentina/Guatemala/Paraguay/Bolivia)	115
Papilionidae	Troidini	<i>Parides</i>		<i>archidamas</i>			12 (Chile)	12
Papilionidae	Troidini	<i>Parides</i>		<i>ingemus</i>			5 (Cuba)	5
Papilionidae	Troidini	<i>Parides</i>		<i>chalcus</i>			1 (Mexico)	1
Papilionidae	Troidini	<i>Parides</i>		<i>deillerei</i>			13 (Paraguay/Colombia)	13
Papilionidae	Troidini	<i>Parides</i>		<i>lanodamas</i>			3 (Mexico)	3
Papilionidae	Troidini	<i>Parides</i>		<i>copaque</i>			7 (Guatemala/Honduras)	7
Papilionidae	Troidini	<i>Parides</i>		<i>lydas</i>			17 (Brazil/Ecuador/Colombia)	17
Papilionidae	Troidini	<i>Parides</i>		<i>chilrodamas</i>			14 (Peru/Brazil)	14

Papilionidae	Papilioninae	Leptocircini	<i>Protographium</i>	-	<i>epidius</i>	<i>epidius</i> <i>repicus</i> <i>franchinisi</i>	9) (Guatemala/Mexico) 11) (Mexico)	9 11
Papilionidae	Papilioninae	Leptocircini	<i>Protographium</i>	-	<i>leathenes</i>	<i>leathenes</i>	5) (Costa Rica)	5
Papilionidae	Papilioninae	Leptocircini	<i>Protographium</i>	-	<i>leucaspis</i>	<i>lanis</i> <i>leucaspis</i>	12) (Australia) 9) (Equator/Colombia)	12 9
Papilionidae	Papilioninae	Leptocircini	<i>Protographium</i>	-	<i>marcellinus</i>	<i>leucaspis</i>	5) (Colombia/Peru)	5
Papilionidae	Papilioninae	Leptocircini	<i>Protographium</i>	-	<i>philolaus</i>	<i>philolaus</i> <i>sanctiles</i> <i>marichandi</i>	11+5) (Mexico/Honduras/Guatemala) + 3) (female form niger - Guatemala) 1) 16) (Guatemala/Mexico)	19 1 16
Papilionidae	Papilioninae	Leptocircini	<i>Protographium</i>	-	<i>thyastes</i>	<i>panamensis</i> <i>thyastinus</i> <i>thyastes</i> <i>zevros</i>	4) (Colombia) 5+9) (Equator/Guatemala/Colombia) 8) (Brazil/Peru) 3) (Bolivia)	4 14 8 3
Papilionidae	Papilioninae	Leptocircini	<i>Protographium</i>	-	<i>zanzara</i>	<i>zevros</i>	5) (Haiti) 36) (Europe/Mediterranean)	5 36
Papilionidae	Papilioninae	Leptocircini	<i>Aphelodes</i>	-	<i>podalirius</i>	<i>pseudopersea</i>	9) (Drome) + 16) (Gard) + 12) (Hautes Alpes) + 7) (Corse) + 27) (Hérault) + 7) (Bouches du Rhône) + 14) (Var) + 13) (Basses Alpes) + 14) (Alpes Maritimes) + 55) (Vaucluse)	160
						<i>flammaris</i>	36) (Germany) + 9) (Tchecoslovaquie) + 5) (Loire) + 1) (Nièvre) + 4) (Saône et Loire) + 18) (Loire) + 6) (Ain) + 10) (Gironde) + 3) (Lot et Garonne) + 3) (Tarn) + 1) (Lot) + 5) (Comté) + 2) (Puy de Dôme) + 1) (Cantal) + 3) (Isère) + 5) (Savoie) + 29+40) (Ile de France) + 5) (Eure) + 3) (Ille et Vilaine) + 1) (Indre et Loire) + 7) (Charente) + 3) (Charente Maritime) + 6) (Vendée) + 5) (Vienne) + 1) (Maine et Loire) + 2) (Gers) + 1) (Pyénées Atlantique) + 1) (Hautes Pyénées) + 6) (Haute Garonne) + 7) (Ariège) + 1) (Aude) + 7) (Aveyron) + 6) (Lozère) + 4) (Ardèche) + 3) (Maurte et Moselle) + 1) (Bas Rhin) + 3) (Haut Rhin) + 3) (Vosges) + 30) (Alsace)	287
						<i>alexandria</i>	2) (Italia)	2
						<i>intermedia</i> <i>zanzara</i>	8) (Italia) + 3) (Austria) + 1) (Croatia) + 1) (Albanie) + 1) (Serbie) + 1) (Dalmatie) + 10) (Macédoine)	25 28
						<i>creta</i>	3) (Italia) + 6) (Espagne) + 6) (Sicile) + 3) (Austria) + 10) (Liban)	15
						<i>zanzara</i>	11) (Greece) + 4) (Rhodes)	21
						<i>elongata</i>	21) (Suisse/Zerland)	21
						<i>intersecta</i>	2) (Hongrie) + 4) (Roumanie)	6
						<i>persica</i>	1) (Syrie)	1
						<i>cantabrigiae</i>	15) (Iran)	15
						<i>flacillus</i>	1) (Russie) + 1) (Zakhanan) + 3) (Azerbaïdjan) + 4) (Crimée) + 5) (Caucase) + 4) (Oural)	18
						<i>juldasa</i>	2) (Russie)	2
						<i>smyrnensis</i>	2) (Turkistan)	2
						<i>lotteri</i>	58) (Turquie)	58
						<i>fishamelli</i>	32) (Maroc) + 1) (Tunisie) + 2) (Ane Mineure) + 35 + 43) (Argente)	113
							42 + 34 + 46) (Pyénées Orientales) + 28) (Aude) + 7 + 48) (Espagne) + 12) (Portugal) + 25+2) (Touraine = Indre et Loire) + 9) (Seine et Marne)	275
								0
						<i>curtus</i>	3) (Vietnam) + 14) (Law/India) + 9) (form walkeri - China) + 16) (form theilades - Indonesia)	42
						<i>strevens</i>	3) (Vietnam) + 25) (Indonésie/Vietnam/India) + 4) (form walkeri - Vietnam)	32
							13) (Indonésie) + 6) (form thaisiens - Indonésie) + 8) (form decius - Philippines) + 5) (form entius - Indonésie)	32
							6+12+36+36+18+15) (Vietnam/Malaysia/Indonésie)	123
							18) (Sri Lanka/India)	18
							5) (Indonésie)	5
							1) (Indonésie)	1
							3) (Indonésie)	3
							1) (Indonésie)	1
							4) (Indonésie)	4
							6) (Indonésie)	6
							7) (Indonésie)	7
							3) (Indonésie)	3
							6) (Papua New Guinea)	6
							1) (Papua New Guinea)	1
						<i>agamemnon</i>		
						<i>merides</i>		
						<i>andaman</i>		
						<i>nigripennis</i>		
						<i>bowenium</i>		
						<i>exilis</i>		
						<i>emodas</i>		
						<i>plithenes</i>		
						<i>guitanus</i>		
						<i>argyranus</i>		
						<i>ligatus</i>		
						<i>neopannemianus</i>		

Popilionidae	Popilioninae	Leptocierini	Graphium	Arctibe	Iconidae	Bierinae	popilidus	28+40 (Congo/Gabon/Guinea)	68
Popilionidae	Popilioninae	Leptocierini	Graphium	Arctibe	Iconidae	Iconidae	popilidus	45 +42+44+44+47+44+41 (Sierra Leone/Ivory Coast/Guinea/Cameroun/Congo)	307
Popilionidae	Popilioninae	Leptocierini	Graphium	Arctibe	Iconidae	Iconidae	popilidus	10 (Afrique du Sud)	10
Popilionidae	Popilioninae	Leptocierini	Graphium	Arctibe	Iconidae	Iconidae	popilidus	7 (Ivory Coast)	7
Popilionidae	Popilioninae	Leptocierini	Graphium	Arctibe	Iconidae	Iconidae	popilidus	3	3
Popilionidae	Popilioninae	Leptocierini	Graphium	Arctibe	Iconidae	Iconidae	popilidus	6 (Ivory Coast)	6
Popilionidae	Popilioninae	Leptocierini	Graphium	Arctibe	Iconidae	Iconidae	popilidus	11 (Angola/Mozambique)	11
Popilionidae	Popilioninae	Leptocierini	Graphium	Arctibe	Iconidae	Iconidae	popilidus	47 (East Africa)	47
Popilionidae	Popilioninae	Leptocierini	Graphium	Arctibe	Iconidae	Iconidae	popilidus	43+1 (Guinea) + 13+9+19 (Gabon) + 27+22+8+15 (Congo) + 9+2 (Cameroun) + 45 (Ivory Coast) + 2 (Sierra Leone) + 48+42+44+44+47+44+41+42 (Afrique Ouest)	432
Popilionidae	Popilioninae	Leptocierini	Graphium	Arctibe	Iconidae	Iconidae	popilidus	6 (Gabon)	6
Popilionidae	Popilioninae	Leptocierini	Graphium	Arctibe	Iconidae	Iconidae	popilidus	4 (East Africa)	4
Popilionidae	Popilioninae	Leptocierini	Graphium	Arctibe	Iconidae	Iconidae	popilidus	17 (East Africa)	17
Popilionidae	Popilioninae	Leptocierini	Graphium	Arctibe	Iconidae	Iconidae	popilidus	63+43 (Gabon/Congo/Central African Republic)	106
Popilionidae	Popilioninae	Leptocierini	Graphium	Arctibe	Iconidae	Iconidae	popilidus	1 (Congo)	1
Popilionidae	Popilioninae	Leptocierini	Graphium	Arctibe	Iconidae	Iconidae	popilidus	1 (Congo)	0
Popilionidae	Popilioninae	Leptocierini	Graphium	Arctibe	Iconidae	Iconidae	popilidus	5 (Angola)	5
Popilionidae	Popilioninae	Leptocierini	Graphium	Arctibe	Iconidae	Iconidae	popilidus	40 +37+36 (Sierra Leone/Gabon/Congo/Central African Republic)	113
Popilionidae	Popilioninae	Leptocierini	Graphium	Arctibe	Iconidae	Iconidae	popilidus	48+38 (Congo/Cameroun/Guinea)	86
Popilionidae	Popilioninae	Leptocierini	Graphium	Arctibe	Iconidae	Iconidae	popilidus	10 (Congo/Cameroun)	10
Popilionidae	Popilioninae	Leptocierini	Graphium	Arctibe	Iconidae	Iconidae	popilidus	30+30+25 (Malaysia/Indonesia/Philippines)	85
Popilionidae	Popilioninae	Leptocierini	Graphium	Arctibe	Iconidae	Iconidae	popilidus	1 (Philippines)	1
Popilionidae	Popilioninae	Leptocierini	Graphium	Arctibe	Iconidae	Iconidae	popilidus	5 (Indonesia)	5
Popilionidae	Popilioninae	Leptocierini	Graphium	Arctibe	Iconidae	Iconidae	popilidus	5 (Indonesia)	5
Popilionidae	Popilioninae	Leptocierini	Graphium	Arctibe	Iconidae	Iconidae	popilidus	4 (Vietnam) + 7 (Sri Lanka/Indonesia)	11
Popilionidae	Popilioninae	Leptocierini	Graphium	Arctibe	Iconidae	Iconidae	popilidus	4+5 (Indonesia)	9
Popilionidae	Popilioninae	Leptocierini	Graphium	Arctibe	Iconidae	Iconidae	popilidus	13 (India)	13
Popilionidae	Popilioninae	Leptocierini	Graphium	Arctibe	Iconidae	Iconidae	popilidus	10 (Malaysia)	10
Popilionidae	Popilioninae	Leptocierini	Graphium	Arctibe	Iconidae	Iconidae	popilidus	1 (Indonesia)	1
Popilionidae	Popilioninae	Leptocierini	Graphium	Arctibe	Iconidae	Iconidae	popilidus	1 (Philippines)	1
Popilionidae	Popilioninae	Leptocierini	Graphium	Arctibe	Iconidae	Iconidae	popilidus	18 (Vietnam)	18
Popilionidae	Popilioninae	Leptocierini	Graphium	Arctibe	Iconidae	Iconidae	popilidus	11 (Indonesia)	11
Popilionidae	Popilioninae	Leptocierini	Graphium	Arctibe	Iconidae	Iconidae	popilidus	2 (Philippines)	2
Popilionidae	Popilioninae	Leptocierini	Graphium	Arctibe	Iconidae	Iconidae	popilidus	8 +40 (Vietnam/China/Malaysia/Thailand)	48
Popilionidae	Popilioninae	Leptocierini	Graphium	Arctibe	Iconidae	Iconidae	popilidus	2 (India)	2
Popilionidae	Popilioninae	Leptocierini	Graphium	Arctibe	Iconidae	Iconidae	popilidus	2 (Vietnam)	2
Popilionidae	Popilioninae	Leptocierini	Graphium	Arctibe	Iconidae	Iconidae	popilidus	3 (Indonesia)	3
Popilionidae	Popilioninae	Leptocierini	Graphium	Arctibe	Iconidae	Iconidae	popilidus	30+23 (Malaysia)	53
Popilionidae	Popilioninae	Leptocierini	Graphium	Arctibe	Iconidae	Iconidae	popilidus	2	2
Popilionidae	Popilioninae	Leptocierini	Graphium	Arctibe	Iconidae	Iconidae	popilidus	1 (Philippines)	1
Popilionidae	Popilioninae	Leptocierini	Graphium	Arctibe	Iconidae	Iconidae	popilidus	1 (Philippines)	1
Popilionidae	Popilioninae	Leptocierini	Graphium	Arctibe	Iconidae	Iconidae	popilidus	3 (Papua New Guinea) + 3 (form fumesa - Papua New Guinea) + 1 (form thule - Papua New Guinea)	7
Popilionidae	Popilioninae	Leptocierini	Graphium	Arctibe	Iconidae	Iconidae	popilidus	6 (Vietnam)	6
Popilionidae	Popilioninae	Leptocierini	Graphium	Arctibe	Iconidae	Iconidae	popilidus	30+4 (India) +8	42
Popilionidae	Popilioninae	Leptocierini	Graphium	Arctibe	Iconidae	Iconidae	popilidus	10 (Indonesia)	10
Popilionidae	Popilioninae	Leptocierini	Graphium	Arctibe	Iconidae	Iconidae	popilidus	20 (Vietnam)	20
Popilionidae	Popilioninae	Leptocierini	Graphium	Arctibe	Iconidae	Iconidae	popilidus	4 (Vietnam) + 4 (Malaysia)	8
Popilionidae	Popilioninae	Leptocierini	Graphium	Arctibe	Iconidae	Iconidae	popilidus	12 (India)	12

Papilionidae	Papilioninae	Leptocleini	Graphium	Pachysa	androcles	insularis androcles elemanes			9 (Indonesia)	9
Papilionidae	Papilioninae	Leptocleini	Graphium	Pachysa	antiphates	antiphates			4 (Indonesia)	4
Papilionidae	Papilioninae	Leptocleini	Graphium	Pachysa		parvulus antiphates		12+ (0+19 Vietnam/India/Cambodia/Philippines)	4 (Indonesia)	4
Papilionidae	Papilioninae	Leptocleini	Graphium	Pachysa		aristatus		30+16 (Vietnam)	3 (Polynésie Française)	46
Papilionidae	Papilioninae	Leptocleini	Graphium	Pachysa		antiscates		26 (India)	26 (Philippines)	26
Papilionidae	Papilioninae	Leptocleini	Graphium	Pachysa		hermocrates		16 (Australia/Indonesia)	12 (Philippines)	12
Papilionidae	Papilioninae	Leptocleini	Graphium	Pachysa		exlonicus		5 (Sri Lanka)	16 (Australia/Indonesia)	16
Papilionidae	Papilioninae	Leptocleini	Graphium	Pachysa		albidulae		8 (Indonesia)	8 (Indonesia)	8
Papilionidae	Papilioninae	Leptocleini	Graphium	Pachysa		taupani		30+26 (Indonesia)	2 (Indonesia)	56
Papilionidae	Papilioninae	Leptocleini	Graphium	Pachysa		antiphonus		1 (Philippines)	1 (Philippines)	1
Papilionidae	Papilioninae	Leptocleini	Graphium	Pachysa	decolor	kaloveris		1 (Indonesia)	1 (Indonesia)	0
Papilionidae	Papilioninae	Leptocleini	Graphium	Pachysa	epaminondas	dorcus		3 (Indonesia)	3 (Indonesia)	1
Papilionidae	Papilioninae	Leptocleini	Graphium	Pachysa	euphrates	euphrates		11 (Philippines/China)	11 (Philippines/China)	11
Papilionidae	Papilioninae	Leptocleini	Graphium	Pachysa	euphratoides	nomius		12 (Laos/Thailand)	12 (Laos/Thailand)	12
Papilionidae	Papilioninae	Leptocleini	Graphium	Pachysa	nomius	svithori		6+6 (Sri Lanka/Vietnam/India)	6+6 (Sri Lanka/Vietnam/India)	12
Papilionidae	Papilioninae	Leptocleini	Graphium	Pachysa	rhesus	rhesus		11 (Indonesia)	11 (Indonesia)	11
Papilionidae	Papilioninae	Leptocleini	Graphium	Pachysa	stratotes	rhesula		1 (Indonesia)	1 (Indonesia)	1
Papilionidae	Papilioninae	Leptocleini	Graphium	Pachysa	alabian	parvinoctia		2 (Indonesia)	2 (Indonesia)	2
Papilionidae	Papilioninae	Leptocleini	Graphium	Pachysa	erous	alabian		5 (Indonesia)	5 (Indonesia)	5
Papilionidae	Papilioninae	Leptocleini	Graphium	Pachysa	erous	erous		20 (Thibe/China/India)	20 (Thibe/China/India)	20
Papilionidae	Papilioninae	Leptocleini	Graphium	Pachysa	incertus	caschmirensis		8 (India)	8 (India)	8
Papilionidae	Papilioninae	Leptocleini	Graphium	Pachysa	glycerion	asakurae		3 (Taiwan)	3 (Taiwan)	3
Papilionidae	Papilioninae	Leptocleini	Graphium	Pachysa	mandarinus			30 (Thibe/India/China)	30 (Thibe/India/China)	0
Papilionidae	Papilioninae	Leptocleini	Graphium	Pachysa	sachauze					0
Papilionidae	Papilioninae	Leptocleini	Graphium	Pachysa	tamaritanus					0
Papilionidae	Papilioninae	Leptocleini	Graphium	Pachysa	timur					0
Papilionidae	Papilioninae	Leptocleini	Graphium	Pachysa	caucasia					0
Papilionidae	Papilioninae	Leptocleini	Graphium	Pachysa	caucasia					0
Papilionidae	Papilioninae	Leptocleini	Graphium	Pachysa	certisy	speciosa		51 (Asie Mineure - Syrie, Greece -)	51 (Asie Mineure - Syrie, Greece -)	51
Papilionidae	Papilioninae	Leptocleini	Graphium	Pachysa	certisy	marini		32 (Greece)	32 (Greece)	32
Papilionidae	Papilioninae	Leptocleini	Graphium	Pachysa	certisy	ferdinandi		29 (Hongrie/Bulgarie)	29 (Hongrie/Bulgarie)	29
Papilionidae	Papilioninae	Leptocleini	Graphium	Pachysa	certisy	certisy		9 (Asie Mineure)	9 (Asie Mineure)	9
Papilionidae	Papilioninae	Leptocleini	Graphium	Pachysa	certisy	certisy		20 (Greece)	20 (Greece)	20
Papilionidae	Papilioninae	Leptocleini	Graphium	Pachysa	certisy	certisy		32+8 (form typique - Asie Mineure) + 6 (female form pallidior - Asie Mineure) + 10 (female form albidior - Asie Mineure) + 14 (female form obscurior - Asie Mineure)	32+8 (form typique - Asie Mineure) + 6 (female form pallidior - Asie Mineure) + 10 (female form albidior - Asie Mineure) + 14 (female form obscurior - Asie Mineure)	60
Papilionidae	Papilioninae	Leptocleini	Graphium	Pachysa	certisy	certisy		90+82 (Europe de l'Est) + 87+66+92+91 (France)	90+82 (Europe de l'Est) + 87+66+92+91 (France)	3
Papilionidae	Papilioninae	Leptocleini	Graphium	Pachysa	certisy	certisy		32 (form honniti element - Bunker) + 3 (form typique Alpes - Bunker) + 68 (Spain/Portugal/Maroc C.H.H.) + 24 (form lusitana Portugal/Spain, C.H.H.) + 83 (Alpes maritimes) + 44 (Spain)	32 (form honniti element - Bunker) + 3 (form typique Alpes - Bunker) + 68 (Spain/Portugal/Maroc C.H.H.) + 24 (form lusitana Portugal/Spain, C.H.H.) + 83 (Alpes maritimes) + 44 (Spain)	0
Papilionidae	Papilioninae	Leptocleini	Graphium	Pachysa	certisy	certisy		73+86+71+23+50 (France/Spain)	73+86+71+23+50 (France/Spain)	303
Papilionidae	Papilioninae	Leptocleini	Graphium	Pachysa	certisy	certisy		17 (Spain)	17 (Spain)	17
Papilionidae	Papilioninae	Leptocleini	Graphium	Pachysa	certisy	certisy		59 (Maroc/Portugal)	59 (Maroc/Portugal)	59
Papilionidae	Papilioninae	Leptocleini	Graphium	Pachysa	certisy	certisy		6 (India)	6 (India)	6
Papilionidae	Papilioninae	Leptocleini	Graphium	Pachysa	certisy	certisy		11 (Thibe/China)	11 (Thibe/China)	0
Papilionidae	Papilioninae	Leptocleini	Graphium	Pachysa	certisy	certisy				11

Papilionidae	Parnassiinae	Parnassini	<i>Parnassius</i>	<i>Dryopa</i>	<i>oreans</i>	<i>consul</i>				1 (China)	1
Papilionidae	Parnassiinae	Parnassini	<i>Parnassius</i>			<i>groomi</i>				1,2 (Tibet)	12
Papilionidae	Parnassiinae	Parnassini	<i>Parnassius</i>			<i>angur</i>				5 (China)	5
Papilionidae	Parnassiinae	Parnassini	<i>Parnassius</i>			<i>dictator</i>				16 (Tibet)	6
Papilionidae	Parnassiinae	Parnassini	<i>Parnassius</i>			<i>bourboni</i>				16 (China)	6
Papilionidae	Parnassiinae	Parnassini	<i>Parnassius</i>	<i>Kallias</i>	<i>antocrator</i>					6 (Afghanistan)	6
Papilionidae	Parnassiinae	Parnassini	<i>Parnassius</i>	<i>Kallias</i>	<i>lorax</i>					1 (China)	1
Papilionidae	Parnassiinae	Parnassini	<i>Parnassius</i>	<i>Kallias</i>	<i>dayshovi</i>					1 (China)	0
Papilionidae	Parnassiinae	Parnassini				<i>bryki</i>				3 (NW Himalaya)	3
Papilionidae	Parnassiinae	Parnassini				<i>elisaritanus</i>				1 (Rupshu)	1
Papilionidae	Parnassiinae	Parnassini				<i>otto</i>				3 (Gya Ladakh)	3
Papilionidae	Parnassiinae	Parnassini	<i>Parnassius</i>	<i>Kallias</i>	<i>charltonius</i>					11 (Cachemire)	11
Papilionidae	Parnassiinae	Parnassini				<i>deckeri</i>				1 (Balistan)	1
Papilionidae	Parnassiinae	Parnassini				<i>corporealis</i>				1 (India)	1
Papilionidae	Parnassiinae	Parnassini				<i>duvalis</i>				2 (Pakistan)	2
Papilionidae	Parnassiinae	Parnassini				<i>romanevi</i>				26 (Tadjikistan)	26
Papilionidae	Parnassiinae	Parnassini	<i>Parnassius</i>	<i>Kallias</i>	<i>inopimus</i>					1	1
Papilionidae	Parnassiinae	Parnassini	<i>Parnassius</i>			<i>vaporosus</i>				4 (Afghanistan)	4
Papilionidae	Parnassiinae	Parnassini				<i>regius</i>		<i>angustus</i>		4	4
Papilionidae	Parnassiinae	Parnassini				<i>imperator</i>				27 (China/Tibet)	27
Papilionidae	Parnassiinae	Parnassini				<i>aino</i>				2	2
Papilionidae	Parnassiinae	Parnassini	<i>Parnassius</i>	<i>Kallias</i>	<i>imperator</i>					7	7
Papilionidae	Parnassiinae	Parnassini				<i>mausgeu</i>				10 (Tibet)	10
Papilionidae	Parnassiinae	Parnassini				<i>regulus</i>				5 (Tibet)	5
Papilionidae	Parnassiinae	Parnassini	<i>Parnassius</i>	<i>Kallias</i>						2 (India)	2
Papilionidae	Parnassiinae	Parnassini	<i>Parnassius</i>	<i>Koromius</i>	<i>angustus</i>					12 (Afghanistan)	12
Papilionidae	Parnassiinae	Parnassini	<i>Parnassius</i>	<i>Koromius</i>	<i>aeolus</i>			<i>ceratialis</i>			0
Papilionidae	Parnassiinae	Parnassini	<i>Parnassius</i>	<i>Koromius</i>	<i>ceratal</i>						0
Papilionidae	Parnassiinae	Parnassini	<i>Parnassius</i>	<i>Koromius</i>	<i>hunca</i>						0
Papilionidae	Parnassiinae	Parnassini	<i>Parnassius</i>	<i>Koromius</i>	<i>jacoboni</i>						0
Papilionidae	Parnassiinae	Parnassini	<i>Parnassius</i>	<i>Koromius</i>	<i>stratosmus</i>						1
Papilionidae	Parnassiinae	Parnassini	<i>Parnassius</i>	<i>Koromius</i>	<i>solitarius</i>				<i>nandacrinensis</i>	1 (Pakistan)	1
Papilionidae	Parnassiinae	Parnassini				<i>albatus</i>				62-67 (Kirghizstan)	129
Papilionidae	Parnassiinae	Parnassini				<i>pulchra</i>				16 (Kirghizstan)	16
Papilionidae	Parnassiinae	Parnassini				<i>karacharica</i>				2 (Kirghizstan)	2
Papilionidae	Parnassiinae	Parnassini				<i>kasakana</i>				5 (Kasaktan)	5
Papilionidae	Parnassiinae	Parnassini				<i>namunganus</i>				22 (Turkestan)	22
Papilionidae	Parnassiinae	Parnassini				<i>manuveri</i>				5 (India Cachemire)	5
Papilionidae	Parnassiinae	Parnassini				<i>nicelliei</i>				5 (India)	5
Papilionidae	Parnassiinae	Parnassini				<i>abissini</i>				2 (Himalaya)	2
Papilionidae	Parnassiinae	Parnassini				<i>zimbakrica</i>				1 (India)	1
Papilionidae	Parnassiinae	Parnassini				<i>temis</i>				1 (Himalaya)	1
Papilionidae	Parnassiinae	Parnassini	<i>Parnassius</i>	<i>Koromius</i>	<i>delphius</i>					3 (Turkestan)	3
Papilionidae	Parnassiinae	Parnassini				<i>haifa</i>				6 (Afghanistan)	6
Papilionidae	Parnassiinae	Parnassini				<i>rufi</i>				1 (Pakistan)	1
Papilionidae	Parnassiinae	Parnassini				<i>shigarenis</i>				1 (Pakistan)	1
Papilionidae	Parnassiinae	Parnassini				<i>workmani</i>				11 (Kirghizstan)	11
Papilionidae	Parnassiinae	Parnassini				<i>interpica</i>				10 (Kirghizstan)	10
Papilionidae	Parnassiinae	Parnassini				<i>tilastri</i>				2	2
Papilionidae	Parnassiinae	Parnassini				<i>delphius</i>				1 (Afghanistan)	1
Papilionidae	Parnassiinae	Parnassini				<i>constans</i>				1 (Afghanistan)	1
Papilionidae	Parnassiinae	Parnassini				<i>condanus</i>				1 (Afghanistan)	10
Papilionidae	Parnassiinae	Parnassini				<i>menander</i>				42 (China/Turkestan)	42
Papilionidae	Parnassiinae	Parnassini	<i>Parnassius</i>	<i>Koromius</i>	<i>infernalis</i>					13 (Kirghizstan)	13
Papilionidae	Parnassiinae	Parnassini	<i>Parnassius</i>	<i>Koromius</i>	<i>maximus</i>					15 (Uzbekistan)	15
Papilionidae	Parnassiinae	Parnassini	<i>Parnassius</i>	<i>Koromius</i>	<i>parvicus</i>			<i>hale + pronus</i>		1 (China)	1
Papilionidae	Parnassiinae	Parnassini				<i>kardacoffi</i>					

Papilionidae	Parnassiinae	Parnassini	Parnassius	<i>phoebus</i>	<i>olympiana</i> <i>stratzei</i> <i>rogersi</i> <i>hollandi</i> <i>montaninus</i> <i>apricinus</i> <i>hermodar</i> <i>magnus</i> <i>idahoensis</i> <i>soy</i> <i>hansi</i> <i>baehleri</i> <i>tesisaron</i> <i>svyatsicus</i> <i>gezei</i>				1 (USA) 2 (USA) 2 (USA) 2 (USA) 9 (USA) 1 (Alaska) 4 (USA) 9 (Canada) 1 (USA) 31 (USA) 24 (Austria) 7 (Switzerland/France) 6 (France/Switzerland) 22 (female - Austria) 31 (France) 9 (USA) 9 (Creta) 17 (Russia) 14 (Russia) 10 (Russia) 3 1 (China) 59 (Switzerland)	1 2 2 2 9 1 4 9 1 31 24 7 6 22 31 9 9 17 14 10 3 1 59
Papilionidae	Parnassiinae	Parnassini	Parnassius	<i>satulicus</i>	<i>halaucinus</i> <i>gracieri</i> <i>breneri</i> <i>compacta</i> <i>solonensis</i> <i>ellenae</i>				9 (USA) 17 (Russia) 14 (Russia) 10 (Russia) 3 1 (China) 59 (Switzerland)	9 17 14 10 3 1 59
Papilionidae	Parnassiinae	Parnassini	Parnassius	<i>doergalensis</i>	<i>rubra</i> + <i>epiphilus</i> <i>bulcyi</i> + <i>prewalskii</i> + <i>rossicollis</i>				4 (Tibet) 2 3	4 2 3
Papilionidae	Parnassiinae	Parnassini	<i>Tadania</i>	<i>atco</i>	<i>mundipheris</i> <i>chamariensis</i> <i>tagalangi</i>				2 2 2	2 2 2
Papilionidae	Parnassiinae	Parnassini	<i>Tadania</i>	<i>maharaja</i>	<i>pythia</i> <i>obani</i>				2 (USA) 1 11 21 (Tibet) 5 6	2 1 11 21 5 6
Papilionidae	Parnassiinae	Parnassini	<i>Tadania</i>	<i>szekelyi</i>	<i>arnoldina</i> <i>germane</i> <i>szekelyi</i> <i>eros</i> <i>kansensis</i> <i>hardwicki</i> <i>albicans</i>				28 (form hardwicki - India) + 2 (form namposterior) 20 (form albicans - India/Tibet) + 39 (form viridicans - India)	2 2 21 5 6 30 59
Papilionidae	Parnassiinae	Parnassini	<i>Tadania</i>	<i>huberi</i>					20 (form albicans - India/Tibet) + 39 (form viridicans - India)	0
Total										3407

Annex II

Patterns of morphological variation shed light on the adaptive evolution of eyespots modularity in the butterfly *Morpho telemachus*

Ariane Chotard¹, Violaine Llaurens¹ and Vincent Debat¹

¹Institut de Systématique, Evolution, Biodiversité (ISYEB, UMR 7205), Muséum National d'Histoire Naturelle, CNRS, Sorbonne Université, EPHE, UA, Paris, France

In revision: Evolution

Abstract: Morphological evolution can be biased by developmental constraints limiting the effect of selection on traits. Eyespots are repeated wing colour pattern elements, widespread across butterfly species. As developmental serial homologues, they are controlled by similar developmental pathways, so that selection on a single eyespot can induce correlated responses in all eyespots. Here we focus on the variations in the ventral eyespots of the butterfly *Morpho telemachus*, where two different selective regimes are likely to act: while most eyespots are always-visible, two eyespots are conditionally-displayed: hidden at rest, they can be exposed when the butterflies are threatened. We investigate how such contrasted selection across eyespots can break up the covariations generated by their shared developmental origin. We quantified eyespots variations and covariations within a large population of *M. telemachus* and compared the observed patterns to those found in *Morpho helenor*, where all eyespots are always-visible and thus probably all affected by a similar selection regime. We found that conditionally-displayed eyespots are less variable than always-visible eyespots and form a separate developmental module in *M. telemachus*. Our results suggest that modularity has been shaped by selection, highlighting how natural selection may overcome developmental constraints.

Keywords: *Stabilizing selection, developmental constraints, variation, modularity, butterflies, fluctuating asymmetry*

Introduction

The level of evolutionary constraints on any given trait depends on its developmental and/or selective links with other traits, *i.e.*, trait modularity. For example, adaptive radiations have been suggested to occur primarily along the genetic lines of least resistance, because of the constraining effects of genetic correlations (Schluter, 1996). Serial homologues, like vertebrate teeth (Valen, 1994) or arthropod segments (Emerson and Schram, 1990), are relevant traits to identify how selection regime can overcome the effect of developmental constraints acting on phenotypic evolution. Such homologous traits stem from the repetition of the same developmental pathway in different locations of the body (Hall, 1995). Serial homologues are thus expected to present a tight covariation due to their shared developmental basis (Young and Hallgrímsson, 2005). In contrast, heterogeneous selection across the elements of a series might drive their divergence and break down their co-variation (Wagner and Altenberg, 1996; Melo and Marroig, 2015). Theoretical models suggest that directional selection can strongly affect the evolution of modularity and that stabilizing selection is required for its long-term maintenance (Melo and Marroig, 2015). The patterns of covariation across serial homologues therefore reflect the prevailing effect of developmental vs. selective factors affecting trait evolution (Beldade and Brakefield, 2003; Breuker *et al.*, 2006; Allen, 2008). Butterfly eyespots are a textbook example of serial homology: these circular colour patterns are repeated across the wings in many butterfly species. All eyespots are formed by the expression of a common developmental cascade at different locations on the wings, as shown by developmental studies carried out in the model species *B. anynana* (see Monteiro, 2015 for a review). Such serial developmental homology results in strong genetic correlations across eyespots: artificial selection on a particular eyespot indeed induces a correlated response on all eyespots, consistent with their developmental integration (Monteiro *et al.*, 1994, 1997; Beldade *et al.*, 2002; Beldade and Brakefield, 2002, 2003). Nevertheless, the seasonal forms of *B. anynana*, displaying different eyespot number and shapes, suggest that the ecological conditions encountered in the different season have promoted adaptive plasticity in eyespot development, leading to different wing patterns from the same shared developmental pathway (Lyytinen *et al.*, 2004).

The wide diversity of eyespot size, shape, and colour composition observed among butterfly species with contrasted ecologies suggests that diverse selective pressures can

affect the evolution of eyespots (Kodandaramaiah, 2011). For instance, in some species, eyespots are conditionally-displayed, usually hidden at rest, but uncovered at will. These eyespots are usually large and strongly contrast with the background colour of the wing: they might intimidate predators if suddenly uncovered during an attack, providing the butterfly some time to escape (Stevens, 2005; Dapporto *et al.*, 2019). Radically different eyespots are observed in other species, with a small size and peripheral location and usually constantly visible at rest. Such eyespots might divert predator attacks away from the vital parts of the body (Lyytinen *et al.*, 2004; Stevens, 2005; Olofsson *et al.*, 2010; Prudic *et al.*, 2015). A continuum of size and shapes exists in between these two extremes, some species harbouring large peripheral eyespots (Kodandaramaiah, 2011). In yet other butterfly species, eyespots can be reduced and poorly contrasting, participating in the crypsis of the wings. These are often highly variable: apostatic selection generated by predator cognitive capacities favours rare cryptic colour patterns and thus promote variability within populations (Bond and Kamil, 1998; Bond, 2007). On top of selection generated by predators, sexual selection might affect variation in eyespot series. In *B. anynana*, males express preference for UV reflectance in the center of the ventral, conditionally-displayed eyespot (Huq *et al.*, 2019), therefore specifically promoting this particular coloration in some specific eyespots. The heterogeneous morphology of eyespots from the same series observed within many butterfly species suggests that contrasted selective pressures may affect them, potentially breaking their covariation and leading to their morphological divergence.

Here we investigate how contrasted selective pressures may disrupt developmental constraints, by focusing on covariation patterns across eyespots within the butterfly species *Morpho telemachus* (Linné, 1758), where the different eyespots are likely submitted to different selective regimes. In the *Morpho* genus, a series of eyespots is observed on the ventral side of the wings (Debat *et al.*, 2020), exposed when butterflies are resting with closed wings. In contrast with most *Morpho* species, *M. telemachus* has two large conditionally-displayed eyespots on the ventral side of the forewing (Figure 1). They are usually hidden by the overlapping hindwing when the butterfly is at rest and can be revealed when the butterfly spreads its wings. These eyespots might have an intimidating effect on predators if unmasked during an attack, as suggested in other butterfly species (Stevens, 2005; Dapporto *et al.*, 2019). Paired eyespots are indeed

suggested to be more intimidating than single eyespots (Stevens, 2005; Inglis *et al.*, 2010). These two highly visible eyespots could also be part of a sexual signal, concealable at will when the butterfly adopts a more cryptic behaviour. The remaining eyespots, located on the hindwing and on the forewing tip, are always-visible, suggesting they might be submitted to a different selective pressure, possibly contributing to the general cryptic appearance of the butterfly at rest. Such contrasted selective regimes across eyespots in *M. telemachus* provide a relevant opportunity to investigate the relative impact of selection and developmental constraints on the pattern of covariation across a series of developmental homologues. Serial homology is expected to impose a tight covariation across all eyespots, leading to their developmental integration (Allen, 2008). In contrast, different selective pressures across eyespots should favour their relative independence (*i.e.*, functional modularity).

Since the precise pattern of covariation among eyespots expected from developmental correlations is unknown, we contrasted patterns of variations observed in *M. telemachus* with another *Morpho* species, *Morpho helenor* (Cramer, 1776). In this species, all eyespots are always-visible, suggesting that, in contrast to *M. telemachus*, similar selective pressure affect all eyespots of the series. Comparing the patterns of eyespot covariation between *M. telemachus* and *M. helenor* should thus shed light on the effect of heterogeneous selection on the evolution of eyespot modularity.

We first assessed the conspicuousness of the different eyespots in the two species, by measuring the reflectance spectra of the yellow and black rings forming the eyespots and computing the colour contrast perceived by avian predators. We measured the size and shape of the two rings within each eyespot and then compared their patterns of variations and covariations in the two species. (1) By comparing the levels of variation of the different eyespots within each species, we predicted a homogeneous and low level of variation in all eyespots in *M. helenor* as a result of stabilizing selection acting on all eyespots. In contrast, a difference in variation across eyespots was expected in *M. telemachus*, with a low variation in the two conditionally-displayed eyespots due to stabilizing selection, and a higher variation in the always-visible eyespots because of a relaxed or apostatic selection. (2) By comparing the covariations between traits within species, we predicted a global pattern of integration across eyespots in *M. helenor*, resulting from congruent developmental and selective effects (developmental and

functional integration). In contrast, in *M. telemachus* we predicted a pattern of modularity opposing conditionally-displayed and always-visible eyespots, as a result of the contrasted selective regimes.

Variation and covariation were assessed at two levels: using among individual variance, reflecting genetic and environmental differences among individuals, and using fluctuating asymmetry (FA, [Palmer and Strobeck, 1986](#)), assessing random developmental variation within individuals. While both individual variance and FA can be affected by stabilizing selection promoting developmental robustness, FA reflects developmental interactions across traits ([Klingenberg, 2014](#), see below). It therefore allows to specifically test whether selection can alter developmental integration ([Breuker et al., 2006](#)).

Materials & Methods

1) Butterfly Samples

M. telemachus is a canopy species distributed throughout the Amazon basin, from the foothills of the Andes to the Brazilian Atlantic Forest ([Blandin and Purser, 2013](#)). We focused on an exceptional sample composed of 370 males from a single emergence bloom of *M. telemachus exsusarion* (Le Moult & Réal 1962) collected in 1995 in Bolivia, in the province of Chapare (Department of Cochabamba CBBA; Gilbert Lachaume, pers. com.). This exceptional sample provides a relevant opportunity to assess variability within natural population. All individuals likely encountered similar environmental conditions, reducing the potential effects of phenotypic plasticity.

We compared the levels of variation in the different eyespots within this population of *M. telemachus* to the variation of the same eyespots in a closely related species, *M. helenor*. We gathered specimens of *M. helenor* from the collections of the Muséum National d'Histoire Naturelle (Paris), by sampling 31 males originating from two localities (Chapare - Bolivia/ Perene - Peru). Since these collection specimens were originally caught by different collectors at different localities, the morphological variation measured in *M. helenor* combines intra- and inter-population differences – either genetic or environmental – and thus likely over-estimates phenotypic variation.

2) Estimating eyespot conspicuousness

To estimate the level of conspicuousness of the different eyespots, we measured their color contrast on a subsample of 10 individuals per species. For each eyespot, the reflectance spectrum of the yellow and the black ring was measured using a spectrophotometer (AvaSpec-ULS2048CL-EVO-RS, software AvaSoft v.8.12.0.0), sensitive to wavelengths between 200 and 1100 nm. A light source (Avalight-DH-S-BAL) covering the visible and UV wavelengths from 300 to 700 nm was used to illuminate the specimens (coupling a deuterium lamp with a spectrum of 215 to 500 nm, and a halogen lamp from 500 to 2500 nm). Our measurements were conducted while minimizing external light sources. To assess the contrast between the two rings as perceived by avian predators, we quantified chromatic and achromatic contrasts (Olsson *et al.* 2018) using the two major visual systems documented in birds (UV and violet-sensitive respectively), as implemented in the R package PAVO2 (Maia *et al.*, 2019). The vision models were all applied with standard conditions (Weber fraction value of 0.05, Dell'Aglio *et al.*, 2018) with the following relative cone densities 0.37:0.7:0.99:1 for UV-sensitive model (UVS:S:M:L) and 0.25:0.5:1:1 for Violet-sensitive model (VS:S:M:L) (Finkbeiner *et al.*, 2017). The chromatic and achromatic contrast analyses were performed using a bootstrap procedure. Contrasts are expressed in JND (*Just Noticeable Difference*) with a threshold of 1 JND. Values above that threshold will be considered as noticeable by an avian observer.

3) Measuring eyespot size and shape: Imaging and morphometric measurements

The four wings of each individual were photographed in a photo studio under controlled LED light using a Nikon D90 (Camera lens: AF-S Micro Nikkor 60 mm 1:2.8G ED), in standardized conditions allowing to minimize shape distortion due parallax. Each eyespot is composed of two concentric rings: an external yellow ring and an internal black ring, around a central white pupil. *M. telemachus* usually has 9 ventral eyespots (Figure 1A-B): 4 on the forewing and 5 on the hindwing. Nevertheless, two of these eyespots (E2 and E6 - visible on Figure 1B) were very often extremely reduced when not simply absent; in addition, these eyespots are absent in *M. helenor* (Figure 1B). We thus decided to exclude them from our protocol and focus on the 7 eyespots observed on all specimens.

For both species, length and width of the yellow and black rings (respectively noted L_y , W_y and L_b , W_b , Figure 1C) were measured on all eyespots using ImageJ (version 1.8.0_112). Following previous studies (Monteiro *et al.*, 1997; Breuker *et al.*, 2007; Adams, 2016), length was measured along the direction parallel to the veins framing the eyespot and passing through the center of the eyespot and width along the perpendicular to that direction (Figure 1C). To characterize the shape of the different eyespots, we computed the ratio between length and width of the two rings for each eyespot ($R_y=L_y/W_y$ and $R_b=L_b/W_b$) and used $(1 - R)$ as a measure of their departure from perfect circularity. All measurements were made on both left and right eyespots, to assess asymmetry.

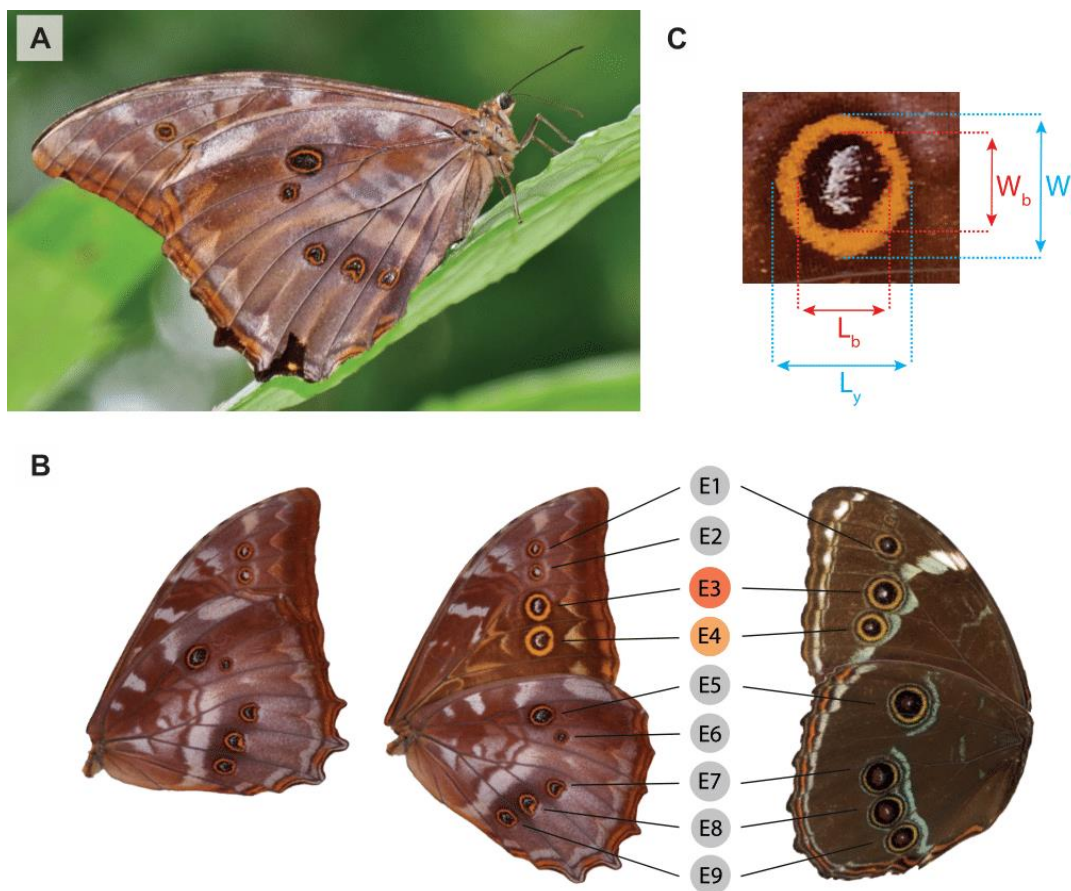


Figure 1: Eyespots observed on the ventral sides of the wings in *Morpho telemachus* and *Morpho helenor*. (A) Picture of *M. telemachus* taken in resting position, showing the always-visible eyespots. Photo credit: Peter Møllmann. (B) Position and numbering of the measured eyespots. Eyespots E3 and E4, figured in dark and light orange, are conditionally-displayed in *M. telemachus* (they are usually hidden by the hindwing at rest), and always exposed in *M. helenor*. The other eyespots are figured in grey. Left - *M. telemachus*: Right - *M. helenor*. (C) The four measurements taken on each eyespot (length and width of the yellow and black rings, respectively noted L_y , W_y , L_b and W_b).

4) Assessing patterns of variations and covariations

Estimating fluctuating asymmetry - To assess the level of developmental control on eyespots variation, we estimated fluctuating asymmetry (FA). FA is the deviation from perfect bilateral symmetry due to developmental noise, *i.e.*, the small, random variation independently affecting the two sides of a trait during development (Palmer and Strobeck, 1986). FA thus reflects developmental stability, *i.e.* the buffering of developmental noise (Palmer and Strobeck, 1986; Klingenberg and Polak, 2003). Developmental stability is generally expected to be favored by stabilizing selection (*e.g.*, Debat and David, 2001, but see Pélabon *et al.*, 2010): eyespots under stabilizing selection are thus predicted to exhibit less FA than eyespots evolving neutrally. We quantified FA as the variance of the right minus left values distribution (FA4 in the terminology of Palmer, 1994). To avoid measurement bias due to the lateralization of the human observer, mirror images of the left wings were used (R package *TransformJ*, Meijering *et al.*, 2001), and the order of measurements (right or left) randomized.

Checking measurement error and allometric effects on FA - To quantify measurement error (ME), which is critical for accurately estimating FA, a random sub-sample of 30 individuals was measured 3 times, and the impact of ME on FA was assessed. We estimated ME on the different traits, using the repeated measurements protocol described in Palmer and Strobeck (1986) and Palmer (1994). We applied two-way mixed model ANOVAs with ‘side’ as a fixed effect and ‘individual’ as a random effect, for each of the 28 variables. In these models, the interaction term (side x individual) assesses FA and its statistical significance tests whether FA is greater than ME, which is included in the residual term. For all measurements, individual variation and fluctuating asymmetry were significantly larger (on average 11.6 times) than ME, suggesting that FA is not strongly affected by error. To test whether larger eyespots display higher asymmetries, we computed the correlation of trait asymmetry values ($L-R$) and trait average size $(L+R)/2$. As no correlation was detected ($r = -0.01$, $p = 0.284$), correction for eyespot size was not applied. In contrast, a significant positive correlation was detected between eyespot size and eyespot variance ($r = 0.79$, $p < 0.001$). Inter-individual variation of linear measurements was thus assessed by their coefficient of variation (CV). Finally, to assess whether larger butterflies tended to display higher asymmetries, we tested the correlation between asymmetry values and wing area, used as a proxy of butterfly size. A significant

correlation was detected, but it was very low ($r = 0.026$, $p < 0.01$), suggesting that allometric effects are weak.

Comparing eyespots variability - We then estimated the levels of variation of the different traits within each of the two species. Differences in mean size (L_y , W_y , L_b and W_b) and shape (ratios R_y and R_b) among eyespots were tested using pairwise Welch tests, which allows to compare means of multiple samples with unequal variances. FA and inter-individual variances were compared across eyespots using pairwise F -tests, because FA was computed as a variance. Coefficients of variation of size were compared using an asymptotic test for the equality of multiple coefficients of variation (based on the calculation of the $D'AD$ statistic proposed by [Feltz and Miller \(1996\)](#), R package *cvequality*, [Marwick and Krishnamoorthy, 2018](#)). Multiple testing was accounted for by using Holm-Bonferroni procedure. We then compared the intraspecific levels of variations of all eyespots between species using F -tests.

Assessing the patterns of modularity across eyespots - To identify the different modules, we estimated covariations between traits within each species. The covariation of morphological traits can result either from direct interactions among the developmental pathways producing the traits, or from parallel variation in those pathways ([Klingenberg, 2008](#); [Klingenberg and Polak, 2003](#)). Parallel variation is due to joint external influences, including environmental effects (plasticity), but also allelic variation in genes involved in the different pathways (pleiotropy), and can be assessed by individual covariation (*i.e.*, the covariation of traits across individuals). In contrast, FA covariation (*i.e.*, the covariation of trait asymmetries across individuals) only results from direct developmental interactions. Since FA is inherently random, its values can be correlated across traits only if those traits directly interact during development: this can happen either if the traits share part of their developmental pathways (*e.g.*, common precursor, or global pre-patterning) and random variation affects this common part, or through inductive signalling between pathways, random variation in one pathway being transmitted to the other through this signal ([Klingenberg, 2008](#)). Comparing covariations based on FA and individual differences thus enables to discriminate direct developmental interactions from parallel variation. We thus quantified both covariation between traits values, averaged across sides (individual covariation) and covariation between traits asymmetries (FA covariation).

Direct interactions are mostly expected among physically close developing traits – typically the different rings of an eyespot, or adjacent eyespots – or among traits that depend on a same pre-patterning – the whole eyespot series being influenced by the general wing patterning. We therefore predicted a tight covariation in FA within eyespots, and a looser covariation across eyespots, possibly opposing forewing and hindwing eyespots. A joint selection on two developmentally distinct structures, by favouring their phenotypic covariation, should nevertheless increase their developmental integration (e.g., Breuker *et al.*, 2006; Klingenberg, 2010): accordingly, we also predicted a tight covariation in FA between the two conditionally-displayed eyespots of *M. telemachus*.

We specifically compared the covariations among always-visible eyespots with those among the two conditionally-displayed eyespots of *M. telemachus*, by computing the average inter-eyespot correlations. The patterns of modularity across eyespots were estimated using correlation matrices restricted to statistically significant correlations among traits. Correlation matrices were visually displayed as networks in which each variable is a node and each correlation an edge, using the R package *qgraph* (Epskamp *et al.*, 2012).

The hypotheses of modularity were then tested using a hierarchical module partition using Ward’s hierarchical cluster analysis (Ward, 1963; Zelditch *et al.*, 2008) using the function *pvclust* of the R package *pvclust* (Suzuki *et al.*, 2006), which calculates *p*-values for hierarchical clustering via multiscale bootstrap resampling. All nodes defined by a significant *p*-value are considered to define a module. This method has the advantage of allowing to detect nested modularity patterns and thus, a simultaneous analysis of the intra- and inter-eyespots modularity.

All statistical analyses were carried out in R version 3.6.3 (R Core Team 2020).

Results

1) Contrasted levels of conspicuousness among eyespots in *M. telemachus*

In *M. telemachus*, conditionally-displayed eyespots E3 and E4 were significantly larger than all other eyespots (41.46% for L_y , 37.10% for W_y , 49.03% for L_b and 37.67% for W_b ,

on average; Figure 2A, Table S1). Their shape was also significantly rounder than in other eyespots (Figure 2B, details in Tables S2). Achromatic contrasts in *M. telemachus* were heterogeneous across eyespots, E3 and E4 eyespots displaying particularly high values (55.69% higher than other eyespots in UV-models and 56.81% higher in Violet-models, on average; Figure 2C). Conversely, achromatic contrasts in *M. helenor* eyespots were homogeneously high, comparable to *M. telemachus* conditionally-displayed eyespots (Figure 2C). The reduced size and achromatic contrast of the always-visible eyespots of *M. telemachus* suggests a strong decrease in conspicuousness in these eyespots as compared to the conditionally-displayed eyespots of *M. telemachus* and to all eyespots of *M. helenor*. Such difference was nevertheless not observed for chromatic contrasts (Figure S1), suggesting that similar coloration was conserved throughout all eyespots in both species.

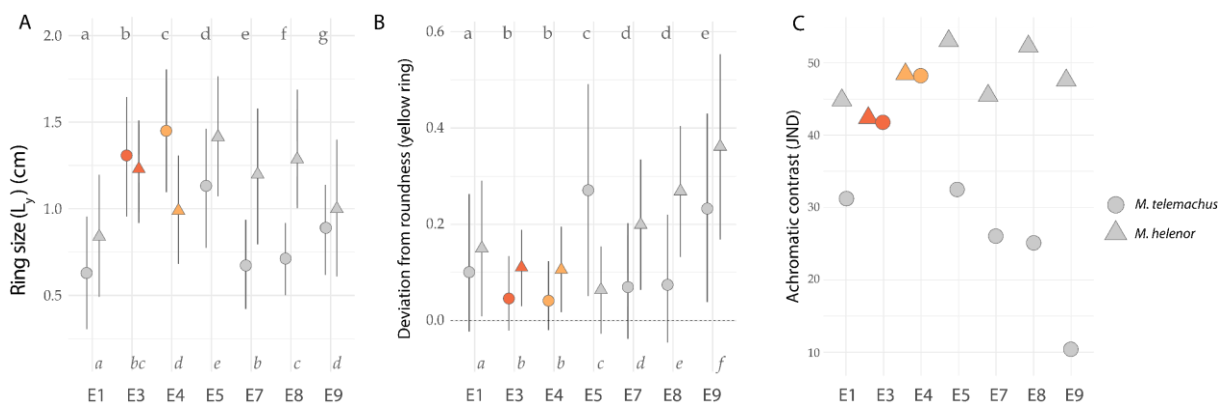


Figure 2: Sizes, shapes and colors of eyespots, revealing contrasted levels of conspicuousness in *M. telemachus* and *M. helenor*. Eyespots E3 and E4 (conditionally-displayed in *M. telemachus*) are figured in orange. Circles: *M. telemachus*; triangles: *M. helenor*. (A) Eyespots sizes. The four measurements are similarly different across eyespots, so only L_y is displayed. Boxplots indicate mean and standard deviation. Significant differences between eyespots are shown using different letters (a, b, c) – results for *M. telemachus* are displayed in full letters (above) and results for *M. helenor* are displayed in italic letters (below). (B) Deviation from roundness of *M. telemachus* eyespots yellow rings (assessed by L_y/W_y ratio). (C) Achromatic contrast (JND) between the yellow and the black rings of each eyespot. Results are similar across the 2 vision models, so only the UV-model results are displayed (see Figure S1 for chromatic contrasts).

2) The shape of always-visible eyespots is more variable and asymmetrical in *M. telemachus*

For both species, the variability of eyespot size, as estimated by the variation among individuals and by fluctuating asymmetry, was quite homogeneous across eyespots: most pairwise comparisons of size variation between eyespots were non-significant (fluctuating

asymmetry see Figures S2; individual variation: L_y : $D'AD = 1.87$, $p = 0.93$; L_b : $D'AD = 0.91$, $p = 0.99$; W_y : $D'AD = 2.84$, $p = 0.83$; W_b : $D'AD = 2.36$, $p = 0.88$ - Figure S3). In contrast, striking differences across eyespots were detected in *M. telemachus* when considering the variability of eyespot shape. Overall, both individual variation and asymmetry of shape were lower in the two conditionally-displayed eyespots than in the always-visible eyespots (Figure 3), and particularly strikingly so for the yellow ring (on average 4.01 times less variable and 10.08 times less asymmetric than the always-visible eyespots). Such low variability of shape in the conditionally-displayed eyespots suggests a selective effect on the roundness of these eyespots.

Overall, eyespot shape variability tended to be lower in *M. helenor* than in *M. telemachus*: among individual variation was on average 1.62 and 2.79 times lower, in the yellow and black rings ($F_{\text{yellow}} = 1.62$, $df = 2566$, $p < 0.001$; $F_{\text{black}} = 2.80$, $df = 2564$, $p < 0.001$ - Figure 3), and FA was 3.13 and 2.27 times lower ($F_{\text{yellow}} = 3.13$, $df = 2566$, $p < 0.001$; $F_{\text{black}} = 2.27$, $df = 2564$, $p < 0.001$ - Figure 3). This difference was particularly strong for always-visible eyespots (E1, E5, E7, E8 and E9), which were very variable between individuals in *M. telemachus*, and much more stable in *M. helenor*. Combined with a generally more conspicuous appearance of all eyespots in *M. helenor*, this stability of eyespot shape points at a similar selection regime acting on all eyespots in this species. Overall, the comparison of the two species suggests a similarly low variability in the whole series of eyespots in *M. helenor*, as well as in the conditionally-displayed eyespots in *M. telemachus*. This points at a similar stabilizing selection in these eyespots. In contrast, the always-visible eyespots of *M. telemachus* are much more variable, suggesting a relaxed or apostatic selection.

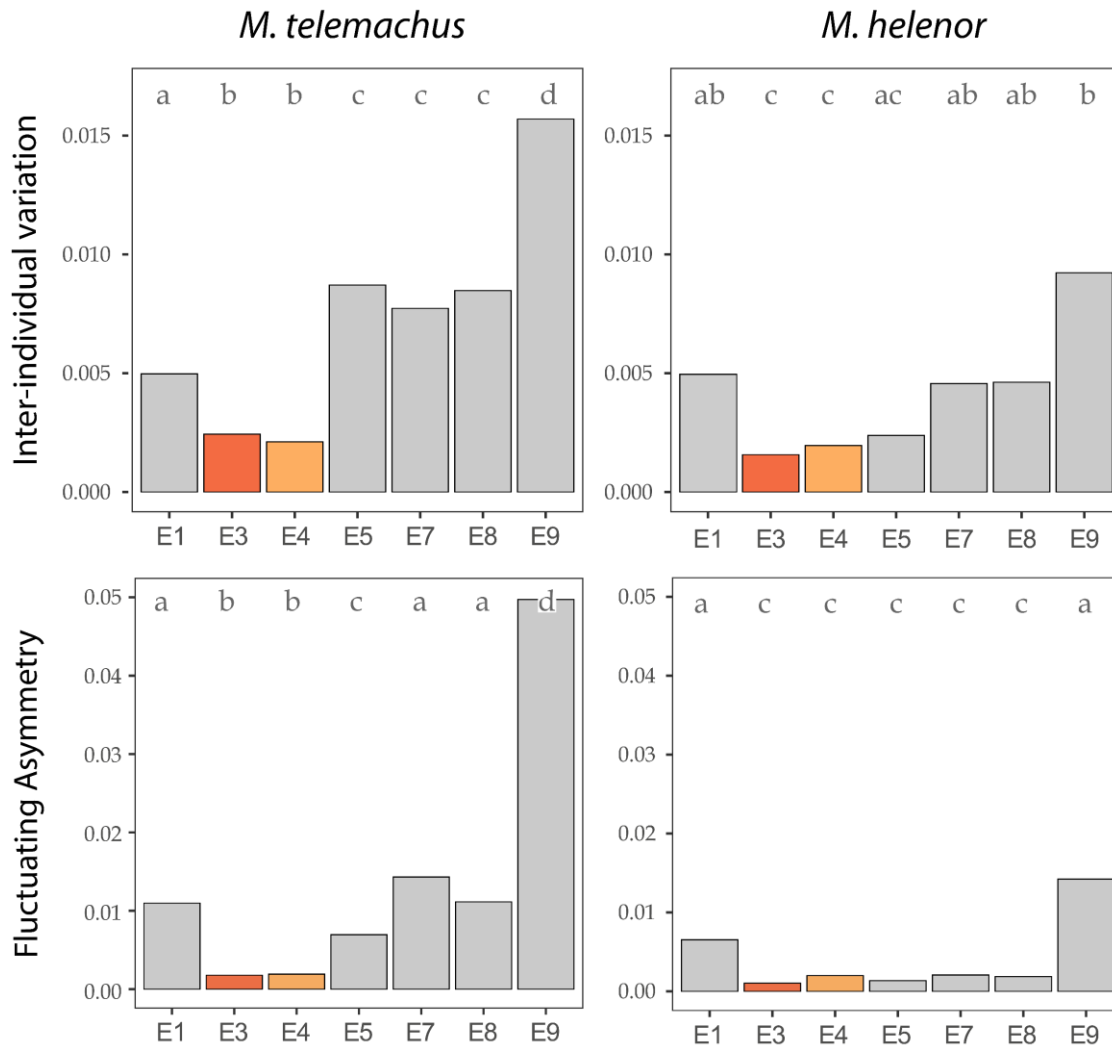


Figure 3: High levels of shape variability in *M. telemachus* always-visible eyespots suggest a relaxed selection. Inter-individual variation (top) and fluctuating asymmetry (bottom) of eyespots yellow ring shape (L_y/W_y). For each species, significant differences between eyespots are shown using different letters (a, b, c; a letter pools non-significantly different traits). Left: *M. telemachus* (n = 370); right: *M. helenor* (n = 31). The relatively low variability of E3 and E4 is comparable to that observed in most *M. helenor* eyespots, suggesting a similar stabilizing selection. The high variability of *M. telemachus* always-visible eyespots in turn suggests a relaxed or apostatic selection.

3) Conditionally-displayed eyespots form a developmental module in *M. telemachus*

Figure 4 clearly shows that there are stronger correlations across traits (individual variation) than across traits asymmetries (FA). Since covariations in FA reflect direct developmental interactions among traits, greater correlations are expected within physically-interacting traits, *e.g.*, within each eyespot, while more limited correlation in FA is expected across eyespots. The patterns of modularity obtained from inter-individual

variation and FA matrices were nevertheless mostly congruent. Overall, the different eyespots tend to form separate modules, the two rings tightly covarying within an eyespot, and more loosely among eyespots. This is particularly striking in *M. helenor* for individual variation (Figures 4A and 5A; mean correlations: $\text{cor}_{\text{within all eyespots}} = 0.94 \pm 0.05$; $\text{cor}_{\text{among all eyespots}} = 0.54 \pm 0.14$; see Table S3 for all correlations categories), but also for FA (Figures 4B and 5B; mean correlations: $\text{cor}_{\text{within all eyespots}} = 0.67 \pm 0.24$; $\text{cor}_{\text{among all eyespots}} = 0.03 \pm 0.19$). A submodular pattern was also observed in both species within eyespots, opposing the yellow and black rings (higher correlations within a ring than among rings of the same eyespot; Figure 5). Consistent with a homogeneous effect of selection on the whole series of eyespots in *M. helenor*, no sub-clustering of eyespots is detected.

In contrast, in *M. telemachus*, the conditionally-displayed eyespots E3 and E4 exhibit strong covariations and clearly form a separate module. Remarkably, their higher FA covariation compared to among always-visible eyespots (noted “AV” below) is indicative of a developmental integration ($\text{cor}_{\text{among E3-E4}} = 0.30 \pm 0.17$; $\text{cor}_{\text{among AV}} = 0.11 \pm 0.12$; see Table S3 for all correlations categories). Contrary to all other eyespots, that display a submodular pattern opposing the two rings, the different measurements of these two eyespots cluster irrespective of eyespot identity (Figure 5C), suggesting a very tight integration. The same pattern is found for individual variation, the E3 and E4 covariation being even almost as high as that measured within a single eyespot ($\text{cor}_{\text{among E3-E4}} = 0.74 \pm 0.12$, $\text{cor}_{\text{among AV}} = 0.49 \pm 0.10$, $\text{cor}_{\text{within all}} = 0.82 \pm 0.18$). Overall, this opposition between conditionally-displayed *vs.* always-visible eyespots suggests that different selective pressures affect the two types of eyespots and may have modified the patterns of modularity in *M. telemachus*.

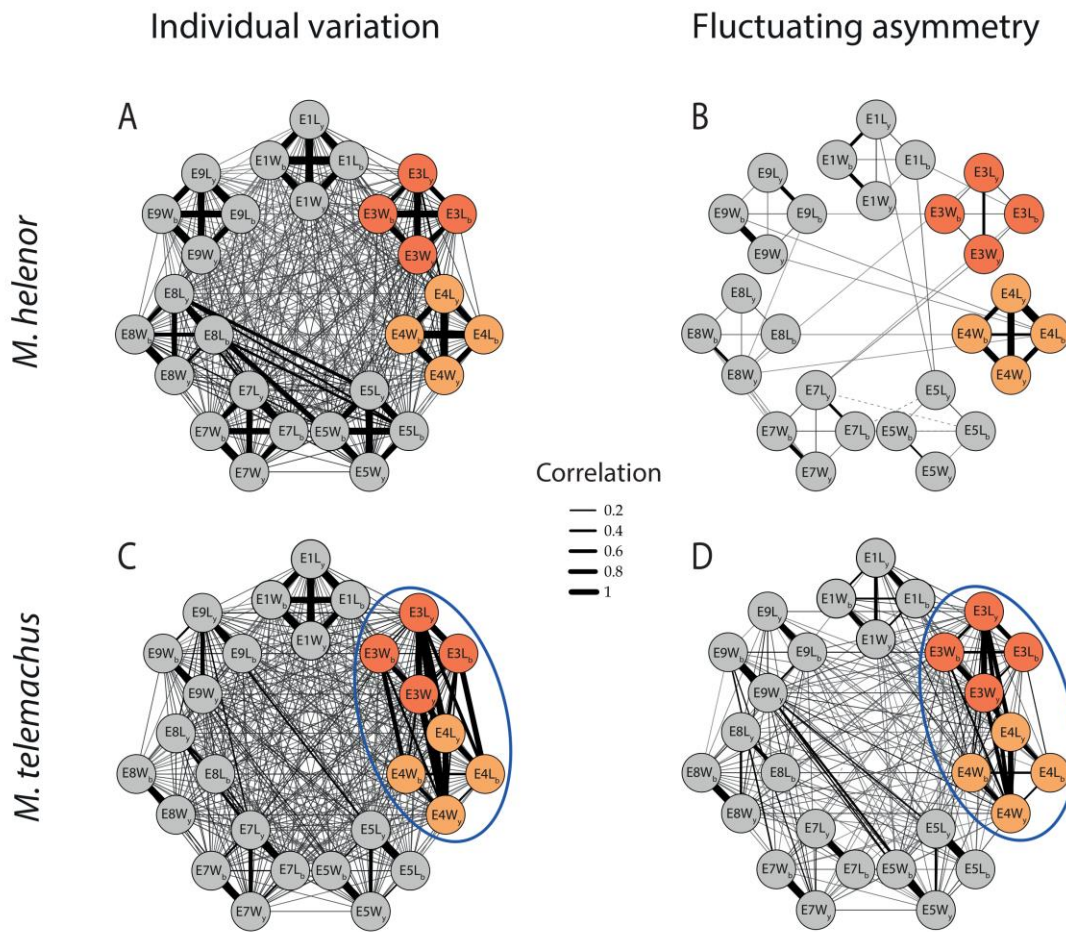


Figure 4: Contrasted patterns of modularity observed in *M. telemachus* and *M. helenor*. as assessed by correlation matrices of linear parameters (L_y , W_y , L_b , W_b) of the 7 different eyespots. Top: *M. helenor* ($n = 31$); Bottom: *M. telemachus* ($n = 370$). Left: modularity patterns inferred from individual variation; Right: modularity patterns inferred from FA. Nodes represent the 4 measured variables and the edges represent the statistically significant correlations. Line thickness is proportional to the correlation. The blue ellipse shows the module regrouping E3 and E4 detected by the hierarchical clustering in *M. telemachus*.

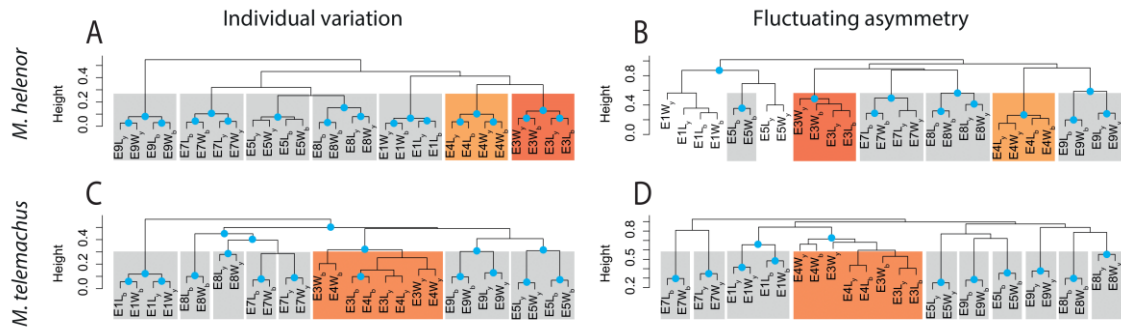


Figure 5: Hierarchical clustering based on the FA and inter-individual correlation matrices of linear parameters (L_y , W_y , L_b , W_b) of the 7 different eyespots. *M. telemachus* ($n = 370$) is shown on the second row and *M. helenor* ($n = 31$) on the first row. Left: Hierarchical clustering based on the inter-individual correlation matrices. Right: Hierarchical clustering based on FA correlation matrices. Hierarchical clustering exploring the networks modularity. The height of the nodes indicates the distance between two observations (here we used correlation matrix as distance matrix, so the higher the height, the less correlated are two traits). A node marked with a blue circle indicate that the associated cluster is significant. The cluster associating the conditionally-displayed eyespots E3 and E4 in *M. telemachus* is the only cluster whose intra-eyespot modularity is overcome by inter-eyespots modularity.

Discussion

1) Differential eyespot variability in *M. telemachus* shaped by contrasted selection regimes

In *M. telemachus*, the large difference in achromatic contrast detected between conditionally-displayed eyespots and the others (Figure 2C), suggests that the two types of eyespots may be submitted to different selective regimes. Achromatic contrast is indeed often used by birds to detect small targets while chromatic contrast is involved in discrimination of large targets and recognition of chromatic patterns (Osorio *et al.*, 1999; Théry *et al.*, 2004; Halpin *et al.*, 2020). Achromatic contrast was also shown to increase prey conspicuousness and detection by mantid predators (Prudic *et al.*, 2007). Our results thus highlight that conditionally-displayed eyespots are more conspicuous than the other eyespots. Their evolution might thus have been influenced by different selective pressures.

Our analyses then show that in *M. telemachus*, conditionally-displayed eyespots are rounder than the always-visible eyespots. Their shape is also strikingly less variable, these low levels of variation and FA being comparable to those detected in *M. helenor* (Figure 3). Traits that are visible – and thus exposed to selection – only part of the time might be

submitted to a weaker selection and would thus be expected to present higher variation than always exposed traits. Our results nevertheless support highlight the converse situation, with a lower variation in the conditionally-exposed eyespots. This observation is consistent with an effect of stabilizing selection, expected to reduce allelic variation in the genes controlling the traits in the population (Boonekamp *et al.*, 2018; Stearns *et al.*, 1995). Stabilizing selection should also favour developmental robustness of the traits, therefore promoting low levels of variation and fluctuating asymmetry via enhanced canalization and developmental stability (Clarke *et al.*, 1968; Palmer and Strobeck, 1986; Leamy and Klingenberg, 2005; Garnier *et al.*, 2006 but see Pélabon *et al.*, 2010). The overall agreement between low fluctuating asymmetry and low inter-individual variation thus likely reflects stabilizing selection on the morphology of the two conditionally-displayed eyespots, and more particularly on their shape.

Since most *Morpho* species display large and quite conspicuous eyespots, rather similar to those found in *M. helenor* (Debat *et al.*, 2020), the always-visible, irregularly shaped eyespots observed in *M. telemachus* are likely a derived condition. The contrasted pattern of variation across *M. telemachus* eyespots might thus be related to a relaxation of selection on the visible eyespots of *M. telemachus*, rather than to an increase in stabilizing selection on the conditionally-displayed eyespots. The large inter-individual variation, and the increased FA in those eyespots are indeed consistent with such a relaxation of selection. A similar increase in FA and individual variation was detected in the wings of the carabid *Carabus solieri*, which are non-functional and vestigial in this species, relative to the legs, that are phenotypically much more stable, and are probably under strong selection linked to prey capture (Garnier *et al.*, 2006); similar results were reported for vestigial wings in a gall thrips by Crespi and Vanderkist (1997). The most variable eyespots in *M. telemachus* may thus be vestigial: consistent with this hypothesis, the two most variable eyespots E2 and E6 (Figure 1B) are absent in many individuals within our sample of *M. telemachus* (in 55.7% and 51.4% of individuals for E2 and E6 respectively). Artificial selection studies in *B. anynana* have suggested a developmental correlation between eyespot size and its variability (Beldade and Brakefield, 2003). In *M. telemachus*, the disappearance of eyespots E2 and E6 in some individuals may be a by-product of the relaxation of selection on the small, always-visible eyespots. In a study of the evolution of eyespots across the whole *Morpho* genus, we recently reported a negative correlation

between eyespot size and intraspecific variability of eyespot size and shape (Debat *et al.*, 2020), suggesting that beyond the particular example of *M. telemachus*, stabilizing selection on the smallest eyespots might be relaxed compared to larger ones.

The high variability of shape of always-visible eyespots in *M. telemachus* could also stem from specific selective regimes, such as apostatic selection (Allen and Clarke, 1968; Ursprung and Nöthiger, 1972; Bond, 2007). This form of negative frequency-dependent selection favours rare phenotypes in prey communities, as they are more difficult to identify by predators, searching for images of already encountered prey. This is for example the case in the cryptic patterns of moths (Bond and Kamil, 2006, 2002). Apostatic selection may favour extreme, low frequency eyespot variants, improving crypsis. While apostatic selection in principle relies on genetic variants, it might also favour low levels of developmental robustness in the always-visible eyespots, leading to their increased plasticity and developmental instability and enhancing their variability. While our data do not allow us to assess plasticity, the high levels of FA in these eyespots attest their instability, raising the interesting possibility of an adaptive developmental instability (see Forde, 2009 for a similar hypothesis in plants).

2) Phenotypic covariation: integration within eyespots, modularity among eyespots

In both species, we observed a strong covariation within all eyespots, for both FA and individual variation. Such a tight integration within eyespots is expected, as the black and yellow rings derive from the same suites of developmental events, from the pre-patterning to the control of pigmentary genes (reviewed in Monteiro, 2015; Beldade and Monteiro, 2021). In particular, FA covariation illustrates this developmental integration: as FA originates from stochastic variation affecting developmental processes, only traits with shared developmental routes exhibit correlated FA (Klingenberg and Polak, 2003; Klingenberg, 2008). The different components of an eyespot are also likely integrated by the joint selection acting on them. In this respect, one could have expected always-visible eyespots to be less tightly integrated than conspicuous eyespots: the mean correlation within an eyespot is indeed slightly lower in always-visible eyespots ($r_{\text{within AV}}=0.53\pm0.34$ vs. $r_{\text{within E3-E4}}=0.57\pm0.30$) but the high standard deviations prevent drawing any robust conclusion.

Except between the two conditionally-displayed eyespots in *M. telemachus*, the covariation among eyespots was markedly lower than within eyespots, for both FA and individual variation. This result was expected for FA, as direct developmental interactions across eyespots are expected to be limited to the common global pre-patterning of the wing. Considering individual variation, the strong modularity of the different eyespots was unexpected. Eyespots serial homology indeed implies that genetic variation affecting any of the components of the shared genetic network should trigger a joint phenotypic variation. Similarly, any environmental influence on this common network should increase phenotypic covariance (e.g., Allen, 2008). A tight covariation across eyespots was in particular predicted in *M. helenor*, where all eyespots are expected to be submitted to the same selection regime. Although the correlation among eyespots was quite high (0.5 in *M. helenor*), the pattern of modularity clearly opposed the different eyespots. This suggests that the patterning of the different eyespots involves locally different processes, allowing some independent variation. This result is consistent with artificial selection experiments in *B. anynana* (Beldade *et al.*, 2002; Beldade and Brakefield, 2003), showing that the independent evolution of eyespots is not strongly constrained by the genetic correlations among eyespots. The evolution of seasonal forms with different eyespot series in *B. anynana* as well as the contrasted evolution of eyespot modularity within the pattern of *M. telemachus* highlight that eyespot modularity in butterflies is a relevant example of developmental series where patterns of modularity are likely to evolve in response to selection.

3) Phenotypic covariation: functional and developmental modularities match in *M. telemachus*

In contrast to *M. helenor*, covariation patterns in *M. telemachus* are clearly heterogeneous across the eyespot series. For both FA and individual variation, the two conditionally-displayed eyespots strongly covary and form a module opposed to the individually-modular always-visible eyespots. In particular, the covariance in FA suggests that specific developmental processes have evolved that jointly affect these two eyespots morphology, leading to the formation of a single developmental module. The change in developmental modularity in the eyespot series of *M. telemachus* coincides with the contrasted selective

pressures affecting it. Such a match between developmental and functional modularity has been predicted to result from the adaptive evolution of pleiotropy across groups of traits submitted to different selective pressures (Cheverud, 1984; Wagner and Altenberg, 1996; Breuker *et al.*, 2006; Wagner *et al.*, 2007; Klingenberg, 2014). The developmental covariation between the two conditionally-displayed eyespots might result from new pleiotropic interactions promoted by the joint selection of these two traits. The exact nature of the selection affecting the modularity of the two conditionally-displayed eyespots remains to be determined.

Documented cases of adaptive evolution of modularity are still largely lacking (Klingenberg, 2010). Our study on the eyespots of *M. telemachus* may thus represent a relevant case where developmental modularity can be tuned by natural selection, in line with the matching hypothesis (Breuker *et al.*, 2006). Similar analysis of morphological variation and modularity should be performed in other species harbouring heterogeneous morphologies of eyespots, to assess the diversity of interactions between developmental and selective constraints. Experiments are now required to identify (1) the exact selection regime affecting conditionally-displayed eyespots in *M. telemachus* and, (2) the developmental bases underlying the evolution of modularity across *Morpho* species.

Supplementary

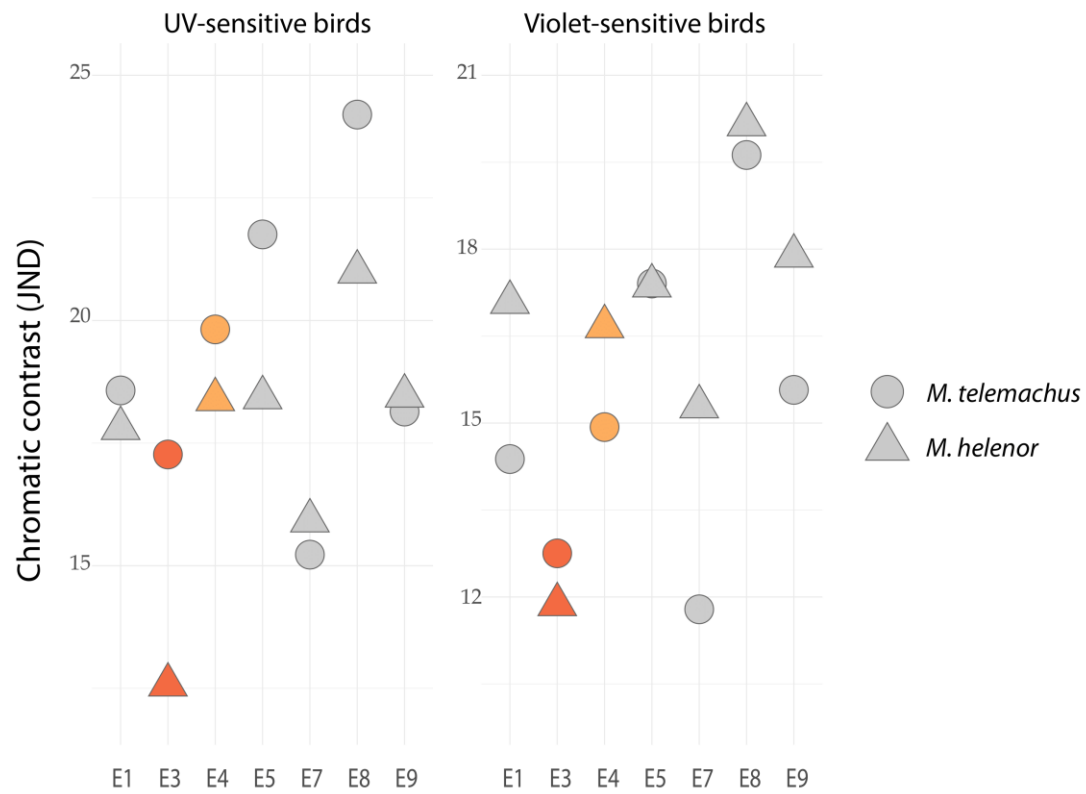


Figure S1: Chromatic contrasts (JND) between the yellow ring and the black ring of eyespots measured in *M. telemachus* (n = 10; circles) and *M. helenor* (n = 10; triangles). The 2 vision models are displayed: UV-sensitive birds (left) and Violet-sensitive birds (right).

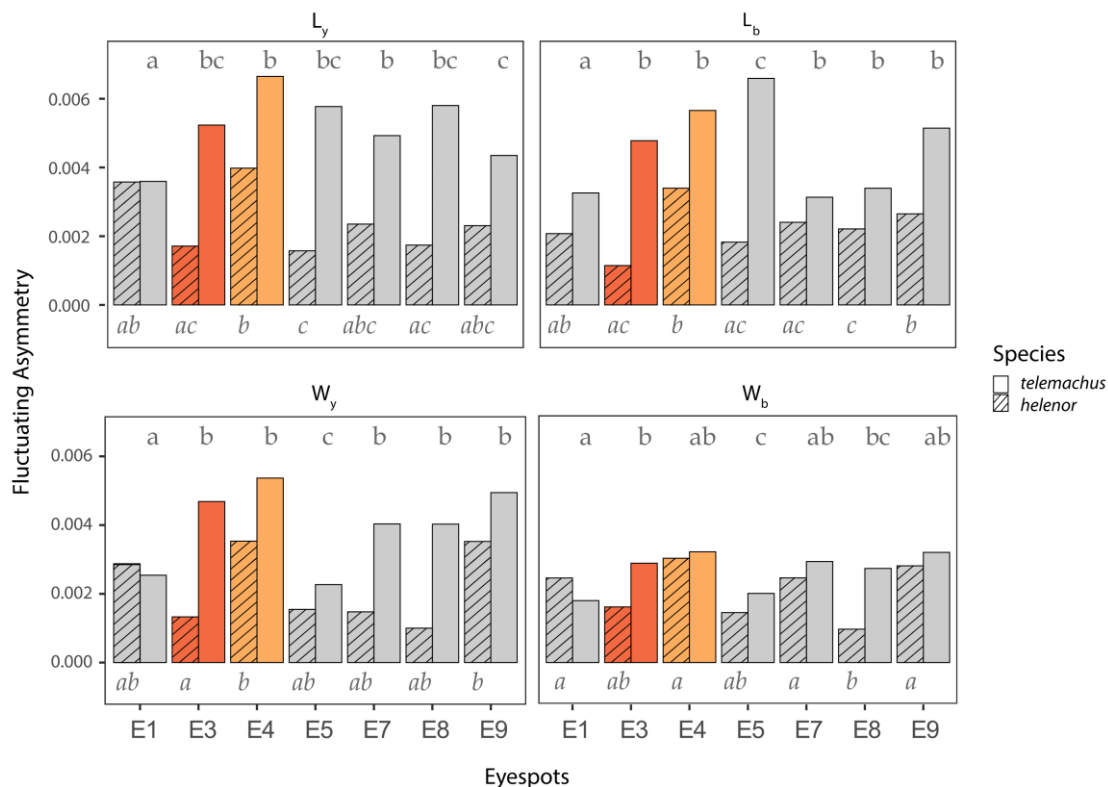


Figure S2: Fluctuating asymmetry of eyespots linear parameters, respectively length and width of the yellow ring (L_y and W_y) and length and width of the black ring (L_b and W_b) of each eyespot (E1, E3, E4, E5, E7, E8 and E9), measured in the *M. telemachus* sample ($n = 370$) and *M. helenor* ($n = 31$). Significant differences between eyespots are shown using different letters (a, b, c) – results for *M. telemachus* are displayed in full letters (above) and results for *M. helenor* are displayed in italic letters (below).

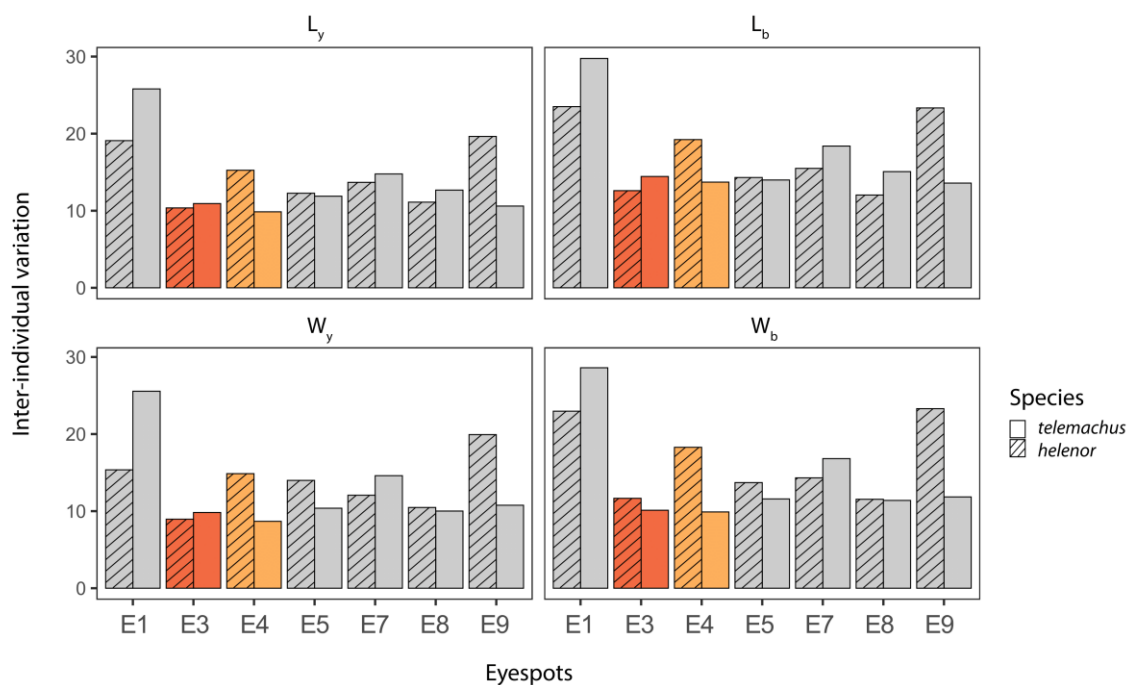


Figure S3: Inter-individual variation of eyespots linear parameters, respectively length and width of the yellow ring (L_y and W_y) and length and width of the black ring (L_b and W_b) of each eyespot (E1, E3, E4, E5, E7, E8 and E9), measured in the *M. telemachus* sample ($n = 370$) and *M. helenor* ($n = 31$).

Table S1: Pairwise comparisons of size differences among *M. telemachus* eyespots (L_y measures), using Welch's tests, and accounting for multiple comparisons using Holm-Bonferroni correction. The sample size for all tests is 370.

Trait1	Trait2	Welch t	df	P
E1	E3	-60.2	726.0	<0.001
E1	E4	-73.0	726.4	<0.001
E1	E5	-45.7	712.9	<0.001
E1	E7	-4.3	611.0	<0.001
E1	E8	-8.6	577.1	<0.001
E1	E9	-26.7	592.7	<0.001
E3	E4	-13.8	738.0	<0.001
E3	E5	17.3	735.3	<0.001
E3	E7	70.1	658.3	<0.001
E3	E8	67.6	623.5	<0.001
E3	E9	46.8	639.9	<0.001
E4	E5	31.4	735.1	<0.001
E4	E7	86.0	657.6	<0.001
E4	E8	84.0	622.7	<0.001
E4	E9	62.9	639.1	<0.001
E5	E7	52.7	679.6	<0.001
E5	E8	49.7	645.9	<0.001
E5	E9	28.1	662.0	<0.001
E7	E8	-5.7	731.4	<0.001
E7	E9	-30.6	736.1	<0.001
E8	E9	-26.2	736.5	<0.001

Table S2: Pairwise comparisons of the yellow ring shape among *M. telemachus* eyespots (R_y measures), using Welch's tests and accounting for multiple testing by using Holm-Bonferroni correction. The sample size for all tests is 370.

Trait1	Trait2	Welch t	df	P
E1	E3	14.7	525.5	<0.001
E1	E4	16.2	501.6	<0.001
E1	E5	-29.1	647.7	<0.001
E1	E7	7.1	689.8	<0.001
E1	E8	5.7	711.7	<0.001
E1	E9	-19.2	545.6	<0.001
E3	E4	1.9	733.2	0.054
E3	E5	-44.0	462.3	<0.001
E3	E7	-7.2	609.8	<0.001
E3	E8	-8.2	574.1	<0.001
E3	E9	-29.0	420.3	<0.001
E4	E5	-45.3	448.7	<0.001
E4	E7	-8.8	580.8	<0.001
E4	E8	-9.6	547.6	<0.001
E4	E9	-29.8	412.7	<0.001
E5	E7	36.1	593.9	<0.001
E5	E8	34.1	633.9	<0.001
E5	E9	3.6	678.8	<0.001
E7	E8	-1.3	727.9	0.211
E7	E9	-24.2	501.1	<0.001
E8	E9	-23.0	530.4	<0.001

Table S3: Summary of the measured correlations between eyespots of *M. telemachus* and *M. helenor* – especially between conditionally-displayed (E3-E4) and always-visible (AV) eyespots. Table indicate mean and standard deviation

FA correlations	<i>telemachus</i>	<i>helenor</i>
correlation among AV	0.11 ± 0.12	0.03 ± 0.18
correlation among E3-E4	0.30 ± 0.17	0.05 ± 0.29
correlation within AV	0.53 ± 0.34	0.63 ± 0.36
correlation within E3-E4	0.57 ± 0.30	0.75 ± 0.34
Individual correlations	<i>telemachus</i>	<i>helenor</i>
correlation among AV	0.49 ± 0.10	0.55 ± 0.13
correlation among E3-E4	0.74 ± 0.12	0.66 ± 0.11
correlation within-AV	0.82 ± 0.19	0.94 ± 0.12
correlation within E3-E4	0.82 ± 0.16	0.93 ± 0.15

Bibliography

- Abadi, M., Agarwal, A., Barham, P., Brevdo, E., Chen, Z., Citro, C., Corrado, G.S., Davis, A., Dean, J., Devin, M., Ghemawat, S., Goodfellow, I., Harp, A., Irving, G., Isard, M., Jia, Y., Jozefowicz, R., Kaiser, L., Kudlur, M., Levenberg, J., Mane, D., Monga, R., Moore, S., Murray, D., Olah, C., Schuster, M., Shlens, J., Steiner, B., Sutskever, I., Talwar, K., Tucker, P., Vanhoucke, V., Vasudevan, V., Viegas, F., Vinyals, O., Warden, P., Wattenberg, M., Wicke, M., Yu, Y., Zheng, X., 2016. TensorFlow: Large-Scale Machine Learning on Heterogeneous Distributed Systems. *OSDI 16*, 265-283.
- Abbasi, R., Marcus, J.M., 2017. A new A-P compartment boundary and organizer in holometabolous insect wings. *Sci Rep* 7, 16337. <https://doi.org/10.1038/s41598-017-16553-5>
- Adams, D.C., 2016. Evaluating modularity in morphometric data: challenges with the RV coefficient and a new test measure. *Methods Ecol Evol* 7, 565–572. <https://doi.org/10.1111/2041-210X.12511>
- Adams, D.C., Otárola-Castillo, E., 2013. geomorph: an R package for the collection and analysis of geometric morphometric shape data. *Methods Ecol Evol* 4, 393–399. <https://doi.org/10.1111/2041-210X.12035>
- Adams, D.C., Rohlf, F.J., Slice, D.E., 2004. Geometric morphometrics: Ten years of progress following the ‘revolution.’ *Ital J Zool* 71, 5–16. <https://doi.org/10.1080/11250000409356545>
- Alcock, J., 1996. Male size and survival: the effects of male combat and bird predation in Dawson’s burrowing bees, *Amegilla dawsoni*. *Ecol Entomol* 21, 309–316. <https://doi.org/10.1046/j.1365-2311.1996.00007.x>
- Allen, C.E., 2008. The “Eyespot Module” and eyespots as modules: development, evolution, and integration of a complex phenotype. *J Exp Zool B Mol Dev Evol* 310B, 179–190. <https://doi.org/10.1002/jez.b.21186>
- Allen, J.A., Clarke, B., 1968. Evidence for Apostatic Selection by Wild Passerines. *Nature* 220, 501–502. <https://doi.org/10.1038/220501a0>
- Allio, R., Nabholz, B., Wanke, S., Chomicki, G., Pérez-Escobar, O.A., Cotton, A.M., Clamens, A.-L., Kergoat, G.J., Sperling, F.A.H., Condamine, F.L., 2021. Genome-wide macroevolutionary signatures of key innovations in butterflies colonizing new host plants. *Nat Commun* 12, 354. <https://doi.org/10.1038/s41467-020-20507-3>
- Allio, R., Scornavacca, C., Nabholz, B., Clamens, A.-L., Sperling, F.A., Condamine, F.L., 2020. Whole Genome Shotgun Phylogenomics Resolves the Pattern and Timing of

- Swallowtail Butterfly Evolution. *Syst Biol* 69, 38–60.
<https://doi.org/10.1093/sysbio/syz030>
- Altizer, S., Davis, A.K., 2009. Populations of monarch butterflies with different migratory behaviors show divergence in wing morphology. *Evolution* 64, 1018–1028.
<https://doi.org/10.1111/j.1558-5646.2009.00946.x>
- Aluthwattha, S.T., Harrison, R.D., Ranawana, K.B., Xu, C., Lai, R., Chen, J., 2017. Does spatial variation in predation pressure modulate selection for aposematism? *Ecol Evol* 7, 7560–7572. <https://doi.org/10.1002/ece3.3221>
- Arnold, E.N., 1984. Evolutionary aspects of tail shedding in lizards and their relatives. *J Nat Hist* 18, 127–169. <https://doi.org/10.1080/00222938400770131>
- Barber, J.R., Leavell, B.C., Keener, A.L., Breinholt, J.W., Chadwell, B.A., McClure, C.J.W., Hill, G.M., Kawahara, A.Y., 2015. Moth tails divert bat attack: Evolution of acoustic deflection. *Proc Natl Acad Sci USA* 112, 2812–2816.
<https://doi.org/10.1073/pnas.1421926112>
- Basset, J.-P., Cartraud, P., Jacquot, C., LEROY, A., Peseux, B., Vaussy, P., 2007. Introduction à la résistance des matériaux.
- Bateman, A.W., Vos, M., Anholt, B.R., 2014. When to Defend: Antipredator Defenses and the Predation Sequence. *Am Nat* 183, 847–855. <https://doi.org/10.1086/675903>
- Bateman, P.W., Fleming, P.A., 2009. To cut a long tail short: a review of lizard caudal autotomy studies carried out over the last 20 years. *J Zool* 277, 1–14.
<https://doi.org/10.1111/j.1469-7998.2008.00484.x>
- Beaulieu, J.M., O’Meara, B.C., 2016. Detecting Hidden Diversification Shifts in Models of Trait-Dependent Speciation and Extinction. *Syst Biol* 65, 583–601.
<https://doi.org/10.1093/sysbio/syw022>
- Beldade, P., Brakefield, P.M., 2003. Concerted evolution and developmental integration in modular butterfly wing patterns. *Evol Dev* 5, 169–179. <https://doi.org/10.1046/j.1525-142X.2003.03025.x>
- Beldade, P., Brakefield, P.M., 2002. The genetics and evo–devo of butterfly wing patterns. *Nat Rev Genet* 3, 442–452. <https://doi.org/10.1038/nrg818>
- Beldade, P., Koops, K., Brakefield, P.M., 2002. Modularity, Individuality, and Evo-Devo in Butterfly Wings. *Proc Nat Acad Sci* 99, 14262–14267.
- Beldade, P., Monteiro, A., 2021. Eco-evo-devo advances with butterfly eyespots. *Curr Opin Genet Dev* 69, 6–13. <https://doi.org/10.1016/j.gde.2020.12.011>

- Beneski, J.T., 1989. Adaptive Significance of Tail Autotomy in the Salamander, *Ensatina*. *J Herpetol* 23, 322. <https://doi.org/10.2307/1564465>
- Berwaerts, K., Van Dyck, H., Aerts, P., 2002. Does Flight Morphology Relate to Flight Performance? An Experimental Test with the Butterfly *Pararge aegeria*. *Funct Ecol* 16, 484–491.
- Blackburn, D.C., Siler, C.D., Diesmos, A.C., McGuire, J.A., Cannatella, D.C., Brown, R.M., 2013. An adaptive radiation of frogs in a Southeast Asian island archipelago. *Evolution* 67, 2631–2646. <https://doi.org/10.1111/evo.12145>
- Blandin, P., Purser, B., 2013. Evolution and diversification of neotropical butterflies: insights from the biogeography and phylogeny of the genus *Morphos fabricus*, 1807 (Nymphalidae: Morphinae) with a review of the geodynamics of South America. *Trop Lepid Res* 23(2), 62:85.
- Bolar, K., 2019. STAT: Interactive Document for Working with Basic Statistical Analysis.
- Bond, A.B., 2007. The Evolution of Color Polymorphism: Crypticity, Searching Images, and Apostatic Selection. *Annu Rev Ecol Evol Syst* 38, 489–514. <https://doi.org/10.1146/annurev.ecolsys.38.091206.095728>
- Bond, A.B., Kamil, A.C., 2006. Spatial heterogeneity, predator cognition, and the evolution of color polymorphism in virtual prey. *Proc Natl Acad Sci India Sect B Biol Sci* 103, 3214–3219. <https://doi.org/10.1073/pnas.0509963103>
- Bond, A.B., Kamil, A.C., 2002. Visual predators select for crypticity and polymorphism in virtual prey. *Nature* 415, 609–613. <https://doi.org/10.1038/415609a>
- Bond, A.B., Kamil, A.C., 1998. Apostatic selection by blue jays produces balanced polymorphism in virtual prey. *Nature* 395, 594–596. <https://doi.org/10.1038/26961>
- Bookstein, F.L., 1997. Landmark methods for forms without landmarks: morphometrics of group differences in outline shape. *Med Image Anal* 1, 225–243. [https://doi.org/10.1016/S1361-8415\(97\)85012-8](https://doi.org/10.1016/S1361-8415(97)85012-8)
- Boonekamp, J.J., Mulder, E., Verhulst, S., 2018. Canalisation in the wild: effects of developmental conditions on physiological traits are inversely linked to their association with fitness. *Ecol Lett* 21, 857–864. <https://doi.org/10.1111/ele.12953>
- Brattström, O., Aduse-Poku, K., van Bergen, E., French, V., Brakefield, P.M., 2020. A release from developmental bias accelerates morphological diversification in butterfly eyespots. *Proc Natl Acad Sci U.S.A.* 117, 27474–27480. <https://doi.org/10.1073/pnas.2008253117>

- Breuker, C.J., Debat, V., Klingenberg, C.P., 2006. Functional evo-devo. *Trends in Ecology & Evolution* 21, 488–492. <https://doi.org/10.1016/j.tree.2006.06.003>
- Breuker, C.J., Gibbs, M., Van Dyck, H., Brakefield, P.M., Klingenberg, C.P., Van Dongen, S., 2007. Integration of wings and their eyespots in the speckled wood butterfly *Pararge aegeria*. *J Exp Zool B Mol Dev Evol* 308B, 454–463. <https://doi.org/10.1002/jez.b.21171>
- Brodsky, A.K., 1994. *The Evolution of Insect Flight*. Oxford University Press.
- Burress, E.D., Muñoz, M.M., 2022. Functional Trade-Offs Asymmetrically Promote Phenotypic Evolution. *Syst Biol* syac058. <https://doi.org/10.1093/sysbio/syac058>
- Carroll, S.B., 1995. Homeotic genes and the evolution of arthropods and chordates. *Nature* 376, 479–485. <https://doi.org/10.1038/376479a0>
- Carroll, S.B., Grenier, J.K., Weatherbee, S.D., 2005. *From DNA to diversity: molecular genetics and the evolution of animal design*, 2nd ed. ed. Blackwell Pub, Malden, MA.
- Carvalho, M.R.M., Peixoto, P.E.C., Benson, W.W., 2016. Territorial clashes in the Neotropical butterfly *Actinote pellenea* (Acraeinae): do disputes differ when contests get physical? *Behav Ecol Sociobiol* 70, 199–207. <https://doi.org/10.1007/s00265-015-2042-6>
- Cespedes, A., Penz, C.M., DeVries, P.J., 2015. Cruising the rain forest floor: butterfly wing shape evolution and gliding in ground effect. *J Anim Ecol* 84, 808–816. <https://doi.org/10.1111/1365-2656.12325>
- Chan, I.Z.W., Ngan, Z.C., Naing, L., Lee, Y., Gowri, V., Monteiro, A., 2021. Predation favours *Bicyclus anynana* butterflies with fewer forewing eyespots. *Proc R Soc B* 288, 20202840. <https://doi.org/10.1098/rspb.2020.2840>
- Chazot, N., Panara, S., Zilbermann, N., Blandin, P., Le Poul, Y., Cornette, R., Elias, M., Debat, V., 2016. Morpho morphometrics: Shared ancestry and selection drive the evolution of wing size and shape in “Morpho” butterflies: “Morpho” morphometrics. *Evolution* 70, 181–194. <https://doi.org/10.1111/evo.12842>
- Cheverud, J.M., 1984. Quantitative genetics and developmental constraints on evolution by selection. *J Theor Biol* 110, 155–171. [https://doi.org/10.1016/S0022-5193\(84\)80050-8](https://doi.org/10.1016/S0022-5193(84)80050-8)
- Chotard, A., Ledamoisel, J., Decamps, T., Herrel, A., Chaine, A.S., Llaurens, V., Debat, V., 2022. Evidence of attack deflection suggests adaptive evolution of wing tails in butterflies. *Proc R Soc B* 289, 20220562. <https://doi.org/10.1098/rspb.2022.0562>
- Ciampaglio, C.N., Kemp, M., McShea, D.W., 2001. Detecting changes in morphospace occupation patterns in the fossil record: characterization and analysis of measures of

- disparity. *Paleobiology* 27, 695–715. [https://doi.org/10.1666/0094-8373\(2001\)027<0695:DCIMOP>2.0.CO;2](https://doi.org/10.1666/0094-8373(2001)027<0695:DCIMOP>2.0.CO;2)
- Clark, C.J., Dudley, R., 2009. Flight costs of long, sexually selected tails in hummingbirds. *Proc R Soc B* 276, 2109–2115. <https://doi.org/10.1098/rspb.2009.0090>
- Clarke, C.A., Sheppard, P.M., Thornton, I.W.B., 1968. The genetics of the mimetic butterfly *Papilio memnon* L. *Philos Trans R Soc Lond B Biol Sci* 254, 37–89. <https://doi.org/10.1098/rstb.1968.0013>
- Codella, S.G., Lederhouse, R.C., 1989. Intersexual comparison of mimetic protection in the black swallowtail butterfly, *Papilio polywenes*: experiment with captive blue jay predators. *Evolution* 43, 410–420. <https://doi.org/10.1111/j.1558-5646.1989.tb04236.x>
- Colombo, M., Damerou, M., Hanel, R., Salzburger, W., Matschiner, M., 2015. Diversity and disparity through time in the adaptive radiation of Antarctic notothenioid fishes. *J Evol Biol* 28, 376–394. <https://doi.org/10.1111/jeb.12570>
- Condamine, F.L., Sperling, F.A.H., Wahlberg, N., Rasplus, J.-Y., Kergoat, G.J., 2012. What causes latitudinal gradients in species diversity? Evolutionary processes and ecological constraints on swallowtail biodiversity: Phylogeny and latitudinal diversity gradient. *Ecol Lett* 15, 267–277. <https://doi.org/10.1111/j.1461-0248.2011.01737.x>
- Cook, S.E., Vernon, J.G., Bateson, M., Guilford, T., 1994. Mate choice in the polymorphic African swallowtail butterfly, *Papilio dardanus*: male-like females may avoid sexual harassment. *Anim Behav* 47, 389–397.
- Cooper, W.E., 1998. Reactive and anticipatory display to deflect predatory attack to an autotomous lizard tail. *Can J Zool* 76, 4.
- Corn, K.A., Martinez, C.M., Burress, E.D., Wainwright, P.C., 2021. A Multifunction Trade-Off has Contrasting Effects on the Evolution of Form and Function. *Syst Biol* 70, 681–693. <https://doi.org/10.1093/sysbio/syaa091>
- Cott, H.B., 1940. Adaptive coloration in animals. Methuen, London.
- Crespi, B.J., Vanderkist, B.A., 1997. Fluctuating asymmetry in vestigial and functional traits of a haplodiploid insect. *Heredity* 79, 624–630. <https://doi.org/10.1038/hdy.1997.208>
- Cuthill, I.C., Partridge, J.C., Bennett, A.T.D., Church, S.C., Hart, N.S., Hunt, S., 2000. Ultraviolet Vision in Birds, in: Slater, P.J.B., Rosenblatt, J.S., Snowdon, C.T., Roper, T.J. (Eds.), *Adv Study Behav* 29, 159–214. [https://doi.org/10.1016/S0065-3454\(08\)60105-9](https://doi.org/10.1016/S0065-3454(08)60105-9)

- Dapporto, L., Hardy, P.B., Dennis, R.L.H., 2019. Evidence for adaptive constraints on size of marginal wing spots in the grayling butterfly, *Hipparchia semele*. *Biol J Linn Soc Lond* 126, 131–145. <https://doi.org/10.1093/biolinnean/bly179>
- Debat, V., Chazot, N., Jarosson, S., Blandin, P., Llaurens, V., 2020. What Drives the Diversification of Eyespots in Morpho Butterflies? Disentangling Developmental and Selective Constraints From Neutral Evolution. *Front Ecol Evol* 8, 112. <https://doi.org/10.3389/fevo.2020.00112>
- Debat, V., David, P., 2001. Mapping phenotypes: canalization, plasticity and developmental stability. *Trends in Ecol Evol* 16, 555–561. [https://doi.org/10.1016/S0169-5347\(01\)02266-2](https://doi.org/10.1016/S0169-5347(01)02266-2)
- Dell’Aglio, D.D., Troscianko, J., McMillan, W.O., Stevens, M., Jiggins, C.D., 2018. The appearance of mimetic *Heliconius* butterflies to predators and conspecifics. *Evolution* 72, 2156–2166. <https://doi.org/10.1111/evo.13583>
- Devries, P., 2002. Differential Wing Toughness in Distasteful and Palatable Butterflies: Direct Evidence Supports Unpalatable Theory. *Biotropica* 34, 176–181. <https://doi.org/10.1111/j.1744-7429.2002.tb00254.x>
- Dockx, C., 2007. Directional and stabilizing selection on wing size and shape in migrant and resident monarch butterflies, *Danaus plexippus* (L.), in Cuba: SELECTION ON THE MONARCH BUTTERFLY. *Biol J Linn Soc Lond* 92, 605–616. <https://doi.org/10.1111/j.1095-8312.2007.00886.x>
- Dudley, R., 2002. The Biomechanics of Insect Flight: Form, Function, *Evolution*. Princeton University Press.
- Durden, C.J., Rose, H., 1978. Butterflies from the middle Eocene : The earliest occurrence of fossil Papilionidae (Lepidoptera) 28.
- Ehrlich, P.R., Raven, P.H., 1964. Butterflies and Plants: A Study in Coevolution. *Evolution* 18, 586–608.
- Emerson, M.J., Schram, F.R., 1990. The Origin of Crustacean Biramous Appendages and the Evolution of Arthropoda. *Science* 250, 667–669. <https://doi.org/10.1126/science.250.4981.667>
- Epskamp, S., Cramer, A.O.J., Waldorp, L.J., Schmittmann, V.D., Borsboom, D., 2012. qgraph : Network Visualizations of Relationships in Psychometric Data. *J Stat Soft* 48. <https://doi.org/10.18637/jss.v048.i04>

- Espeland, M., Breinholt, J., Willmott, K.R., Warren, A.D., Vila, R., Toussaint, E.F.A., Maunsell, S.C., Aduse-Poku, K., Talavera, G., Eastwood, R., Jarzyna, M.A., Guralnick, R., Lohman, D.J., Pierce, N.E., Kawahara, A.Y., 2018. A Comprehensive and Dated Phylogenomic Analysis of Butterflies. *Curr Biol* 28, 770-778.e5. <https://doi.org/10.1016/j.cub.2018.01.061>
- Evans, R., Thomas, L.R., 1992. The aerodynamic and mechanical effects of elongated tails in the scarlet-tufted malachite snnbird: measuring the cost of a handicap. *Anim Behav* 43, 11.
- Feltz, C.J., Miller, G.E., 1996. An asymptotic test for the equality of coefficients of variation from k populations. *Statist Med* 15, 647–658. [https://doi.org/10.1002/\(SICI\)1097-0258\(19960330\)15:6<647::AID-SIM184>3.0.CO;2-P](https://doi.org/10.1002/(SICI)1097-0258(19960330)15:6<647::AID-SIM184>3.0.CO;2-P)
- Finkbeiner, S.D., Fishman, D.A., Osorio, D., Briscoe, A.D., 2017. Ultraviolet and yellow reflectance but not fluorescence is important for visual discrimination of conspecifics by *Heliconius erato*. *J Exp Biol* 220, 1267–1276. <https://doi.org/10.1242/jeb.153593>
- FitzJohn, R.G., 2012. Diversitree : comparative phylogenetic analyses of diversification in R: *Diversitree. Methods Ecol Evol* 3, 1084–1092. <https://doi.org/10.1111/j.2041-210X.2012.00234.x>
- Forde, B.G., 2009. Is it good noise? The role of developmental instability in the shaping of a root system. *J Exp Bot* 60, 3989–4002. <https://doi.org/10.1093/jxb/erp265>
- Fordyce, J.A., 2010. Host shifts and evolutionary radiations of butterflies. *Proc R Soc B* 277, 3735–3743. <https://doi.org/10.1098/rspb.2010.0211>
- Fordyce, J.A., 2000. A Model Without a Mimic: Aristolochic Acids from the California Pipevine Swallowtail, *Battus philenor hirsuta*, and Its Host Plant, *Aristolochia californica*. *J Chem Ecol* 26, 2567–2578.
- Foster, D.J., Cartar, R.V., 2011. What causes wing wear in foraging bumble bees? *J Exp Biol* 214, 1896–1901. <https://doi.org/10.1242/jeb.051730>
- Foth, C., Tischlinger, H., Rauhut, O.W.M., 2014. New specimen of Archaeopteryx provides insights into the evolution of pennaceous feathers. *Nature* 511, 79–82. <https://doi.org/10.1038/nature13467>
- Fox, J., Weisberg, S., Price, B., Adler, D., Bates, D., Baud-Bovy, G., Bolker, B., Ellison, S., Firth, D., Friendly, M., Gorjanc, G., Graves, S., Heiberger, R., Krivitsky, P., Laboissiere, R., Maechler, M., Monette, G., Murdoch, D., Nilsson, H., Ogle, D., Ripley,

- B., Venables, W., Walker, S., Winsemius, D., Zeileis, A., R-Core, 2021. *car*: Companion to Applied Regression. R Foundation for Statistical Computing 1109.
- French, J., P., 2017. autoimage: Multiple Heat Maps for Projected Coordinates. *The R Journal* 9, 284. <https://doi.org/10.32614/RJ-2017-025>
- Fritz, S.A., Purvis, A., 2010. Selectivity in Mammalian Extinction Risk and Threat Types: a New Measure of Phylogenetic Signal Strength in Binary Traits: Selectivity in Extinction Risk. *Conserv Biol* 24, 1042–1051. <https://doi.org/10.1111/j.1523-1739.2010.01455.x>
- Gamboa, S., Condamine, F.L., Cantalapiedra, J.L., Varela, S., Pelegrín, J.S., Menéndez, I., Blanco, F., Hernández Fernández, M., 2022. A phylogenetic study to assess the link between biome specialization and diversification in swallowtail butterflies. *Glob Chang Biol* gcb.16344. <https://doi.org/10.1111/gcb.16344>
- Garland, T., Downs, C.J., Ives, A.R., 2022. Trade-Offs (and Constraints) in Organismal Biology. *Physiol Biochem Zool* 95, 82–112. <https://doi.org/10.1086/717897>
- Garnier, S., Gidaszewski, N., Charlot, M., Rasplus, J.-Y., Alibert, P., 2006. Hybridization, developmental stability, and functionality of morphological traits in the ground beetle *Carabus solieri* (Coleoptera, Carabidae): FA in *Carabus solieri* hybrids. *Biol J Linn Soc Lond* 89, 151–158. <https://doi.org/10.1111/j.1095-8312.2006.00668.x>
- Gaunet, A., Dincă, V., Dapporto, L., Montagud, S., Vodă, R., Schär, S., Badiane, A., Font, E., Vila, R., 2019. Two consecutive *Wolbachia* -mediated mitochondrial introgressions obscure taxonomy in Palearctic swallowtail butterflies (Lepidoptera, Papilionidae). *Zool Scr* 48, 507–519. <https://doi.org/10.1111/zsc.12355>
- Gibb, T.J., Oseto, C.Y., Oseto, C., 2006. *Arthropod Collection and Identification: Laboratory and Field Techniques*. Academic Press.
- Gould, S.J., Vrba, E.S., 1982. Exaptation-A Missing Term in the Science of Form. *Paleobiology* 8, 4–15.
- Guidi, R. dos S., São-Pedro, V. de A., da Silva, H.R., Costa, G.C., Pessoa, D.M.A., 2021. The trade-off between color and size in lizards' conspicuous tails. *Behav Processes* 192, 104496. <https://doi.org/10.1016/j.beproc.2021.104496>
- Hall, B.K., 1995. Homology and Embryonic Development, in: Hecht, M.K., Macintyre, R.J., Clegg, M.T. (Eds.), *Evol Biol*, 1-37. <https://doi.org/10.1007/978-1-4615-1847-1>
- Halpin, C.G., Penacchio, O., Lovell, P.G., Cuthill, I.C., Harris, J.M., Skelhorn, J., Rowe, C., 2020. Pattern contrast influences wariness in naïve predators towards aposematic patterns. *Sci Rep* 10, 9246. <https://doi.org/10.1038/s41598-020-65754-y>

- Heard, S.B., Hauser, D.L., 1995. Key evolutionary innovations and their ecological mechanisms. *Hist Biol* 10, 151–173.
- Hervé, M., 2022. RVAideMemoire: Testing and Plotting Procedures for Biostatistics.
- Hill, R.I., Vaca, J.F., 2004. Differential Wing Strength in Pierella Butterflies (Nymphalidae, Satyrinae) Supports the Deflection Hypothesis. *Biotropica* 36, 362–370. <https://doi.org/10.1111/j.1744-7429.2004.tb00328.x>
- Holmes, G.G., Delferrière, E., Rowe, C., Troscianko, J., Skelhorn, J., 2018. Testing the feasibility of the startle-first route to deimatism. *Sci Rep* 8, 10737. <https://doi.org/10.1038/s41598-018-28565-w>
- Holzman, R., Collar, D.C., Price, S.A., Hulsey, C.D., Thomson, R.C., Wainwright, P.C., 2012. Biomechanical trade-offs bias rates of evolution in the feeding apparatus of fishes. *Proc R Soc B* 279, 1287–1292. <https://doi.org/10.1098/rspb.2011.1838>
- Hothorn, T., Bretz, F., Westfall, P., Heiberger, R.M., Schuetzenmeister, A., Scheibe, S., 2022. multcomp: Simultaneous Inference in General Parametric Models.
- Humphreys, R.K., Ruxton, G.D., 2018. What is known and what is not yet known about deflection of the point of a predator’s attack. *Biol J Linn Soc Lond* 123, 483–495. <https://doi.org/10.1093/biolinnean/blx164>
- Hunter, J.P., Jernvall, J., 1995. The hypocone as a key innovation in mammalian evolution. *Proc Natl Acad Sci U.S.A.* 92, 10718–10722. <https://doi.org/10.1073/pnas.92.23.10718>
- Huq, M., Bhardwaj, S., Monteiro, A., 2019. Male *Bicyclus anynana* Butterflies Choose Females on the Basis of Their Ventral UV-Reflective Eyespot Centers. *J Insect Sci* 19. <https://doi.org/10.1093/jisesa/iez014>
- In welchem die in sechs Classen eingetheilte Papilionen mit ihrem Ursprung, Verwa, 1746. . Zoologica.
- Inglis, I.R., Huson, L.W., Marshall, M.B., Neville, P.A., 2010. The Feeding Behaviour of Starlings (*Sturnus vulgaris*) in the Presence of ‘Eyes.’ *Z Tierpsychol* 62, 181–208. <https://doi.org/10.1111/j.1439-0310.1983.tb02151.x>
- Jantzen, B., Eisner, T., 2008. Hindwings are unnecessary for flight but essential for execution of normal evasive flight in Lepidoptera. *Proc Natl Acad Sci India Sect B Biol Sci* 105, 16636–16640. <https://doi.org/10.1073/pnas.0807223105>
- Kassambara, A., 2021. rstatix: Pipe-Friendly Framework for Basic Statistical Tests.
- Kawahara, A.Y., Plotkin, D., Espeland, M., Meusemann, K., Toussaint, E.F.A., Donath, A., Ginnich, F., Frandsen, P.B., Zwick, A., dos Reis, M., Barber, J.R., Peters, R.S., Liu, S.,

- Zhou, X., Mayer, C., Podsiadlowski, L., Storer, C., Yack, J.E., Misof, B., Breinholt, J.W., 2019. Phylogenomics reveals the evolutionary timing and pattern of butterflies and moths. *Proc Natl Acad Sci USA* 116, 22657–22663. <https://doi.org/10.1073/pnas.1907847116>
- Kim, Y., Hwang, Y., Bae, S., Sherratt, T.N., An, J., Choi, S.-W., Miller, J.C., Kang, C., 2020. Prey with hidden colour defences benefit from their similarity to aposematic signals. *Proc R Soc B* 287, 20201894. <https://doi.org/10.1098/rspb.2020.1894>
- Kiritani, K., Yamashita, H., Yamamura, K., 2013. Beak marks on butterfly wings with special reference to Japanese black swallowtail. *Popul Ecol* 55, 451–459. <https://doi.org/10.1007/s10144-013-0375-4>
- Klein, T., 2001. Wing disc development in the fly: the early stages. *Curr Opin Genet Dev* 11, 470–475. [https://doi.org/10.1016/S0959-437X\(00\)00219-7](https://doi.org/10.1016/S0959-437X(00)00219-7)
- Klingenberg, C.P., 2014. Studying morphological integration and modularity at multiple levels: concepts and analysis. *Phil Trans R Soc B* 369, 20130249. <https://doi.org/10.1098/rstb.2013.0249>
- Klingenberg, C.P., 2010. Evolution and development of shape: integrating quantitative approaches. *Nat Rev Genet* 11, 623–635. <https://doi.org/10.1038/nrg2829>
- Klingenberg, C.P., 2008. Morphological Integration and Developmental Modularity. *Annu Rev Ecol Evol Syst* 39, 115–132. <https://doi.org/10.1146/annurev.ecolsys.37.091305.110054>
- Klingenberg, C.P., Polak, M., 2003. Developmental instability as a research tool: using patterns of fluctuating asymmetry to infer the developmental origins of morphological integration. *Developmental Stability: Causes and Consequences* 427–442.
- Kodandaramaiah, U., 2011. The evolutionary significance of butterfly eyespots. *Behav Ecol* 22, 1264–1271. <https://doi.org/10.1093/beheco/arr123>
- Koutrouditsou, L.K., Nudds, R.L., 2021. No evidence of sexual dimorphism in the tails of the swallowtail butterflies *Papilio machaon gorganus* and *P. m. britannicus*. *Ecol Evol* 11, 4744–4749. <https://doi.org/10.1002/ece3.7374>
- Kunte, K., 2009. The diversity and evolution of batesian mimicry in *Papilio* Swallowtails butterflies. *Evolution* 63, 2707–2716. <https://doi.org/10.1111/j.1558-5646.2009.00752.x>
- Kuznetsova, A., Brockhoff, P.B., Christensen, R.H.B., 2017. lmerTest Package: Tests in Linear Mixed Effects Models. *J Stat Soft* 82. <https://doi.org/10.18637/jss.v082.i13>

- Landowski, M., Kunicka-Kowalska, Z., Sibilski, K., 2020. Mechanical and structural investigations of wings of selected insect species. *Acta Bioeng Biomech* 22. <https://doi.org/10.37190/ABB-01525-2019-03>
- Le Roy, C., Amadori, D., Charberet, S., Windt, J., Muijres, F.T., Llaurens, V., Debat, V., 2021. Adaptive evolution of flight in *Morpho* butterflies. *Science* 374, 1158–1162. <https://doi.org/10.1126/science.abh2620>
- Le Roy, C., Cornette, R., Llaurens, V., Debat, V., 2019a. Effects of natural wing damage on flight performance in Morphobutterflies: what can it tell us about wing shape evolution? *J Exp Biol* 222, jeb204057. <https://doi.org/10.1242/jeb.204057>
- Le Roy, C., Debat, V., Llaurens, V., 2019b. Adaptive evolution of butterfly wing shape: from morphology to behaviour. *Biol Rev* brv.12500. <https://doi.org/10.1111/brv.12500>
- Leamy, L.J., Klingenberg, C.P., 2005. The Genetics and Evolution of Fluctuating Asymmetry. *Annu Rev Ecol Evol Syst* 36, 1–21. <https://doi.org/10.1146/annurev.ecolsys.36.102003.152640>
- Li, W., Cong, Q., Shen, J., Zhang, J., Hallwachs, W., Janzen, D.H., Grishin, N.V., 2019. Genomes of skipper butterflies reveal extensive convergence of wing patterns. *Proc Natl Acad Sci USA* 116, 6232–6237. <https://doi.org/10.1073/pnas.1821304116>
- Linke, D., Elias, M., Klečková, I., Mappes, J., Matos-Maraví, P., 2022. Shape of Evasive Prey Can Be an Important Cue That Triggers Learning in Avian Predators. *Front Ecol Evol* 10, 910695. <https://doi.org/10.3389/fevo.2022.910695>
- Llaurens, V., Whibley, A., Joron, M., 2017. Genetic architecture and balancing selection: the life and death of differentiated variants. *Mol Ecol* 26, 2430–2448. <https://doi.org/10.1111/mec.14051>
- Lucas, T., Goswami, A., 2017. paleomorph: Geometric Morphometric Tools for Paleobiology. *R package*.
- Lyytinen, A., Brakefield, P.M., Lindström, L., Mappes, J., 2004. Does predation maintain eyespot plasticity in *Bicyclus anynana*? *Proc Royal Soc B* 271, 279–283. <https://doi.org/10.1098/rspb.2003.2571>
- Macdonald, W.P., Martin, A., Reed, R.D., 2010. Butterfly wings shaped by a molecular cookie cutter: evolutionary radiation of lepidopteran wing shapes associated with a derived Cut/wingless wing margin boundary system: Butterfly wings shaped by a molecular cookie cutter. *Evol Dev* 12, 296–304. <https://doi.org/10.1111/j.1525-142X.2010.00415.x>

- Maia, R., Gruson, H., Endler, J.A., White, T.E., 2019. PAVO 2: New tools for the spectral and spatial analysis of colour in R. *Methods Ecol Evol* 10, 1097–1107. <https://doi.org/10.1111/2041-210X.13174>
- Mappes, J., Marples, N., Endler, J., 2005. The complex business of survival by aposematism. *Trends in Ecology & Evolution* 20, 598–603. <https://doi.org/10.1016/j.tree.2005.07.011>
- Martin, L.J., Carpenter, P.W., 1977. Flow-visualization experiments on butterflies in simulated gliding flight. *Fortschr Zool* 24, 308–316.
- Marwick, B., Krishnamoorthy, K., 2018. cvequality: Tests for the equality of coefficients of variation from multiple groups. *R software package* version 0.1 3.
- McKenna, K.Z., Kudla, A.M., Nijhout, H.F., 2020. Anterior–Posterior Patterning in Lepidopteran Wings. *Front Ecol Evol* 8, 146. <https://doi.org/10.3389/fevo.2020.00146>
- Meijering, E.H.W., Niessen, W.J., Viergever, M.A., 2001. Quantitative evaluation of convolution-based methods for medical image interpolation. *Med Image Anal* 5, 111–126. [https://doi.org/10.1016/S1361-8415\(00\)00040-2](https://doi.org/10.1016/S1361-8415(00)00040-2)
- Melo, D., Marroig, G., 2015. Directional selection can drive the evolution of modularity in complex traits. *Proc Natl Acad Sci USA* 112, 470–475. <https://doi.org/10.1073/pnas.1322632112>
- Mitteroecker, P., Gunz, P., 2009. Advances in Geometric Morphometrics. *Evol Biol* 36, 235–247. <https://doi.org/10.1007/s11692-009-9055-x>
- Molleman, F., Javoš, J., Davis, R.B., Whitaker, M.R.L., Tammaru, T., Prinzing, A., Õunap, E., Wahlberg, N., Kodandaramaiah, U., Aduse-Poku, K., Kaasik, A., Carey, J.R., 2020. Quantifying the effects of species traits on predation risk in nature: A comparative study of butterfly wing damage. *J Anim Ecol* 89, 716–729. <https://doi.org/10.1111/1365-2656.13139>
- Monteiro, A., 2015. Origin, Development, and Evolution of Butterfly Eyespots. *Annu Rev Entomol* 60, 253–271. <https://doi.org/10.1146/annurev-ento-010814-020942>
- Monteiro, A., Brakefield, P.M., French, V., 1997. Butterfly eyespots: the genetics and development of the color rings. *Evolution* 51, 1207–1216. <https://doi.org/10.1111/j.1558-5646.1997.tb03968.x>
- Monteiro, A.F., Brakefield, P.M., French, V., 1994. The evolutionary genetics and developmental basis of wing pattern variation in the butterfly *Bicyclus anynana*. *Evolution* 48, 1147–1157. <https://doi.org/10.1111/j.1558-5646.1994.tb05301.x>

- Montejo-Kovacevich, G., Smith, J.E., Meier, J.I., Bacquet, C.N., Whiltshire-Romero, E., Nadeau, N.J., Jiggins, C.D., 2019. Altitude and life-history shape the evolution of *Heliconius* wings. *Evolution* 73, 2436–2450. <https://doi.org/10.1111/evo.13865>
- Murali, G., Kodandaramaiah, U., 2016. Deceived by stripes: conspicuous patterning on vital anterior body parts can redirect predatory strikes to expendable posterior organs. *R Soc open sci* 3, 160057. <https://doi.org/10.1098/rsos.160057>
- Museum für Naturkunde Berlin, n.d. Global Butterfly Information System (GloBIS). <https://doi.org/10.15468/112dgb>
- Myette, A.L., Hossie, T.J., Murray, D.L., 2019. Defensive posture in a terrestrial salamander deflects predatory strikes irrespective of body size. *Behav Ecol* 30, 1691–1699. <https://doi.org/10.1093/beheco/arz137>
- Naef-Daenzer, L., Naef-Daenzer, B., Nager, R.G., 2000. Prey selection and foraging performance of breeding Great Tits *Parus major* in relation to food availability. *J Avian Biol* 31, 206–214. <https://doi.org/10.1034/j.1600-048X.2000.310212.x>
- Nakae, M., 2021. Papilionidae of the World. Roppon-Ashi Entomological Books.
- Norberg, U.M., 1995. How a Long Tail and Changes in Mass and Wing Shape Affect the Cost for Flight in Animals. *Funct Ecol* 9, 48. <https://doi.org/10.2307/2390089>
- Novelo Galicia, E., Luis Martínez, M.A., Cordero, C., 2019. False head complexity and evidence of predator attacks in male and female hairstreak butterflies (Lepidoptera: Theclinae: Eumaeini) from Mexico. *PeerJ* 7, e7143. <https://doi.org/10.7717/peerj.7143>
- Olofsson, M., Vallin, A., Jakobsson, S., Wiklund, C., 2010. Marginal Eyespots on Butterfly Wings Deflect Bird Attacks Under Low Light Intensities with UV Wavelengths. *PLoS ONE* 5, e10798. <https://doi.org/10.1371/journal.pone.0010798>
- Orme, D., Freckleton, R., Thomas, G., Petzoldt, T., Fritz, S., Isaac, N., Pearse, W., 2013. The Caper Package: Comparative Analysis of Phylogenetics and Evolution in R. *R package version 5*, 1–36.
- Ortega Ancel, A., Eastwood, R., Vogt, D., Ithier, C., Smith, M., Wood, R., Kovač, M., 2017. Aerodynamic evaluation of wing shape and wing orientation in four butterfly species using numerical simulations and a low-speed wind tunnel, and its implications for the design of flying micro-robots. *Interface Focus* 7, 20160087. <https://doi.org/10.1098/rsfs.2016.0087>

- Osorio, D., Miklósi, A., Gonda, Zs., 1999. Visual Ecology and Perception of Coloration Patterns by Domestic Chicks. *Evol Ecol* 13, 673–689. <https://doi.org/10.1023/A:1011059715610>
- Ostrom, J.H., 1974. Archaeopteryx and the Origin of Flight. *Q Rev Biol* 49, 27–47. <https://doi.org/10.1086/407902>
- Ota, M., Yuma, M., Mitsuo, Y., Togo, Y., 2014. Beak marks on the wings of butterflies and predation pressure in the field: Beak mark and predation pressure. *Entomol Sci* 17, 371–375. <https://doi.org/10.1111/ens.12076>
- Outomuro, D., Söderquist, L., Nilsson-Örtman, V., Cortázar-Chinarro, M., Lundgren, C., Johansson, F., 2016. Antagonistic natural and sexual selection on wing shape in a scrambling damselfly: antagonistic selection on wing shape. *Evolution* 70, 1582–1595. <https://doi.org/10.1111/evo.12951>
- Owens, H.L., Lewis, D.S., Condamine, F.L., Kawahara, A.Y., Guralnick, R.P., 2020. Comparative Phylogenetics of *Papilio* Butterfly Wing Shape and Size Demonstrates Independent Hindwing and Forewing Evolution. *Syst Biol* 69, 813–819. <https://doi.org/10.1093/sysbio/syaa029>
- Páez, E., Valkonen, J.K., Willmott, K.R., Matos-Maraví, P., Elias, M., Mappes, J., 2021. Hard to catch: experimental evidence supports evasive mimicry. *Proc Royal Soc B* 288, 20203052. <https://doi.org/10.1098/rspb.2020.3052>
- Palmer, A.R., 1994. Fluctuating asymmetry analyses: a primer, in: Markow, T.A. (Ed.), *Developmental Instability: Its Origins and Evolutionary Implications*. Springer Netherlands, Dordrecht, pp. 335–364. https://doi.org/10.1007/978-94-011-0830-0_26
- Palmer, A.R., Strobeck, C., 1986. Fluctuating Asymmetry: Measurement, Analysis, Patterns. *Annu Rev Ecol Evol Syst* 17, 391–421. <https://doi.org/10.1146/annurev.es.17.110186.002135>
- Park, H., Bae, K., Lee, B., Jeon, W.-P., Choi, H., 2010. Aerodynamic Performance of a Gliding Swallowtail Butterfly Wing Model. *Exp Mech* 50, 1313–1321. <https://doi.org/10.1007/s11340-009-9330-x>
- Parsons, M.J., 1996. A phylogenetic reappraisal of the birdwing genus *Ornithoptera* (Lepidoptera: Papilionidae: Troidini) and a new theory of its evolution in relation to Gondwanan vicariance biogeography. *J Nat Hist* 30, 1707–1736. <https://doi.org/10.1080/00222939600771001>

- Pau, G., Fuchs, F., Sklyar, O., Boutros, M., Huber, W., 2010. EBImage--an R package for image processing with applications to cellular phenotypes. *Bioinformatics* 26, 979–981. <https://doi.org/10.1093/bioinformatics/btq046>
- Pélabon, C., Hansen, T.F., Carter, A.J.R., Houle, D., 2010. Evolution of variation and variability under fluctuating, stabilizing, and disruptive selection. *Evolution* 64, 1912–1925. <https://doi.org/10.1111/j.1558-5646.2010.00979.x>
- Pennell, M.W., Eastman, J.M., Slater, G.J., Brown, J.W., Uyeda, J.C., FitzJohn, R.G., Alfaro, M.E., Harmon, L.J., 2014. geiger v2.0: an expanded suite of methods for fitting macroevolutionary models to phylogenetic trees. *Bioinformatics* 30, 2216–2218. <https://doi.org/10.1093/bioinformatics/btu181>
- Pinheiro, C.E.G., 2011. On the evolution of warning coloration, Batesian and Müllerian mimicry in Neotropical butterflies: the role of jacamars (Galbulidae) and tyrant-flycatchers (Tyrannidae). *J Avian Biol* 42, 277–281. <https://doi.org/10.1111/j.1600-048X.2011.05435.x>
- Pinheiro, C.E.G., Cintra, R., 2017. Butterfly Predators in the Neotropics: Which Birds are Involved? *J Lepid Soc* 71, 109–114. <https://doi.org/10.18473/lepi.71i2.a5>
- Pinheiro, J., S., Bates, D., DebRoy, S., Sarkar, D., Heisterkamp, S., Van Willigen, B., Ranke, J., 2022. nlme: Linear and Nonlinear Mixed Effects Models. *R package* version, 3(57), 1-89.
- Pliske, T.E., 1972. Sexual Selection and Dimorphism in Female Tiger Swallowtails, *Papilio glaucus* L. (Lepidoptera: Papilionidae) : a Reappraisal. *Ann Entomol Soc Am* 65, 1267–1270. <https://doi.org/10.1093/aesa/65.6.1267>
- Prudic, K.L., Skemp, A.K., Papaj, D.R., 2007. Aposematic coloration, luminance contrast, and the benefits of conspicuousness. *Behav Ecol* 18, 41–46. <https://doi.org/10.1093/beheco/arl046>
- Prudic, K.L., Stoehr, A.M., Wasik, B.R., Monteiro, A., 2015. Eyespots deflect predator attack increasing fitness and promoting the evolution of phenotypic plasticity. *Proc R Soc B* 282, 20141531. <https://doi.org/10.1098/rspb.2014.1531>
- Prum, R.O., Brush, A.H., 2002. The Evolutionary Origin And Diversification Of Feathers. *Q Rev Biol* 77, 261–295. <https://doi.org/10.1086/341993>
- R Core Team, 2018. R: A language and environment for statistical computing. R Foundation for Statistical Computing.

- Rabosky, D.L., 2014. Automatic Detection of Key Innovations, Rate Shifts, and Diversity-Dependence on Phylogenetic Trees. *PLoS ONE* 9, e89543. <https://doi.org/10.1371/journal.pone.0089543>
- Rabosky, D.L., Grudler, M., Anderson, C., Title, P., Shi, J.J., Brown, J.W., Huang, H., Larson, J.G., 2014. BAMMtools: an R package for the analysis of evolutionary dynamics on phylogenetic trees. *Methods Ecol Evol* 5, 701–707. <https://doi.org/10.1111/2041-210X.12199>
- Racheli, T., Pariset, L., 1992. Il Genere Battus (Lepidoptera, Papilionidae): Tassonomica e Storia Naturale, *Fragmenta Entomologica*. Universita Degli Studi di Roma.
- Raia, P., Castiglione, S., Serio, C., Mondanaro, A., Melchionna, M., Febbraro, M.D., Profico, A., Carotenuto, F., 2022. RRphylo: Phylogenetic Ridge Regression Methods for Comparative Studies. *R package version*, 2(0).
- Rawlins, J.E., 1980. Thermoregulation by the Black Swallowtail Butterfly, *Papilio Polyxenes* (Lepidoptera: Papilionidae). *Ecology* 61, 345–357. <https://doi.org/10.2307/1935193>
- Rebel, H., 1898. *Dorittes bosniaskii*. Sitzungsberichte der akademie der wissenschaften. Mathematischen-Naturwissenschaftliche classe. *Abt 1*, 734–741.
- Revell, L.J., 2012. phytools: Phylogenetic Tools for Comparative Biology (and Other Things). *Methods Ecol Evol* 2, 217–223.
- Robbins, R.K., 1981. The “False Head” Hypothesis: Predation and Wing Pattern Variation of Lycaenid Butterflies. *Am Nat* 118, 770–775. <https://doi.org/10.1086/283868>
- Robbins, R.K., 1980. The Lycaenid “false head” hypothesis: quantitative analysis. *J Lepid Soc* 34, 15.
- Rohlf, F.J., 2015. The tps series of software. *Hystrix, the Italian J Mammal* 26. <https://doi.org/10.4404/hystrix-26.1-11264>
- Rohlf, F.J., Slice, D., 1990. Extensions of the Procrustes Method for the Optimal Superimposition of Landmarks. *Syst Biol* 39, 40–59. <https://doi.org/10.2307/2992207>
- Rubin, J.J., Hamilton, C.A., McClure, C.J.W., Chadwell, B.A., Kawahara, A.Y., Barber, J.R., 2018. The evolution of anti-bat sensory illusions in moths. *Sci Adv* 4, eaar7428. <https://doi.org/10.1126/sciadv.aar7428>
- Ruxton, G.D., Sherratt, T.N., Speed, M.P., 2004. *Avoiding attack: the evolutionary ecology of crypsis, warning signals, and mimicry*, Oxford biology. Oxford University Press, Oxford ; New York.

- Sane, S.P., 2003. The aerodynamics of insect flight. *J Exp Biol* 206, 4191–4208. <https://doi.org/10.1242/jeb.00663>
- Schluter, D., 1996. Adaptive radiation along genetic lines of least resistance. *Evolution* 50, 1766–1774. <https://doi.org/10.1111/j.1558-5646.1996.tb03563.x>
- Scoble, M.J., 1992. The Lepidoptera. Form, function and diversity. The Lepidoptera. Form, function and diversity.
- Scudder, S.H., 1875. Fossil Butterflies: Memoirs of the American Association for the Advancement of Science, I. Salem, Massachusetts.
- Sekimura, T., Nijhout, H.F. (Eds.), 2017. Diversity and Evolution of Butterfly Wing Patterns: An Integrative Approach. Springer Singapore, Singapore. <https://doi.org/10.1007/978-981-10-4956-9>
- Sourakov, A., 2015. Antipredation and “antimimicry”: wing pattern is supported by behavior in *Archaeoprepona chromus* (Lepidoptera: Nymphalidae: Preponini). *ATL Notes* December 2015, 1–7.
- Sourakov, A., 2013. Two heads are better than one: false head allows *Calycopis cecrops* (Lycaenidae) to escape predation by a Jumping Spider, *Phidippus pulcherrimus* (Salticidae). *J Nat Hist* 47, 1047–1054. <https://doi.org/10.1080/00222933.2012.759288>
- Stearns, S.C., Kaiser, M., Kawecki, T.J., 1995. The differential genetic and environmental canalization of fitness components in *Drosophila melanogaster*. *J Evol Biol* 8, 539–557. <https://doi.org/10.1046/j.1420-9101.1995.8050539.x>
- Stevens, M., 2005. The role of eyespots as anti-predator mechanisms, principally demonstrated in the Lepidoptera. *Biol Rev* 80, 573. <https://doi.org/10.1017/S1464793105006810>
- Stoddard, M.C., 2012. Mimicry and masquerade from the avian visual perspective. *Curr Zool* 58, 630–648. <https://doi.org/10.1093/czoolo/58.4.630>
- Strauss, R.E., 1990. Patterns of quantitative variation in lepidopteran wing morphology: the convergent groups Heliconiinae and Ithomiinae (Papilionoidea: Nymphalidae). *Evolution* 44, 86–103. <https://doi.org/10.1111/j.1558-5646.1990.tb04281.x>
- Suzuki, R., Terada, Y., Shimodaira, H., 2006. pvclust: Hierarchical Clustering with P-Values via Multiscale Bootstrap Resampling version 2.2-0 from CRAN. *Bioinformatics* 22, 1540–1542.
- Swallow, J., Husak, J., 2011. Compensatory traits and the evolution of male ornaments. *Behav* 148, 1–29. <https://doi.org/10.1163/000579510X541265>

- Theriault, D.H., Fuller, N.W., Jackson, B.E., Bluhm, E., Evangelista, D., Wu, Z., Betke, M., Hedrick, T.L., 2014. A protocol and calibration method for accurate multi-camera field videography. *J Exp Biol* 217, 1843–1848. <https://doi.org/10.1242/jeb.100529>
- Théry, M., Debut, M., Gomez, D., Casas, J., 2004. Specific color sensitivities of prey and predator explain camouflage in different visual systems. *Behav Ecol* 16, 25–29. <https://doi.org/10.1093/beheco/arh130>
- Thomas, A.L.R., 1993. On the Aerodynamics of Birds' Tails. *Phil Trans R Soc Lond B* 361–380. <https://doi.org/doi:10.1098/rstb.1993.0079>
- Tonner, M., Novotny, V., Leps, J., Komarek, S., 1993. False Head Wing Pattern of the Burmese Junglequeen Butterfly and the Deception of Avian Predators. *Biotropica* 25, 474. <https://doi.org/10.2307/2388871>
- Ursprung, H., Nöthiger, R. (Eds.), 1972. The Biology of Imaginal Disks, Results and Problems in Cell Differentiation. Springer Berlin Heidelberg, Berlin, Heidelberg. <https://doi.org/10.1007/978-3-540-37185-4>
- Van Valen, L.V., 1994. Serial homology: the crests and cusps of mammalian teeth. *Acta Palaeontol Pol* 38, 145–158.
- Wagner, G.P., Altenberg, L., 1996. Perspective: Complex adaptations and the evolution of evolvability. *Evolution* 50, 967–976. <https://doi.org/10.1111/j.1558-5646.1996.tb02339.x>
- Wagner, G.P., Pavlicev, M., Cheverud, J.M., 2007. The road to modularity. *Nat Rev Genet* 8, 921–931. <https://doi.org/10.1038/nrg2267>
- Walker, J.A., 2007. A General Model of Functional Constraints on Phenotypic Evolution. *Am Nat* 170, 681–689. <https://doi.org/10.1086/521957>
- Ward, J.H., 1963. Hierarchical Grouping to Optimize an Objective Function. *J Am Stat Assoc* 236–244.
- Watson, C.M., Roelke, C.E., Pasichnyk, P.N., Cox, C.L., 2012. The fitness consequences of the autotomous blue tail in lizards: an empirical test of predator response using clay models. *Zoology* 115, 339–344. <https://doi.org/10.1016/j.zool.2012.04.001>
- Welch, G., Bishop, G., 1995. An Introduction to the Kalman Filter 127–132.
- Wourms, M.K., Wasserman, F.E., 1985. Butterfly wing markings are more advantageous during handling than during the initial strike of an avian predator. *Evolution* 39, 845–851. <https://doi.org/10.1111/j.1558-5646.1985.tb00426.x>
- Wright, S., 1932. The roles of mutation, inbreeding, crossbreeding, and selection in evolution.

-
- Wu, T.-S., Leu, Y.-L., Chan, Y.-Y., 2000. Aristolochic Acids as a Defensive Substance for the Aristolochiaceae Plant-Feeding Swallowtail Butterfly, *Pachliopta aristolochiae interpositus*. *Jnl Chinese Chemical Soc* 47, 221–226. <https://doi.org/10.1002/jccs.200000026>
- Young, N.M., Hallgrímsson, B., 2005. Serial homology and the evolution of Mammalian limb covariation structure. *Evolution* 59, 2691. <https://doi.org/10.1554/05-233.1>
- Zakharov, E.V., Caterino, M.S., Sperling, F.A.H., 2004. Molecular Phylogeny, Historical Biogeography, and Divergence Time Estimates for Swallowtail Butterflies of the Genus *Papilio* (Lepidoptera: Papilionidae). *Syst Biol* 53, 193–215. <https://doi.org/10.1080/10635150490423403>
- Zelditch, M.L., Wood, A.R., Bonett, R.M., Swiderski, D.L., 2008. Modularity of the rodent mandible: Integrating bones, muscles, and teeth: Modularity of the rodent mandible. *Evol Dev* 10, 756–768. <https://doi.org/10.1111/j.1525-142X.2008.00290.x>

Evolution of tails in Swallowtail butterflies (Papilionidae, Lepidoptera): macro-evolutionary and experimental approaches

The evolution of butterfly wing shape is driven by multiple selective, phylogenetic and developmental influences. In my thesis, I focused on the evolution of wing shape in Papilionidae, a butterfly family presenting a high diversity of wing shapes. Papilionidae are collectively referred to as Swallowtail butterflies, owing to the tails that many species harbour on the hindwings. While this feature is particularly striking and diversified, its evolutionary drivers have never been investigated. *Did tails evolve neutrally? What are the selective pressures affecting it? Do forewings and hindwings evolve independently?* By combining micro- and macro-evolutionary approaches, my thesis aimed at answering these questions and identifying the main factors affecting the evolution of wing shape, with a particular focus on hindwing tails. Focusing on *Iphiolides podalirius*, I first tested whether tails deflect birds attacks away from the butterfly body (the *deflecting effect* hypothesis; Chapter I). I showed that natural wing damages mostly concern hindwings tails and colour-pattern, suggestive of predation attempts; I then conducted a behavioural assay with dummy butterflies, and showed that great tits (*Parus major*) focus their attacks on the tails; finally, quantifying the mechanical properties of fresh wings, I found that the tails are particularly fragile. Altogether, these results support a deflecting effect of hindwing tails, suggesting that predation is an important selective driver of the evolution of tails in butterflies. I then investigated the relative aerodynamic importance of tails in flapping flight (the *aerodynamic effect* hypothesis; Chapter II), conducting flight analyses of phenotypically altered *I. podalirius*. I showed that hindwing tails have a significant stabilising impact on flapping flight, suggesting that selection on aerodynamic performance likely affects the evolution of tails. Based on these experimental results, I then quantified the variation of fore- and hindwing wing shape at the macro-evolutionary scale (across the Papilionidae family; Chapter III). I compared the shape diversity and evolutionary rate among the two wings, and tested the link between diversification and phenotypic disparity. I specifically characterized the evolution of the tail at the family level. My results show that hindwings are strikingly more diversified than forewings, suggesting contrasted selective regimes on the two pairs of wings. Forewings might be under stabilizing selection in relation to flight anteromotorism, while hindwings might be submitted to a diversity of selective pressures. Our results on *I. podalirius* suggest a possible trade-off between attack deflection and aerodynamic effects, promoting the diversity of hindwing shape, and particularly the evolutionary lability of tails and associated colour patterns. Contrary to previous work, my results also suggest a tight coevolution of the two wing pairs, the presence of tails possibly affecting the selection on the forewings. Overall, this study shows that the combination of behavioural ecology and macro-evolutionary studies might shed light on key factors affecting morphological evolution.

Altogether, my PhD work has brought some insights on the selection pressures involved in hindwing tail evolution and highlighted the complex links existing between forewings and hindwings evolution, between contrasted selection, developmental constraints and co-evolution.



